Title
Modeling and Analysis of Bacterial Survival Strategies

Author
Morimoto, Michael Toshiro

Publication Date
2011

Peer reviewed|Thesis/dissertation

Modeling and Analysis of Bacterial Survival Strategies

by

Michael Toshiro Morimoto

A dissertation submitted in partial satisfaction of the

requirements for the degree of

Doctor of Philosophy

in

Engineering – Mechanical Engineering

in the

Graduate Division

of the

University of California, Berkeley

Committee in charge:

Professor Kameshwar Poolla, Chair
Professor Adam Arkin
Professor J. Karl Hedrick

Fall 2011

Abstract

Modeling and Analysis of Bacterial Survival Strategies

by

Michael Toshiro Morimoto

Doctor of Philosophy in Engineering – Mechanical Engineering

University of California, Berkeley

Professor Kameshwar Poolla, Chair

An interesting way to study biological systems is from the perspective of control theory. Most of these systems can only operate within a narrow range of conditions, and external disturbances typically conspire to push them out of their normal operating domains. This has necessitated the development of mechanisms for physiological and environmental sensing to ensure that vital internal variables are regulated. Without these feedback control systems, life itself would be impossible due to daily and seasonal variations in environmental conditions. Survival therefore depends largely on the effectiveness of these control systems, and it is commonly assumed that natural selection has led to the evolution of optimal control strategies. This framework of evolutionary optimality is used in this dissertation to examine sporulation, a bacterial survival strategy employed by *Bacillus subtilis*.

Sporulation is the process of forming a morphologically-distinct, dormant structure that is able to withstand severe environmental insults. This dormant cell structure, called an endospore (or spore), is typically formed in response to nutrient limitation or other environmental signals associated with low food supply. A signal transduction pathway integrates intra- and extra-cellular signals to arrive at a decision to sporulate, effectively acting as a control mechanism that allows survival in the face of environmental nutrient limitation and other serious disturbances. In the framework of evolutionary optimality, this control strategy is hypothesized to be optimal in the sense of maximizing a fitness reward function for the *B. subtilis* colony.

In this dissertation, sporulation is analyzed from this perspective to uncover some interesting characteristics of the decision policy. It is shown that sporulation provides a higher fitness than a simpler bacterial survival strategy with many of the same benefits (called dormancy in this study). The particular environment in which this is verified features a catastrophic event several generations into the future, after which only the survival structures remain. This result agrees with the morphological differences between a spore and a simple dormant cell. Moreover, the optimal sporulation policy qualitatively agrees with experimental data, while the optimal dormancy strategy is significantly different from observed behavior in literature studies. These results offer a candidate evolutionary justification for

the existence of sporulation.

Fitness-maximizing sporulation policies are then studied in the contexts of simple population-level models with food-per-growing-cell rate dependencies. Since the results for a single population model are not consistent with expected results, a second model is postulated based on resource competition between two bacterial populations. The competitive exclusion principle is shown to hold for the proposed model structure, which provides an extension of previous resource competition results due to the sporulation model's "storage-like" spore states. For specialized cases of this competing populations model (birth and death rates equal for both populations), an approximation of the steady state solution is derived and input-output stability is analytically proved using perturbation methods. Both of these are notable due to the model's non-unique steady state solutions and the nonlinearity of the proposed model. Though the steady state approximation imposes nutrient influx changes to be small, it is intended to model adiabatic system trajectories for slowly-changing nutrient conditions. In response to these changes, a game theoretic analysis yields two policies that cannot be invaded by rare mutants: 100% steady state sporulation efficiency if nutrient influx decreases on average, and 0% steady state sporulation efficiency if nutrient influx increases on average. Evolutionary dynamics are introduced to model changes between these two optimal policies, and the nutrient influx is assumed to randomly switch between positive and negative values based on a two-state Markov chain. A non-equilibrium policy is derived for these modeling and environmental conditions, which is much closer to experimental data than the optimal policies. The "choice" of the non-equilibrium policy over the optimal policies is then examined in a prospect theory framework, and it is shown that the preference of the non-optimal policy could be explained with appropriate shifts of reference: when nutrient influx increases on average, the bacterium expects the worst (pessimistic), and when nutrient influx decreases on average, the bacterium expects the best (optimistic). While the non-equilibrium policy appears to fall within the class of bet-hedging (risk-spreading) strategies, this is not the case as the probability of population extinction is not decreased.

The work presented in this dissertation yields some interesting results on *B. subtilis* behavior, some of which may generalize to other organisms that are capable of entering an inactive state.

For Anne and my family.

Contents

List of Figures

List of Tables

Chapter 1

Introduction

Biological organisms are intricately engineered systems. With few exceptions (such as show animals from fancy breeds), they are designed to maximize the survival of their species. With over 3.5 billion years of research and development by evolution to address this objective, biological organisms have evolved into extremely complex systems. For example: human arms have more degrees of freedom (seven) and muscle groups than are necessary for three-dimensional positioning, yet most human beings are able to use this redundancy to improve performance or adapt to internal/external changes [136, 143]; human kidneys excrete blood-borne waste by non-selective filtration followed by selective re-absorption, which allows unanticipated toxins to be excreted from the body [269]; and the metabolic pathways that are conserved across most living organisms are composed of extremely complex interconnected subsystems (a *simplified* map is shown in Figure 1.1).

Despite these apparent complexities, biological systems exhibit resilient multi-functional properties and robust architectures [36, 46]. From an engineering point of view, many biological organisms appear to be the products of carefully-engineered designs. Realizing the paramount goal of improving survival draws on diverse elements from many engineering disciplines, ranging from mechanical engineering to materials science. For example:

1. The dimorphic chelae (claws) of many American lobsters differ in size and design according to functionality. The smaller chela typically holds prey while the larger chela crushes its shell, a strategy that is possible due to the disparity between mechanical advantages of the chelae. Studies on some species have shown that the larger chela has twice the mechanical advantage of the smaller chela [68].

2. Flying fish (family Exocoetidae) exhibit "good aerodynamic designs," such as hypertrophied fins and a cylindrical body with a ventrally flattened surface, for proficient gliding flight. Behavioral aspects of flying fish suggest that they initiate flight patterns with a maximum lift coefficient and follow maximum-distance gliding paths [196].

3. The hypodermal blubber layer in marine mammals primarily serves to insulate and provide energy reserves. Blubber in harbor seals experiences seasonal variations in volume, mean depth, and ratio of blubber depth to body radius (d/r ratio). The d/r ratio exhibits relatively small temporal and spatial variations (along the body length)

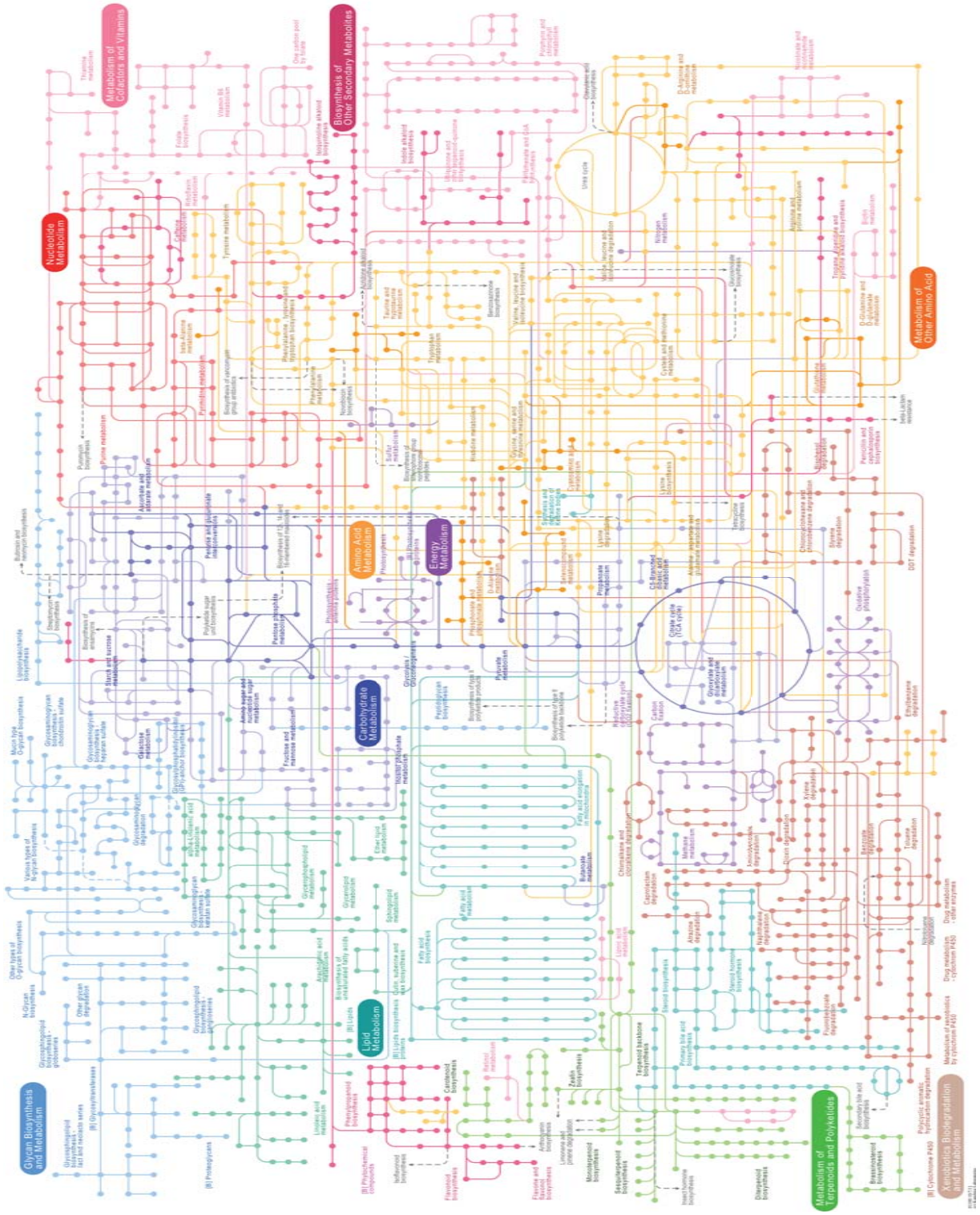

Figure 1.1: Metabolic pathways, from Kanehisa and Goto [134].

for a single seal, and blubber is preferentially lost from over-insulated areas of the body. This suggests that blubber mass is adjusted to maintain maximal insulation effectiveness [223].

4. Besides their obvious uses in dexterous maneuvers, human hands aid in body temperature regulation. Some of the responses to increased core body temperature are vasodilation of skin vessels and sweating [269], which increases the heat transfer away from the body. The high surface area to volume ratio of a human hand makes it extremely adept at cooling, much like fins or extended surfaces. Studies have shown that hand cooling during exercise attenuates the rise in tympanic temperature and may increase certain measures of exercise performance [119].

5. Wood is widely used as an engineering material because it has a remarkable combination of mechanical properties. On a normalized mass basis (accounting for densities), wood has comparable stiffness, strength, and toughness (in certain orientations to the grain) to aluminum, steel, and other glass-fiber composites [124].

6. Silk produced by spiders and other insects has very high strength, stiffness, and toughness in both compression and tension, is reliable across a wide range of temperatures and humidities, and is biodegradable [260]. Dragline silk is three times as tough as aramid fibers and five times stronger (by weight) than steel. Spider silk has significantly influenced the design of high-performance materials that may be used in applications requiring high energy absorption and elongation [149].

There are countless other examples from which to draw, but the point is clear: Studying biological organisms from an engineering point of view is natural due to the design philosophy behind most evolved traits, where functionality to improve survival is prized and rewarded. In fact, biological systems often provide inspiration for the design of actual engineering systems, which has spawned the relatively new paradigm of biomimicry [19].

One of the most striking features of biological systems is their ability to contend with unknown environmental conditions. Though many are deliberately over-designed for average use (e.g. bone thickness [233]), most are able to adapt to various situations by means of sensor measurements and feedback control. This pervasive trait is briefly reviewed in the next section.

1.1 Control systems in biology

One of the most interesting engineering perspectives of biological organisms and systems comes through the lens of control theory. The study of feedback systems is a natural framework within which to study biological organisms because they are constantly changing and interacting with surrounding environments. Survival is intimately related to these *a priori* unknown conditions, which has necessitated the evolution of sensing mechanisms to help regulate key biological variables that are influenced by wide ranges of disturbances. For example, many animals rely on sight or smell to detect predators, which is processed in the

brain to create control signals to actuate muscles in the legs. At the highest levels, feedback is involved in path planning and conscious decision-making, and at lower levels, feedback is involved in muscle recruitment and balance. Even the evolutionary histories of biological traits can be studied from a control theory point of view, where optimal control provides a compelling interpretation of natural selection. Many interesting biological phenomenon have simple feedback interpretations [46], which makes control theory a powerful tool to use in the study of biological systems.

An exhaustive survey of control systems in biological organisms and systems is beyond the scope of this dissertation. In just one field of biology (e.g. physiology, molecular cell biology, or evolutionary biology), this would prove to be a monumental task. However, to provide some idea of the broad applicability of control theory, three examples are listed below:

1. **Motor control**: Skeletal muscle movements rely on a hierarchy of interrelated control systems. For example, grasping a coffee mug on the kitchen table would be nearly impossible without visual or tactile feedback. On top of this, equilibrium organs aid in balancing while the arm is outstretched, and initial visual localization is used to plan a spatial path to the final hand position. Though it may seem that feedforward control may be able to accomplish seemingly trivial tasks such as walking or grabbing objects, feedback is essential for these operations at most levels.

   At the lowest levels, mechanical feedback is provided by the viscoelastic behavior of the musculoskeletal system in its resistance to deformation, which has a stabilizing effect on the high neural controller gains [52]. Slightly higher in the control hierarchy is the neuronal feedback provided by the stretch reflex arcs, which help to regulate the magnitudes and dynamics of force and length in the musculoskeletal system. Higher still are the neuronal control loops which create large-scale muscle movements, which are affected by tonic input from directional sensors, equilibrium organs, and mechanosensory cells [52]. These are responsible for directing an animal to a desired location or providing stabilization in the face of environmental perturbations. Additionally, combined with the lower-level control loops, neuronal control systems help to regulate and coordinate force generation and braking mechanisms that are essential for quick, accurate, and harmonized movements [221]. Finally, at the highest level, neuronal control in the higher centers of the brain relies on visual, olfactory, auditory, or other sensors to command voluntary changes in muscle movement that are essential for guidance, obstacle avoidance, hunting prey, or avoiding predators [52].

   It is evident that the musculoskeletal movements can be represented as the product of a complex, interconnected control system. Analysis is difficult since it is a distributed, nonlinear, time-varying control system with redundancies on many levels [136]. In particular, dissecting the controllers involved in path planning and overall muscle movements is difficult, though observed muscle movements have been replicated by assuming the nervous system minimizes an objective function that relies on jerk [136].

2. **Biochemical networks**: Genetic and protein cellular networks are widely studied systems where control theoretic ideas have brought a deeper understanding of underly-

ing processes. Though comparatively straightforward, these networks are responsible for some extremely important cellular phenomena. For instance, they govern and regulate processes such as the management of intracellular energy stores, the establishment of periodic cycles or rhythms, and gene expression and enzyme activation due to environmental stimuli. It has been shown that some models of these networks can reproduce many cellular processes, most of which contain feedback properties. These applications of control theory were significant enough to cause Brian Goodwin (a key contributor to early theoretical biology) to declare "the demonstration of negative feedback control processes operating at the molecular level in cells is one of the most significant developments in modern biology" [89].

One ubiquitous example of a biochemical network with feedback is the repression of mRNA synthesis by a protein encoded by that mRNA or a metabolite formed under the catalytic control of the protein [92]. In this case, the feedback is often negative and nonlinear, since a simplified representation of protein (repressor) binding dynamics leads to Michaelis-Menton kinetics [252]. Some examples of this general network structure are the synthesis of the protein PER, which plays a crucial role in circadian rhythms in *Drosophilia*, and the regulation of the enzyme phosphofructokinase (PFK), which allows the formation of adenosine triphosphate (ATP) from adenosine diphosphote (ADP) during glycolysis [252]. PER proteins inhibit the transcription of their own mRNA while PFK activity is inhibited and triggered by ATP and ADP, respectively. Slightly more complicated is the case of a regulator/operator gene that controls the synthesis rate of a different protein through cytoplasmic interactions, where the regulator protein is sensitive to environmental stimuli [122]. Examples of this system structure are the *lac* operon in *E. coli*, which is only expressed when lactose and glucose are high and low, respectively [122, 222], and the regulation of two cyclins in well-nourished yeast cells, which are important for normal growth and division [252]. Expression of the *lac* operon is negatively-regulated by the *lac* repressor and positively-regulated by the catabolite gene activator protein (CAP), while the cyclins and their associated kinase subunits affect their own synthesis and the synthesis/degradation of the other cyclin to produce periodic accumulation and degradation of both proteins.

More complex biochemical networks exist (see Figure 1.1), but even in these higher-order systems, feedback is invariably present [65]. Control theory has provided tools for the analysis of biological systems, and conversely, complex biochemical networks have provided inspiration for new analytical results for general control systems (for example, see [229]).

3. **Blood glucose control**: Some of the most immediate applications of control theory in biology are the physiological systems that maintain homeostatic conditions in the human body. For example, blood pressure, blood acidity, and electrolyte balance are all tightly regulated in a disease-free human. Each of these physiological variables varies narrowly around an operating point using biological sensors, actuators, and controllers. The blood pressure system, for instance, uses baroreceptor pressure

sensors in the carotid arteries and aortic arch to measure arterial pressure, and the central nervous system (medullary cardiovascular center in the medulla oblongota) sends signals to the peripheries and heart to affect total peripheral resistance (via arterioles constriction) and cardiac output, respectively [269]. In the long term, blood volume regulation by renal mechanisms also plays a major factor in blood pressure control.

One of the most interesting homeostatic control systems is the relatively tight regulation of blood glucose (BG) levels. This control system is extremely important because central nervous system cells use BG almost exclusively for fuel under non-starvation conditions (most other cells have intracellular fuel stores such as glycogen) [269]. Negative deviations from normal BG levels (hypoglycemia) lead to alterations in neural activity due to lack of fuel, ranging from subtle impairment of neural activity to seizures, coma, or even death; deviations in the positive direction (hyperglycemia) lead to excess glucose, ketone, sodium, and water excretion in the urine, which reduces blood volume, blood pressure, and brain blood flow, and increased blood hydrogen ion concentrations due to accumulation of ketones in the blood, which can cause brain dysfunction [269]. To maintain proper neural activity, tight BG regulation is required. This objective is often challenged by extremely variable food levels in the gut.

A balanced meal contains all three of the major nutrients– carbohydrates, proteins, and fat– with the majority of the energy content coming from carbohydrates [269]. For the purposes of BG control, proteins and fat will be ignored in the sequel. Food enters the gastrointestinal tract, where salivary and pancreatic amylases produce products that are broken down into monosaccharides (glucose, galactose, and fructose) by enzymes in the luminal membranes of the small intestine epithelial cells [269]. These monosaccharides are transported into the blood and into the liver, where galactose and fructose are converted to glucose or enter similar metabolic pathways to glucose. The meal therefore acts to raise BG levels when food is in the gut, which is emptied approximately four hours after ingestion [269].

To deal with this irregular supply of BG, the human body has developed a control system with BG sensors, actuators, and controllers. The BG sensors are pancreatic β- and α-cells, neural cells, other endocrine cells, and possibly liver cells; the main actuators are various hormones released by pancreatic β-cells (insulin), α-cells (glucagon), adrenal medulla (epinephrine), and adrenal cortex (cortisol); and the controllers are distributed throughout the pancreas and central nervous system [269]. Insulin is the main control signal, which triggers the net uptake, utilization, and storage of fuel in cells when blood insulin levels are high, and the net release and breakdown of stored fuels when insulin levels are low. The effect of increased insulin levels is a reduction in BG levels, so it is no surprise that insulin levels increase after meal ingestion. Interestingly, there is a feedforward component of insulin release that is triggered from the gut, which provides an increase of insulin levels before BG levels rise. Glucagon is released when BG levels fall too low, which causes the breakdown and release of stored fuel in the liver. The stress hormones epinephrine and cortisol are also released when BG

levels decrease below the operating point, which both act to increase the breakdown and release of fuel in the liver, skeletal muscle, and fat cells [269]. These hormones that oppose the action of insulin and raise BG levels are called glucose-counterregulatory controls.

Control theory is being used to develop treatments for a pathology in the BG control system. Type-I diabetes mellitus patients suffer from an autoimmune disorder in which the pancreatic β-cells are destroyed, effectively wiping out the main BG sensor and actuator from the BG feedback interconnection. Until recently, all type-I diabetics used insulin injections and irregular BG measurements (via finger pricks) as a surrogate for the controller, but we are now on the verge of a closed-loop mechanical system based on (nearly) continuous BG measurements and continuous infusion of insulin. Successful and safe implementation of the so-called "artificial pancreas" will be one of the crowning achievements of control theory applications, but complexities in BG dynamics, large disturbances, and significant inter- and intra-patient variability present serious roadblocks [20]. These obstacles have prompted many different approaches and controller designs for automatic BG regulation for type-I diabetics [16, 118, 199].

Control theory can also provide analysis tools for biological behavior, where decisions are made in response to environmental stimuli or conditions. This interesting perspective is covered in the next section.

1.2 Control systems in behavior

The motor control overview in the previous section alluded to an interesting application of control theory. The highest level of the control hierarchy lies in advanced brain centers which integrate sensor signals to command high-level voluntary changes in muscle movement. These commands are used to trace paths which are chosen on the basis of some performance criterion. For example, the highest level motor controller will coordinate muscles to move away a predator with a survival maximization goal, move in a straight line between two points for a distance minimization goal, or move along the path of least resistance in an energy minimization goal. Interestingly, all of these commands are the results of conscious thought, where biological *behavior* is used as "actuation" to accomplish the objective. Though lower-level control systems are involved in the execution of the chosen behavior (i.e. regulation of Ca^{2+} during muscle shortening or temporal recruitment of motor units during whole-muscle contractions [269]), the highest-level controller provides a general "plan" that the lower-level systems aim to accomplish.

For human beings, these highest-level control actions (behaviors) are typically the results of conscious thought. Information is gathered by our senses, processed in the nervous system, and integrated into the pathways that determine our behavior. Unlike many physiological control systems that operate autonomously from conscious thought, behavioral actions can often be influenced by our awake, alert state. We are therefore actively participating "in the loop" of this control system, which is an interesting departure from most control theory

applications. This means that everything that can be accessed from consciousness (and unconscious thoughts in many cases) affects the behavioral outcome to a set of environmental stimuli, which adds considerable complexity to this problem. Life histories, for example, may affect our behaviors when confronted with a particular task; a dark, forbidding path may be preferred over a sunny, well-lit path for someone who does not watch cartoons or has had positive experiences with dark paths in the past. Indeed, this complexity in behavioral outcomes is a reflection of the complexity of the brain itself– one neuron may be connected (via synapses) to as many as 2×10^5 other neurons, and there is still a great deal that is still unknown about brain function and consciousness [269].

Despite the complexities involved in conscious decision-making, the resulting behaviors are typically driven by the same objective as other biological systems: maximization of survival. Analysis of animal behavior usually adopts this paradigm of natural selection, where it is assumed that decision makers with higher survival will more heavily influence the propensities of future generations than decision makers with lower survival (see Chapter 2). Of course, since conscious decision-making is influenced by life history, survival-maximizing behavior will not always be observed experimentally. Hypothesizing that decisions are made to maximize some measure of survival is an intuitive and simple way to analyze animal behavior.

Examples of survival-maximizing behavioral mechanisms resulting from high-level decision-making include:

1. Core temperature in the human body is tightly regulated to insulate vital biochemical reactions from fluctuating external temperatures and to protect against nerve malfunction and protein denaturation [269]. Though lower-level control systems exist (shivering thermogenesis or sweating), behavioral mechanisms are used to help regulate core temperature. For example, a reduction in surface area by curling up into a ball reduces heat loss by radiation and conduction, while adding or removing clothing can decrease or increase heat loss, respectively. Choice of surroundings is another behavioral mechanism to aid thermoregulation, where a preference for shade will help protect against hyperthermia.

2. Foraging is important for solitary animals with relatively high energy expenditures, small energy stores, and periodic interruptions in feeding (e.g. small birds or rodents) [270]. Survival-maximizing behavioral mechanisms have resulted in risk sensitive foraging for animals in experimental settings. For example, if an animal is offered a choice between two food rewards where one amount is deterministic at the constant value σ, and the other is random with expected value σ, it has been observed that most animals will prefer the certain food choice when σ is large enough for survival and the random food choice otherwise [220]. These behaviors have been labeled "risk averse" and "risk seeking," respectively. Intuitively, the deterministic food choice guarantees survival when σ is large enough for survival, and the random food choice gives the animal a chance of surviving when σ is too small for survival (there is a positive probability that the realization of food is large enough for survival). See Section 7.10.1 for more details.

3. Economic theory usually assumes that survival is equivalent to monetary reward [241]. In this setting, humans seek to maximize their monetary assets by means of behavioral mechanisms (e.g. decisions based on utility maximization). Interestingly, social experiments have shown that behavior can be controlled by means of incentive or charging mechanisms. For example, traffic congestion may be reduced by charging tolls during peak commute times (reduction of monetary reward) or providing incentives during off-peak times (augmentation of monetary reward). A six-month experiment was performed in Bangalore that provided an incentive mechanism (credits in weekly lottery drawings) to reduce morning commute times, and resulted in a drop of average commute times from 71 minutes to 54 minutes [178]. The study was enthusiastically adopted by commuters, management, and Indian national newspapers, which suggests that it was successful in shaping the behavioral mechanisms of the participants.

One interesting aspect of behavioral control is the ability to qualitatively characterize the controllers. Besides claiming optimality, characterizations can be borrowed from descriptions of human decision-making. This is evident in the foraging example above, where "risk averse" and "risk seeking" are used to characterize the behaviors (and controllers) of foraging animals, depending on environmental conditions. Since behavior results from conscious decision-making, we are able to relate to these characterizations because it is easy to imagine what we would do when placed in a similar situation. When formulated correctly, these biological behavior control problems provide a fascinating interpretation of ourselves and the biological organisms with which we share the world.

1.3 General research aims

The research presented in this dissertation explores a simple biological organism from a control theoretic perspective. The intent is to characterize and gain a better understanding of its observed behavioral mechanisms. More precisely, this research aims to answer the following questions:

1. Why does a behavioral mechanism exist?
2. What is the optimal behavior under certain environmental conditions?
3. What are the characteristics of the actual, observed behavior? Is this behavior optimal?

Of course, "optimality" will depend on the biological organism and specific circumstances under which it is studied. For example, the optimal feeding behavior for a field mouse will be very different than the optimal feeding behavior for a wolf pack. Nevertheless, most behavioral mechanisms are assumed to optimize survival (which is context-specific) because of natural selection, which provides a framework of evolutionary optimality in which to perform the analysis. This allows the first two questions to be addressed in a straightforward manner, and experimental data will provide the answer to the third question.

The research platform used to address the research aims is the (relatively) well-understood bacterium, *Bacillus subtilis*. It is a model organism for laboratory studies due to its amenability to genetic manipulation [105], which has resulted in a comparatively thorough account of its behavioral mechanisms. The particular behavior mechanism examined in this dissertation is the bacterium's distinguishing ability to form an endospore under adverse environmental conditions. Though seemingly a departure from conscious decision-making, the "decision" to sporulate represents a high-level control system in the bacterium's physiology– several lower-level control systems are activated in response to the sporulation decision. Since endospore formation directly affects survival, we can examine this behavioral mechanism in the framework of evolutionary optimality to try to explain and understand the existence of this survival strategy, optimal sporulation policies in different environmental conditions, and characterizations of actual, experimental sporulation behaviors. In short, *Bacillus subtilis* provides an accessible system for which the general research goals of this dissertation can be accomplished.

The objectives of this dissertation have been examined in the context of several other biological organisms. Researchers have investigated the reasons for the existence of certain clutch sizes for birds [49, 171]; variability of hunting group numbers for African lions [117]; intense bursts of song (the dawn chorus) by many songbirds [117]; ordering of the T-cell independent immune response cascade [12]; stochastic phenotype switching in clonal populations [1, 146]; and the dependence of international relations on the characteristics of decision makers and context of the situation [172], to name a few examples. Though this is a very small sample size of related research, all of the studies in the preceding list were performed in the context of optimality, where the existence of a behavioral mechanism was the result of a reward or survival maximization problem. In many cases, the optimal behavioral mechanisms were found to be consistent with experimental observations, such as hunting group numbers for lions, the dawn chorus, and ordering of immune response steps. The experimental and theoretical consistencies in these studies, taken collectively, provide compelling evidence of evolutionary optimality in real biological systems.

1.4 Summary of contributions

Several original results were obtained while addressing the general research aims of this dissertation. These are summarized below:

1. Three population-level, phenomenological models were developed to capture the effects of the decision to sporulate. A discrete time model based on a mean-valued, growing collection of Markov chains provided the dynamics for examining a reason why sporulation has evolved. A simpler, continuous time model with food-per-growing-cell rate dependencies provided an optimal sporulation policy for a single colony, while a competing populations model provided a different optimal policy based on evolutionary stable strategies. Each model was able to capture population-level dynamical features that experimental data revealed.

2. A possible reason for the existence of sporulation was postulated based on a com-

parison to a similar survival strategy. This survival strategy, called *dormancy*, is a relatively ubiquitous strategy that offers many of the same benefits as sporulation. It was found that sporulation can confer higher fitness than dormancy in catastrophic environments, which is consistent with the morphological differences between an endospore and a dormant cell. The sporulation policy that maximized fitness in the catastrophic environment was qualitatively much more similar to experimental data than the optimal dormancy policy, which further supports the proposition that sporulation has evolved specifically to deal with extremely harsh environmental conditions.

3. The competitive exclusion principle, a classical result in resource competition theory where the population with the lowest equilibrium resource level competitively excludes another population, was shown to apply for the general competing populations sporulation model. In contrast to models typically exhibiting this principle, the sporulation model had storage-like states that were immune from death by resource limitation (endospores). Thus, the competitive exclusion principle was shown to apply to a broader class of models than previously studied.

4. An analytical method to prove the input-output stability of the competing populations model with identical birth and death rates was developed. This model was nonlinear, had equilibrium values that depended on the initial conditions, and yielded a linearized model with an eigenvalue at the origin, so the model could not be analyzed using many classical techniques. Instead, perturbation methods were used to expand the states in a power series of a perturbed variable, and it was analytically shown that the dynamics of the expansion terms were each input-output stable. This allowed the stability of the competing populations model with identical birth and death rates to be established for the class of inputs considered in the subsequent analysis.

5. The optimal policy for the competing populations model was derived and characterized. The optimal policy was derived as an evolutionary stable strategy (fitness could not be increased by adopting another strategy), and the characterization was performed in relation to a non-equilibrium policy converging towards the optimal strategy. Prospect theory was used to show that the choice of the non-equilibrium policy over the optimal policy is pessimistic during "good" times (nutrient influx increasing on average) and optimistic during "bad" times (nutrient influx decreasing on average). Since the non-equilibrium policy was qualitatively more consistent with experimental observations than the optimal policy, it may be argued that *Bacillus subtilis* exhibits optimistic and pessimistic behavioral mechanisms depending on the environmental conditions.

The general contribution of the work done in this dissertation is an example of the analysis of a biological system from a control theory point of view. This interdisciplinary approach lead to small advancements in both fields, and added to the collection of interesting research performed in this paradigm.

1.5 Dissertation organization

Chapter 2 provides biological background information on *Bacillus subtilis* and evolutionary biology. Included in the *Bacillus subtilis* background information are the signal integration network responsible for the sporulation decision, the environmental variables that affect sporulation, and the process of spore formation. The evolutionary biology background focuses on defining and measuring fitness, which are key components of natural selection and evolution. A presentation of the evolutionary optimality framework concludes the chapter.

Chapter 3 provides background on the sporulating microcolony datasets that guided the model development in this dissertation. Two of these datasets are presented and a modeling exercise on parameter estimation is shown. This provides a more natural interpretation of the datasets in terms of quantified sporulation decision policies.

A possible reason why sporulation exists (the first general research aim) is postulated in Chapter 4. Background on dormancy is provided and the first sporulation model is derived. A catastrophic environmental model is described, and evolutionary optimality is used to derive the optimal sporulation and dormancy survival strategies. The chapter concludes with some biological and experimental evidence that the proposed reason for sporulation existence is not invalid.

Chapter 5 presents the second (single population) sporulation model, which is a simpler, continuous time model. The rate dependencies are consistent with recent work on the decision to sporulate. Evolutionary optimality is again used to find the fitness-maximizing sporulation policy, which in this case is not consistent with experimental observations. This necessitates the development of the competing populations model derived in the next chapter.

Chapters 6 and 7 address the shortcoming of the single population, continuous time model. Specifically, it is shown that the optimal policy for the single population model does not produce the highest fitness under certain environmental conditions. Chapter 6 examines the competing populations model with different birth and death rates (for both populations), where it is shown that the competitive exclusion principle holds (i.e. one population becomes extinct). Chapter 7 examines the specialized case of identical birth and death rates, where coexistence between two competing populations is possible. However, this model necessitates the development of a stability analysis based on perturbation methods and an approximation of the steady state solution (since steady state values depend on initial conditions). Since fitness depends on the competing population's sporulation strategy, an evolutionary stable strategy analysis allows the derivation of the optimal strategy. Evolutionary dynamics and an environmental model are proposed, which allows a non-equilibrium strategy to be derived and compared to the optimal strategy and a broader class of risk-spreading strategies. The chapter concludes with the results of the comparisons and some possible drawbacks of the analysis.

The last chapter provides general conclusions from the research performed in this dissertation. General future research directions are suggested to complete the main body of text. Appendices A and B provide supporting material for many of the presented results.

Chapter 2

Biological Background

2.1 *Bacillus subtilis* background

2.1.1 Overview

Bacillus subtilis is a member of the genus *Bacillus*, which is one of the most diverse and commercially useful groups of microorganisms that is composed of all endospore-forming, Gram-positive, rod-shaped, straight or nearly straight bacteria capable of growing aerobically [39, 102]. *Bacillus* species are used commercially for producing enzymes, antibiotics, fine biochemicals such as flavor enhancers and food supplements, and insecticides, and are classified as "generally recognized as safe" by the FDA (though *B. anthracis* and *B. cereus* are pathogenic to humans, and *B. thuringiensis* produces an insecticide) [102]. Found almost everywhere in nature, *Bacillus* species are generally not studied in great detail due to their non-pathogenesis, which induces a lack of interest or funding [217]. This general dearth of information does not hold true for *B. subtilis*, though, which is one of the most intensively-studied and well-understood bacteria known today.

B. subtilis was discovered in 1835 (named *Vibrio subtilis* at the time), one of the first species of *Bacillus* to be characterized [39]. Primarily known for its ability to form endospores and ease of genetic manipulation, *B. subtilis* is a relatively benign bacteria with several biotechnological uses [105]. One of the enzymes it produces, subtilisin, is an alkaline protease that accounts for a large portion of the world enzyme market due to its use in detergents [97]. Other *B. subtilis* practical applications include veterinary food supplements [8, 154], probiotics [115], fermentation agents [120], and biofungicides [187].

Isolates of *B. subtilis* have been found all over the world, from deserts to the Antarctic [217]. Though difficult to ecologically classify due to endospore transport by wind [63], *B. subtilis* has been collected from a variety of different habitats. Primarily characterized as a soil-dwelling microorganism, this bacteria has been shown to vegetatively grow in soil-like conditions [190], which suggests that the soil is more than an accumulation location for windborne endospores. Indeed, many of the natural *B. subtilis* isolates studied in the literature are taken from soil samples. Found in low-organic content soils [168, 217] to nutrient-rich soils [240], *B. subtilis* can flourish in a variety of different environments. Strains have been

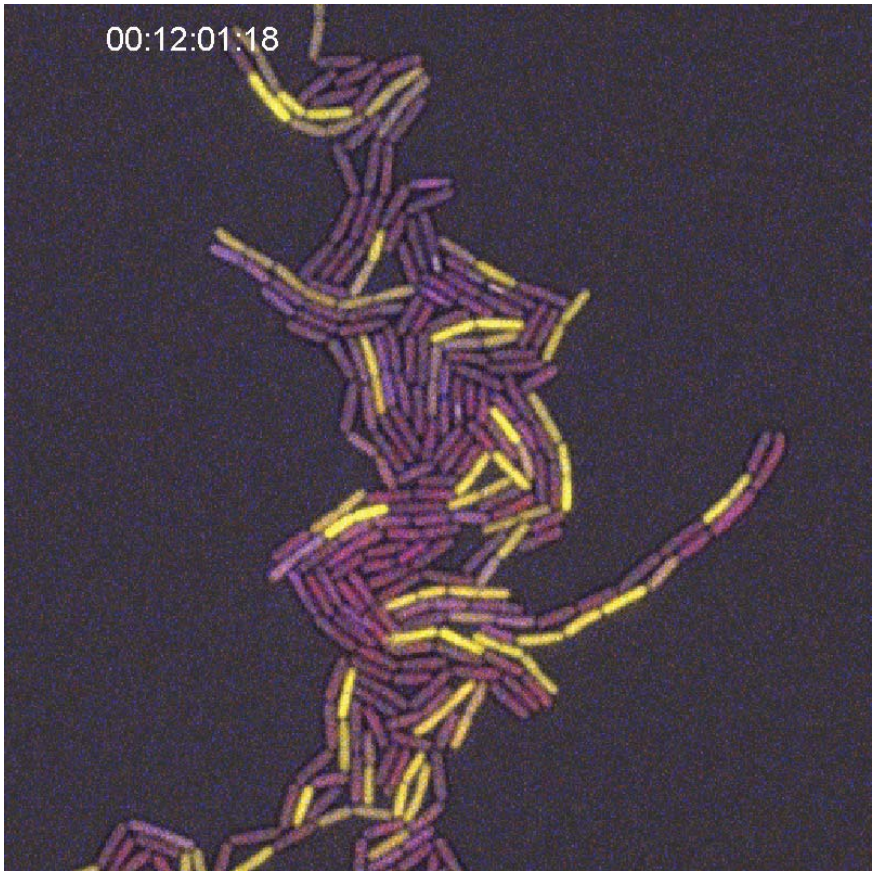

Figure 2.1: Sporulating microcolony of *B. subtilis*. The white, small objects in some of the cells are the precursors to spores. This colony was transformed to create yellow fluorescent protein when *rapA* is expressed, cyan fluorescent protein when *spoIIA* is expressed, and red fluorescent protein when *spo0A* is expressed. See Section 2.1.3 for more details.

isolated from plant root surfaces, where it is believed they have a symbiotic relationship with plants [63], and even in marine (primarily coastal) and freshwater environments [217]. Due to is pervasiveness in soil, water, and plants ecosystems, *B. subtilis* can be found in various foods such as spices, cocoa, milk, seeds, and bread [217]. This, in turn, leads to bacterial samples found in animal and human feces, though it has long been thought that the passage through the gastrointestinal tract is transient. However, recent evidence suggests that *B. subtilis* can grow and divide inside chicken, pig, and human GI tracts [8, 116, 154, 248] due to the presence of genes encoding for a respiratory nitrate reductase, which allows anaerobic growth in the presence of nitrate [63]. Given the extent of its presence, we are fortunate that *B. subtilis* is generally considered a harmless microorganism (though there have been a few cases of food poisoning and open wound infections [86]).

There is an abundance of *B. subtilis* bacteria is the research laboratory because *B. subtilis* is a model bacterial organism [105]. It is genetically and physiologically one of the most well-understood bacteria (second only to *Escherichia coli*) due to its ease of isolation and "simple" process of cellular differentiation. This differentiation process, the outcome

of which is a bacterial endospore (or spore in the sequel), has provided the richest area of research on this microorganism [102]. First observed by Ferdinand Cohn in 1876, spores are the final product of a bacterial survival strategy to protect against harsh environmental conditions (even extraterrestrial environments [188]). They are resistant to a variety of noxious treatments, which makes *B. subtilis* spores important to food-processing and sterile products industries. However useful this research may be for addressing *B. subtilis*'s more harmful relatives, the main thrust of *B. subtilis* research is the cellular differentiation process itself. Though relatively simpler than other cellular differentiation processes (e.g. human stem cells), the process of forming spores is very complex, both in its biochemistry and the mechanisms used for control [102]. The following sections provide a brief overview of this defining feature of *B. subtilis*.

2.1.2 Sporulation

Sporulation is a process where a *B. subtilis* bacterium forms a resilient, metabolically inactive, and morphologically distinct cell type that is capable of reanimation (germination) in the future [70, 109]. This event is primarily triggered by nutrient deprivation and protects against possible environmental stressors such as heat, radiation, and harmful chemicals [55, 211, 236]. Sporulation has evolved to deal with unfavorable environmental conditions, as it allows a cell to preserve its genome until favorable conditions return. Though other bacterial survival strategies exist (e.g. persistence, see Section 4.2), spore morphology suggests that sporulation is tailored to survival in extreme environmental conditions.

B. subtilis spores have special features that protect them from environmental insults; see Nicholson *et al.* for a detailed review [188]. The spore coat provides the first line of defense against harmful conditions, particularly noxious chemicals (iodine, glutaraldehyde, and peroxides), due to its relative impermeability that prevents peptidoglycan-lytic enzymes from entering the spore cortex. Further inside the spore, the reduced water content in the core protects against wet heat damage and is hypothesized to provide resistance against γ-radiation. The relatively high mineral content of the spore core (particularly Ca^{2+}) contributes to wet and dry heat resistance as well as protection against oxidizing agents. Finally, spore DNA is specifically protected by α/β-type small, acid-soluble proteins (SASP), which saturate DNA to straighten, stiffen, and shape the DNA to an α-like helix. This has been shown to protect against desiccation (dehydration), wet and dry heat, UV radiation, alkylating agents, and formaldehyde. Damaged spore DNA can be repaired during germination, where experimental studies of spores lacking DNA repair mechanisms were susceptible to desiccation, dry heat, γ-radiation, UV radiation, alkylating agents, and formaldehyde. Figure 2.2 shows the general structure of a spore. Though many of the factors involved in spore resistance and longevity are still unknown, it is clear that a spore provides a very secure storage site for bacterial DNA.

The process of spore formation is irreversible after the earliest stages are completed [198, 247]. In other words, if nutrient deprivation triggers the formation of a spore but nutrients are reintroduced during the spore formation process, the *B. subtilis* bacterium will continue to form a spore until it is finished. This will place the bacterium at a severe competitive

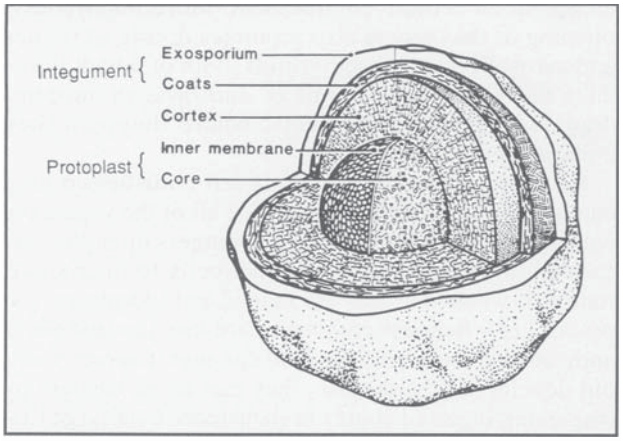

Figure 2.2: General structure of bacterial endospores, from Dragon and Rennie [53].

disadvantage against other bacteria that made the "correct" sporulation decision. Therefore, the decision to sporulate should not be taken lightly by the cell. Since the survival and competitive ability of the colony depend on making the correct sporulation decision at the right time, it is expected that a relatively sophisticated mechanism governs the decision to sporulate. This cellular mechanism, called the phosphorelay, is reviewed in the next section.

B. subtilis is not the only bacteria that is capable of forming spores. Other sporulating bacteria include: *Sporosarcina* spp., *Sporohalobacter* spp., *Sporolactobacillus* spp., *Clostridium* spp., *Anaerobacter* spp., *Desulfotomaculum* spp., *Heliobacterium* spp., *Heliophilum* spp, and other *Bacillus* spp. [188]. Table 2.1 lists some of these bacteria (as well as other organisms for the sake of comparison) and their sporulation efficiencies. This characterization describes the ratio between spores and vegetative (growing) cells in stationary phase, or during conditions that approximate steady state. Implicit in this measurement is the fact that sporulation is heterogeneous, even in an isogenic population. Though this measurement is procured at different times for different experiments, it is typically taken 24-hours after inoculation in a sporulation media. From Table 2.1, a general trend emerges regarding sporulation efficiencies: A bacterium from a nutrient-rich environment will have a low sporulation efficiency, whereas a bacterium from a nutrient-poor environment will have a high sporulation efficiency. Intuitively, an organism used to low nutrient conditions will devote more resources to spores, while an organism used to high nutrient conditions will devote more resources to vegetative growth. This general subject will be covered in more detail in Section 2.2.3.

Table 2.1: Sporulation efficiencies of other bacteria

Bacteria	Sporulation Efficiency	Specimen Origin	Measurement Notes	References
B. subtilis	58%	168 evolved 5000 generations with < 800 sporulation selection events	Exhaustion in glucose-lacking medium, 24-hr after inoculation	[167, 168]
B. subtilis	$0\% - \approx 10\%$	168 evolved 6000 generations with relaxed selection for sporulation (DSM with 1% glucose, lacking sporulation salts)	Exhaustion in glucose-lacking medium, 24-hr after inoculation	[167]
B. subtilis and *B. pumilus sensu lato*	$\approx 100\%$	Sonoran Desert basalt	Exhaustion in SSM, 24-hr after inoculation (entered stationary phase $\approx$ 5-hr after inoculation)	[17, 168]
B. subtilis	$\approx 98\%$	Dust particles on "low nutrient" spacecraft surfaces in cleanrooms ($>$ 7.7 month exposure time)	Exhaustion in SSM, 24-hr after inoculation	[166, 167, 168, 258]
B. thuringiensis	$50\% - 64\%$	Leaf surfaces of chickpea, pigeon pea, pea, and mung bean	Exhaustion in LB medium, overnight-grown culture	[137]
C. cellulolyticum[a]	0.05% – 20%, depending on chemostat dilution rate	Decayed grass[b]	Steady state conditions with different dilation rates in a chemostat	[202, 209]

continued on next page

[a] *C. cellulolyticum* has similar sporulation mechanisms as *B. subtilis* [272].

[b] *B. subtilis* is most often in vegetative form when associated with decaying organic material [63].

continued from previous page

Bacteria	Sporulation Efficiency	Specimen Origin	Measurement Notes	References
B. megaterium *B. subtilis* *B. licheniformis* *B. pumilus*	116%[a] 98.6%, 100%, 108.3%[c] 44.4%, 172.7%[b] 90%	Fecal matter and GI tract of chickens[c]	Exhaustion in DSM broth, 24-hr after inoculation	[8]
B. subtilis *Bacillus* sp.[d]	A_1 : 32.5% C : 81% H : 15.7% A_1 : 46% C : 21.3%	H layer, A_1 horizon, and C horizon in an acid forest soil[e]	Exhaustion in peptone yeast extract agar	[240]
B. subtilis CH201 and *B. licheniformis* CH200	4, 6-hr: 72% 24-hr: 12%	Vetinary dietary supplements administered orally to pigs as spores	Samples collected by killing pigs at hours 4, 6, 8, and 24; flow cytometry used to measure spore/cell counts	[154]
B. subtilis var. natto	1% 2% 25.12% 3.98% 0.13% 0.40% 15.85% 0.50% 0.40%	Nine samples from N. Thailand fermented food (Thua nao, 2-3 days of fermentation)	(not specified)	[120]

continued on next page

[a] Within the error of the method.

[b] Exhibited an extended lag phase.

[c] There is evidence to suggest that bacteria have evolved to live in gut ecosystems due to intense selection prior to the intestines [248]; GIT *B. subtilis* isolates exhibit increased growth and sporulation under anaerobic conditions than other strains, in which sporulation is highly reduced [182, 113].

[d] Including *circulans*, *subtilis*, *cereus*, *lichenformis*, *polymyxa*, *sphaericus*, *megaterium*, *firamus*, *lentus*, and *brevis*.

[e] H layer composed primarily of decomposing pine needles; A_1 horizon composed of mineral soil, decomposing leaves, and pieces of decaying root; C horizon composed of mineral soil and decaying roots/root exudates.

continued from previous page				
Bacteria	Sporulation Efficiency	Specimen Origin	Measurement Notes	References
B. subtilis: PY79 (reference) var. natto feces isolates gut biopsies	Max spore time[a]: 16-hr 7-hr 9.6-hr 11.8-hr	Human gut biopsies (ileum) and fecal samples	Exhaustion in DSM medium	[116]
B. subtilis MB24	$\approx 15\%$[b]	"Wild-type" laboratory strain (*trpC2 metC3*)	Exhaustion in DSM batch culture, $\approx$ 38-hr after fed-batch phase	[182]
S. cerevisiae[c]: Oak tree isolates Wine isolates	 100% $\approx 25 - 70\%$	North American oak trees and wine fermentations	Exhaustion in 1% potassium acetate (sporulation medium), 24-hr after inoculation	[83]
M. xanthus[d]	$\approx 2 - 5\%$	Soil samples from NY state, Greece, Minnesota, India, Japan, and Taiwan[e]	Exhaustion in CCT soft agar, 5-days after inoculation	[129]

[a]Quicker sporulation may indicate an adaptation to the GIT environment [248], and possible increased sporulation efficiency.

[b]No pH control, labeled as "spore fraction" (not efficiency) in paper

[c]Included for comparison to *Bacillus* sp.

[d]Included for comparison to *Bacillus* sp.

[e]Isolates were selected based on their ability to sporulate similarly to model strain 1622.

2.1.3 Control of sporulation: The phosphorelay

Though not understood in its entirety, each cell possesses a relatively complex cellular network that governs the important decision to sporulate [69, 109]. This genetic and protein network, called the phosphorelay, integrates environmental and intracellular signals to ensure that a cell initiates sporulation only when appropriate conditions are met. This is accomplished by activation of the "master regulator" protein Spo0A through addition or subtraction of phosphate from proteins within the relay [32, 109, 245, 254]. If a phosphate passes through the phosphorelay, the number of Spo0A$\sim$P (the activated form of Spo0A) molecules will increase until the concentration is high enough to turn on the remaining genes of the sporulation pathway. For a single cell, once the number of Spo0A$\sim$P molecules exceeds a certain threshold, sporulation is initiated [38, 78]. Figure 2.3 shows a schematic of the phosphorelay and some of the regulatory pathways that influence phosphate transfer through the signal integration network.

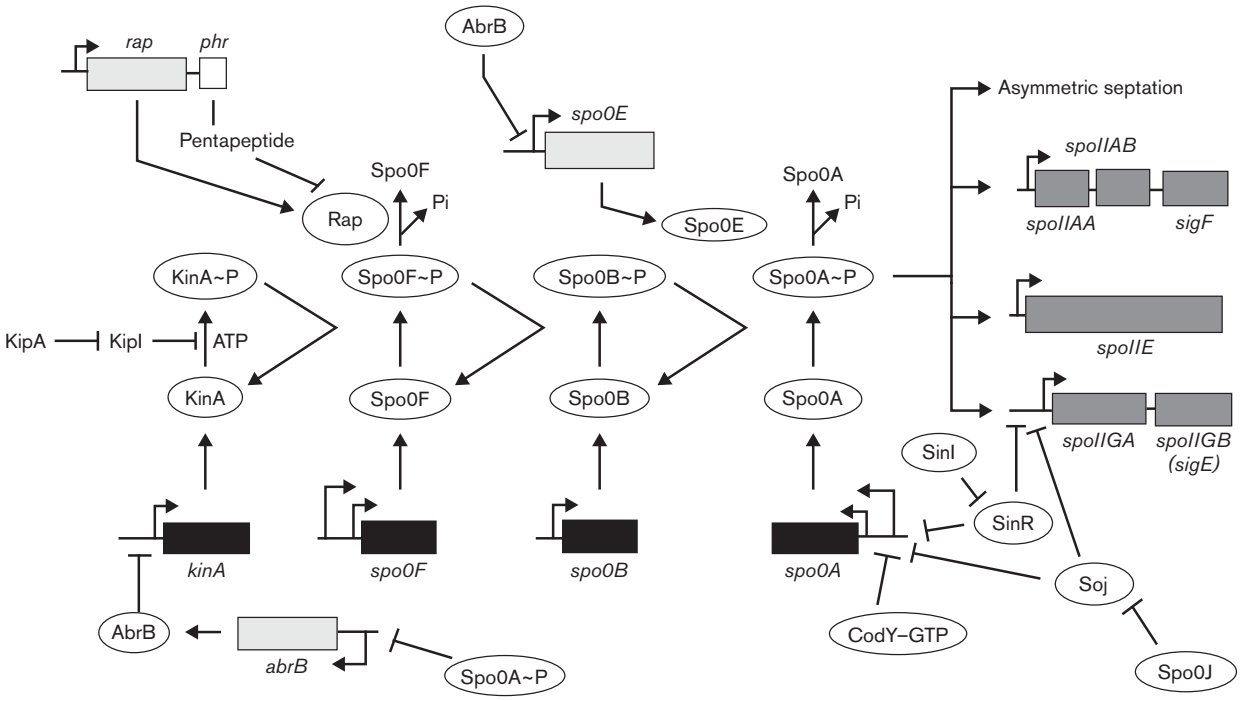

Figure 2.3: Schematic of the phosphorelay and regulatory pathways that influence sporulation, from Sonenshein [245].

Many of the experiments examining the functionality of the phosphorelay are resuspension experiments, which consist of growing cells in a nutrient-rich broth, separating the cells from the nutrients using a centrifuge, and transferring the cells to a chemically-defined media (see Section 3.2). This media is primarily nutrient-poor (though other environmental stressors may also be involved), and it has been observed that certain proteins autophosphorylate and add phosphate to the relay in response to this supposed nutrient deprivation [4, 205]. One of these proteins that is widely studied is KinA, which is postulated to act as a nutrient sensing device that increases the level of Spo0A∼P in response to nutrient limitation [32, 72, 93]. This model hypothesizes that *B. subtilis* has a mechanism that increases the propensity to sporulate when nutrient levels are diminished. Other phosphatases exist (KinB, KinC, KinD, and KinE [254]), though they have not been studied as rigorously as KinA.

KinA adds phosphate to the phosphorelay, but as mentioned above, there are also proteins that remove phosphate from the phosphorelay. One of the most well-understood of these proteins is RapA, which removes phosphate from Spo0F∼P (an intermediate protein in the relay). RapA is co-expressed with PhrA, which is a protein that is exported from the cell, processed extracellularly, and re-imported. The processed and re-imported PhrA binds to and inactivates RapA, which reduces the amount of phosphate removal from the relay [185, 203, 204, 206, 214]. Extracellular PhrA is higher around areas of high RapA-expressing cell density, which makes the RapA/PhrA system a rough population sensing apparatus. If the sub-population of RapA-expressing cells is locally high, there will be more

PhrA present, which will subsequently be imported into the cells and inactivate the RapA molecules. This will allow more phosphate to pass through the phosphorelay and activate Spo0A, which drives sporulation. Thus, high (sub)population densities will also drive the cell towards sporulation, though nutrient deprivation is also required since the phosphorelay needs a source of phosphate.

The subpopulation of the cells expressing RapA are all growing and dividing ("vegetative"). However, especially in the early stages of colony growth, not all vegetative cells are expressing RapA [24, 254]. It is not clear if imported PhrA has any effect in non-high-RapA cells since its quorum sensing role has only been studied in the context of RapA. If it is assumed, however, that the high-RapA cells are the only ones factored into the population size measurements, then the population densities used to influence sporulation is only a subpopulation measurement. However, especially after entry into stationary phase, the number of RapA-expressing cells is typically close to the total number of vegetative cells since Spo0A∼P represses *rapA* gene expression [254]. Thus, claiming that a *B. subtilis* cell knows the total number of microcolony vegetative cells may only be valid during certain periods of microcolony growth.

As mentioned before, once the level of Spo0A∼P (activated master regulator proteins) exceeds a certain threshold, sporulation is initiated. Spo0A∼P causes several regulatory proteins and sigma factors to be transcribed, which in turn regulate the expression of the genes required for the second stage of sporulation [109]. These second stage sporulation genes, collectively labeled *spoII* genes, give rise to third stage sporulation genes (*spoIII*) through an additional round of regulatory protein and sigma factor transcription. This "cascade of sigma factors" continues through six stages of sporulation until stage VII, when the spore is released [69, 95]. The progression of stages II through VII typically occurs deterministically; even if nutrients are reintroduced and population densities are dropped, Spo0A∼P remains at a high level to drive the remaining stages of sporulation. This is due to the positive feedback effects of the master regulator protein [78]. Spo0A∼P represses *arbB* and *sinR*, which repress the expression of *kinA* and *spo0A*, respectively [109, 245, 254]. Therefore, more phosphate is fed into the phosphorelay and a larger pool of Spo0A is created to absorb this phosphate, which make Spo0A∼P levels remain high. Due to this effect, genetic markers for *spoIIA* (one of the operons controlled by Spo0A∼P) are used to identify when a cell is irreversibly committed to sporulation [254]. Cell cycle and metabolic factors influence also influence the positive feedback targets of Spo0A∼P [245], which provide a stabilizing effect on Spo0A∼P levels when they are low.

2.1.4 Spore formation

Once a *B. subtilis* cell commits to sporulation, a specialized cell division takes place [71]. Instead of forming two identical daughter cells, a sporulating cell forms distinct daughter cells that act together to create a single spore. The larger daughter cell, the "mothercell," engulfs the smaller "prespore" daughter cell shortly after the division occurs in a process similar to phagocytosis [71]. These steps are mediated by the expression of the *spoII* and *spoIII* operons, which also create some transcription factors that differentiate gene expres-

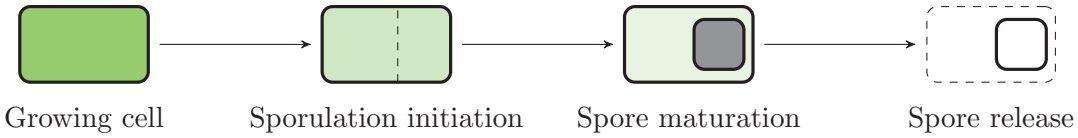

Figure 2.4: Simplified representation of spore formation.

sion in the mothercell and prespore [69]. The prespore continues to develop (core, cortex, and coat) with the help of the mothercell until it is fully mature, at which point the mothercell releases the spore by lysing (bursting). These spore developmental and lysis steps rely on the *spoVI* through *spoVII* operons and the transcription factors that they encode [69, 71]. Figure 2.4 illustrates these general steps. Mothercell lysis provides an additional source of nutrients for other vegetative cells, though the event takes place several hours after the initial commitment to sporulation [24]. Thus, the sporulation process not only reduces the number of vegetative cells that are consuming nutrients, but it also provides an additional source of food when the mothercell lyses.

In the context of sporulation, it is important to examine the ability of a bacteria cell to internally store energy. For example, if there is an overabundance of intracellular nutrient storage molecules in a *B. subtilis* cell, sporulation by environmental nutrient deprivation would almost never occur. It is known that there are nutrient storage molecules in several types of bacteria [30, 130, 239, 263, 275], but it is interesting to examine the role of these molecules in sporulating bacteria. In *Bacillus cereus*, cells that accumulate the energy storage polymer polyhydroxyalkanoate (PHA) do not have this molecule after sporulation and the degradation products are incorporated into the spore [140, 186]. It is concluded that the storage molecule is utilized during the spore formation process. In *Bacillus megaterium*, PHA-negative mutants formed more spores than the wild-type cells, suggesting that cells depleted of these intracellular energy stores commit to sporulation earlier than wild-type cells [157]. In this example, the nutrient storage molecule seemed to provide an alternative energy source when extracellular nutrients were depleted. Though neither of the experiments studied *B. subtilis*, they provide evidence that there exist intracellular storage molecules in *B. subtilis*, and these molecules may be important during the decision to sporulate. In particular, they may provide an alternative source of energy in a nutrient-poor environment or the energy required for spore formation.

2.1.5 Germination

A spore can transform into a vegetative cell after it undergoes germination and outgrowth. Germination characterizes the steps involved in the activation of spore metabolism while outgrowth refers to the macromolecular synthesis needed to convert a metabolically-active spore to a vegetative cell [235]. Since germination is irreversible, the steps involved in outgrowth will not be covered here.

Commitment to germination may occur within seconds of exposure to germinants. These are typically single amino acids, sugars, or purine nucleosides, but laboratory studies have shown that cationic surfactants, salts, high pressure, or lysozyme can also trigger germina-

tion [121, 235]. Recently, it has also been shown that muropeptide fragments of growing cell walls act as potent germinants [237, 238], which may ensure that a spore is germinated if environmental conditions allow growth for other cells. Germinants bind to germinant receptors located in the spores inner membrane [235], which trigger several steps in the germination pathway that can be grouped into two stages [235]:

1. Stage I:
   (a) Release of spore H^+, monovalent cations, and Zn^{2+} from the spore core. This raises the core pH to allow for future metabolic acitivities.
   (b) Release of the spore core's large depot of dipicolinic acid (DHA) and associated cations (Ca^{2+}).
   (c) Replacement of DPA by water. This results in an increase in core hydration and causes some decrease in spore wet-heat resistance, though it is not enough to allow metabolism.
2. Stage II:
   (a) Hydrolysis of spore's peptidoglycan spore cortex.
   (b) Swelling of the spore core through further water uptake and expansion of the germ cell wall. After this step is completed, the core is hydrated enough to allow for protein mobility and enzyme action, and hence, metabolism. This marks the cessation of dormancy.

These stages of germination do not require metabolic activity and are thought to be primarily biophysical [121, 235]. Intuitively, this situation is similar to triggering a spring-loaded mousetrap, where no energy is required to maintain the "armed" state. This allows for increased spore longevity (up to $10^5 - 10^7$ years [188]) since monitoring the environment does not require energy.

Like sporulation, the commitment to germination is heterogeneous [277]. Though the precise steps in germination commitment are not known, various factors (such as heat, germinant levels, and average germinant receptors/spore) have been shown to influence germination commitment and timing [277]. In the presence of high germinant levels that are typically sufficient to trigger germination, some spores germinate extremely slowly or not at all [84]. These spores, called superdormant spores, pose a problem with pathogenic spore-forming bacteria like *B. cereus* or *B. anthracis* because incomplete germination within a microcolony may cause antibacterial treatments to be less effective. Superdormant spores are not genetically different from other spores within the colony, since germination, outgrowth, and sporulation of superdormant spores resulted in a similar fraction of superdormant spores ($\approx 4\% - 12\%$) [84]. Because of this fact, it is postulated that stochastic variation of the number of germinant receptors or other structures necessary for germination is responsible for germination heterogeneity [84]. This is an issue related to spore formation, which emphasizes the intricate complexity of this cellular differentation process.

2.1.6 Cell cycle timing

The phosphorelay is influenced by other cellular regulatory pathways, including processes that regulate the cell cycle. It has long been observed that sporulation may only be initiated at certain times during the cell cycle; specifically, a starvation stimulus must be applied while DNA is replicating, and the peak capacity for sporulation is reached around fifteen minutes after chromosome replication has begun [48, 161]. Recently, it has been shown that a sporulation inhibitor protein, Sda, acts as a "genetic timer" that only allows sporulation during a certain part of the cell cycle [256]. This protein, which inhibits KinA's autokinase activity, reduces the levels of Spo0A∼P and is positively regulated by DnaA, a chromosome replication initiation protein [225, 264]. Therefore, Spo0A∼P levels may only accumulate when Sda levels are low, which only happens during a certain part of the cell cycle. More precisely, Sda levels are low when a cell has the correct copy number and has completed DNA replication and repair [256]. This protects spores against an abnormal number of chromosome copies and an associated decrease in spore viability. Since cell cycle timing is an important factor in sporulation initiation, a brief overview is provided below.

Control of cell cycle timing is a complex process. The typical stages of the bacterial cell cycle are divided into periods: the time between division (birth) and the initiation of chromosome replication (the B period); the time required for chromosome replication (the C period); and the time between the completion of chromosome replication and the completion of cell division (the D period) [264]. These periods most likely proceed temporally via checkpoints that depend on the other two periods [27], though it is typically accepted that a major metabolic control point for cell cycle timing regulation is the initiation of chromosome replication [279]. The rate-limiting factor in chromosome replication initiation, DnaA, unwinds certain regions of DNA at the origin of replication (*oriC*) and needs to be synthesized before a new round of replication may occur [264]. The rate of synthesis of DnaA is subject to nutrient availability through the actions of small transcription-inhibiting nucleotides collectively called (p)ppGpp [279]; higher nutrient availability leads to higher accumulation rates of DnaA (faster replication frequency), while lower nutrient availability leads to lower accumulation of DnaA (slower replication frequency). The C and D periods are usually relatively constant [264], suggesting that chromosome replication initiation is the major controller of cell cycle timing. Therefore, nutrient availability is inversely related to the cell cycle length. In the context of sporulation, which can only be initiated at certain times during the cell cycle, this implies that spore formation becomes rarer (on an absolute time scale) as nutrients are depleted.

2.2 Evolutionary biology background

2.2.1 Overview

Charles Darwin's groundbreaking work in *On The Origin of Species* can be grossly simplified to the idea of natural selection or "the survival of the fittest" [201]. This statement applies to traits, individual organisms, or groups of organisms, and intuitively means that the

best-performing trait/individual/group will endure. Darwin proposed this hypothesis after careful observation of unique animal traits that seemed to be the results of adaptation to particular environments; for example, flightless birds on isolated oceanic islands with no predators do not need to fly from danger, insects and birds susceptible to predation are colored similarly to their habitats, burrowing rodents have small eyes covered by skin and fur to protect against eye inflammation, and giraffe tails help to resist the attacks of insects (to save strength) by acting as "fly-flappers" [47]. The principle thesis is that these adaptations represent the fittest strategies under each set of environmental constraints, which suggests that they have evolved to solve certain evolutionary optimization problems. In this case, fitness maximization is the evolutionary objective and natural selection is the optimization method. Although this has not been defined with mathematical rigor at this point, the idea seems natural at its core: evolution has produced biological traits/individuals/groups that are optimally-adapted to the environments in which they developed.

In order to provide a descriptive model of the actions of natural selection, the ideas presented in the preceded paragraph must be formalized. Specifically, fitness needs to be carefully examined from a biological perspective to guide its mathematical representation, and natural selection must be dissected to provide evidence for evolutionary optimality. This section will present some background on fitness and fitness metrics, followed by the hypothesis of natural selection. A sampling of the great many mathematical studies on the survival of the fittest illustrates the utility of this framework, and the evolutionary objective used throughout this dissertation concludes the chapter.

2.2.2 Fitness

The concept of fitness or evolutionary objective is central to the theory of evolutionary biology. Fitness can be interpreted as:

- The ability to produce offspring [100];
- Future reproductive success [117];
- Viability and fertility [244]; or
- Survival, mating success, and fecundity [194].

A common theme underlying these definitions is the ability to pass genetic information to the next generation(s) in a given environment. For example, an organism is more likely to pass genetic information to the next generation if it has a high probability of surviving to adulthood, finding a mate, and producing several offspring. If any of the three probabilities are small, then the fitness of an organism will also be small. Though fitness may be applied to traits, individual organisms, populations, or species [9, 117], in each case, the general concept of passing genetic information to the next generation applies. Natural selection favors high relative fitness, and it is easy to imagine evolution as solving an optimization problem where fitness for a particular environment is maximized (see Section 2.2.4).

Though the idea of fitness is clear, measuring fitness is not. This makes the idea of "maximizing fitness" ambiguous because the ability to pass genetic information to the next

generation in a given environment can be quantified differently for even a single experiment. The following methods of measuring fitness have been widely used:

- Probability of surviving to adulthood [117];
- Expected number of offspring [210, 244];
- Probability of survival relative to the highest survival probability in the environment [194];
- Dominant Lyapunov exponent [145, 146, 160, 179]; and
- Expected growth rate of the population (for both continuous and discrete models) [44, 169, 171, 194].

For a rapidly-reproducing population, fitness is often measured as number of progeny or growth rate [152, 208, 213]. A generational time scale is almost always used for these fitness measurements [29], so the fitness of a trait, organism, population, or species is defined for a specific generation. This is consistent with defining fitness as the ability to pass genetic information to the next generation(s) in a given environment. For example, the fitness of an adult organism may be the expected number of offspring it produces that are able to survive to adulthood, or it may be some multiplicative factor of viable offspring number to fertile parent number. The fitness may also be defined as the expected number of grand-offspring it produces that are able to survive to adulthood, or some multiplicative factor of the ratio between viable grand-offspring and fertile parent number.

There has been some debate pertaining to the appropriate horizon length for defining an evolutionary objective. Should we only look at the fitness measurement one generation into the future? Or, should we look several generations into the future? Some researchers have argued that a longer-term measure of fitness is more appropriate in an evolutionary setting, such as a million or ten-million years [249] or the expected time to extinction [42]. Others have argued that a short term fitness measure is more realistic because it relates adaptedness to the process of natural selection; that is, long term measures fail to explain how the process of natural selection can be sensitive to differences in long term fitness measurements of surviving offspring [29, 244]. In other words, selection has no foresight: unless long term fitness is directly correlated with short term fitness, there is no way that the success of distant generations will affect the ability of the current generation to transmit genetic information. On the other hand, a long term fitness metric may be more appropriate when examining an evolutionarily-optimized organism because its fitness has been maximized since the origin of its existence. For the evolution of survival strategies in particular, long term fitness is able to deal with species extinction. This becomes important in the context of environmental uncertainty, where long term fitness measurements can illustrate the tradeoff between offspring number and probability of extinction [43, 210].

2.2.3 Natural selection and evolution

An introductory explanation of the theory of evolution and natural selection can easily require several hundred pages, so this section will focus on providing some evidence that

adaptation is the process of (nearly) maximizing fitness by natural selection. The basic mechanisms of natural selection and a brief review of optimality results in various fields of biology will be covered in the sequel.

Natural selection is the differential survival and reproduction of entities that differ from one another in one or more respects [79]. There are two major components of this definition: genetic variability and selection pressure. Genetic strategies are heritable, so high-fitness characters beget high-fitness offspring. Variability at the genetic level (imperfect heredity) is needed to explore deviations from the parents' strategies, where selection pressure weeds out the poor-performing strategies and lets the best-performing strategies flourish. After each iteration of heritable changes and selection pressure, the fittest traits/individuals/groups increase in frequency relative to the less-fit strategies, until "survival of the fittest" is realized.

$$\left.\begin{array}{lcl} \text{Genetic changes} & \rightarrow & \text{Heritable changes} \\ \text{Environmental interactions} & \rightarrow & \text{Selection pressure} \end{array}\right\} \Rightarrow \text{Natural selection}$$

Genetic variability and selection pressure are necessary for natural selection [79]. Without heritable changes, it is possible for fitness to decrease with each generation, and without selection pressure, fitness may not increase. These two critical components are examined below.

Mechanisms of genetic variability

Adaptation by natural selection relies on genetic inheritance, the primarily accepted method of passing information to future generations. "Information" in this context refers to the factors that affect an organism's ability to survive and reproduce, such as the growth of specialized appendages, the ability to eliminate competition, or (in the case of *B. subtilis*) the development of decision-making genetic networks. All of these genetically-inherited traits are realizations of the expressions of genes, which are portions of DNA that give rise to particular proteins/enzymes/protein-assembly machines. A single gene will encode a single protein or enzyme via the "central dogma" of molecular biology: DNA is transcribed to RNA (messenger, ribosomal, or transfer) which is then translated to proteins or enzymes [2]. These proteins and enzymes are the building blocks and machinery used to fabricate an organism and its ability to survive and reproduce, and are used in everything from organic structures to biological propensities to behave a certain way [151]. This is readily apparent in an embryo of an animal: a mixture of DNA is inherited from the parents that directs, through the expression of genes to form proteins/enzymes, the observed characteristics of the offspring. This genetic inheritance is consistent with the fact that offspring resemble their parents, and is traditionally considered the most important factor in determining biological fitness since genetic makeup largely dictates how an organism develops and behaves.

If genes affect the phenotypes (observed characteristics) of an organism, then differences in genetic makeup (genotype) between two organisms will lead to differences in fitness be-

tween the two organisms. Differences in genotype may arise from a multitude of sources, though the most commonly studied source is sexual reproduction. Discussion of the details of sexual reproduction, such as meiosis, dominant and recessive genes, and chromosomal crossing over, is not completely relevant for an asexually-reproducing organism like *B. subtilis*, but the basic idea is that each parent donates different regions to the complete DNA of the offspring [269]. The genes of the next generation will therefore be a combination of the genes from the previous generation and may therefore bestow higher (and lower) fitness measurements than the parents' generation. The genetic diversity resulting from sexual reproduction is very large compared to the diversity resulting from binary fission (the type of asexual reproduction found in *B. subtilis*), since the parent DNA is simply replicated and the daughter cells (offspring) each receive an identical copy. Though it may seem that genetic homogeneity is the only possibility in asexually-reproducing species, some organisms have developed strategies to promote genetic diversity such as the development of natural genetic transformation (competence) in bacteria. This event, typically occurring after the onset of stationary phase in microcolony growth, allows horizontal gene transfer by the uptake of the extracellular DNA resulting from the death of other cells [56, 94]. Other horizontal gene transfer mechanisms include conjugation (transfer of genetic material through direct cell-cell contact) and transduction (injection of foreign DNA by a bacteriophage) [158]. In addition to sexual reproduction or horizontal gene transfer, genetic variation may also result from random mutations of cellular DNA or errors during chromosomal replication (though the resulting phenotypes most likely have lower fitness [171]), which allow novel genes to be introduced into the population. However, horizontal gene transfer plays the most important role in bacterial genetic diversity [63]. Whatever the dominant method of genetic variability, the end result is a heritable diversification of phenotypes and fitnesses for each generation.

In addition to genetic inheritance, some information may be passed to future generations in other forms. Though not as significant in determining phenotype as genetic inheritance, one example is extranuclear inheritance. Besides parental DNA, other parts of the parent cells may be inherited to the offspring. In sexual reproduction, for example, the ovum contains other cellular organelles in addition to maternal DNA. Some organelles, such as mitochondria and chloroplasts, have DNA that replicates independently of nuclear DNA [23]. The offspring therefore receives information from the mother that is not coded into the DNA of the offspring (recall that the offspring DNA is from both the mother and father). This phenomenon is apparent in several cases, such as identical egg color in genetically-different hen offspring, identical shell coil orientations in pond snail offspring not necessarily resembling their mother's, and the inheritance of altered cilia on the surface of the protozoa *Paramecium* [171]. A more controversial way that an acquired characteristic may be passed to future generations is by selectively-increased alterations to an organism's DNA. Experiments have suggested that an organism lacking an essential gene for survival will increase directed mutations until the gene is recovered [33, 141], indicating that there is an indirect way for the environment to alter DNA. Phenotypic differences can therefore be also attributed to factors that are non-genetic in origin.

Regardless of the way in which phenotypic differences occur, each distinct phenotype will give rise to a specific fitness measurement. These differences in fitness are the means

by which adaptation occurs.

Selection pressure

A population of organisms with different fitness measurements in a constant environment will likely be eventually composed of those organisms that increase the population's average fitness. Given enough time, the population's average fitness will often be nearly maximized [117, 194]. This is because a high-fitness organism will typically be descended from high-fitness parents. Though easy to see for asexually-reproducing organisms, this makes sense even for sexually-reproducing organisms. Assuming high-fitness DNA sequences at a particular locus do not vary dramatically from other high-fitness DNA sequences at the same locus, combinations of genes producing high fitness are likely to produce an organism with high fitness. Although phenotypic variability still results when two high-fitness organisms sexually reproduce, the expected fitness of the offspring will likely be higher than the fitness of an offspring from two low-fitness organisms (it has been proposed that evolution has rendered the more-favorable genes dominant [75]). These high-fitness members of the population will consequently be more viable and fertile than the relatively low-fitness members, which will eventually lead to the elimination of the subpopulation harboring the less-favorable genes. Higher-fitness organisms will always eventually replace lower-fitness organisms from our definition of fitness, so the population's fitness level will always be non-decreasing; indeed, as Darwin stated in *On The Origins of Species*, "The larger and more dominant groups thus tend to go on increasing in size; and they consequently supplant many smaller and feebler groups" [47]. Given enough time, a finite fitness metric, a large population, and a constant environment, this process of adaptation will tend towards a (possibly local) maximal average fitness for the population [192, 197].

The simplistic description given above proposes that the average fitness for a population will always be non-decreasing, but this is not necessarily true. Though non-decreasing average fitness may seem to logically follow from the preceding arguments, it does not explain how some organisms exhibit decreased fitness over time [194] or how some may gradually become extinct (for example, the gradual extinction of several vertebrates during the Upper Permian period of the Paleozoic Era [265]). These facts seemingly contradict Ronald Fisher's Fundamental Theorem of Natural Selection, which states "The rate of increase in fitness of any organism at any time is equal to its genetic variance in fitness at that time" [74], thus implying that fitness is always non-decreasing. The theorem, as stated, is true in the semantics and context in which it was stated [73, 216]; however, it does not imply that the population's *average* fitness is always non-decreasing. The theorem refers to the partial change in a single organism's fitness due to selection and does not take the (possibly) detrimental effects of mutation or environmental changes into account (note that extinction events can usually be attributed to environmental changes) [64, 212]. If, however, we can assume that the effects of disadvantageous mutations are negligible and the environment is constant, then the Fundamental Theorem of Natural Selection may be approximately true for a population's average fitness. Assuming that the mutation rate is similar in *B. subtilis* as it is in *Drosophilia*, a single mutation will affect approximately one cell for every

240 cells produced [75]. Combined with the facts that some mutations are beneficial and only 272 genes (of ≈ 4100) are essential in *B. subtilis* [139], detrimental mutations in *B. subtilis* cannot be concluded to be significant in its evolution. The environment in which the bacteria usually resides in the wild (see Section 2.1.1) may be approximated as constant if the time scale for ecological change are long compared to the generational time scale for *B. subtilis* (of course, we are ignoring any adverse affects that overcrowding may impinge on the environment). Thus, it may be possible to assume that the population's average fitness has been non-decreasing for *B. subtilis* during the course of its evolution, which would imply that its fitness has been nearly maximized. Even without the assumptions of negligible detrimental mutations and a nearly constant environment, it is not unreasonable to claim that the bacteria's fitness is nearly maximized due to its ubiquity in the wild and its relatively sophisticated decision-making processes.

The description of adaptation given above fits into the framework of an optimization problem, even without the mutation and environment assumptions. The cost function is the fitness metric, the decision variables are genotypes giving rise to different phenotypes, and the constraints model the interactions between phenotype, environment, and fitness. The optimization problem is solved using a non-descent method (assuming the population's average fitness always increases) or some randomized algorithm (assuming the population's average fitness may decrease) [159]. The random optimization implementation adds the original gene sequence to random gene vectors drawn from the distribution resulting from inter-generational genetic variability, and the highest-fitness gene sequence (possibly excluding the original seed if each generation produces offspring only once) is assigned the starting point for the next iteration. Adaptation can be roughly visualized using the "adaptive topography" description provided by Wright [194, 273], where a multidimensional field of discrete gene frequencies produces a fitness surface that is shaped by the constraints. The non-descent method provides a way to climb the hills of this surface, while the random optimization method proceeds in the direction of steepest ascent from the set of random gene vectors (this may result in a descent direction that lowers fitness if there does not exist a gene vector that increases fitness). Figure 2.5 provides a visualization of this "hill climbing" algorithm, where possible local maxima are present. Though the adaptive topography idea is now widely disregarded due to mathematical inconsistencies [64], it provides an intuitive way to argue that the fitness is at least locally maximized when evolution is allowed to proceed for a long time. It has been shown that some biological systems do not attain the maximum fitness values, but these may be due to environmental variation (which changes the fitness landscape), finite time, or inability of genetic combinations to achieve the maximum value [197, 207].

The optimization problem becomes more complex when competition is involved, since the fitness associated with a genotype will depend on the genotypes of other organisms. Though it is possible to model competition as environmental constraints in the problem, it is commonly approached using evolutionary stable strategies (ESS) which rely on mathematical techniques from game theory [170]. The genetic strategy for an ESS typically does not correspond to the same genotype that would be obtained with simple fitness maximization, though organisms not utilizing the ESS always have lower fitness [197]. Thus, when

dealing with organisms that evolved while facing severe competition, special care must be taken in the examination and assumptions of optimal behavior. Background information on ESSs and their relationships to optimal policies are given in Section 7.7.1.

Examples

Several examples have been examined that show the optimality of certain observed characteristics in the wild. The Great Tit bird has been shown to lay the number of eggs that maximizes the fitness of the offspring by artificially increasing or enlarging the clutch size [49], and other species (swifts and starlings) most commonly lay the number of eggs that gives the greatest number of survivors [171]. The optimal clutch size is dependent on the environment, and the ability to adjust clutch size annually is an adapted trait; for example, the Great Tit can adjust the sizes of its first and second broods according to the predicted food supply in the future [85]. Other bird examples include the explanations of songbird behavior at dawn and the foraging behavior of small birds in the winter as solutions to optimization problems [117].

The vertebrate immune response has also been shown to be optimal [12]. Specifically, the instantaneous antibody production rate is maximized by allocating the large lymphocyte population among 1) proliferation to more lymphocytes (which secrete some antibodies), 2) differentiation to plasma cells (which secrete a lot of antibodies), and 3) differentiation to memory cells (which have surface antibodies and guard against future infections from the same antigen). The authors take a "cybernetic" approach to solving this optimization problem and show that the temporal ordering of the lymphocyte allocation in mice (proliferation→plasma cells→memory cells) is optimal. They also show that the increase in memory cell production and decrease in response time is consistent with the solution to the optimization problem.

The cellular heat shock response has also been shown to be nearly optimal in *Escherichia coli* [66]. When the temperature rises above the normal operating temperature in a cell, essential proteins become misfolded or unfolded, which results in the failure of the cellular

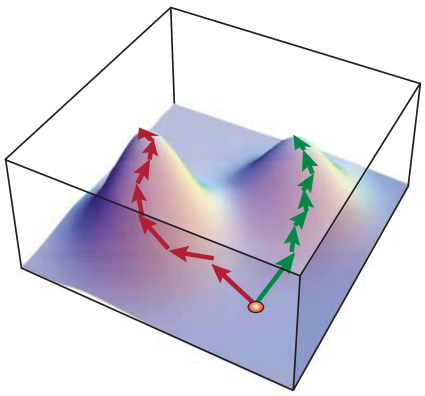

Figure 2.5: "Fitness landscape" visualization of adaptation, from Elena and Lenski [67].

networks in which they operate. Most cells have evolved heat shock proteins to 1) refold and reorganize misfolded proteins and 2) destroy damaged proteins in order to survive temperature increases. Since the cost of creating heat shock proteins may be large relative to the detrimental effects of misfolded proteins, there is a trade off between producing large quantities of heat shock proteins and minimizing the number of misfolded/damaged proteins. By varying a weighting parameter between the L^2 norms of the number of misfolded proteins and the number of heat shock proteins, the authors showed that the wild type norms nearly coincide with the optimal solution for a particular value of the weighting parameter.

2.2.4 Fitness maximization problem

With fitness quantified and an argument for natural selection presented, we are ready to state the problem that underlies our evolutionary optimal framework. In some form or another, it is the same as every other evolutionary biology-inspired mathematical study of biological systems [91, 170, 197]. The evolutionary optimal framework provides an intuitive and simple foundation in which to study evolved traits, where a behavior exists solely to accomplish an evolutionary objective. Though there are serious critiques of this framework [58, 90, 218], it provides a plausible starting point for the study of natural biological organisms.

Sporulation is a prime candidate for examination in the framework of evolutionary optimality. Since it results from a genetic network, it is heritable and can be optimized after several rounds of selection. In this case, selection pressure is exerted by competitors and the environment, where poor sporulation strategies are dominated by more fit strategies after several rounds of selection. With the typical microbial fitness measurement of offspring in the future [152, 208, 213], sporulation "parameters" $\mathbf{u}^*$ can be assumed to be selected so

$$\begin{aligned} \mathbf{u}^* = \arg\max_{\mathbf{u}\in\mathcal{U}} \quad & \text{(offspring in the future)} \\ \text{s.t.} \quad & \text{(system dynamics)} \end{aligned} \tag{2.1}$$

where the constraints depend on the chosen sporulation model. Chapters 4–7 solve this problem under various circumstances in an attempt to provide a formal study of sporulation in a mathematical framework.

Chapter 3

Experimental Data

3.1 Introduction

The qualitative biological background in Chapter 2 may elucidate a suitable structure for a sporulation model, but quantitative data is needed to verify that the proposed model is able to capture the general behavior of the biological system. A good candidate model structure will be able to explain the quantitative data with a reasonable choice of model parameters; on the other hand, a bad candidate model will require biologically-unreasonable values for model parameters to explain the data, if at all. Data is especially valuable for biological systems, where modeling may help to corroborate or discover novel findings. For example, Alan Hodgkin and Andrew Huxley used data to hypothesize the existence of voltage-gated ion channels in a giant squid axon. This was confirmed several years later and won them the 1963 Nobel Prize in Physiology or Medicine [110, 189].

The research in this dissertation is fortunate to have access to experimental *B. subtilis* sporulation data from the Arkin Laboratory for Systems and Synthetic Biology. As a member of the *B. subtilis* group, I was able to observe experimental procedures and supervise some data processing and analysis for experiments devoted to the study of the sporulation decision process. Though the experimental conditions did not necessarily correspond to the assumed environmental conditions in this dissertation, the data was able to guide the model developments in Chapters 4–7.

Two experimental datasets are presented in Section 3.3 after a rough description of the experimental conditions in Section 3.2. Though I processed data for several more experiments, the two experiments exhibited in this chapter correspond to the most complete datasets. This data is analyzed in the context of a very simple Markov model for a single cell in Section 3.4. Parameter identification is performed for the Markov model parameters, which are used as a verification source for subsequent models in this dissertation.

3.2 Experimental conditions

Sporulation, one of the most well-known stress responses for the model organism *B. subtilis*, has been the focus of numerous studies. There are standardized procedures used to

make a microcolony of *B. subtilis* sporulate effectively [103], most of which involve nutrient limitation as the primary stressor. Sporulation resuspension experiments, where a colony is grown and transferred to a nutrient-poor media that promotes sporulation, allow the stress response to be examined using time-lapse fluorescence microscopy imaging. The general experimental setup and conditions we used are described below.

3.2.1 Experimental setup

Common to most sporulation protocols is the induction of sporulation by nutrient limitation. "Nutrients" can be defined as the chemicals that trigger sporulation when they are scarce. These essential chemicals are carbon (energy source), nitrogen (protein/amino acid building blocks), and phosphorus. The medium upon which sporulation occurs should be limited in at least one of these three chemicals. Different methodologies for inducing sporulation were developed to be "most effective" at producing nice experimental results for particular strains of *B. subtilis*, so it is unclear which of the three chemicals acts as the sporulation-inducing nutrient [103].

In the experiments done in Arkin Lab, cells are grown in "growth medium" (GM), which is a chemically-defined medium (i.e. known composition) with enough nutrients for growth. After reaching a certain optical density, some cells are resuspended in a nutrient-poor medium. The nutrient-poor medium is made up of Sterlini-Mandelstam medium (SM), which contains "sporulation salts" that promote sporulation, and a little bit of GM. Experimentalists have found that residual GM introduced into the SM-GM mixture does not interfere with subsequent sporulation [103], meaning that the control over initial nutrient concentrations may not be tightly regulated. Some of the same batch of SM-GM is combined with agarose (agar) to make gel pads, and once the gel construction and resuspension are complete, some of the cells are squirted on top of the gel pad. The gel pad is then rotated around to allow a more even distribution of cell solution, after which it is inverted onto a microscope slide container. At this point, many of the bacteria are in a monolayer between the agar pad and container boundary. The container is then sealed to prevent moisture from escaping. Figure 3.1 shows the experimental environment during data collection.

The experimental protocol calls for the SM-GM to be well mixed. This suggests that the carbon/nitrogen/phosphorus concentrations are relatively uniform throughout the solution. Therefore, the liquid that is introduced with the cells onto the gel pad should have a relatively uniform distribution of nutrients, though as mentioned before, the initial nutrient level may be variable from experiment to experiment. On the other hand, it is hard to conjecture about the nutrient makeup of the gel. It is unknown if the nutrient distribution changes while crosslinks are formed in the gel, and this is probably very difficult to verify on the order of the size of the bacteria ($\approx 2\mu$m). However, it is probably safe to assume that the nutrient distribution in the gel is also initially uniform, simply because a better hypothesis is not available.

Another issue related to the nutrients in the gel is diffusion. The data shows that cells initially have enough nutrients to sustain exponential growth, after which sporulation occurs (as evident in Figures 3.8 and 3.13, where the cell cycle times become shorter before getting

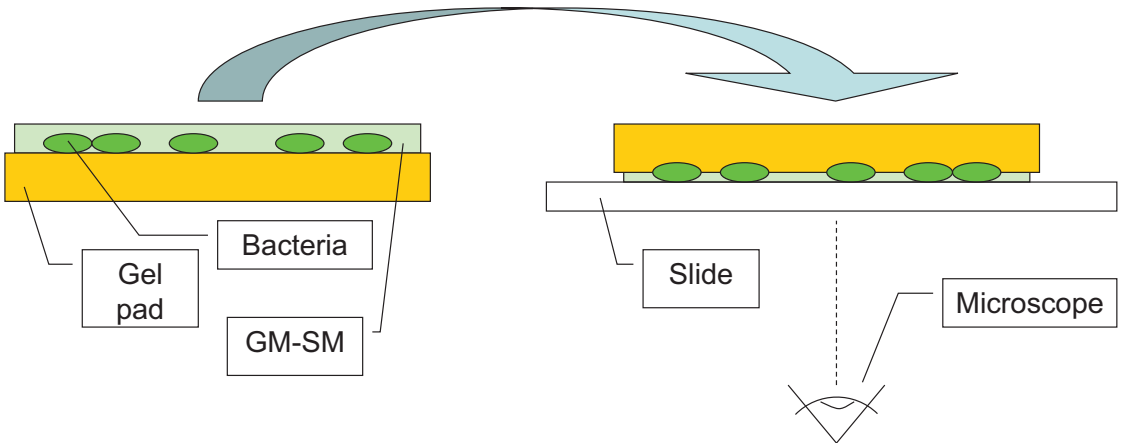

Figure 3.1: Experimental setup during data collection.

longer). This implies that the nutrient availability eventually goes down since spores form at locations with different cell densities. This also implies that the diffusivity of nutrients through the gel pad is not very high, or else the bacteria would almost never run out of nutrients (the gel pad is 0.5 mm thick, so there is a large nutrient reservoir). Estimates of diffusivity of glucose in some gels are available ($\sim 10^{-10}$ m^2/s [3]), which are still quite high considering the length scales of the experiment. The problem with low diffusivity of nutrients through the gel arises when a spore is released: if the nutrients cannot travel very quickly through the gel, then the spatial effects of mothercell lysis nutrient distribution should not be ignored. However, one may argue that the nutrients are also released into the SM-GM liquid that was introduced when the cells were inoculated, which would have a higher diffusivity for the nutrients than the gel. It is difficult to conclude the validity of ignoring spatial effects either way, but for the sake of simplicity, it will be assumed that the experimental conditions yield a homogeneous spatial distribution of nutrients.

In essence, there is no quantitative information about nutrient levels during the experiments. Qualitatively, the best description is a nutrient-poor medium.

After the colony is resuspended and mounted in the microscope, spatially-isolated bacteria are found to ensure that the resulting microcolonies are isogenic. The locations of several candidate points are recorded in a microscope camera motion-control program, and these points are revisited every 15 minutes for 2-3 days. A digital camera (Photometrics CoolSNAP HQ^2) is used to record the microscopy images at a pixel resolution of 512×512. The room that houses the microscope is temperature-controlled and the microscope is insulated from vibrations using an anti-vibration table.

3.3 Data

The experimental data comes from time-lapse microscopy videos of sporulating colonies of *B. subtilis* with fluorescence proteins tied to the expression of key genes in the sporulation pathway. These videos are automatically processed and manually checked/processed to seg-

ment (identify) cells that are growing/dividing. Once the prespore appears in the mothercell (this time does not correspond to when a cell commits to sporulation), segmentation stops for that cell. A cell's lineage is constructed from tracking software after manual processing, so individual cells can be tracked and the segments give average (over the area of the cell) fluorescence intensity versus time for each track. From these tracks, several time series can be extracted, which include the numbers of vegetative cells, spores, and dead cells.

Some examples of the raw data for two different experiments are given in Figures 3.2 and 3.3. Experiment 090731 was initiated on July 31, 2009, and experiment 090810 started on August 10, 2009. The experimental procedures were identical.

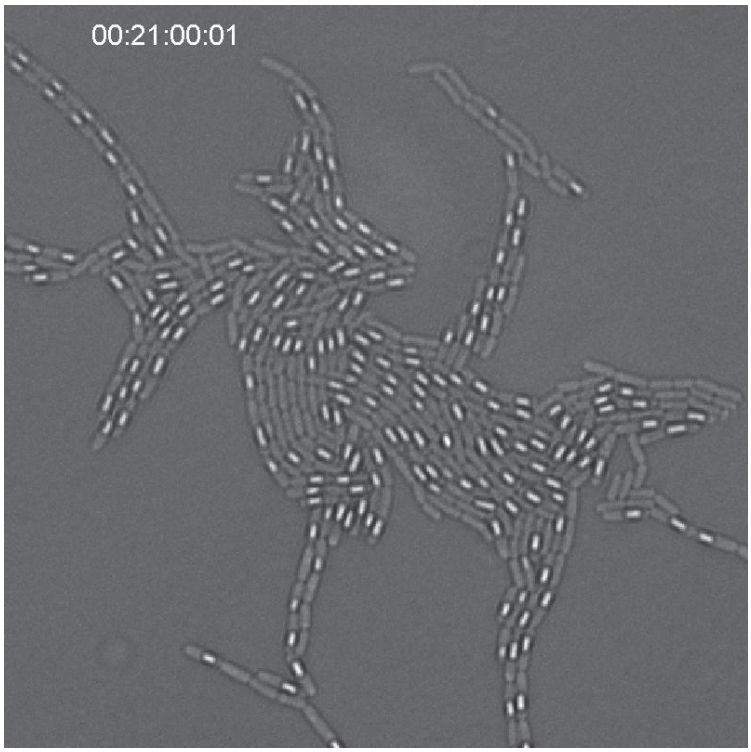

Figure 3.2: Example of raw data for experiment 090731.

Though it may be easy to distinguish between the cells and background in Figures 3.2 and 3.3, it is difficult to implement an algorithm to automatically segment an experimental movie. Though automatic segmentation packages exist, they are designed for movies of cells that are much easier to segment (large cells with high background/foreground contrast) [35, 61, 234]. None of them proved to be effective for segmenting our experimental findings, so an imaging processing/segmentation/manual correction program was created in Matlab to process the data. Most of the programming was done by Dr. Ilka Bischofs, and will not be covered in this dissertation. Though effective for some movies, the adopted segmentation package typically required ≈ 40 hours of manual corrections. A much more effective segmentation package has been developed by my colleague, Gavin Price, and will be released shortly.

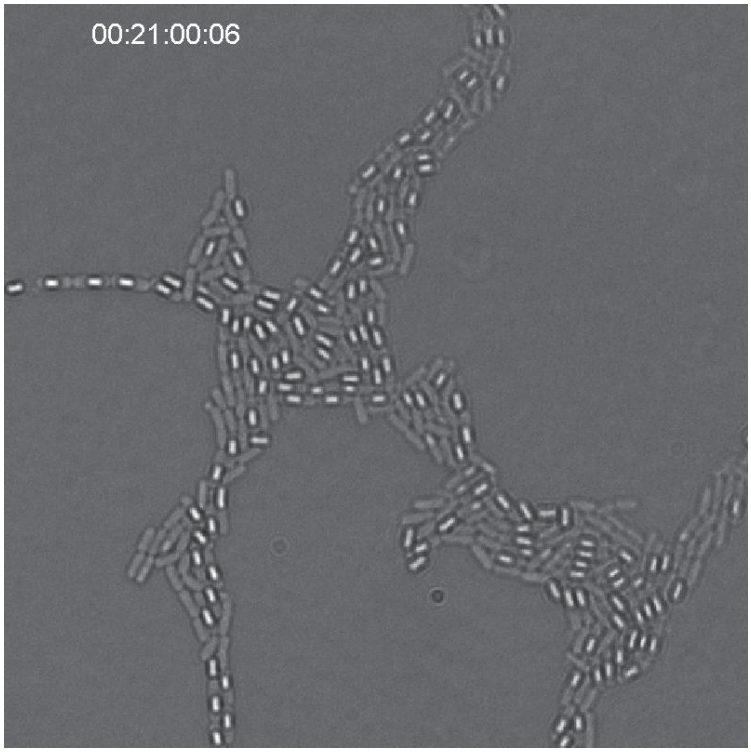

Figure 3.3: Example of raw data for experiment 090810.

After segmentation, the numbers of vegetative cells and dead cells versus time can be plotted. Additional data sets for the numbers of cells making the decision to sporulate and cells committed to sporulation can also be obtained, though this is not directly observable from the data (see Section 3.4.3). Average cell cycle times can also be computing, indexed at the beginning of each cell cycle. These data sets are given in Figures 3.4 – 3.13 for experiments 090731 and 090810.

3.4 Exercise: A simple Markov model interpretation of the data

3.4.1 Overview

This section will outline a parameter estimation exercise for a simple model based on a set of assumed operating modes for *B. subtilis* during nutrient limitation. The purpose of this exercise is to gain quantitative information about bacterial behavior, especially the decision to sporulate. Some of the results of this exercise will be used later in this dissertation to test the validity of theoretical conclusions.

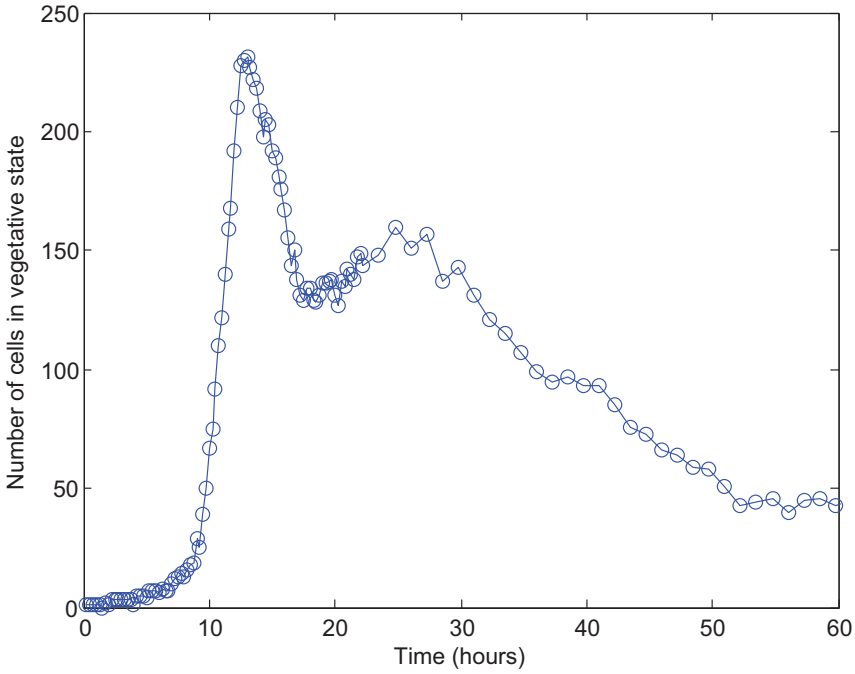

Figure 3.4: Number of vegetative cells for experiment 090731.

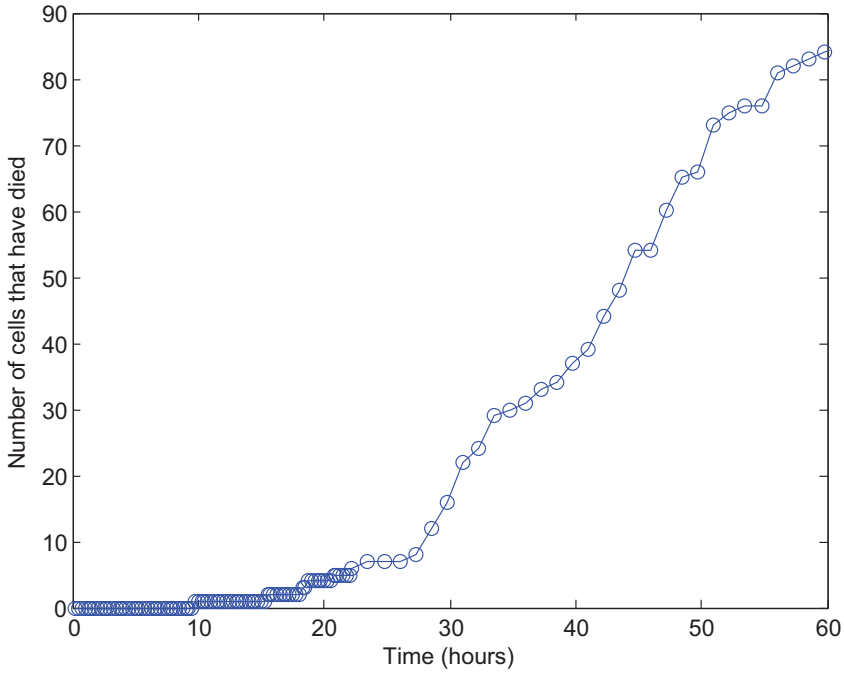

Figure 3.5: Number of dead cells for experiment 090731.

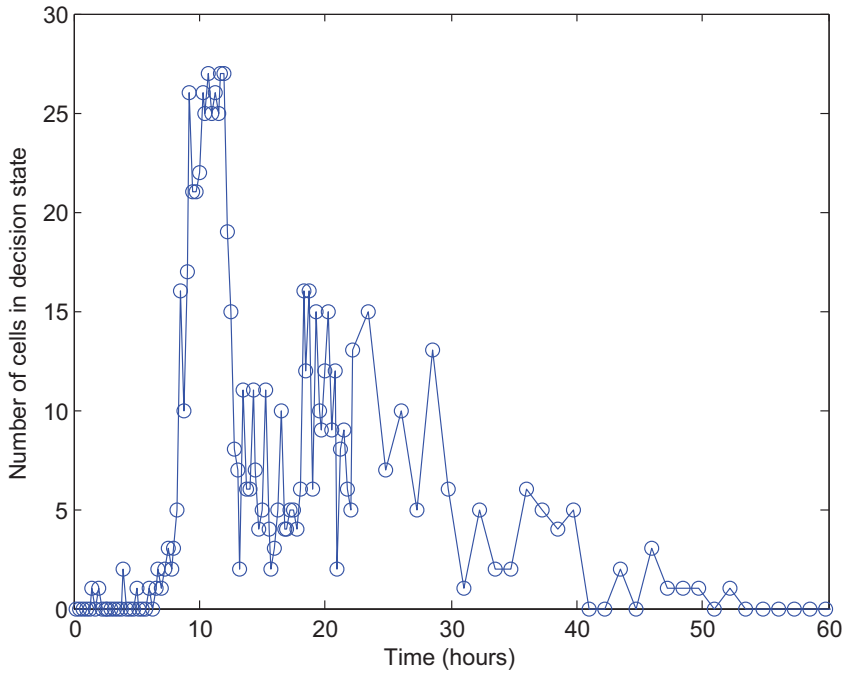

Figure 3.6: Estimated number of decision cells for experiment 090731.

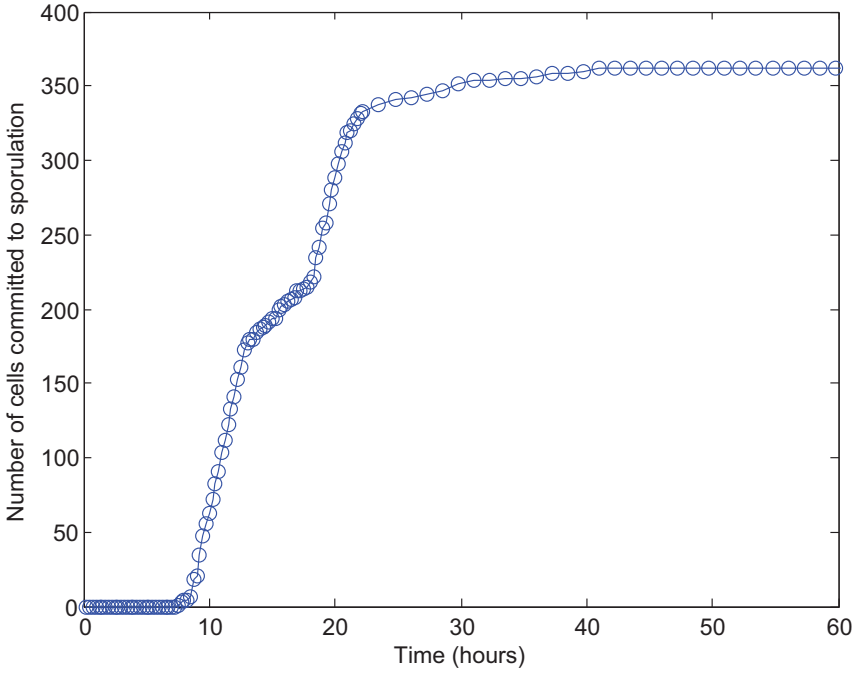

Figure 3.7: Estimated number of cells committed to sporulation and spores for experiment 090731.

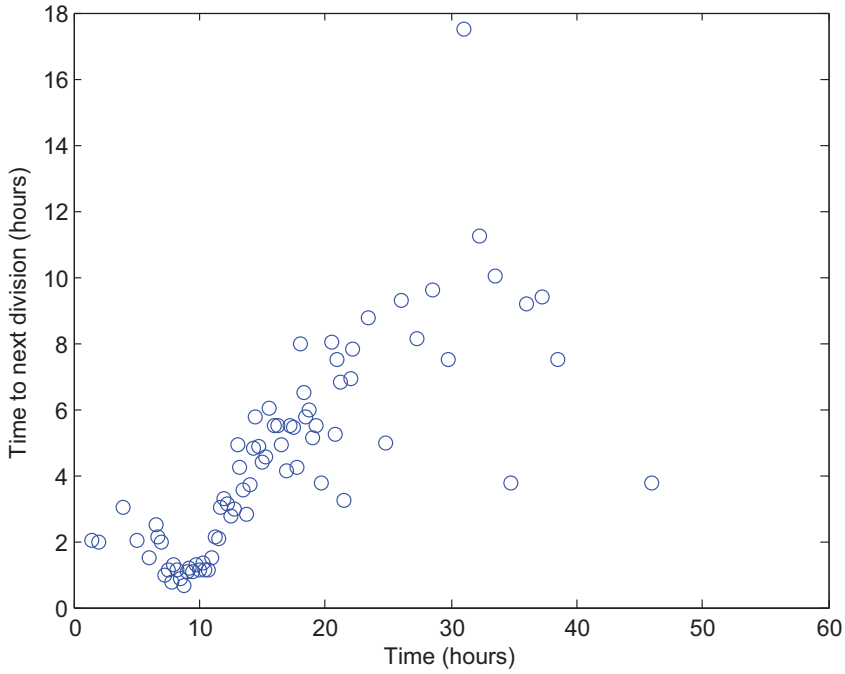

Figure 3.8: Cell cycle times for experiment 090731.

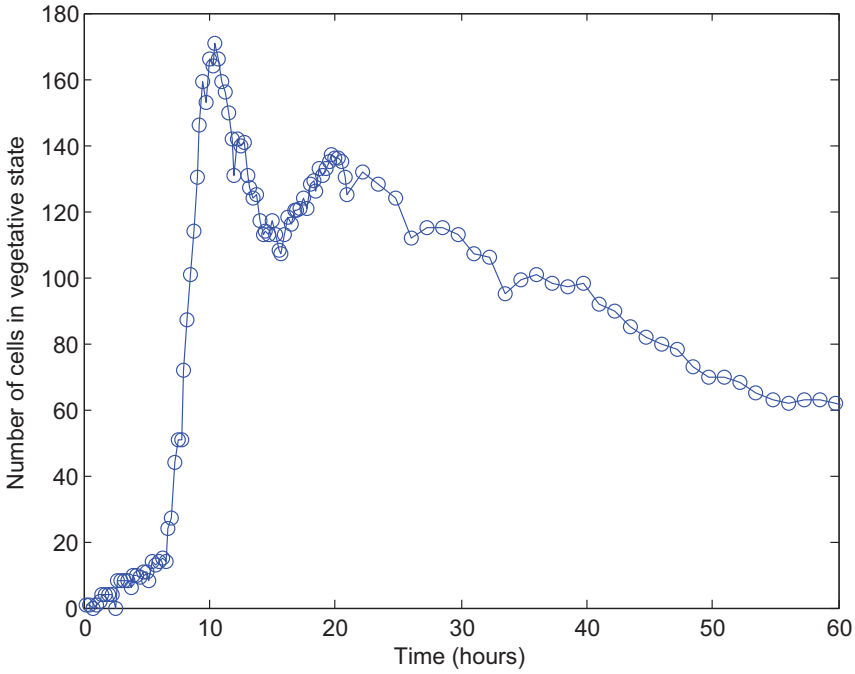

Figure 3.9: Number of vegetative cells for experiment 090810.

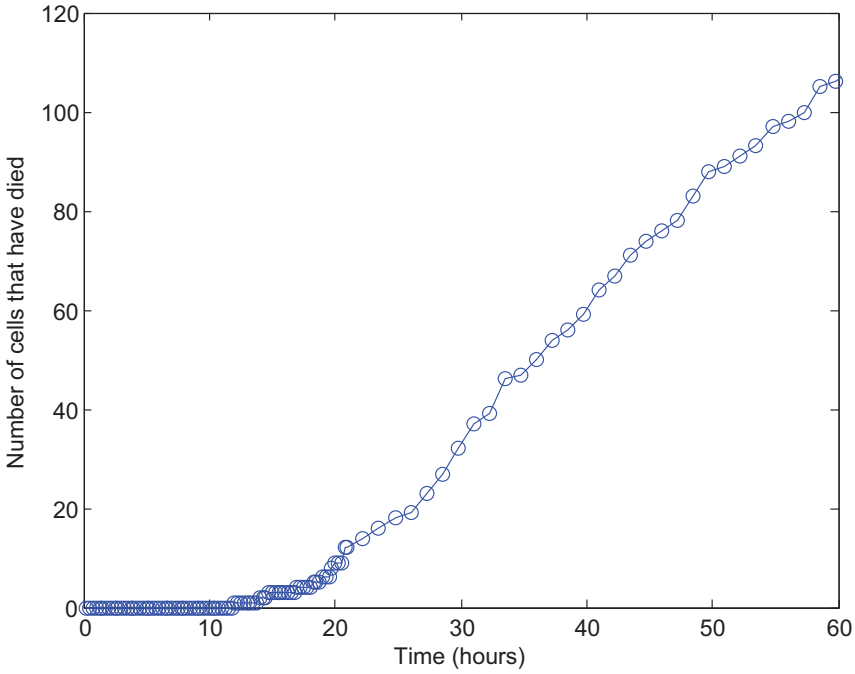

Figure 3.10: Number of dead cells for experiment 090810.

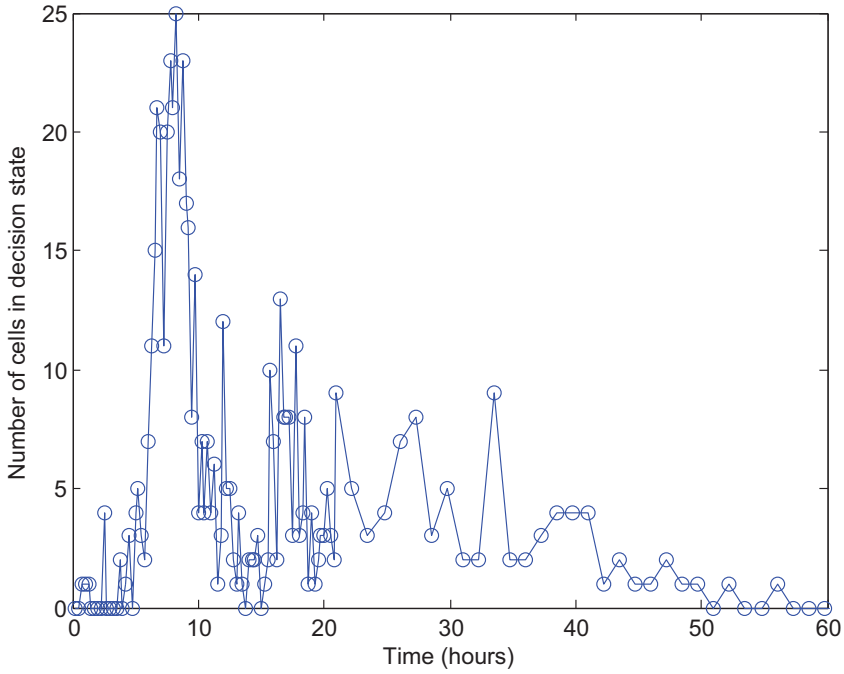

Figure 3.11: Estimated number of decision cells for experiment 090810.

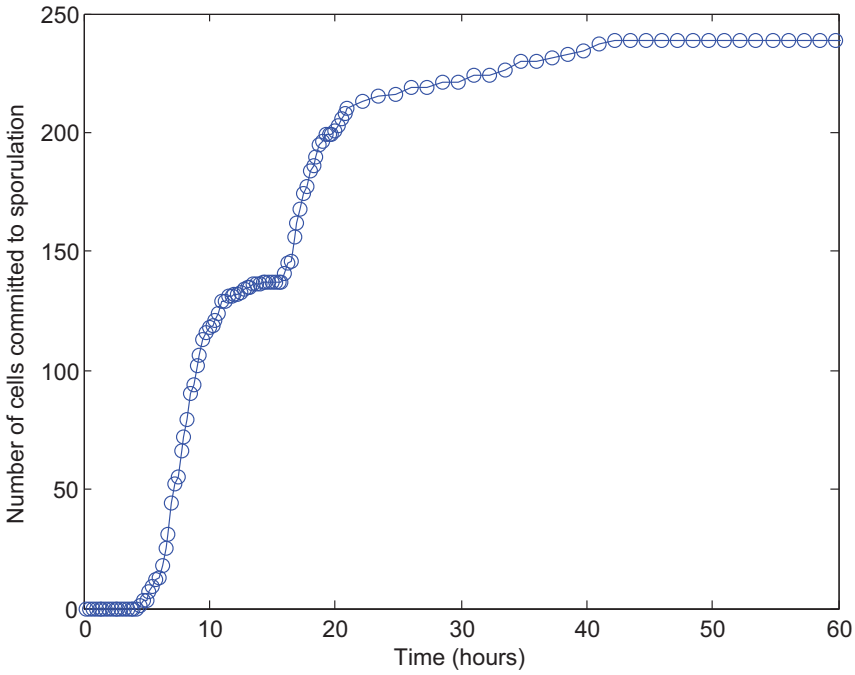

Figure 3.12: Estimated number of cells committed to sporulation and spores for experiment 090810.

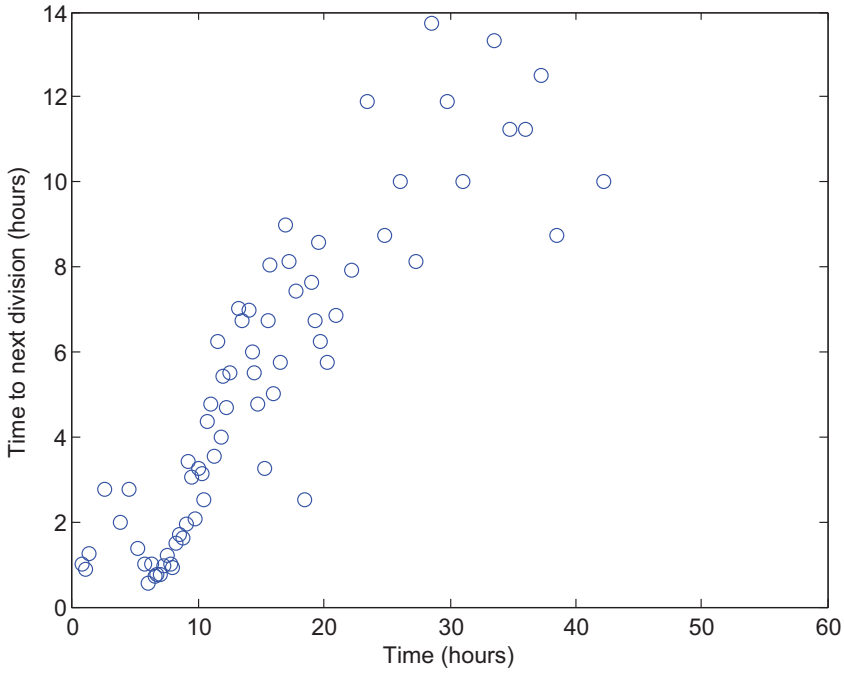

Figure 3.13: Cell cycle times for experiment 090810.

3.4.2 Model

The actual system that governs the decision to sporulate, the phosphorelay, is very complex and interconnected. Using a first-principles model to describe the sporulation decision is not possible; capturing the important dynamics will lead to high order, nonlinear systems [24] which are impossible to corroborate with data because of the many unknown parameters and difficulty in manipulating inputs into the phosphorelay. Therefore, instead of starting with a complicated, detailed model to examine the control policies in the decision to sporulate, a simplified, phenomenological model for *B. subtilis* will be used that treats the phosphorelay as a black box that processes inputs and returns control actions. The model, depicted in Figure 3.14, assumes that each cell is operating in one of five modes ($death$ = cell is dead; V = vegetative growth; D = decision mode; C = committed to sporulation; and S = fully mature spore). These modes were chosen because they can be observed from the data[1].

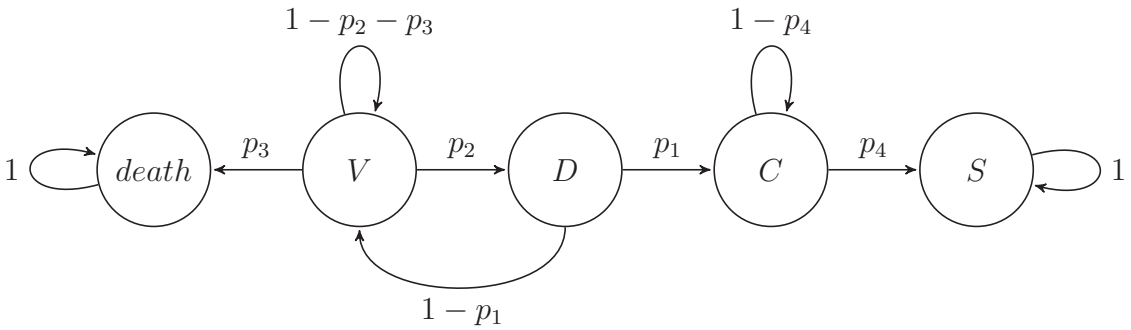

Figure 3.14: Markov model for a single cell.

When a single cell transitions from mode D to mode V (continuing to grow/divide), another copy of the Markov model is created for the new offspring. The parameter p_3 reflects the nutrient availability and other adverse environmental conditions.

The cell cycle time is characterized by the variable p_2, and the decision to sporulate shows up in the variable p_1. Modeling the decision to sporulate as a probability has been adopted in at least one other study [230]. The decision to sporulate takes place only at the end of the cell cycle in my model, which is consistent with the fact that the decision to sporulate only occurs within a certain period of the cell cycle [161, 256].

Cell cycle times change during the course of microcolony development. Researchers have observed that the two daughter cells from a single parent cell are more likely to form spores as a pair rather than separately [48, 257]. Since the decision to sporulate takes place only during a certain period of the cell cycle, the cell cycle times for both daughter cells must be similar. Therefore, it is assumed that the cell cycle parameter p_2 for both daughter cells is chosen by the parent cell while it is in mode D. Similarly, the parent cell also chooses the spore maturation parameter p_4 while in decision mode D since one may view spore formation as a specialized form of cell division [108]; in other words, after the division to

[1]The transition into mode "committed to sporulation" is estimated for the collected data because the prespore appears several hours after sporulation is initiated.

produce mothercell and prespore, a cell cycle with only one period takes place. Though not as well-studied as the phosphorelay, there is a brief review on the cell cycle timing decision in Section 2.1.6.

A simpler model would have lumped the C and S modes together since there is no return from committing to sporulate under our experimental conditions. However, since nutrient release from mothercell lysis presumably influences the vegetative cells, the model needs to keep track of the transition from committed to sporulation, to spore release.

Another simpler model would have no *death* mode since there are relatively few deaths that occur during the course of the resuspension experiments. However, the *death* mode must be present because it is essential to understand the trade-off between the decision to grow or sporulate. For example, suppose there was no *death* mode and a *B. subtilis* cell was in decision mode at time t. Maximization of "fitness" would mean choosing $p_1 = 0$ and $p_2 = 1$, which is clearly not consistent with a wild-type *B. subtilis* sporulating microcolony phenotype. A cell may only transition into *death* from V because it may spend a long time in V, and it does not actively choose to die (so it is not accessible from mode D). This mode is also not accessible from C because it is not possible to distinguish between cells transitioning to *death* from C or V.

3.4.3 Parameter estimation

The bacteria chooses p_1 through the phosphorelay, and there is evidence to support that p_2 and p_4 are also chosen since the processes that they influence fluctuate during the experiments. These parameters, which change in response to environmental conditions, are therefore the control parameters/policies for nutrient-deprived *B. subtilis*. We are interested in estimating these parameters from the data so we can analyze a bacterium's behavior in the framework of the model presented in the previous section.

The data naturally lead to examination of the number of cells in each operating mode as a way to extract useful information about the probabilities. Rough estimates of some of the probabilities can be obtained using the number of cells in each operating mode and some information about the cell tracks. These numbers are realizations of random variables since the underlying system is assumed to be stochastic. In the sequel, let $X_{death}(t)$ be the random variable (RV) representing the number of cells in *death* at time t; $X_V(t)$ be the RV for the number of cells in V at t; $X_D(t)$ be the RV for the number of cells in D at t; $X_C(t)$ be the RV for the number of cells in C at t; and $X_S(t)$ be the RV for the number of cells in S at time t. The (non-normalized) population distribution at time t can be described by the vector $X(t) := \left[\begin{array}{ccccc} X_{death}(t) & X_V(t) & X_D(t) & X_C(t) & X_S(t) \end{array} \right]^T$.

Since the prespore appears several hours after the cell commits to sporulation, only estimates of the number of cells in D and C can be constructed at a given time. Specifically, the number of cells entering C at time t is the number of prespore appearances at time $t+T_C$, where T_C is the time between commitment to sporulation and prespore appearance. The number of cells in mode D at time t is the number of cell divisions between t and $t+1$, plus the number of new commitments to sporulation at time $t+1$. It will be assumed that $T_C = 4.5$ hours is known in the following analysis [24], though this is likely to be violated

during later parts of the experiments (see Sections 3.4.3 and 3.4.4).

The number of cells entering S is difficult to observe from the videos because mothercell lysis events are typically difficult to detect when cell densities are high.

Problem formulation

Assume that at time t, a bacterium in the decision mode chooses and fixes $p_1(t)$, $p_2(t)$, and $p_4(t)$. These values will be constant for this particular bacterium until it chooses them again (the next time it enters D, if at all). Assume also that the time scale of environmental effects is much smaller than the sampling time, which means that we can ignore spatial effects and that global cell number measurements (from extracellular Phr molecules, for example) have no delay. This implies that every cell in mode D at time t will choose the same numbers for their individual $p_1(t)$, $p_2(t)$, and $p_4(t)$. A point of emphasis is that the probabilities for each *B. subtilis* cell are only chosen each time it enters D, so it may be possible that the microcolony may be composed of individual cells with entirely different probability parameters at a particular time during stationary phase.

This fact is important because the expected population distribution $m_X(t) := \mathbb{E}\{X(t)\}$ cannot be easily written as $m_X(t+1) = A(p_1(t), p_2(t), p_3(t), p_4(t))m_X(t)$ since there are a whole bunch of different choices for $p_1(t)$, $p_2(t)$, and $p_4(t)$ floating around in the colony. Again, this is due to the asynchronous entry into mode D.

Estimating the probability of sporulation $p_1(t)$

Based on the model described in Figure 3.14, the conditional probability mass function of the random variable $\Delta_C(t) := X_C(t+1) - X_C(t)$ given $X_D(t)$ is

$$\Pr\{\Delta_C(t) = \delta_C(t) | X_D(t) = x_D(t)\} = \begin{pmatrix} x_D(t) \\ \delta_C(t) \end{pmatrix} p_1(t)^{\delta_C(t)}(1-p_1(t))^{x_D(t)-\delta_C(t)}.$$

The likelihood of the data $(\delta_C(t), x_D(t))$ is

$$\begin{aligned}\mathcal{L}(\delta_C(t), x_D(t)) &= \Pr\{\Delta_C(t) = \delta_C(t), X_D(t) = x_D(t)\} \\ &= \Pr\{\Delta_C(t) = \delta_C(t) | X_D(t) = x_D(t)\} \Pr\{X_D(t) = x_D(t)\}.\end{aligned}$$

Since the system is causal, $\Pr\{X_D(t) = x_D(t)\}$ is not a function of $p_1(t)$.

The maximum likelihood estimate (MLE) for $p_1(t)$ based on the data $(\delta_C(t), x_D(t))$ can now be easily found to be:

$$\hat{p}_1(t) = \frac{\delta_C(t)}{x_D(t)}.$$

It can be verified that, under the distribution implied by the model in Figure 3.14, this estimate is also unbiased. Is it also easy to verify that the statistic δ_C is a complete sufficient statistic for the family of distributions conditioned on $X_D(t) = x_D(t)$, which implies that $\hat{p}_1(t)$ is the uniform minimum variance unbiased estimator of $p_1(t)$ [150]. This estimator is also asymptotically efficient (it has the minimum mean squared error between the estimate and the actual parameter as the sample size $x_D(t)$ goes to ∞), which can be verified by comparison to the Cramér-Rao lower bound.

Estimating the cell cycle parameter $p_2(t)$ and death probability $p_3(t)$

Preliminaries and assumptions As mentioned in Section 5.2, the cell cycle parameter $p_2(t)$ is chosen when the cell is in mode D and held fixed until the next time (if any) the cell is in D. In other words, suppose that a cell chooses its sporulation probability, cell cycle parameter, and spore maturation parameter at time Z_1. The parameters $p_1(Z_1)$, $p_2(Z_1)$, and $p_4(Z_1)$ are held fixed until the next time the cell enters D. So, the cell cycle time will have a *constant* parameter $p_2(Z_1)$ in its Markov chain even though the current time t may be greater than Z_1.

The death probability, on the other hand, varies continuously with time since it reflects the environmental effect of nutrient consumption and depletion. To make the analysis easier, we can make the assumption that the cells consume nutrients on a first come, first serve basis, so the nutrient availability at the *beginning* of the cell cycle is what determines the probability of death. This may be plausible, for example, if each cell imported nutrients only during the beginning of the cell cycle. This is most likely not representative of what the physical system is doing, but it allows for much easier calculations. It will therefore be assumed that $p_3(t)$ is constant throughout the cell cycle, and only changes for a single cell upon entry into mode V.

This approximation will break down when the probability of death is relatively high. If a significant fraction of the cells are dying while in V, the number of cells consuming nutrients may dramatically fluctuate with time. For example, if 90% of the population dies while in V and the cell cycle time is very large, then we would expect that the probability of death should decrease as the population is dwindling. This is because the nutrient-per-cell level is increasing, which intuitively should lead to higher survival rates. Under this condition we will require a different parameter identification approach than the ones given in Sections 3.4.3 and 3.4.3 since $p_3(t)$ is no longer constant for a single cell during its cell cycle.

Since $p_2(t)$ is assumed to be constant throughout the cell cycle, other events taking place around the cell do not influence the cell cycle timing. This assumption simplifies our analysis because certain random variables become independent (see next section).

Estimating $p_2(t)$ and $p_3(t)$ Suppose that at time $t+1$, $\Delta_V(t)$ cells enter mode V with fixed parameters $p_2(t)$ and $p_3(t)$. Of these $\Delta_V(t)$ cells, some may die and the remaining will transition to mode D. These numbers are realizations of random variables representing the number of cells that move to D, L_D, and the number of cells that die, L_{death}. Notice that, under the model in Figure 3.14, $L_D + L_{death} = \Delta_V(t)$. The distributions for L_D and L_{death} are binomial with parameters $\frac{p_2(t)}{p_2(t)+p_3(t)}$ and $\frac{p_3(t)}{p_2(t)+p_3(t)}$, respectively, but these will not help much with the identification of the probability parameters (we can only get an expression for the ratio of the parameters because, conditioned on knowledge of $\Delta_V(t)$, the distributions are dependent on one another). We can, however, look at realizations of the random variable governing the exit time from V for each cell to extract more useful information from the data.

A cell in mode V can either go to D or to *death*. Denoting the random variables for exit

time to D and *death* as T_D and T_{death} respectively, the possible realizations are:

$$T_D = \begin{cases} t_D & \text{with prob. } (1-p_2(t)-p_3(t))^{t_D-1}p_2(t) \text{ for } t_D \in [1,\infty) \\ z_1 & \text{with prob. } \frac{p_2(t)}{p_2(t)+p_3(t)} \text{ for } z_1 \notin [1,\infty) \end{cases}$$

$$T_{death} = \begin{cases} t_{death} & \text{with prob. } (1-p_2(t)-p_3(t))^{t_D-1}p_3(t) \text{ for } t_{death} \in [1,\infty) \\ z_2 & \text{with prob. } \frac{p_3(t)}{p_2(t)+p_3(t)} \text{ for } z_2 \notin [1,\infty) \end{cases}$$

where realizations of z_1 for T_D corresponds to the event in the sample space when the cell dies (and vice versa for z_2). Now, suppose that we have $\Delta_V(t)$ cells entering mode V and L_D of them transition to D while L_{death} of them transition to *death*. The L_D cells transitioning to D will have realizations of $T_{D,i} = t_{D,i} \neq z_1$ and $T_{death,i} = z_2$ for $i = 1, \ldots, L_D$. Since $T_{D,i} \neq z_1 \Rightarrow T_{death,i} = z_2$,

$$\Pr\left\{T_{D,i} = t_{D,i} \cap T_{death,i} = z_2\right\} = \Pr\left\{T_{D,i} = t_{D,i}\right\}.$$

The same can be said about the remaining probabilities for the L_{death} cells that die. Since it is assumed that cells transitioning away from mode V do not affect the timing of the cells currently in mode V (implying independence of the exit times for the $\Delta_V(t)$ cells), the likelihood of the data $\mathcal{D} := (t_{D,1} \cap z_2, t_{D,2} \cap z_2, \ldots, t_{D,L_D} \cap z_2, z_1 \cap t_{death,1}, \ldots, z_1 \cap t_{death,L_{death}})$ is:

$$\begin{aligned} \mathcal{L}(\mathcal{D}) &= \prod_{i=1}^{L_D} (1-p_2(t)-p_3(t))^{t_{D,i}-1} p_2(t) \prod_{i=1}^{L_{death}} (1-p_2(t)-p_3(t))^{t_{death,i}-1} p_3(t) \\ &= (1-p_2(t)-p_3(t))^{\sum_{i=1}^{L_D} t_{D,i} + \sum_{i=1}^{L_{death}} t_{death,i} - L_D - L_{death}} p_2^{L_D} p_3^{L_{death}}. \end{aligned}$$

The log-likelihood is concave in the parameter vector $\begin{bmatrix} p_2(t) & p_3(t) \end{bmatrix}^T$, so we can maximize the log-likelihood to get MLE estimates for the probabilities. For notational convenience, define $\alpha_1 := \sum_{i=1}^{L_D} t_{D,i}$ and $\alpha_2 := \sum_{i=1}^{L_{death}} t_{death,i}$. The maximum likelihood estimators are:

$$\hat{p}_2(t) = \frac{(\alpha_1+\alpha_2-L_D)L_D - L_D L_{death}}{(\alpha_1+\alpha_2-L_{death})(\alpha_1+\alpha_2-L_D) - L_D L_{death}}$$

$$\hat{p}_3(t) = \frac{(\alpha_1+\alpha_2-L_{death})L_{death} - L_D L_{death}}{(\alpha_1+\alpha_2-L_{death})(\alpha_1+\alpha_2-L_D) - L_D L_{death}}$$

These estimators are biased. For example, the relatively common occurrence when $L_D =$

$\Delta_V(t)$ and $L_{death} = 0$ yields

$$\begin{aligned}
\hat{p}_2(t) &= \frac{L_D}{\sum_{i=1}^{L_D} t_{D,i}} \\
\mathbb{E}\left\{\hat{p}_2(t)\right\} &= \mathbb{E}\left\{\mathbb{E}\left\{\left.\frac{L_D}{\sum_{i=1}^{L_D} t_{D,i}}\right| L_D\right\}\right\} \\
&> \mathbb{E}\left\{L_D \frac{1}{\mathbb{E}\left\{\left.\sum_{i=1}^{L_D} t_{D,i}\right| L_D\right\}}\right\} \\
&= \mathbb{E}\left\{L_D \frac{p_2(t)}{L_D}\right\} \\
&= p_2(t)
\end{aligned}$$

by Jensen's Inequality. The corresponding estimate for $p_3(t)$ is 0. This is a lower bound on the actual parameter, since $p_3(t) = 0.001$ for $\Delta_V(t) = 10$ would likely yield $L_D = 10$ and $\hat{p}_3(t) = 0$.

An alternative method to estimate $p_2(t)$ and $p_3(t)$ It may seem natural to view the arrival times from V as events in a Bernoulli process, where the exit from V is governed by the probability $p_2(t)+p_3(t)$ (the probability that a cell exits V at each time). This Bernoulli process then splits to arrivals in D or *death*, which leads to a new Bernoulli process for the arrivals in D or *death*. Parameterizing these processes can be found as follows:

$$\begin{aligned}
\Pr\left\{\text{arrival from } V\right\} &= p_2(t) + p_3(t) \\
\Pr\left\{\text{choose } D | \text{arrival from } V\right\} &= \frac{p_2(t)}{p_2(t) + p_3(t)} \\
\Pr\left\{\text{arrive at } D\right\} &= \Pr\left\{\text{choose } D \cap \text{arrival from } V\right\} \\
&= \Pr\left\{\text{choose } D | \text{arrival from } V\right\} \Pr\left\{\text{arrival from } V\right\} \\
&= p_2(t).
\end{aligned}$$

Thus, the process describing the arrivals at D has a probability of success $p_2(t)$, and the probability of success for arrivals in *death* can be found similarly to be $p_3(t)$. Denoting the inter-arrival times for D as $T_D^{\mathcal{B}}$ and using the assumptions in the previous section, we can estimate $p_2(t)$ by the (biased) maximum likelihood estimator

$$\hat{p}_2(t) = \frac{L_D}{\sum_{i=1}^{L_D} t_{D,i}^{\mathcal{B}}}$$

where L_D is the total number of arrivals at D for the cells that enter V at time $t+1$. A similar estimator can be found for $p_3(t)$. Notice the effort in making the distinction between T_D and $T_D^{\mathcal{B}}$, because these random variables are *not* the same: T_D represents some of the interarrival times (the ones that "choose" D) for the original Bernoulli process parameterized

by $p_2(t) + p_3(t)$, while $T_D^{\mathcal{B}}$ represents the interarrival times for the split Bernoulli process. For every realization, $T_D^{\mathcal{B}} \geq T_D$. Analogous statements apply for arrivals at *death*. Figure 3.15 illustrates these processes.

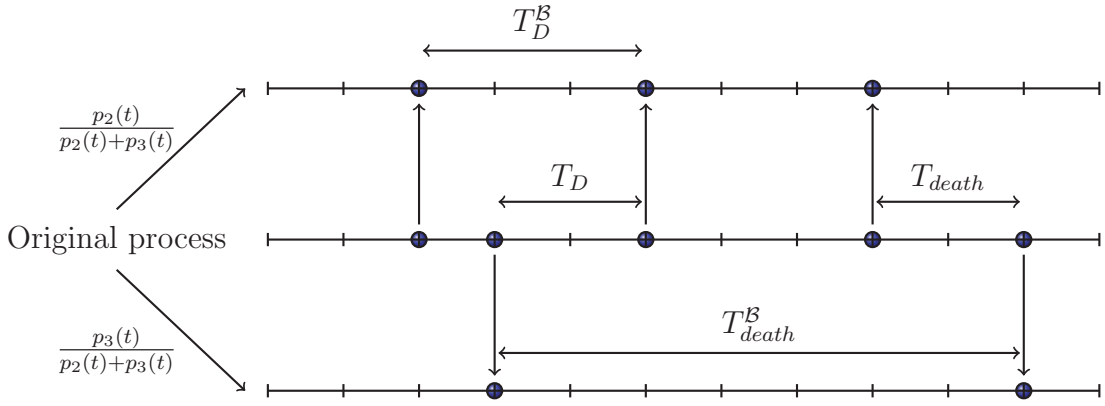

Figure 3.15: Graphical representation of Bernoulli process splitting.

Though it may seem natural to think of this problem as a Bernoulli splitting process, it is easier to deal with the available data using the approach given previously. This is primarily because of the additional step of constructing the original process (parameterized by $p_2(t) + p_3(t)$) from the raw cell cycle data.

Estimating the spore maturation parameter $p_4(t)$

Preliminaries and assumptions Similar to the methodology in in the previous section, it will be assumed that $p_4(t)$ remains constant for a particular cell when it is in C. An additional simplifying assumption is that mothercell lysis by some cells in C will not affect the spore development of the remaining cells in C. As before, this will allow the exit times from C to be independent.

Estimating $p_4(t)$ An estimate for $p_4(t)$ can be found by examining the case in Section 3.4.3 and setting either $p_3(t) = 0$ or $p_2(t) = 0$ (so there is only one way a cell may exit V). This leads to the maximum likelihood estimator:

$$\hat{p}_4(t) = \frac{\delta_C(t)}{\sum_{i=1}^{\delta_C(t)} t_{S,i}}$$

where $\delta_C(t)$ is a realization of the number of cells entering C at time $t + 1$ and $t_{S,i}$ is a realization of the dwell time in C for cell i. As mentioned at the end of Section 3.4.3, this estimator is biased.

Data windowing

The performance of the estimators degrades when the data is sparse. For example, there are several instances of time in the collected datasets where only one cell is in mode D.

The MLE for $p_1(t)$ will be either 0 or 1, which may not even be close to the actual decision variable.

One way to compensate for this problem is to window the data so the variances of the estimators are "small," or below some specified threshold. Though this may improve the performance of the estimators, windowing the data will reduce the temporal resolution of the parameter estimates. This is an extremely important trade-off to analyze, but will not be addressed in this work.

3.4.4 Results

This section shows some data from the two processed videos. No data windowing was performed, which makes the results toward the end of each experiment less reliable (when there are few transition events). The last part of this section shows some results from a study on mothercell lysis events, which relates $p_2(t)$ and $p_4(t)$.

Estimates for $p_1(t)$

Figures 3.16 and 3.17 show the $p_1(t)$ estimates for experiments 090731 and 090810, respectively. As mentioned before, there was no data windowing performed on these data sets, so the estimates at certain parts of the datasets (especially near the ends of the experiments) are not very good. Despite this drawback, it is clear that there is an initial wave of sporulation events in both experiments, followed by another sporulation wave ≈ 15 hours afterwards. This is consistent with qualitative observations.

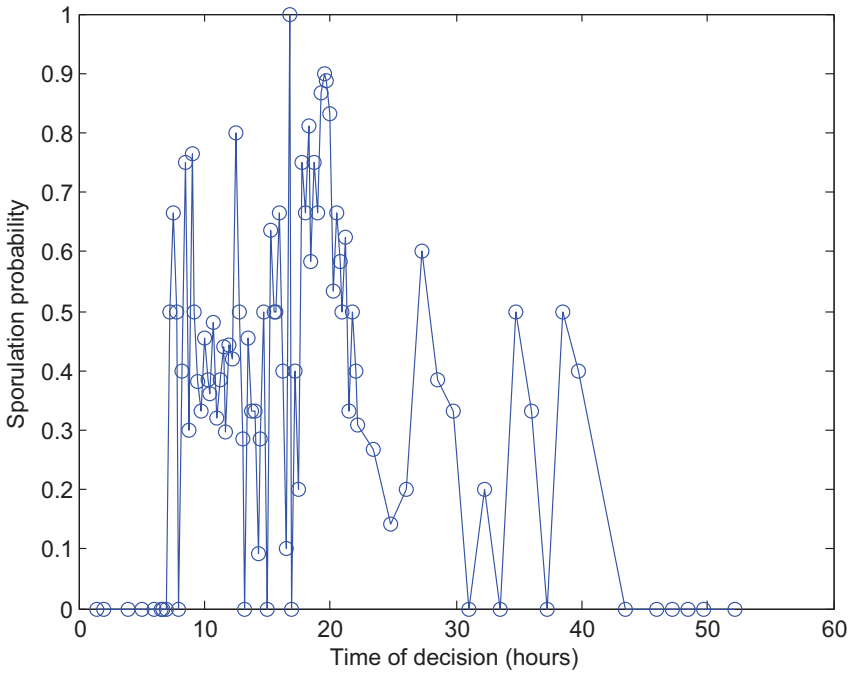

Figure 3.16: Estimate of $p_1(t)$ for experiment 090731.

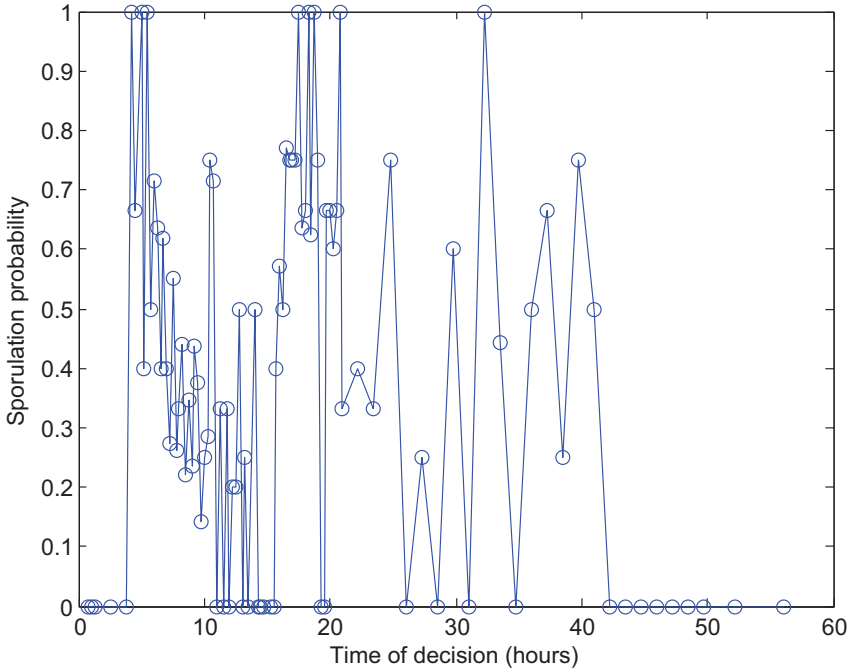

Figure 3.17: Estimate of $p_1(t)$ for experiment 090810.

From these estimates, the "population heterogeneity" that characterizes the sporulation decision is evident– the majority of the estimates for $p_1(t)$ are between 0 and 1. In other words, from these isogenic colonies (grown from a single ancestor), the decision to sporulate varies across the population. Assuming that this bacterial strain is indeed "wild" (i.e. these experimental responses are evolutionary optimal), we should therefore expect any theoretical sporulation policies in this dissertation to exhibit population heterogeneity.

Estimates for $p_2(t)$

Figures 3.18 and 3.19 show the $p_2(t)$ estimates for experiments 090731 and 090810, respectively. Aside from the initial ≈ 7 hours, these estimates seem to be decreasing with time. This is consistent with the hypothesis that cell cycle times are correlated with nutrient availability [264, 279], since the experimental setup does not introduce nutrients during the data collection phase; nutrients are exhausted from the SM-GM as the microcolony grows. This claim makes intuitive sense: cell growth involves the transformation of nutrients to cell matter, so the higher the nutrient level, the faster the cell may grow and progress though cell cycles. Everything "slows down" for the cell when nutrients run low, which is consistent with the integral of nutrient level directly affecting cell cycle timing. Therefore, $p_2(t)$ can be used as an estimate of the nutrient available to the bacteria.

Estimates greater than 1 correspond to events where a single cell has more than one division septum, which are commonly observed during the early stages of the experiments. This event was not considered in the proposed Markov model, so the corresponding estimates are not valid.

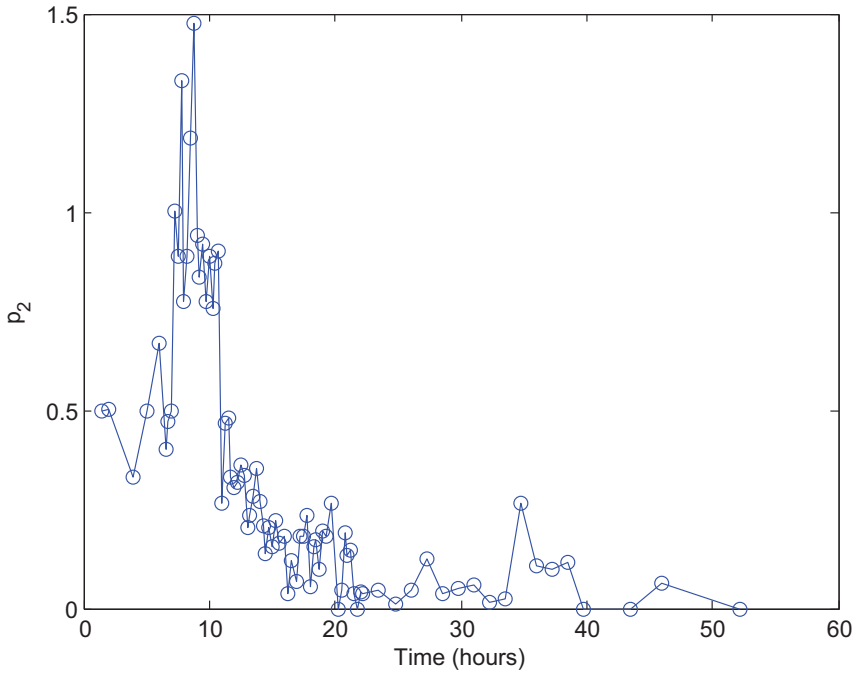

Figure 3.18: Estimate of $p_2(t)$ for experiment 090731.

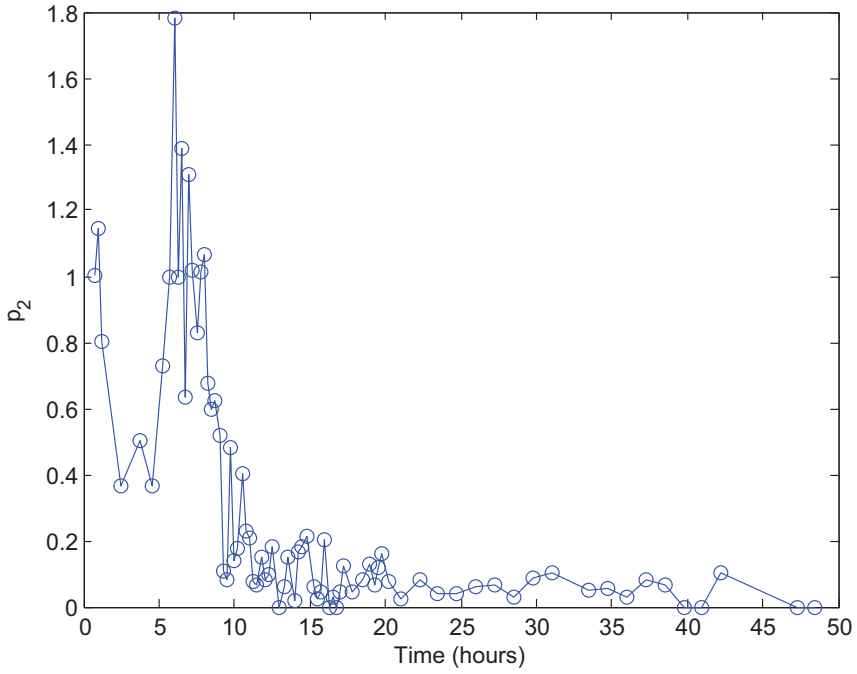

Figure 3.19: Estimate of $p_2(t)$ for experiment 090810.

Though the performance of the estimator may be poor due to the small number of cells, the initial ≈ 7 hours of the experiments exhibit interesting behavior. If the parameter $p_2(t)$ was a direct indicator of nutrient availability, then both experiments suggest that nutrients increase initially from the point of view of the bacteria. Alternatively, the initial concentration of nutrients on the agar pad may be higher than the cellular environmental conditions immediately preceding resuspension, resulting in a decrease in $p_2(t)$. The interesting thing about this explanation is that the first wave of sporulation occurs while the average cell cycle time is decreasing ($p_2(t)$ increasing), which implies that sporulation occurs when nutrient availability increases. This may be due to a food-per-growing-cell shortage during this time (the presumed dependence for sporulation), assuming that $p_2(t)$ is selected on absolute nutrient availability.

Estimates for $p_3(t)$

Figures 3.20 and 3.21 show the $p_3(t)$ estimates for experiments 090731 and 090810, respectively. With the same caveat about data windowing and the reliability of these estimators, it appears that death is a relatively infrequent occurrence for *B. subtilis* during nutrient limitation in these experiments. It is difficult to observe any trends in the estimates, though if death depended on absolute nutrient availability, it would be expected that these increase with time. On the other hand, if $p_3(t)$ depended on food-per-growing-cell, then regulation of the vegetative population to keep this metric constant would ensure that $p_3(t)$ remained constant. Indeed, the vegetative population is constantly decreasing in size. It is unclear from the data if any of these hypotheses are not invalid.

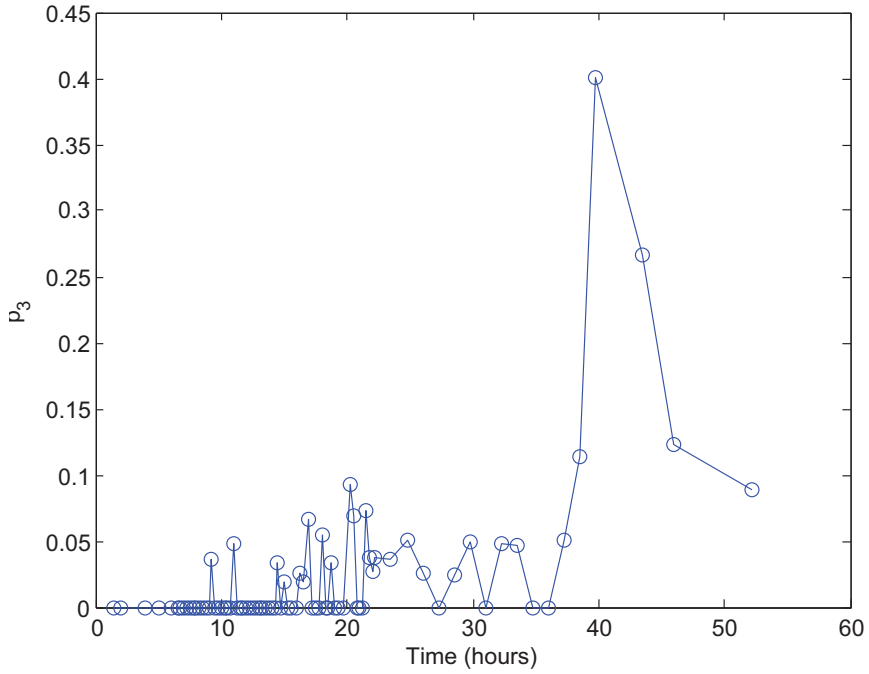

Figure 3.20: Estimate of $p_3(t)$ for experiment 090731.

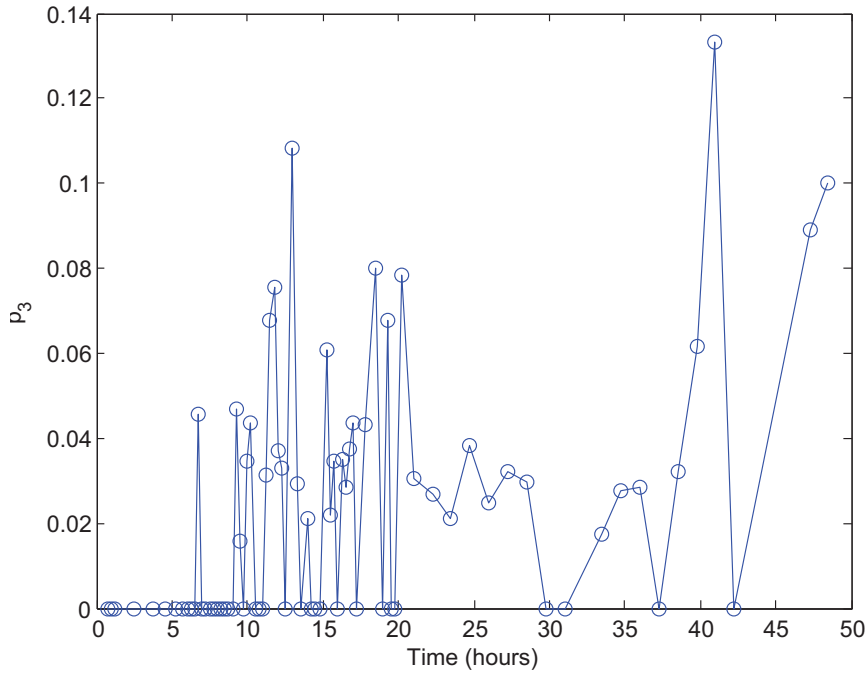

Figure 3.21: Estimate of $p_3(t)$ for experiment 090810.

Estimates for $p_4(t)$ (via mothercell lysis events)

Cells from experiment 090731 were picked that clearly exhibit mothercell lysis events, and the tracks were recorded from prespore appearance to mothercell lysis. We originally wanted to see a correlation between autofluorescence intensity of the prespore and mothercell lysis (e.g. mothercell lysis occurs once the normalized CFP level crosses some threshold), but it did not show anything useful. We noticed, however, that the timing between commitment to sporulation and mothercell lysis resembled the cell cycle timing plot for this experiment (see Figure 3.22).

A nice result, which is consistent with the idea of spore formation as a specialized form of cell division [71], is that the average mothercell lysis time is related to the average cell cycle time. Figure 3.23 shows an illustration of this relationship. In the figure, intermediate points were resampled to provide more data points in the illustration.

It appears that the parameters $p_2(t)$ and $p_4(t)$ are related. In this dataset, $p_4(t) \approx \frac{1}{5}p_2(t)$.

3.5 Concluding remarks

This chapter presented experimental conditions and data from resuspension experiments performed in the Arkin Lab. In the context of a simple Markov model, a parameter identification exercise was performed to quantify certain aspects of *B. subtilis* behavior. Specifically, the sporulation decision policies for two experimental microcolonies were found, as well as cell cycle timing, death, and spore maturation parameters. Since this dissertation is devoted

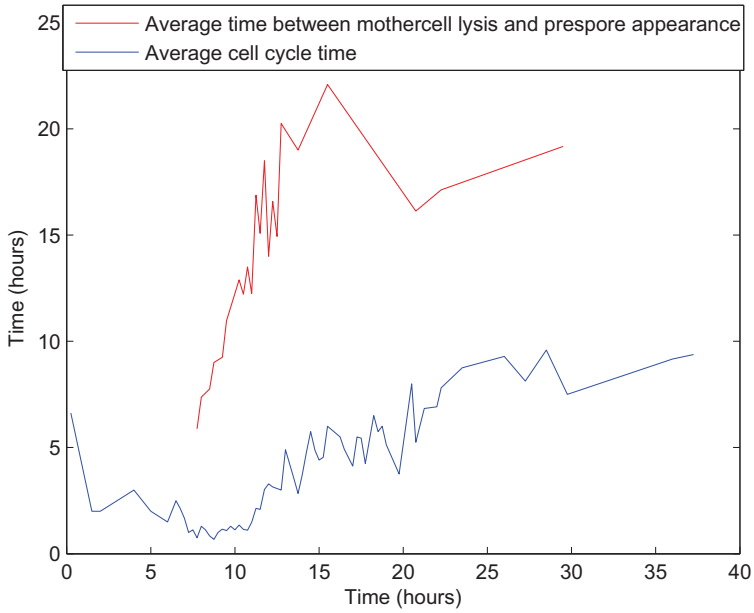

Figure 3.22: Averaged mothercell lysis and cell cycle times for experiment 090731.

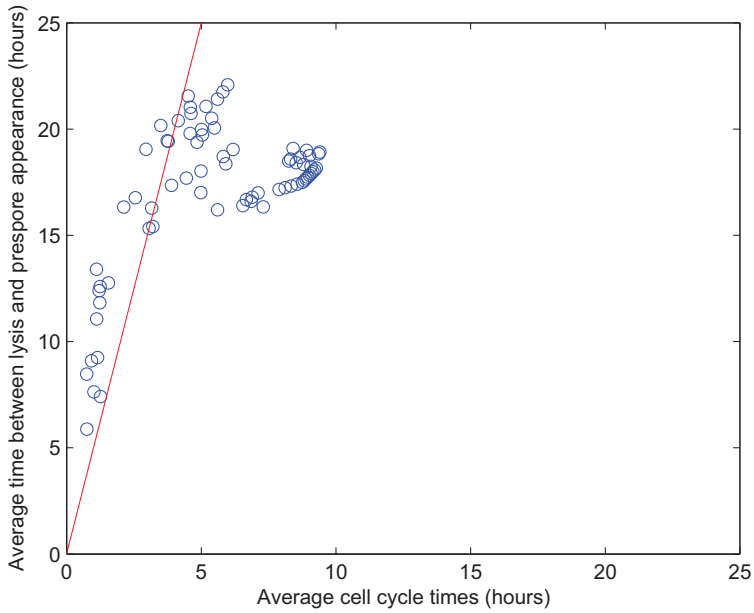

Figure 3.23: Relationship between average mothercell lysis time and average cell cycle time.

to the study of sporulation, the estimates for $p_1(t)$ will prove useful in the sequel. The other parameters will not be revisited.

Using this data to guide model development has some drawbacks, all of which are related to corroborating theoretical results with experimental findings:

1. Nutrient information: As mentioned before, there is no quantitative information about nutrient availability in these datasets. Though it may be possible to infer these values from average cell cycle times (see Section 3.4.4), an extensive literature review suggests that this has not been verified quantitatively using experiments. Thus, there is no direct way to monitor the nutrient availability in these resuspension experiments. Even if it were possible to directly record nutrient values, the experimental nutrient conditions may not facilitate a tractable solution for nonlinear sporulation models, where constant or "catastrophic" nutrient conditions are needed (see Chapters 4 and 5).

2. "Wildness" of experimental strain: In an evolutionary optimal framework (see Section 2.2.4), care must be taken when utilizing experimental results. More precisely, there is no guarantee that the laboratory organism under study has been selected to respond optimally to the experimental conditions. This can be due to a variety of reasons, one of which is that the laboratory organism does not exhibit "wild"-type phenotypes (assuming wild organisms have been selected long enough to behave optimally). Common laboratory strains, such as 168 (the strain used in these experiments), have been domesticated long enough that some important phenotypes have been lost [28, 63, 195]. This implies that the data collected from experiments with these domesticated strains do not correspond to evolutionary optimal decision-making.

3. Experimental conditions: Another reason that a laboratory organism might not exhibit an evolutionary optimal response is the experimental conditions may not mirror the environment conditions in which the organism underwent natural selection. For example, an organism that evolved inside a volcano will not respond optimally (i.e. maximal fitness) to nutrient abundance in a rain forest, and vice versa. Unless it is known that the experimental conditions are similar to the conditions in which the laboratory organism evolved, then it is difficult to compare a theoretically-optimal decision policy to the available data. Even if the organism exhibits an optimal response for the experimental environment, the experimental setup may not allow the optimal phenotype to manifest; for example, biofilm formation is not possible when bacteria grow in a monolayer (as in our experiments), but is supposedly essential for an optimal sporulation response [45, 114, 246].

Thus, corroborating theoretical findings with experimental results may not be possible, even if the theoretical work is correct. However, data is still useful in assessing the general behavior and results of a candidate model. The two datasets presented in this chapter will provide, at the very least, a quick litmus test for theoretical work presented in this dissertation.

There is clearly a need to strengthen the ties between experimental conditions and theoretical assumptions as much as possible. For the work in this dissertation, directly recording nutrient levels will increase the biological impact of any research more than any other experimental modification. Microfluidic devices are a step in the right direction [7, 18], though quantification of nutrient levels is still not direct. The solution to this problem is admittedly complex due to the required understanding of the actual inputs into the phosphorelay and the implementation of devices to measure these inputs.

Another way to increase the biological relevance of evolutionary optimal theoretical work is to work with bacteria that have evolved in environments similar to the experimental settings. This requires isolation of strains from natural ecosystems, where they have presumably maximized their fitnesses due to repeated rounds of natural selection. This also requires the experimental nutrient conditions and physical constraints to mirror those from the natural ecosystem. While these tasks may be difficult to accomplish in practice, they may help counter criticisms of work based on the evolutionary optimality assumption.

Chapter 4

Sporulation Versus Dormancy

4.1 Introduction

The decision to sporulate is governed by a complex cellular network (the phosphorelay), and the formation of a spore itself is a complex developmental process (see Chapter 2). Due to its sophistication and the fact that several bacteria are capable of forming spores (other bacteria in the genera *Bacillus* and *Clostridium* [224]), it is unlikely that sporulation is a neutral or deleterious mutation that hitchhiked with beneficial mutations [67]. There must be a compelling reason why sporulation has evolved, and this chapter will examine a possible explanation for the existence of sporulation by comparing it to a simple reduction in metabolic activity, a similar bacterial survival strategy.

The survival strategy comparison will be done in fitness space. Natural selection has maximized the fitness of an organism in a particular environmental condition, so the maximal fitnesses associated with each survival strategy can be directly compared. If there exists an environment in which sporulation has a higher fitness than another survival strategy, then it is possible that sporulation has evolved because it provides a better chance of survival. The comparison becomes stronger when the proposed environmental condition reflects the actual environment in which the bacteria have evolved.

Though most traits have been selected to increase an organism's fitness [171], quantitative comparisons between different traits has not received much attention. Many studies have been performed on evolutionary optimality in the abstracted context of optimizing parameters for a particular model structure [66, 117, 170, 194, 197], but comparing maximal fitnesses for different model structures is an often unexplored direction. This chapter will provide an exercise in this area, where two different models for sporulation and metabolic reduction are proposed in Sections 4.3.1 and 4.3.2. Section 4.5 formulates the specific fitness maximization problem for the environmental profile suggested in Section 4.4, and the results of the comparison between sporulation and metabolic reduction are given in Section 4.6.

4.2 Dormancy background

A simple reduction in metabolic activity provides many of the benefits of sporulation without the complexity and energetic costs of spore formation [59]. Metabolic reduction, or "dormancy" in the sequel[1], is common across the microbial world [7] and does not result in the formation of a morphologically-distinct protective structure. Instead, dormancy is a reversible state that reduces the amount of nutrient needed for survival and protects against stressors that rely on cellular metabolism [59, 127, 160]. Thus, dormancy is a way to deal with nutrient limitation and protect against a certain class of environmental stressors.

Example of strategies that reduce metabolic activity are "viable but non-culturable cells" and "persisters" [59]. Persister cells were discovered in the 1940s from the observation that bacteria cultures cannot be completely killed by antibiotic treatment– a small portion of the population "persists" [145]. However, these cells did not acquire a genetic resistance to the antibiotics, since subsequent regrowth and antibiotic treatment results in the similar persistent population [81]. This heterogeneous response to antibiotics is the result of a reversible dormant state, in which a bacterium severely reduces or suspends its growth; this makes the bacterium resistant to treatments that affect cell wall synthesis or translation, which are common antibiotic targets [59]. Though dormancy is most often studied in the context of antibiotic treatments (due to its application to human health [160]), a reduction in metabolic activity or growth rate will also protect against nutrient deprivation [264, 279].

There are several similarities between sporulation and dormancy. They both protect against certain environmental stressors and allow survival in the face nutrient limitation. At the same time, there are many differences between the survival strategies, the most obvious being the formation of a morphologically-distinct protective structure for sporulation. The physiological differences between a spore and a non-active cell allow the spore to survive harsher environmental conditions (see Section 4.7), though the energetic costs of spore formation and phosphorelay maintenance may be much greater than the reversible switching to the dormant state. However, for the purposes of this study, the two survival strategies confer many of the same starvation-related benefits.

4.3 Models

4.3.1 Sporulation model

The decision to sporulate is made once per cell cycle [256]. Assume that a group of $m_V(t)$ cells makes a decision to commit $p(t)$ cells to spores at time t. The remaining $1-p(t)$ cells not committed to sporulation will divide to produce $2(1-p(t))m_V(t)$ growing cells. A fraction of this group $q(t)$ will die during the course of their cell cycles, and at the end of the cell cycle the decision to sporulate is repeated [48, 257]. Since spores are resilient to environmental stressors, they are assumed to not die. It is implicitly assumed that there exist sufficient intracellular nutrient stores to complete spore formation or cell division, possibly in the form

[1]Technically, sporulation is a type of dormancy strategy. However, I will define dormancy as a strategy that simply reduces metabolic activity. This is consistent with other studies [160].

of polyhydroxyalkanoates [130], so a vegetative cell will perish only after the completion of the cell division event. It is also assumed the nutrient level is not high enough to exit the spore state, so sporulation is an irreversible process (i.e. no germination). Denoting one generation as the time between cell cycles and assuming the cell cycles for all cells are synchronous, a simple (deterministic) model describing the colony dynamics is given below:

$$\begin{aligned} m_V(t+1) &= 2(1-p(t))(1-q(t))m_V(t) \\ m_S(t+1) &= m_S(t) + p(t)m_V(t) \\ q(t+1) &= \begin{cases} 0 & \text{if } z(t) < 0 \\ z(t) & \text{if } 0 \leq z(t) \leq 1 \\ 1 & \text{if } z(t) > 1 \end{cases} \end{aligned}$$

where $z(t) = q(t) + KM(t+1)$.

In these equations, the variables are

$$\begin{aligned} M(t) &= m_V(t) - \delta p(t-\Delta)m_V(t-\Delta) - N(t) \\ m_V(t) &= \text{number of vegetative/growing cells} \\ m_S(t) &= \text{number of cells committed to sporulation} \\ p(t) &= \text{decision variable for the fraction of cells that commit to sporulation} \\ q(t) &= \text{fraction of growing cells that perish during a cell cycle} \\ N(t) &= \text{nutrient added over one generation (normalized)} \\ \delta &= \text{parameter that describes the amount of nutrient released from mothercell lysis} \\ \Delta &= \text{time between commitment to sporulation and mothercell lysis} \\ K &= \text{parameter to describe the nutrient consumption by a growing cell} \end{aligned}$$

Since cells are assumed to strictly consume nutrients, $\delta < 1$. Also, since cell cycle times depend on nutrient level (see Section 3.4.4) [27, 264, 279], $N(t)$ is defined relative to a single generation.

A useful picture for the dynamics of $q(t)$ is offered in Figure 4.1. Notice that it is possible for $M(t) < 0$ if more nutrients are released from mothercell lysis and/or exogenously added to the environment than consumed by growing cells. In this case, the fraction of surviving growing cells increases. On the other hand, if $M(t) > 0$, then the nutrient level decreases and the fraction of dying cells increases. The motivation for choosing to model the death fraction dynamically is to capture the fact that without nutrient infusion, the nutrient level will always be decreasing with time. A static relationship between vegetative cells and death fraction would not display this behavior.

Figure 4.2 provides a graphical representation of the vegetative cell and spore dynamics.

Except for the dynamics of $q(t)$, this sporulation model corresponds to the mean-valued model of the stochastic model presented in Chapter 3 (with C and S grouped into a single operating mode).

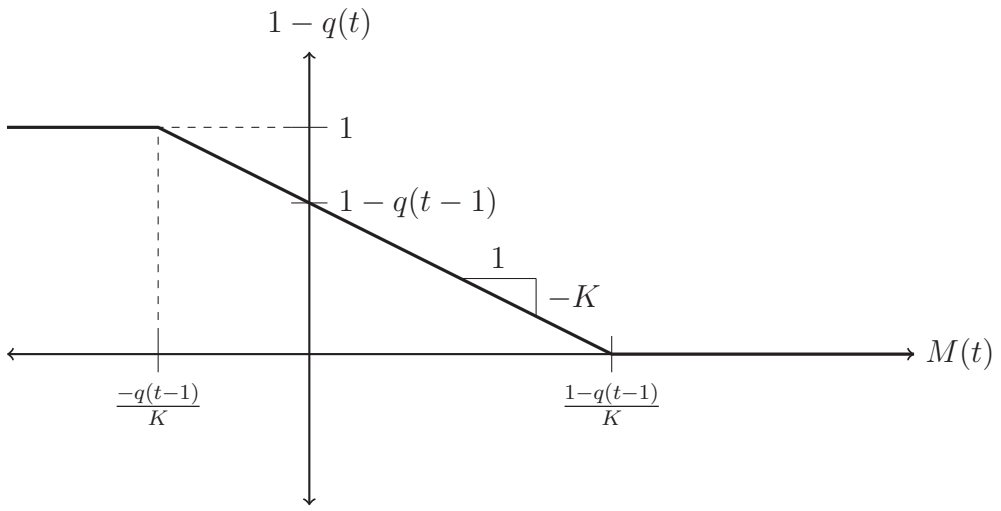

Figure 4.1: Dynamics of $q(t)$.

4.3.2 Dormancy model

A simple, population-level model for dormancy is very similar to the sporulation model. However, the following differences need to be accommodated: non-negligible exit from dormant state even with low nutrient levels [145], and no mothercell lysis events. The energetic cost of forming a spore is assumed, for the sake of simplicity, to be negligibly higher than forming a dormant cell. We also assume that a dormant cell has no metabolic activity, so no growth or death are possible in the dormant state ("perfect" dormant structures). A simple dormancy model can therefore be written as:

$$
\begin{aligned}
m_V(t+1) &= 2(1-\alpha_1(t))(1-q(t))m_V(t) + \alpha_2(t)m_P(t) \\
m_P(t+1) &= (1-\alpha_2(t))m_P(t) + \alpha_1(t)m_V(t) \\
q(t+1) &= \begin{cases} 0 & \text{if } z_P(t) < 0 \\ z_P(t) & \text{if } 0 \le z_P(t) \le 1 \\ 1 & \text{if } z_P(t) > 1 \end{cases}
\end{aligned}
$$

where $m_P(t)$ is the number of dormant cells, $\alpha_1(t)$ and $\alpha_2(t)$ are decision variables for the fraction of cells that commit to and exit dormancy, respectively, $z_P(t) = q(t) + KM_P(t+1)$, and $M_P(t) = m_V(t) - N(t)$.

Figure 4.3 provides a graphical representation of the vegetative and dormant cell dynamics.

4.4 Environmental model

To gain insight into the possible reasons why sporulation may be preferable to dormancy, attention must be restricted to a situation where these strategies are the dominant mechanisms for species survival. A scenario with constant environmental conditions turning

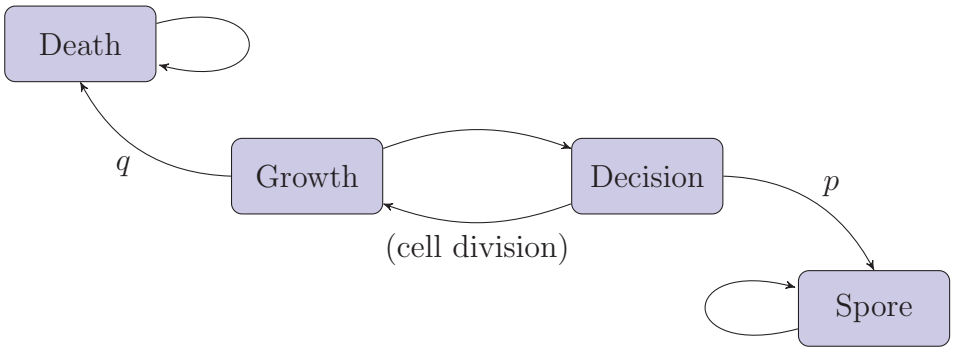

Figure 4.2: Vegetative cell and spore dynamics for the sporulation model. The nodes represent allowable states of the cell, and the parameters p and q are the fraction of cells that transition to the indicated state. The transition from Decision to Growth doubles the number of cells originally present in the Decision mode.

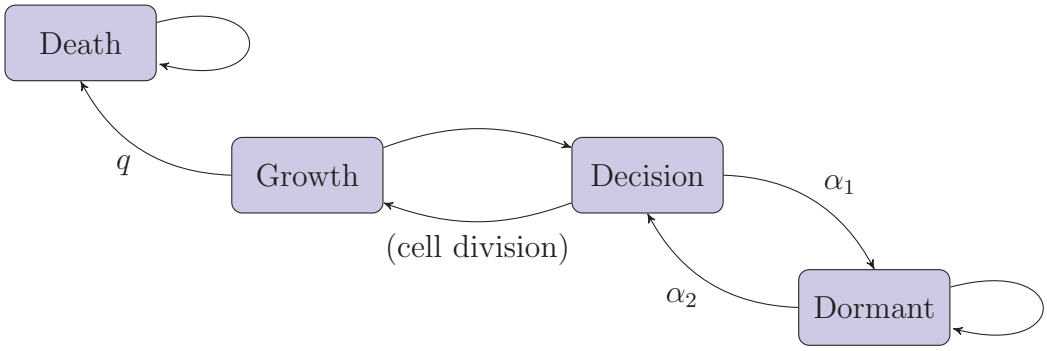

Figure 4.3: Vegetative and dormant cell dynamics for the dormancy model. The nodes represent allowable states of the cell, and the parameters α_1, α_2, and q are the fraction of cells that transition to the indicated state. The transition from Decision to Growth doubles the number of cells originally present in the Decision mode.

catastrophic at the $T-1$ generation ($T \gg 1$) provides a suitable environmental profile that will select for a survival strategy, where it is assumed that the survival structures (spores and dormant cells) can survive the catastrophe. A "catastrophic" environment will force $q(t) = 1 \; \forall t \geq T-1$. In this case, the best strategy is the one that is produces the largest number of survival structures, so increased sporulation or dormancy is crucial for survival in this environment. It is assumed that $N(t) \equiv N$ is large enough to support a nonzero growing cell population to the $T-1$ generation, to avoid the trivial sporulation policy $p \equiv 1$ (immediate sporulation/dormant cell formation by all vegetative cells). For the sake of simplicity, constant decision policies are assumed because N is constant and T is very large (much larger than the settling time of the system dynamics). These conditions will produce a constant optimal policy over most of the optimization horizon, so the constant decision policy presumption is a minor simplification.

This environmental model may be consistent with actual conditions that a soil-dwelling bacterium may encounter. For example, intermittent drought conditions, frigid winter temperatures, or flooding may destroy plant life and impose extremely harsh conditions for soil-dwelling organisms. The proposed environmental profile is similar to that used in another bacterial survival study [80], and it is consistent with the heat treatment mechanisms used to select for increased sporulation [166, 168] and spore isolation (see references in Table 2.1).

4.5 Problem statement

As mentioned in the introduction to this chapter, we are interested in comparing sporulation to dormancy. Using the proposed population-level dynamics and environmental model, this comparison can be done by focusing on the effects of the differences between the two model structures. More precisely, the effects of these differences on fitness maximization will be used to perform the comparison between the two survival strategies.

With the proposed environmental model and constant decision policy assumption, the long term fitness maximization problem (Problem 2.1) is

$$\begin{aligned} &\max_{\mathbf{u}} J(T) \\ &\text{s.t. system dynamics} \\ &0 \preceq \mathbf{u} \preceq 1 \end{aligned}$$

where $\preceq$ denotes element-wise inequality and the specific forms for $J(T)$ and $\mathbf{u}$ are given in Table 4.1. This particular fitness maximization problem will henceforth be referred to as the "long term catastrophe" problem.

Table 4.1: Parameters for fitness maximization problem

	Sporulation	Dormancy
$J(T)$	$m_S(T)$	$m_P(T)$
$\mathbf{u}$	p	(α_1, α_2)

After the solutions for the long term catastrophe problems are computed for each survival strategy, the two optimal strategies can be compared. Theoretically, the strategy with the higher fitness would be preferred since it maximizes a population's fitness. This does not imply, however, that the lower-fitness strategy disappears due to competitive advantages that it may offer. In other words, the strategy that maximizes the fitness of a population does not necessarily correspond to an evolutionary stable strategy [169, 197] (see Section 7.7.1 for more details). Nonetheless, we will judge the performance of a survival strategy based on its fitness measurement $J(T)$.

4.6 Results

Without loss of generality, assume $m_P(0) = m_S(0) = 0$.

4.6.1 Dormancy strategy for long term catastrophe problem

Since T is assumed to be much larger than the settling time of the system dynamics, the fitness maximization problem for the dormancy strategy is very straightforward because we may ignore the transient response of the model. The objective function for constant decision variables is

$$J(T) = m_P(T) = \sum_{i=0}^{T-1} \alpha_1 (1-\alpha_2)^i m_V(T-1-i),$$

from which it is immediately clear that the optimal resuscitation term is $\alpha_2^* = 0$ since, although the dormancy model is generally not stable, $m_V(t)$ and $q(t)$ will always remain bounded (though not necessarily constant). If K is chosen small enough such that $q(t) < 1$ $\forall t$, then $m_V(t) > 0$ $\forall t$. For $m_V(t)$ and $q(t)$ periodic,

$$\sum_{i=0}^{T-1} q(i+1) - q(i) = \sum_{i=0}^{T-1} K M_P(i) \approx 0$$

since T is much larger than the system dynamics timescale. The objective function may be closely approximated by

$$J(T) \approx \alpha_1 N T. \tag{4.1}$$

Obviously, the argument that maximizes this cost function (α_1^*) is the maximum allowable α_1. From the dynamics for $m_P(t)$,

$$\frac{1}{T}\sum_{i=0}^{T-1} \frac{m_V(i+1)}{m_V(i)} = \frac{1}{T}\sum_{i=0}^{T-1} 2(1-\alpha_1)(1-q(i)) \approx 1$$

where the approximation is good when T is much larger than the system dynamics timescale and $m_V(t)$ is periodic and has an average value much larger than the amplitude of its oscillations. Since the dormancy model is a population model, $m_V(t)$ should always be large, so the approximation is valid.

The average value of $q(t)$ is $\overline{q} = 1 - \frac{1}{2(1-\alpha_1)}$. From the constraint $0 \le \overline{q} < 1$, the maximum value of α_1 is $\alpha_1^* = \frac{1}{2}$.

Note that by ignoring the transient response, it has been assumed that the states $m_V(0)$ and $q(0)$ were already at the optimal configuration. Dropping this assumption will give approximately the same result (if T is large), though α_1^* will be very slightly less than $\frac{1}{2}$ if the optimal states are not reachable from the initial conditions with $\alpha_1 = \frac{1}{2}$ and $\alpha_2 = 0$. Nonetheless, we will assume $(\alpha_1^*, \alpha_2^*) = \left(\frac{1}{2}, 0\right)$ is the optimal dormancy strategy for the long term catastrophe environment.

4.6.2 Sporulation strategy for long term catastrophe problem

The optimal constant decision variable p for the sporulation strategy is found analogously. The cost function is

$$J(T) = m_S(T) = \sum_{i=0}^{T-1} p m_V(i),$$

where periodicity in $q(t)$ and large T give the following result, obtained from $\sum_{i=0}^{T-1} M(i) \approx 0$:

$$\sum_{i=0}^{T-1} m_V(i) \approx \frac{NT}{1-\delta p}$$

The cost function can therefore be closely approximated by

$$J(T) \approx \frac{p}{1-\delta p} NT \tag{4.2}$$

subject to the constraint $p \leq \frac{1}{2}$, which is derived in a similar manner as the constraint on α_1 for the dormancy model. Since it is assumed that cells do not create nutrients (i.e. $\delta < 1$), the maximizing p is readily found to be $p^* = \frac{1}{2}$.

The same caveat about reachability of the optimal states for the dormancy model applies to the sporulation model. Also, for both models, the approximations are exact if the numerical values for the parameters are chosen such that $m_V(t)$ and $q(t)$ approach constant values.

Figures 4.4 and 4.5 provide simulation support for the analytical claims above. In the simulations, $K = 0.01$, $N = 10$, $T = 500$, $m_V(0) = 11$, $m_S(0) = m_P(0) = 0$, $q(0) = 0.01$, $\delta = 0.5$, and $\Delta = 2$. Though not obvious from these figures, the reachability issue is present because the optimal p and α_1 are just below 0.5 (corresponding to one increment of the gridded space).

From Equations 4.1 and 4.2, it is clear that the sporulation survival strategy has a higher fitness than the dormancy survival strategy due to the mothercell lysis term.

4.6.3 Time-varying decision policies

The result of higher fitness for sporulation with constant decision policies can be extended to special cases of time-varying decision policies, as long as $\alpha_2^* \equiv 0$. When the condition $\alpha_2^* \equiv 0$ is satisfied, the dormancy model is equivalent to the sporulation model with $\delta = 0$. By examining the effect of mothercell lysis on fitness maximization, presented in Theorems 4.6.1 and 4.6.4, conclusions about time-varying decision policies for both survival strategies can be drawn.

Theorem 4.6.1. *Let δ be the amount of nutrient release by mothercell lysis. Suppose the decision policy is $\mathbf{p} = \{p(0), p(1), p(2), \ldots\}$ and initial conditions are independent of δ. Suppose*

$$K \leq \frac{1}{2 \max_t m_V^{\delta}(t)} \tag{4.3}$$

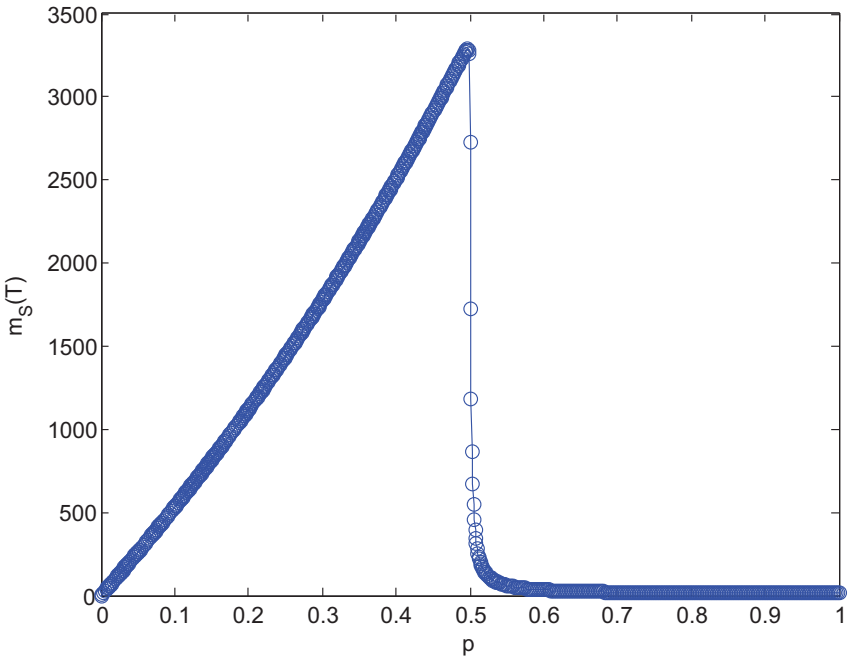

Figure 4.4: Fitness for different values p.

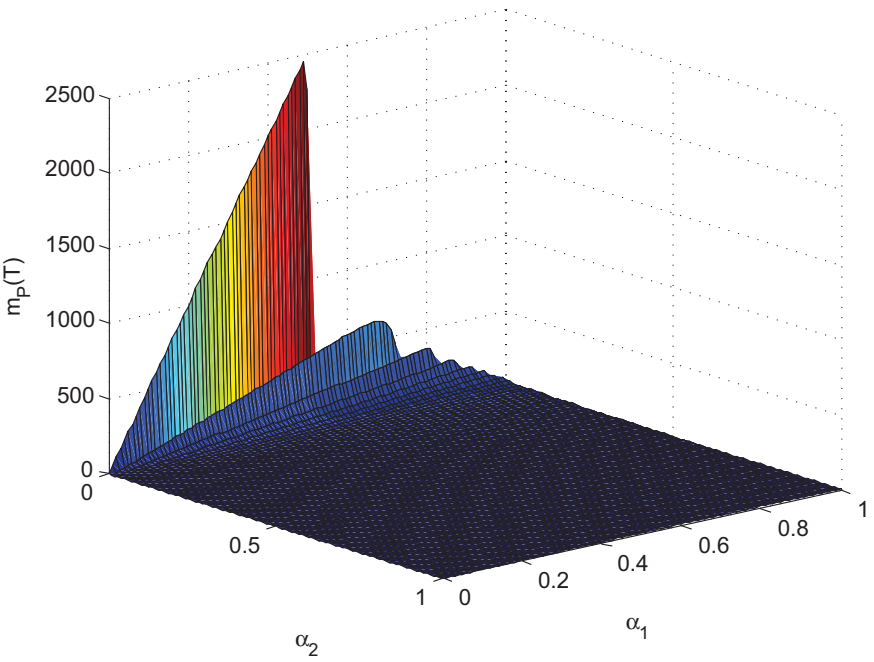

Figure 4.5: Fitness for different values α_1 and α_2.

and

$$\delta \geq \frac{m_V^\delta(t) - m_V(t)}{m_V^\delta(t) m_V^\delta(t+1-\Delta) p(t+1-\Delta) K}, \ \forall t \tag{4.4}$$

where $m_V^\delta(t)$ is the number of growing cells when $\delta > 0$. Then, for all initial conditions,

$$1 - q^\delta(t) \geq 1 - q(t), \ \forall t$$

where $q^\delta(t)$ corresponds to the case with mothercell lysis nutrient release, and $q(t)$ corresponds to the case without mothercell lysis nutrient release.

Equivalently, suppose the policy $\mathbf{p}$ and the initial conditions are independent of δ, the death fraction does not increase too rapidly, and δ is greater than some number. Then, the fraction of cells surviving to the next generation with mothercell lysis nutrient release for any $\delta > 0$ is always greater than or equal to the fraction of cells surviving to the next generation without mothercell lysis nutrient release.

Proof. Denote a variable $y^\delta(t)$ as being associated with the case of mothercell lysis nutrient release ($\delta > 0$) and $y(t)$ (without the superscript) as being associated with the case of no mothercell lysis nutrient release ($\delta = 0$). The result will be shown by induction.

For the base case, let $t = 1$. Since the initial conditions are identical ($q^\delta(0) = q(0)$ and $m_V^\delta(0) = m_V(0)$), and since the decision policies are the same, then $m_V^\delta(1) = m_V(1)$. Letting $M^\delta(1) = m_V^\delta(1) - \delta p(1-\Delta) m_V^\delta(1-\Delta) - N(1)$ and $M(1) = m_V(1) - N(1) = m_V^\delta(1) - N(1)$, the definitions for $q^\delta(1)$ and $q(1)$ clearly show that $1 - q^\delta(1) \geq 1 - q(1)$.

For the inductive step, suppose $1 - q^\delta(\tau) \geq 1 - q(\tau)\ \forall \tau \leq t$. This implies that $m_V^\delta(\tau) \geq m_V(\tau)\ \forall \tau \leq t$ since the initial conditions are assumed to be identical and the control $\mathbf{p}$ is identical.

Showing that $1 - q^\delta(t+1) \geq 1 - q(t+1)$ is equivalent to showing that

$$\begin{aligned} & q^\delta(t) + K M^\delta(t+1) \leq q(t) + K M(t+1) \\ \Leftrightarrow\ & m_V^\delta(t+1) - m_V(t+1) \leq \delta p(t+1-\Delta) m_V^\delta(t+1-\Delta) + \frac{q(t) - q^\delta(t)}{K}. \end{aligned} \tag{4.5}$$

From the system dynamics,

$$\begin{aligned} m_V^\delta(t+1) - m_V(t+1) &= 2(1 - p(t)) \left[(1 - q^\delta(t)) m_V^\delta(t) - (1 - q(t)) m_V(t) \right] \\ &\leq 2 m_V^\delta(t) \left[1 - \frac{m_V(t)}{m_V^\delta(t)} - q^\delta(t) + q(t) \frac{m_V(t)}{m_V^\delta(t)} \right] \\ &\leq 2 m_V^\delta(t) \left[1 - \frac{m_V(t)}{m_V^\delta(t)} - q^\delta(t) + q(t) \right] \end{aligned}$$

where the first inequality results from $1 - p(t) \leq 1$ and the second inequality results from $m_V^\delta(t) \geq m_V(t)$. From conditions (4.3) and (4.4), respectively,

$$\begin{aligned} m_V^\delta(t+1) - m_V(t+1) &\leq \frac{m_V^\delta(t) - m_V(t)}{m_V^\delta(t) K} + \frac{q(t) - q^\delta(t)}{K} \\ &\leq \delta p(t+1-\Delta) m_V^\delta(t+1-\Delta) + \frac{q(t) - q^\delta(t)}{K} \end{aligned}$$

$\forall t$, which satisfies Equation 4.5. Therefore, $1 - q^\delta(t+1) \geq 1 - q(t+1)$. □

Remark 4.6.2. *The condition (4.3) on K ensures that $q^\delta(t) - q^\delta(t+1) \leq \frac{1}{2}, \forall t$.*

Remark 4.6.3. *It is possible that condition (4.4) may not be satisfied with the constraint $\delta < 1$.*

Though Theorem 4.6.1 may seem obvious, the subtlety lies in the fact that a decreased fraction of cells dying puts a larger load on the nutrient supply, which will correspondingly increase the parameter $q(t)$.

Theorem 4.6.4. *Suppose conditions (4.3) and (4.4) hold, and the initial conditions are independent of δ. Then, for all $T > 0$,*

$$\max_{\mathbf{p}} m_S^\delta(T) \geq \max_{\mathbf{p}} m_S(T),$$

where $\mathbf{p} = \{p(0), p(1), \ldots, p(T-1)\}$.

Equivalently, suppose the initial conditions are independent of δ, $q(t)$ does not increase too rapidly, and δ is greater than some number. Then, the spore component of the fitness metric with mothercell lysis is at least as large as the spore component of the metric without mothercell lysis.

Proof. For any $T > 0$, the objective functions can be written as

$$m_S(T) = \sum_{t=0}^{T-1} p(t) 2^t m_V(0) \prod_{i=0}^{t-1} (1 - p(i))(1 - q(i))$$
$$m_S^\delta(T) = \sum_{t=0}^{T-1} p^\delta(t) 2^t m_V(0) \prod_{i=0}^{t-1} (1 - p^\delta(i))(1 - q^\delta(i)).$$

Denote the optimal policy and states with $*$. By definition,

$$\sum_{t=0}^{T-1} p^{\delta *}(t) 2^t m_V(0) \prod_{i=0}^{t-1} (1 - p^{\delta *}(i))(1 - q^{\delta *}(i)) \geq \sum_{t=0}^{T-1} p(t) 2^t m_V(0) \prod_{i=0}^{t-1} (1 - p(i))(1 - q^\delta(i))$$

for any other policy with elements $p(t)$, including the optimal policy corresponding to the model with no mothercell nutrient release (with elements $p^*(t)$). Then,

$$\sum_{t=0}^{T-1} p^{\delta *}(t) 2^t m_V(0) \prod_{i=0}^{t-1} (1 - p^{\delta *}(i))(1 - q^{\delta *}(i)) \geq \sum_{t=0}^{T-1} p^*(t) 2^t m_V(0) \prod_{i=0}^{t-1} (1 - p^*(i))(1 - q^\delta(i))$$

but since $1 - q^*(i) \leq 1 - q^\delta(i)\ \forall i \leq T-1$ (both under the same policy with elements $p^*(t)$), then

$$\sum_{t=0}^{T-1} p^*(t) 2^t m_V(0) \prod_{i=0}^{t-1} (1 - p^*(i))(1 - q^\delta(i)) \geq \sum_{t=0}^{T-1} p^*(t) 2^t m_V(0) \prod_{i=0}^{t-1} (1 - p^*(i))(1 - q^*(i)).$$

So, end to end, we are left with the inequality

$$\sum_{t=0}^{T-1} p^{\delta*}(t)2^t m_V(0) \prod_{i=0}^{t-1}(1-p^{\delta*}(i))(1-q^{\delta*}(i)) \geq \sum_{t=0}^{T-1} p^*(t)2^t m_V(0) \prod_{i=0}^{t-1}(1-p^*(i))(1-q^*(i)),$$

or

$$\max_{\mathbf{p}} m_S^{\delta}(T) \geq \max_{\mathbf{p}} m_S(T)$$

for all $T > 0$. □

Theorem 4.6.4 indicates that a model with mothercell lysis nutrient release will always have a higher fitness in the long term catastrophe problem than a similar model lacking mothercell lysis nutrient release, as long as some parametric conditions are satisfied. Therefore, even without the constant decision policy assumption, sporulation may provide a higher fitness than dormancy for the proposed environmental conditions.

4.7 Discussion

Examining Equations 4.1 and 4.2, it is evident that the sporulation survival strategy has a higher fitness than the dormancy survival strategy in the long term catastrophe environment described in Section 4.5. With conditions on K and δ, Theorems 4.6.1 and 4.6.4 extend the selection of sporulation over dormancy for time-varying decision policies in environments where $\alpha_2^* \equiv 0$ (no exit from dormant state) because the dormancy model becomes equivalent to the sporulation model with $\delta = 0$.

The choice of $\alpha_2^* \equiv 0$ is corresponds to extremely harsh environmental conditions, where it is better to "wait out the storm" and remain dormant instead of risk increased death in the growing state; indeed, since the cells know of the catastrophe $T-1$ generations into the future in the proposed example, it was better to devote resources to the accumulation of survival structures. Though difficult to detect in morphologically-indistinct survival structures (e.g. persistence [59]), there is evidence to suggest that resuscitation from the dormant state is not necessarily common. For example, some spores have been dated to $10^5 - 10^7$ years old [188], and several bacterial species produce a subpopulation of "superdormant" spores that do not germinate even in high-nutrient conditions [84].

The quantitative preference of sporulation over dormancy in extremely harsh environments is also consistent with the morphological differences between spores and metabolically-inactive cells. Inactive cells survive by simply not interacting with their environment, which reduces energetic demands and resists stressors that rely on metabolic activity (e.g. antibiotics disrupt cell replication machiner [7, 59, 81]). On the other hand, spores are specifically designed to protect the cell from harsh environmental conditions and have been recognized as the "hardiest known form of life on Earth" [188]; indeed, since spores do not have any metabolic activity (germination is initiated by passive mechanisms [121, 235, 277]), there is no way to repair potential damage to cellular DNA prior to germination. The outer parts of the spore (integument) have evolved to protect against noxious

chemicals, disinfectants, and degradative enzymes, while the inner parts of the spore (cortex and protoplast) protect against heat, dehydration, and radiation [53] (see Section 2.1.2 for more details). Thus, a spore does a better job protecting a genome copy than a dormant cell in scenarios that are similar to the proposed environmental profile, where conditions are harsh enough such that all vegetative cells perish. The results of this modeling exercise should therefore be expected.

The optimal constant sporulation decision policy is qualitatively consistent with experimental evidence. Though the available data were sourced from nutrient exhaustion conditions (not exactly a catastrophic event; see Section 3.2), the parameter $p^* = \frac{1}{2}$ is similar to maximum likelihood estimates of p (see Section 3.4.4). Figure 4.6 illustrates this agreement with the "wild type" *B. subtilis* 168 strain. Due to this close, qualitative agreement

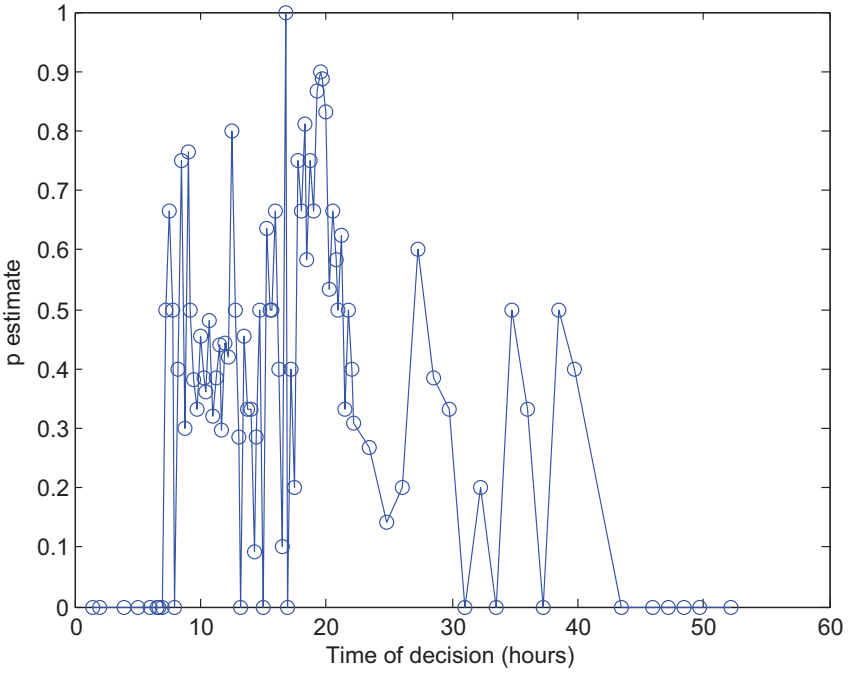

Figure 4.6: Estimate for p for experiment 090731.

with experimental evidence, it seems that sporulation may have evolved to specifically deal with these types of "catastrophic" conditions. On the other hand, experimental dormancy studies (albeit for *E. coli*) suggest a non-zero resuscitation rate ($\alpha_2 > 0$) and a dormancy commitment fraction of $10^{-6} - 10^{-5}$ [183], which corresponds to $\alpha_1 \ll 1$. Since these are not qualitatively consistent with the optimal dormancy policy derived in this chapter, it is possible that dormancy is ill-suited to deal with catastrophes and has evolved to address other environmental conditions.

Thus, the fitness space comparison performed in this chapter and the above considerations suggest that sporulation has evolved specifically to deal with catastrophic environments.

4.8 Concluding remarks

This chapter provided a quantitative assessment of the benefit of sporulation over a simple reduction in metabolic activity. It was shown that the proposed survival strategy models predict that sporulation provides a fitness advantage over dormancy in a long term catastrophic environment with constant decision policies. This result was extended to time-varying decision policies under certain conditions. Thus, if the modeling assumptions are valid, it seems that sporulation is a better survival strategy than dormancy for a long term catastrophic environment. This result is consistent with the difference between dormant cell and spore physiology.

There are several possible points of contention with the modeling assumptions:

1. Timing: The assumed ordering of the cell cycle may not be accurate. For example, it is assumed that a bacterium makes the sporulation/dormancy decision at the end of the cell cycle, and it can die only during a certain part of the cell cycle (after division but before the sporulation/dormancy decision is made). The time between the decision and cell division is not necessarily small, so there may be sufficient time for death. Also, the models assume a single point during the cell cycle when nutrients are consumed, whereas they are likely absorbed throughout the entire cell cycle.

2. Energetic difference between spore and dormant cell formation: Sporulation has been characterized as an "energy-intensive" process [109, 165]. Dormancy, on the other hand, does not require any additional energy because the cell just slows its metabolism. Energetic costs associated with environmental sensing may also differ between the two strategies. Incorporating these differences into the model may provide an important trade-off for spore formation.

3. Independence of spores from environment: Though spores are highly resistant to environmental stressors, they are not immune to them. Physical constraints such as space availability are not considered in this study, which makes the unbounded population growth predicted by the optimal policies unrealistic (spores are affected by mechanical stress [126]). This spore independence assumption does not admit a clear relationship between nutrient influx and population size, a feature which seems appealing to exhibit in a population-level model.

Though it may seem that many of these objections are important, they were omitted in order to obtain the relatively clean results presented in this chapter. However, it is clear that some of these assumptions need to be revisited because some (e.g. energetic difference between spore and dormant cell formation and finite steady state) would significantly increase the accuracy of model.

Aside from the incorporation of possibly important modeling assumptions into the analysis, there are several directions that will significantly improve the impact of the work presented in this chapter. The most outstanding extension is the comparison of sporulation to other bacterial survival strategies other than dormancy, such as cannibalism [87], reduction in cell surface area [224], or competence [184]. These comparisons will provide more

clues about reasons for the evolution of sporulation. Additionally, modeling environmental conditions to more closely resemble experimental conditions (e.g. nutrient exhaustion resuspension experiments) will allow a direct comparison to data. These extensions will increase the relevance of the work presented in this chapter.

Chapter 5

Bacterial Behavior; Single Population Model

5.1 Introduction

The previous chapter provided a possible explanation for why sporulation has evolved. The attention of this dissertation will now shift to the analysis of the characteristics of sporulation in an attempt to explain the general behavior of this evolutionary optimal decision policy. In particular, sporulation will be studied in the context of human decision-making in order to provide a qualitative understanding to which we may easily relate.

Understanding animal behavior in the context of human decision-making is common in biological systems since it is natural to frame unfamiliar ideas using concepts with which we are accustomed. However, beyond this trivial relationship, there have been significant strides in understanding animal behavior by assuming animals will act like humans. In other words, it is hypothesized that animal behavior is the result of "rational" decision-making, where an observed behavior can be explained by asking what a (rational) human would do if it was in the animal's position. Ignoring the technicality that not all humans act rationally, this framework is appealing because it provides self-centered characterizations that are consistent with the way we may act. Though it may be true that many biological organisms lack the cognitive capabilities of humans, their behaviors have been shaped to resemble rational choices to maximize certain measures of fitness (see Section 2.2.4). For example, we are able to explain many evolved phenotypes in the context of game theory (see Section 7.7.1), and we can characterize many foraging animals as risk seeking or risk averse (see Section 7.10.1). The remainder of this dissertation will be devoted to deriving an evolutionary optimal sporulation decision policy and carefully labeling *B. subtilis*'s behavior using human behavioral terms, in hopes of providing a relatable characterization of a bacterial survival strategy.

The population-level, discrete time sporulation model proposed in Chapter 4 is insufficient to study the characteristics of sporulation. Specifically, when considering maximization of total population number over a long time horizon, the optimal sporulation policy is to devote $\approx \frac{1}{2}$ of the vegetative cells to spores with no germination. This leads to the unrealistic

scenario of an unbounded total population level. In a control volume (i.e. a typical laboratory setting), an unbounded population number will necessitate the inclusion of mechanical stress and nutrient gradient effects into the model. Though studies have been done on the effects of mechanical stress on vegetative *B. subtilis* cells [226] and spores [126], introducing these effects and spatial modeling into the discrete time sporulation model would make it cumbersome to analyze. It is therefore desired to construct a model that predicts a steady state population in response to a constant nutrient influx, where the steady state population number depends on the magnitude of the nutrient influx. These features were both absent from the discrete time model.

In order to facilitate the finite steady state population number goal, a simple, population-level, continuous time sporulation model is developed in Section 5.2. Switching to continuous time allows the timing assumptions on nutrient consumption, sporulation decision and formation, and germination to be dropped. Though a matter of taste, treating sporulation, germination, birth, and death transitions as rates allows a more natural representation of a dynamical system. In order to maintain the validity of a population-based model, it is assumed that the nutrient influx is large. Because of this assumption, it is also assumed that the nutrient release from mothercell lysis is negligible and the germination rate is no longer zero. Finally, for the sake of simplicity, the spore formation time is assumed to be folded into the sporulation rate parameterization, which eliminates pure time delays in the model.

After the development of the continuous time model, Section 5.3.1 verifies the finite steady state property. Section 5.3.2 then formulates and solves the population maximization problem.

5.2 Model

Suppose a living population is composed only of vegetative cells and spores, which are supported by a nutrient influx. At each instance in time, vegetative cells form spores at a rate of α_2, spores germinate to form vegetative cells at a rate of α_3, vegetative cells grow at a rate of α_4, and vegetative cells die at a rate of α_1. It is assumed that spores are independent of nutrient conditions (similar to the modeling assumption in Chapter 4), the spore maturation time is incorporated into the sporulation rate parameterization, and the nutrients released from mothercell lysis are negligible compared to the nutrient infusion. The last assumption necessitates the inclusion of non-zero germination.

A graphical interpretation of the population model is given in Figure 5.1, which shows the assumed operating modes a single cell may occupy and the rates of transition between each mode.

It is assumed that all of the α_i's depend on $\frac{f}{X}$, the population-average nutrient level, which depends on time. α_1 and α_2 should be non-increasing in $\frac{f}{X}$ while α_3 and α_4 should be non-decreasing in $\frac{f}{X}$. In other words, there should be a relative increase in growth and germination with higher nutrient levels, and a relative increase in death and sporulation with lower nutrient levels.

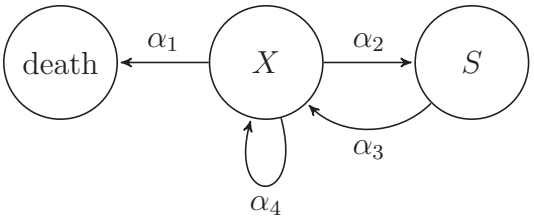

Figure 5.1: Schematic of population model showing the operating modes of the cells. X is the vegetative state and S is the committed to sporulation/spore state.

The single population model is therefore

$$\begin{aligned}\dot{X} &= (\alpha_4 - \alpha_1 - \alpha_2)\, X + \alpha_3 S \\ \dot{S} &= \alpha_2 X - \alpha_3 S \\ \dot{f} &= -\gamma X + e\end{aligned}$$

where

States:

$X =$ number of vegetative (growing) cells

$S =$ number of spores

$f =$ nutrients available to bacteria

Input:

$e =$ nutrient influx rate

Parameters:

$\alpha_1 =$ death rate

$\alpha_2 =$ sporulation rate

$\alpha_3 =$ germination rate

$\alpha_4 =$ birth rate

$\gamma =$ nutrient consumption parameter

and it is assumed that nutrient consumption is proportional to the number of vegetative cells.

The assumed parameterizations for the α_i's are piecewise linear

$$\begin{aligned}\alpha_1 &= \max\left\{0, u_1 - \frac{u_1}{l_1}\frac{f}{X}\right\} \\ \alpha_2 &= \max\left\{0, u_2 - \frac{u_2}{\theta}\frac{f}{X}\right\} \\ \alpha_3 &= \min\left\{u_3, \frac{u_3}{\beta}\frac{f}{X}\right\} \\ \alpha_4 &= \min\left\{u_4, \frac{u_4}{l_4}\frac{f}{X}\right\}\end{aligned}$$

where the u_i's and l_i's can be identified from data and θ and β describe the sporulation and germination decision processes, respectively. Illustrations of the parameterizations for the α_i's are given in Figure 5.2. In simulations in the sequel, the chosen parameter values are

$$\begin{aligned} u_1 &= 0.3 \\ u_2 &= 0.5 \\ u_3 &= 3\ln 2 \\ u_4 &= 3\ln 2 \\ l_1 &= 1 \\ l_4 &= 30, \end{aligned}$$

which are justified in Appendix A. It is assumed that germination takes only one cell cycle to complete, so the maximum germination rate is equal to the maximum birth rate.

The nutrient consumption parameter γ should be chosen so the population is "large enough" to not invalidate the population-level modeling assumptions. The values $\gamma = 0.01$ or $\gamma = 0.001$ are used throughout the remainder of this dissertation.

It is important to emphasize that this model is a *population*-level model while examining the parameterizations for the α_i's because they are not consistent with the expected parameterizations for a single cell. For example, it might be expected that the death rate α_1 should saturate at low $\frac{f}{X}$ because a cell presumably needs a minimum amount of food (> 0) to survive. However, if we consider a fixed control volume with a non-homogeneous spatial distribution of nutrients, the local nutrient level may be significantly different from the average nutrient level (which we are calling $\frac{f}{X}$ in this model). For example, even if the average nutrient level lies below the threshold of nutrients needed for survival, there may be patches in the control volume where the local nutrient level is much higher. Even as the average nutrient level approaches zero, there still may be patches that are able to sustain growth. Hence, the population-level death rate α_1 does not saturate at low nutrient levels.

5.3 Single population model results

5.3.1 Steady state

Assume a constant nutrient influx $e(t) = \overline{e} \geq 0$ and restrict the state variables to be non-negative ($X \geq 0, S \geq 0$, and $f \geq 0$). For $\overline{e} > 0$, there is a single equilibrium point $\left(\overline{X}, \overline{S}, \overline{f}\right)$ with $\overline{X} > 0$, $\overline{S} > 0$, and $\overline{f} > 0$, and another "equilibrium" point $(0, 0, f(t))$ where $f(t)$ is non-constant (for $\overline{e} = 0$, the only point where cell numbers are constant is $(0, 0, 0)$).

The non-trivial equilibrium point $\left(\overline{X}, \overline{S}, \overline{f}\right)$ has an important, intuitive feature: the birth rate α_4 is equal to the death rate α_1, which defines a **constant** operating point $c := \frac{\overline{f}}{\overline{X}}$ that is completely determined by the parameterizations for α_1 and α_4. For example, if the birth

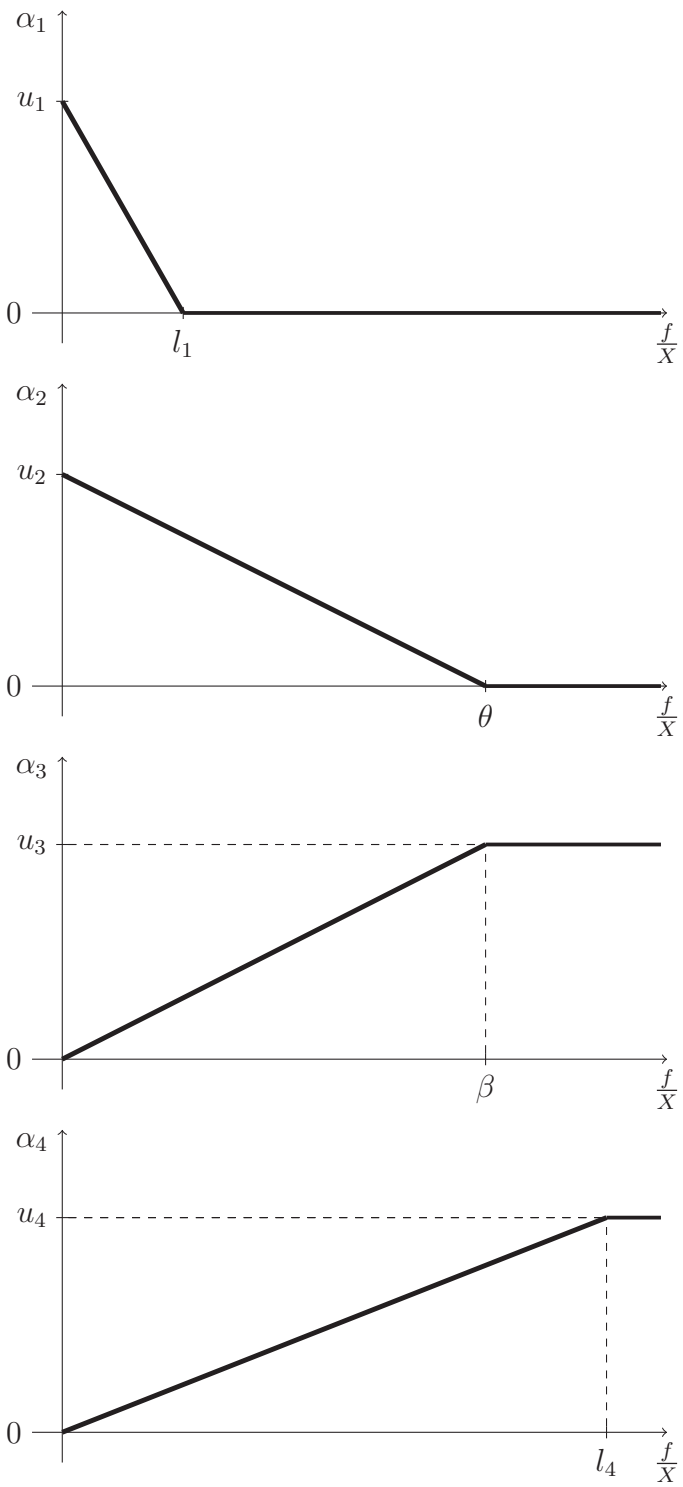

Figure 5.2: Illustrations of the parameterizations for the population model transition rates. α_1 is the death rate, α_2 is the sporulation rate, α_3 is the germination rate, and α_4 is the birth rate.

and death rates are

$$\alpha_1 = \max\left\{0, u_1 - \frac{u_1}{l_1}\frac{f}{X}\right\}$$
$$\alpha_4 = \min\left\{u_4, \frac{u_4}{l_4}\frac{f}{X}\right\},$$

where $u_i > 0$ and $l_4 \geq l_1 > 0$, then the (unique) constant operating point is given by

$$c = \frac{u_1}{\frac{u_4}{l_4} + \frac{u_1}{l_1}}.$$

Expressions for the states at this equilibrium point are

$$\overline{X} = \frac{\overline{e}}{\gamma}$$
$$\overline{S} = \frac{\max\left\{0, u_2 - \frac{u_2}{\theta}c\right\}}{\min\left\{u_3, \frac{u_3}{\beta}c\right\}}\overline{X}$$
$$\overline{f} = \frac{\overline{e}}{\gamma}c$$

and it can be shown that $\left(\overline{X}, \overline{S}, \overline{f}\right)$ is locally stable under certain conditions.

Corollary 5.3.1. *The equilibrium point $\left(\overline{X}, \overline{S}, \overline{f}\right)$ described above is locally stable if $u_i > 0$ $(i = 1, 2, 3, 4)$, $l_i > 0$ $(i = 1, 4)$, $\gamma > 0$, $\theta > 0$, and $\beta > 0$.*

Proof. For the equilibrium point $\left(\overline{X}, \overline{S}, \overline{f}\right)$ described by

$$\overline{X} = \frac{\overline{e}}{\gamma}$$
$$\overline{S} = \frac{\max\left\{0, u_2 - \frac{u_2}{\theta}c\right\}}{\min\left\{u_3, \frac{u_3}{\beta}c\right\}}\overline{X}$$
$$\overline{f} = \frac{\overline{e}}{\gamma}c,$$

four cases need to be examined: $\theta \geq c$ and $\beta \geq c$, $\theta < c$ and $\beta \geq c$, $\theta \geq c$ and $\beta < c$, and $\theta < c$ and $\beta < c$.

Case I: $\theta \geq c$ and $\beta \geq c$

The deviation variables $\delta X = X - \overline{X}$, $\delta S = S - \overline{S}$, $\delta f = f - \overline{f}$, and $\delta e = e - \overline{e}$ are described by the linearized dynamics

$$\frac{d}{dt}\begin{bmatrix} \delta X \\ \delta S \\ \delta f \end{bmatrix} = \begin{bmatrix} -u_1 - 2u_2 + \frac{u_2}{\theta}c & \frac{u_3}{\beta}c & \frac{u_4}{l_4} + \frac{u_1}{l_1} + \frac{u_2}{\theta} \\ 2u_2 - \frac{u_2}{\theta}c & -\frac{u_3}{\beta}c & -\frac{u_2}{c} \\ -\gamma & 0 & 0 \end{bmatrix}\begin{bmatrix} \delta X \\ \delta S \\ \delta f \end{bmatrix} + \begin{bmatrix} 0 \\ 0 \\ 1 \end{bmatrix}\delta e$$
$$= \begin{bmatrix} -a_1 & a_2 & a_3 \\ a_4 & -a_5 & -a_6 \\ -a_7 & 0 & 0 \end{bmatrix}\begin{bmatrix} \delta X \\ \delta S \\ \delta f \end{bmatrix} + \begin{bmatrix} 0 \\ 0 \\ 1 \end{bmatrix}\delta e$$

where $a_i > 0$, $i = 1, 2, \ldots, 7$, if $u_j > 0$, $j = 1, 2, 3, 4$, $l_j > 0$, $j = 1, 2$, $\gamma > 0$, $\theta > 0$, and $\beta > 0$. The characteristic equation for the linearized system is

$$\lambda^3 + (a_1 + a_5)\,\lambda^2 + (a_1 a_5 + a_3 a_7 - a_2 a_4)\,\lambda + (-a_2 a_6 a_7 + a_3 a_5 a_7) = 0.$$

Necessary and sufficient conditions for all roots of the equation $\lambda^3 + b_1\lambda^2 + b_2\lambda + b_3 = 0$ to have negative real part are $b_1 > 0$, $b_3 > 0$, and $b_1 b_2 > b_3$. It will be shown that the characteristic equation above satisfies these conditions.

Clearly, since all of the a_i's positive, the condition $b_1 > 0$ is satisfied. The condition $b_3 > 0$ means that we require

$$-a_2 a_6 a_7 + a_3 a_5 a_7 > 0$$

to be true. Since $a_2 = a_5$,

$$\begin{aligned} &-a_2 a_6 a_7 + a_3 a_5 a_7 > 0 \\ \Leftrightarrow \quad &a_5 a_7\,(a_3 - a_6) > 0 \end{aligned}$$

and since

$$\begin{aligned} a_3 - a_6 &= \frac{u_4}{l_4} + \frac{u_1}{l_1} + \frac{u_2}{c} - \frac{u_2}{c} \\ &= \frac{u_4}{l_4} + \frac{u_1}{l_1} > 0, \end{aligned}$$

the condition $b_3 > 0$ is satisfied. Finally, the condition $b_1 b_2 > b_3$ requires

$$(a_1 + a_5)\,(a_1 a_5 + a_3 a_7 - a_2 a_4) > (-a_2 a_6 a_7 + a_3 a_5 a_7)\,,$$

which is equivalent to

$$a_1 a_3 a_7 + a_2 a_6 a_7 + (a_1 a_5 + a_5 a_5)\,(a_1 - a_4) > 0,$$

which is satisfied since

$$\begin{aligned} a_1 - a_4 &= u_1 + 2u_2 - \frac{u_2}{\theta}c - 2u_2 + \frac{u_2}{\theta}c \\ &= u_1 > 0. \end{aligned}$$

The dynamics of the deviation variables are therefore stable when $\theta \geq c$ and $\beta \geq c$.

Case II: $\theta < c$ and $\beta \geq c$

The linearized dynamics are

$$\begin{aligned} \frac{d}{dt}\begin{bmatrix} \delta X \\ \delta S \\ \delta f \end{bmatrix} &= \begin{bmatrix} -u_1 & \frac{u_3}{\beta}c & \frac{u_4}{l_4} + \frac{u_1}{l_1} \\ 0 & -\frac{u_3}{\beta}c & 0 \\ -\gamma & 0 & 0 \end{bmatrix}\begin{bmatrix} \delta X \\ \delta S \\ \delta f \end{bmatrix} + \begin{bmatrix} 0 \\ 0 \\ 1 \end{bmatrix}\delta e \\ &= \begin{bmatrix} -a_1 & a_2 & a_3 \\ 0 & -a_2 & 0 \\ -a_4 & 0 & 0 \end{bmatrix}\begin{bmatrix} \delta X \\ \delta S \\ \delta f \end{bmatrix} + \begin{bmatrix} 0 \\ 0 \\ 1 \end{bmatrix}\delta e \end{aligned}$$

where again the a_i's are positive under the conditions described above. The characteristic equation for the linearized system is

$$\lambda^3 + (a_1 + a_2)\,\lambda^2 + (a_1 a_2 + a_3 a_4)\,\lambda + a_2 a_3 a_4 = 0.$$

Clearly, $a_1 + a_2 > 0$ and $a_2 a_3 a_4 > 0$, and

$$\begin{aligned} &(a_1 + a_2)\,(a_1 a_2 + a_3 a_4) > a_2 a_3 a_4 \\ \Leftrightarrow\ &a_1\,(a_1 a_2 + a_3 a_4) + a_1 a_2^2 > 0 \end{aligned}$$

which is satisfied. The dynamics of the deviation variables are therefore stable when $\theta < c$ and $\beta \geq c$.

Case III: $\theta \geq c$ and $\beta < c$

The linearized dynamics are

$$\begin{aligned} \frac{d}{dt}\begin{bmatrix} \delta X \\ \delta S \\ \delta f \end{bmatrix} &= \begin{bmatrix} -u_1 - u_2 & u_3 & \frac{u_4}{l_4} + \frac{u_1}{l_1} + \frac{u_2}{\theta} \\ u_2 & -u_3 & -\frac{u_2}{\theta} \\ -\gamma & 0 & 0 \end{bmatrix}\begin{bmatrix} \delta X \\ \delta S \\ \delta f \end{bmatrix} + \begin{bmatrix} 0 \\ 0 \\ 1 \end{bmatrix}\delta e \\ &= \begin{bmatrix} -a_1 & a_2 & a_3 \\ a_4 & -a_5 & -a_6 \\ -a_7 & 0 & 0 \end{bmatrix}\begin{bmatrix} \delta X \\ \delta S \\ \delta f \end{bmatrix} + \begin{bmatrix} 0 \\ 0 \\ 1 \end{bmatrix}\delta e \end{aligned}$$

Note that

$$\begin{aligned} a_3 - a_6 &= \frac{u_4}{l_4} + \frac{u_1}{l_1} + \frac{u_2}{\theta} - \frac{u_2}{\theta} \\ &= \frac{u_4}{l_4} + \frac{u_1}{l_1} > 0 \end{aligned}$$

and

$$\begin{aligned} a_1 - a_4 &= u_1 + u_2 - u_2 \\ &= u_1 > 0, \end{aligned}$$

so the conditions for stability derived for the previous case are valid for this case. Thus, the dynamics of the deviation variables are stable when $\theta \geq c$ and $\beta < c$.

Case IV: $\theta < c$ and $\beta < c$

The linearized dynamics are

$$\begin{aligned} \frac{d}{dt}\begin{bmatrix} \delta X \\ \delta S \\ \delta f \end{bmatrix} &= \begin{bmatrix} -u_1 & u_3 & \frac{u_4}{l_4} + \frac{u_1}{l_1} \\ 0 & -u_3 & 0 \\ -\gamma & 0 & 0 \end{bmatrix}\begin{bmatrix} \delta X \\ \delta S \\ \delta f \end{bmatrix} + \begin{bmatrix} 0 \\ 0 \\ 1 \end{bmatrix}\delta e \\ &= \begin{bmatrix} -a_1 & a_2 & a_3 \\ 0 & -a_2 & 0 \\ -a_4 & 0 & 0 \end{bmatrix}\begin{bmatrix} \delta X \\ \delta S \\ \delta f \end{bmatrix} + \begin{bmatrix} 0 \\ 0 \\ 1 \end{bmatrix}\delta e \end{aligned}$$

where the Jacobian matrix has elements with the same signs as Case II. Therefore, we can immediately conclude that the dynamics of the deviation variables are stable when $\theta < c$ and $\beta < c$. □

By looking at the dynamics, it is clear that the "equilibrium" point $(0, 0, f(t))$ is unstable, so the point $\left(\overline{X}, \overline{S}, \overline{f}\right)$ is a globally stable equilibrium in the allowable state space. Therefore, for a set of initial conditions where either $X(0) > 0$ or $S(0) > 0$ and for $\overline{e} > 0$, the steady state solution is given by $\left(\overline{X}, \overline{S}, \overline{f}\right)$.

The steady state expressions reveal several intuitive facts that the model is able to capture:

- The steady state vegetative cell and spore numbers are monotonically increasing in $\overline{e}$.
- For a fixed $\overline{e}$, the steady state spore number increases as θ or β increase.
- The relative allocation of the population to spores increases as θ or β increase.

The number of steady state vegetative cells does not depend on θ or β; it is only dependent on the nutrient influx. This is because of the assumption that spores do not consume any nutrients.

5.3.2 Steady state population number maximization

The long term fitness maximization problem (Problem 2.1) for this model is

$$\begin{aligned} \max_{\theta,\beta} \ & \overline{X} + \overline{S} \\ \text{s.t. } & \text{steady state relationships} \\ & \theta > 0 \\ & \beta > 0 \end{aligned}$$

with a constant nutrient influx $\overline{e}$. Examination of the steady state expressions gives the solution of the optimization problem– the maximum is approached as $\theta \to \infty$ and $\beta \to \infty$.

In other words, it is always better to allocate as much of the population to spores as possible. This is qualitatively consistent with the optimal constant policies derived in the previous chapter.

If steady state population maximization is the driving factor behind evolution, and nutrient influx in the wild is always approximately constant, then we should expect that a *B. subtilis* colony will always form spores, even as the nutrient influx approaches infinity. This is obviously not the case, and will be further examined in Chapters 6 and 7.

5.4 Concluding remarks

This chapter provided an alternative model to address some of the drawbacks of the discrete time model presented in Chapter 4. The issue of the ordering of cell cycle events is resolved by posing the model in continuous time, and a steady state population level is achieved by germination parameterization (non-zero for positive nutrient levels). The proposed model also captures an intuitive relationship between nutrient level and steady state population number, and relative spore allocation with varying θ and β. This model was used to solve

the long term fitness problem for a constant nutrient influx $\overline{e}$, where it was found that the optimal policy is the one that approaches maximal sporulation ($\theta \to \infty$) and zero germination ($\beta \to \infty$). Though similar to the optimal constant policies derived in the previous chapter, the result is not expected since it is suboptimal to have a vegetative population.

The derived optimal policy does not agree with biological observations of sporulating bacterial colonies, where a non-zero vegetative population persists with a non-zero nutrient supply. This leads to interesting questions that motivate the work in Chapters 6 and 7: Why would a colony every choose finite θ and β? Is there a benefit to choosing smaller θ and β? What conditions may lead to a smaller choice of θ and β?

The question pertaining to why a smaller θ and β may be preferable can be answered by looking at Figure 5.3, which shows two (non-competing) populations with identical initial conditions but different θ and β, each subjected to the same nutrient level change $f(t) = 1 + 49 \cdot \mathbf{1}(t - 200)$. In this figure, it is clear that a smaller θ and β will give a faster

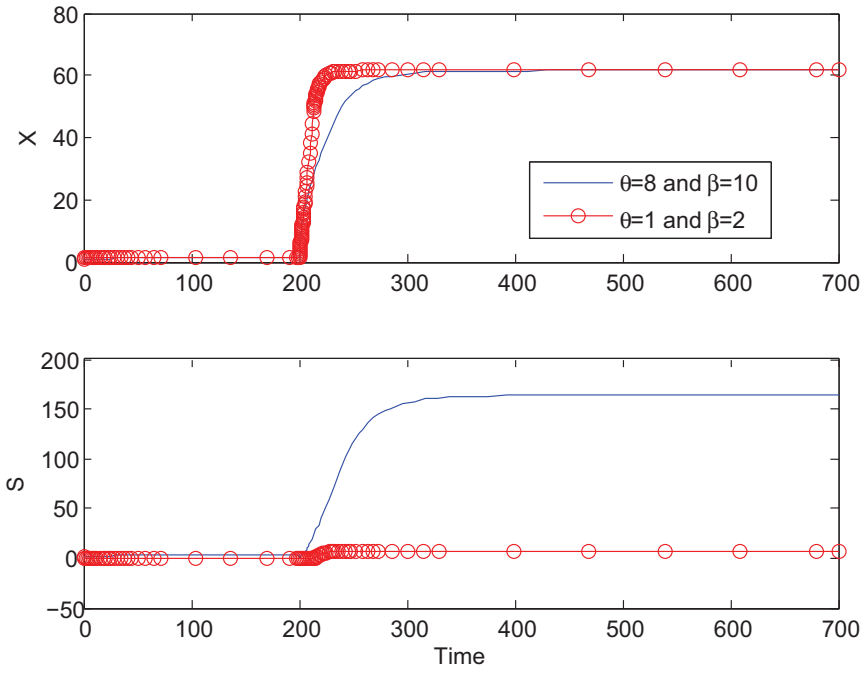

Figure 5.3: Effect of choosing different values for θ and β.

speed of response and settling time, even though the steady state population level may be smaller (relative to the population with larger θ and β). This is important because if these two populations were competing for the *same* resources, the one that is able to respond quicker will have a competitive advantage when nutrients increase. A smaller θ and β can therefore be characterized as being more "aggressive" than the strategy employing larger parameter choices. Since the model developed in this chapter assumed a single population evolving in a vacuum, it is not surprising that the results are not consistent with experimental observations; after all, most biological organisms evolve in a competitive setting [259].

Therefore, competition seems like it should affect the optimal sporulation and germination policies. This important aspect of selecting θ and β leads to the model developed in the next chapter.

Another drawback of the proposed model (and the subsequent models in Chapters 6 and 7) is the assumed rate dependencies for sporulation and germination. Specifically, it is expected that the relative spore allocation should increase when $\overline{f}$ decreases; however, for the assumed sporulation and germination rate dependencies, this spore allocation is independent of $\overline{f}$. This may be remedied by letting sporulation and germination depend on f instead of $\frac{f}{X}$. This does not, however, affect the optimal policies in this chapter, nor will it affect the work in Chapter 7 (see Section 7.5). Thus, for the sake of simplicity, it will be assumed that all of the rates depend on the population-average nutrient level in the sequel.

Chapter 6

Bacterial Behavior; Competing Populations Model I

6.1 Introduction

It was demonstrated at the end of the previous chapter that there may be a benefit to survival strategies that do not commit all resources to spores. Specifically, with identical initial population sizes, a colony with relatively more vegetative cells can respond more quickly to increases in nutrient availability (see Figure 5.3). This leads to a competitive advantage for a population that does not devote all resources to sporulation, but it also introduces a severe drawback: the population becomes more susceptible to decreases in nutrient availability.

Before exploring this trade off in Chapter 7, a general model of competing populations is presented in this chapter. It will be shown in Section 6.4 that a more specialized model is required to perform the desired trade off analysis due to the general model's insensitivity to sporulation and germination policies. This result is consistent with the so-called competitive exclusion principle, discussed in Sections 6.5 and 6.6.

6.2 Model

The competing populations models presented below and in Chapter 7 augment the model from Chapter 5 with an additional population that competes for the same resources.

The general competing populations model is

$$\begin{aligned}
\dot{X}_1 &= (\alpha_{4,1} - \alpha_{1,1} - \alpha_{2,1})\, X_1 + \alpha_{3,1} S_1 \\
\dot{X}_2 &= (\alpha_{4,2} - \alpha_{1,2} - \alpha_{2,2})\, X_2 + \alpha_{3,2} S_2 \\
\dot{S}_1 &= \alpha_{2,1} X_1 - \alpha_{3,1} S_1 \\
\dot{S}_2 &= \alpha_{2,2} X_2 - \alpha_{3,2} S_2 \\
\dot{f} &= -\gamma\,(X_1 + X_2) + e
\end{aligned}$$

where the α_i parameterizations are $(i = 1, 2)$

$$\begin{aligned}
\alpha_{1,i} &= \max\left\{0, u_{1,i} - \frac{u_{1,i}}{l_{1,i}}\frac{f}{X_1 + X_2}\right\} \\
\alpha_{4,i} &= \min\left\{u_{4,i}, \frac{u_{4,i}}{l_{4,i}}\frac{f}{X_1 + X_2}\right\} \\
\alpha_{2,i} &= \max\left\{0, u_2 - \frac{u_2}{\theta_i}\frac{f}{X_1 + X_2}\right\} \\
\alpha_{3,i} &= \min\left\{u_3, \frac{u_3}{\beta_i}\frac{f}{X_1 + X_2}\right\}.
\end{aligned}$$

It is assumed that the two competing populations are identical except for their birth, death, sporulation, and germination rates. In particular, we are assuming that any quorum sensing molecules (e.g. Phr molecules) are the same for both populations, so each cell is able to sense the *total* population density. This is the reason why the α_i's depend on $\frac{f}{X_1+X_2}$, not $\frac{f}{X_1}$ or $\frac{f}{X_2}$. Mathematically, this rate dependence assumption avoids the situation where each population maximizes the total population number by letting $\theta \to \infty$ and $\beta \to \infty$ (similar to the situation presented in Section 5.3.2).

6.3 Equilibria

Suppose that $e = \overline{e}$ is constant. For this input, the corresponding equilibrium values $(\overline{X}_1, \overline{X}_2, \overline{S}_1, \overline{S}_2, \overline{f})$ can be found by setting the derivatives in the model to zero:

$$\begin{aligned}
0 &= (\alpha_{4,1} - \alpha_{1,1} - \alpha_{2,1})\,\overline{X}_1 + \alpha_{3,1}\overline{S}_1 \\
0 &= (\alpha_{4,2} - \alpha_{1,2} - \alpha_{2,2})\,\overline{X}_2 + \alpha_{3,2}\overline{S}_2 \\
0 &= \alpha_{2,1}\overline{X}_1 - \alpha_{3,1}\overline{S}_1 \\
0 &= \alpha_{2,2}\overline{X}_2 - \alpha_{3,2}\overline{S}_2 \\
0 &= -\gamma(\overline{X}_1 + \overline{X}_2) + \overline{e}.
\end{aligned}$$

These equations yield the following set of equations:

$$\begin{aligned}
\alpha_{2,1}\overline{X}_1 &= \alpha_{3,1}\overline{S}_1 \\
\alpha_{2,2}\overline{X}_2 &= \alpha_{3,2}\overline{S}_2 \\
\overline{X}_1 + \overline{X}_2 &= \frac{\overline{e}}{\gamma} \\
\alpha_{4,1} &= \alpha_{1,1} \\
\alpha_{4,2} &= \alpha_{1,2}.
\end{aligned}$$

For $\alpha_{4,1} \neq \alpha_{4,2}$ and $\alpha_{1,1} \neq \alpha_{1,2}$, the last two equalities cannot typically be satisfied simultaneously. However, it is possible to satisfy one equality at a time, which leads to two possible

equilibria. For example, if $\alpha_{4,1} = \alpha_{1,1}$, then all derivatives of the model are zero as long as $\overline{X}_2 = \overline{S}_2 = 0$ and $\alpha_{2,1}\overline{X}_1 = \alpha_{3,1}\overline{S}_1$.

The two equilibria are given in Table 6.1, where c_i is the value of $\frac{f}{X_1+X_2}$ where $\alpha_{4,i} = \alpha_{1,i}$, $i = 1, 2$, which describes the operating points of each equilibrium. Assume that $l_4 \geq l_1$ to reflect the fact that the birth rate becomes smaller when cells start dying, so $c_i = \dfrac{u_{1,i}}{\frac{u_{4,i}}{l_{4,i}} + \frac{u_{1,i}}{l_{1,i}}}$.

Table 6.1: Equilibria for competing populations model with different birth and death rates

	Equilibrium 1 ($\alpha_{4,1} = \alpha_{1,1}$)	Equilibrium 2 ($\alpha_{4,2} = \alpha_{1,2}$)
$\overline{X}_1$	$\frac{\overline{e}}{\gamma}$	0
$\overline{X}_2$	0	$\frac{\overline{e}}{\gamma}$
$\overline{S}_1$	$\frac{\alpha_{4,1}(c_1)}{\alpha_{1,1}(c_1)}\overline{X}_1$	0
$\overline{S}_2$	0	$\frac{\alpha_{4,2}(c_2)}{\alpha_{1,2}(c_2)}\overline{X}_2$
$\overline{f}$	$c_1\overline{X}_1$	$c_2\overline{X}_2$

It will be shown in the next section that under certain conditions, one of these equilibria is locally unstable and the other is locally stable.

6.4 Stability

Without loss of generality, let $c_1 < c_2$, where c_i corresponds to Equilibrium i in Table 6.1.

Theorem 6.4.1. *If X_1, X_2, S_1, S_2, and f are non-negative, the birth, death, sporulation, and germination rates are finite and positive over a nonempty set of values of $\frac{f}{X_1+X_2}$, and $\gamma \ll 1$, then Equilibrium 1 is locally stable and Equilibrium 2 is locally unstable.*

Proof. See Appendix B.1. □

Remark 6.4.2. *The condition $\gamma \ll 1$ allows a simplified proof of the claim. Numerical simulations suggest that the condition is not necessary, but the proof then becomes extremely messy. Since γ should be chosen small to not invalidate the population-level model, the simplification is warranted.*

Remark 6.4.3. *Equilibrium 1 is globally stable if X_1, X_2, S_1, S_2, and f are non-negative. Indeed, the proof of Theorem 6.4.1 included the case when $\frac{f}{X_1+X_2} > c_2$. The only other case that needs to be examined is the point $\left(\overline{X}_1, \overline{X}_2, \overline{S}_1, \overline{S}_2, \overline{f}\right) = (0, 0, 0, 0, f(t))$, which can be shown to be locally unstable; see Appendix B.2.*

6.5 The competitive exclusion principle

Theorem 6.4.1 shows that, in the case of competing populations with different birth and death rates, only one population persists. In particular, the population with the smaller c_i

will survive while the other population becomes extinct. Recall that each c_i is the "resource" level (i.e. value of $\frac{f}{X_1+X_2}$) at which the birth rate is equal to the death rate, or the steady state resource level for population i. Theorem 6.4.1 therefore states that the population that is able to survive at the smaller resource level in steady state will eventually exclude the other population.

This result is consistent with the competitive exclusion principle. Though derived for chemostat models following Lotka-Volterra growth dynamics, this principle states that the population with the smallest steady state, abiotic resource level will approach a finite nonzero density, while the remaining competitors will become extinct [96]. Also called the "R^*-rule" in some texts, the competitive exclusion principle traces its roots back to Volterra [261] and has since then been applied to several extensions of the chemostat models. Though the proof generalizing this principle to a broader class of population models is incorrect (in [6], the "Lyapunov function" is not positive definite), the simplicity of this statement makes it an attractive proposition in ecology.

There are several experimental studies of organisms that seem to follow the competitive exclusion principle. Competition experiments between *E. coli* and *P. aeruginosa* [101], *P. fluorescens* and *A. tumefaciens* [15], *L. casei* and *S. cerevisiae* [176], *C. cochlearium* and *C. tetanomorphum* [147], *Spirillum* sp. and *Pseudomonas* sp. [123, 164], and *Aerobacer* sp. and *Achromobacter* sp. [123] all follow the competitive exclusion principle. In addition, several experimental studies on phytoplankton, higher plants, and some metazoa reveal that this principle is valid when the modeling assumptions are satisfied [96].

Though the competitive exclusion principle predicts low diversity in the wild, it is often (subjectively) observed that ecological systems exhibit a large amount of diversity. This diversity may be maintained by violating the oversimplified modeling assumptions (spatial homogeneity, population interactions only through resource consumption, and time-invariance [96]), but it has also been shown that diversity may be preserved under conditions more closely resembling natural systems. For example, if the resource level fluctuates [98, 155] or if competing populations can consume different resources [5, 6], then different species may coexist (the latter situation giving rise to ecological niches). However, for systems that satisfy the modeling assumptions of Volterra's original system, the competitive exclusion principle is a comforting theoretical result.

Though competitive exclusion has been shown to apply broadly, it does not directly apply to the proposed competing populations model. This is because the proposed model incorporates a "storage-like" state (spores) that make many of the competitive exclusion proofs invalid. However, Theorem 6.4.1 proves that this principle still applies for this specific model.

6.6 Discussion

Though it is appealing that the proposed competing populations model agrees with previous work (even though the rate parameterizations/dependencies and model structure are different), the case of different birth and death rates does not shed any significant insights into the evolutionary roles of the sporulation or germination policies. This is because Theorem

6.4.1 holds regardless of the values of the sporulation or germination parameters (as long as they are positive and finite), so independent tuning of these policies will have no effect on the competitive abilities of a population. In other words, a population may adopt optimal sporulation and germination policies for a particular environment, but it will become extinct when competed against a population with inferior sporulation and germination policies but a lower c_i.

It is possible that the sporulation, germination, birth, and death rates are all dependent, e.g. adjusting the sporulation rate will also change the birth rate. This may be due to genetic interactions or epistasis, a phenomenon where changing one gene affects more than one phenotype in a non-additive manner [180]. Due to the relative complexity of the phosphorelay and its dependence on other cellular networks within the bacteria [161, 245, 255], it is likely that this occurs in *B. subtilis*. However, adjustment of the sporulation and germination policies still takes a back seat to achieving the smallest possible c_i, even if it implies that the associated sporulation and germination policies are severely suboptimal. Bacterial decision-making for populations with different birth and death rates will therefore be disregarded in the remainder of this dissertation since this framework does not provide any insight about the evolution of sporulation.

6.7 Concluding remarks

This chapter introduced a competing populations extension to the continuous time model developed in Chapter 5. In its most general form, both populations have different birth, death, sporulation, and germination rates, and they interact only through resource competition. It was shown that this general model conforms to the competitive exclusion principle, where the population that equilibrates at a higher resource level (in this case, resource $=\frac{f}{X_1+X_2}$) will eventually become extinct. Assuming that the sporulation and germination policies can be tuned independently of the cellular machinery that governs the birth and death rates, the competitive exclusion principle implies that the long term fitness problem does not depend on sporulation or germination. In other words, this situation does not elucidate any interesting information about the survival strategies under study.

Aside from the competitive exclusion outcome, there are other possible shortcomings in the general competing populations model. While it is assumed that the populations only interact through resource competition, there may be other forms of interaction related to the sporulation and germination policies. For example, it has been found that sporulating *B. subtilis* cells export a killing factor and a signaling protein that act cooperatively to block sister cells from sporulating and to cause them to lyse, which introduces a cannibalistic nutrient source [87, 88]. This is also related to the modeling assumption that the nutrient infusion is much larger than the nutrients released from mothercell lysis or cell death, which may affect sporulation decision policies in a competitive setting. For instance, a population that does not sporulate as readily as a competing population will benefit from the release of nutrients from competing mothercells lysing. Though these interactions may be important, they add complexity to a model that is already non-trivial to analyze, so we will continue to employ the simple resource competition assumption in the next chapter.

The assumption of total population sensing may also be invalid. Since the competing populations are genetically distinct, the quorum sensing molecules (i.e. Phr molecules) may be unique for each population. In this case, the rate dependencies would be altered and each population would persist indefinitely. This is because they would be consuming different "resources" in the forms of $\frac{f}{X_1}$ and $\frac{f}{X_2}$, and it has been shown that the competitive exclusion principle does not generally hold for two populations consuming different resources [6, 96]. Though entirely plausible, the inclusion of different rate dependencies for both populations would allow each population to exist almost independently from the other population, which defeats the purpose of the competing populations framework. Therefore, total population sensing will be assumed in the sequel.

The next chapter will examine the special case where the competitive exclusion principle does not hold: Equal birth and death rates for both populations. This framework permits the analysis of various sporulation and germination policies.

Chapter 7

Bacterial Behavior; Competing Populations Model II

7.1 Introduction

The previous chapter examined a competing populations model with different birth and death rates, and it was found that this scenario does not shed much insight into the evolution of sporulation (see Section 6.6). This chapter will therefore study the specialized case of identical birth and death rates for both competing populations. With this restriction, competitive performance will depend on the remaining differences between the populations, which are confined to be the sporulation and germination policies in the following analysis of bacterial survival strategies.

Though often ignored in comparable studies of competing populations due to the difficulty in distinguishing between the two populations [96], the identical birth and death rates scenario may occur in constant natural ecosystems due to natural selection. Since extinction will occur unless a population's c_i is less than or equal to the other population's c_i, selection pressure will result in a non-increasing (with time) overall value of c_i. Since there is a minimum resource level at which a cell can survive (to preserve basic metabolic functions [2]), there is a minimum $c_i^* > 0$ that can be adopted by a population to competitively exclude any other population with a different $c_i \neq c_i^*$. Thus, all populations will be evolving to attain c_i^*. With sufficient evolutionary time, this value will be procured and maintained because any other strategy will be competitively excluded. Therefore, the situation of identical birth and death rates is plausible from an evolutionary point of view.

Within this framework, the population maximization problem presented in Section 5.3.2 can be more closely analyzed. In the next section, it is shown that $\approx 100\%$ sporulation is no longer the best strategy under all conditions due to the trade off between population number volatility and insensitivity to nutrient change. After a type of input-output stability is proved in Section 7.4, approximations for the total population numbers are derived in Section 7.5 for the nonlinear competing populations model. With the introduction of environmental and evolutionary models, it is shown in Section 7.10.1 that, relative to the theoretically-optimal behavior, sporulating bacteria behave optimistically in poor conditions

and pessimistically in favorable conditions. This behavior is compared to a general class of risk-spreading strategies in Section 7.10.2.

7.2 Model

The second competing populations model is

$$\begin{aligned}
\dot{X}_1 &= (\alpha_4 - \alpha_1 - \alpha_{2,1})\, X_1 + \alpha_{3,1} S_1 \\
\dot{X}_2 &= (\alpha_4 - \alpha_1 - \alpha_{2,2})\, X_2 + \alpha_{3,2} S_2 \\
\dot{S}_1 &= \alpha_{2,1} X_1 - \alpha_{3,1} S_1 \\
\dot{S}_2 &= \alpha_{2,2} X_2 - \alpha_{3,2} S_2 \\
\dot{f} &= -\gamma\,(X_1 + X_2) + e
\end{aligned}$$

where the α_i parameterizations are

$$\begin{aligned}
\alpha_1 &= \max\left\{0, u_1 - \frac{u_1}{l_1}\frac{f}{X_1 + X_2}\right\} \\
\alpha_4 &= \min\left\{u_4, \frac{u_4}{l_4}\frac{f}{X_1 + X_2}\right\} \\
\alpha_{2,i} &= \max\left\{0, u_2 - \frac{u_2}{\theta_i}\frac{f}{X_1 + X_2}\right\} \\
\alpha_{3,i} &= \min\left\{u_3, \frac{u_3}{\beta_i}\frac{f}{X_1 + X_2}\right\}.
\end{aligned}$$

for $i = 1, 2$. Note that this model is identical to the model in Chapter 6 except for $\alpha_{4,1} = \alpha_{4,2} = \alpha_4$ and $\alpha_{3,1} = \alpha_{3,2} = \alpha_3$ (identical birth and death rates).

7.2.1 Benefit of "aggressive" decision policy

The simple simulation results given in Figure 7.1 (created with $X_1(0) = X_2(0) = 1$, $S_1(0) = S_2(0) = 1$, $f(0) = 1$, and $e(t) = 0.001 + .999 \cdot \mathbf{1}(t - 400)$) indicate that this model captures the competitive advantage of the population with smaller θ and β due to the quicker response time. The competitive advantage leads to better performance with respect to the $\max \overline{X} + \overline{S}$ metric. As in the single population model, the numerical values $u_1 = 0.3$, $u_2 = 0.5$, $u_3 = u_4 = 3 \ln 2$, $l_1 = 1$, and $l_4 = 30$ were used in the simulations.

The behavior captured by the model brings up the obvious questions: under what environmental conditions is it better to choose a larger θ and β, and under what conditions is it better to choose a smaller θ and β? Unfortunately, this question is not as easy to answer as the single population model (where is was always better to choose θ and β large) because there are infinitely many equilibrium points for a given constant nutrient influx $\overline{e}$ (see Section 7.3). Simulations suggest that the equilibrium point that the system converges to is dependent on the initial conditions of the simulation; this makes it possible to choose

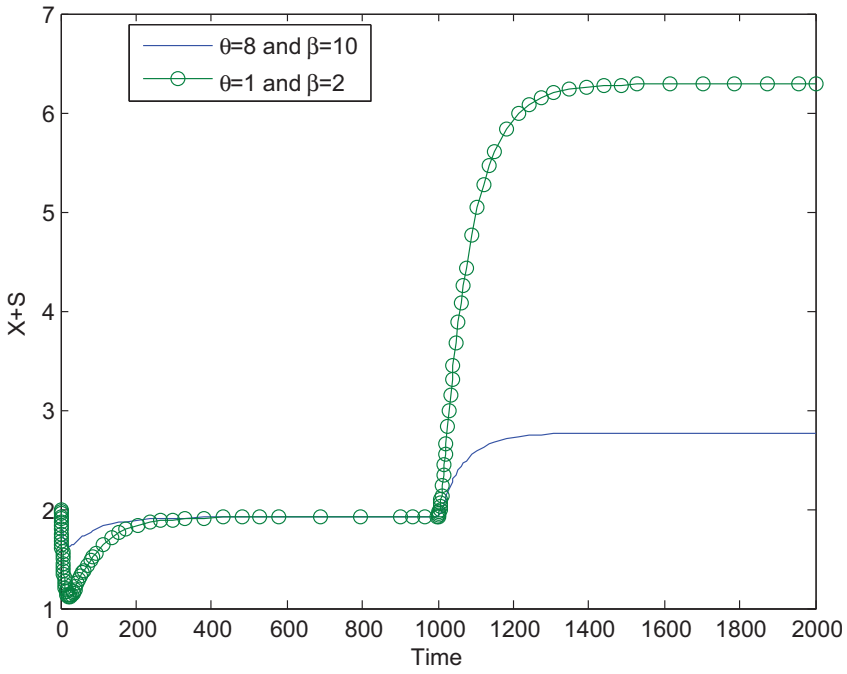

Figure 7.1: Demonstration of a population with smaller θ and β performing better (w.r.t. $\max \overline{X} + \overline{S}$).

initial conditions to favor any particular choice of θ and β with respect to $\max \overline{X} + \overline{S}$, for the same nutrient influx $\overline{e}$. An expression for the solution of the system of equations cannot be explicitly found due to the nonlinearities, which makes analytical results difficult to find/prove.

7.3 Equilibria

Suppose that $e = \overline{e} > 0$ is constant. For this input, the corresponding equilibrium values $(\overline{X}_1, \overline{X}_2, \overline{S}_1, \overline{S}_2, \overline{f})$ can be found by setting the derivatives of the model to zero:

$$\begin{aligned}
0 &= (\alpha_4 - \alpha_1 - \alpha_{2,1})\,\overline{X}_1 + \alpha_{3,1}\overline{S}_1 \\
0 &= (\alpha_4 - \alpha_1 - \alpha_{2,2})\,\overline{X}_2 + \alpha_{3,2}\overline{S}_2 \\
0 &= \alpha_{2,1}\overline{X}_1 - \alpha_{3,1}\overline{S}_1 \\
0 &= \alpha_{2,2}\overline{X}_2 - \alpha_{3,2}\overline{S}_2 \\
0 &= -\gamma(\overline{X}_1 + \overline{X}_2) + \overline{e}.
\end{aligned}$$

These equations yield the following set of equations:

$$\begin{aligned}
\alpha_{2,1}\overline{X}_1 &= \alpha_{3,1}\overline{S}_1 \\
\alpha_{2,2}\overline{X}_2 &= \alpha_{3,2}\overline{S}_2 \\
\overline{X}_1 + \overline{X}_2 &= \frac{\overline{e}}{\gamma} \\
\alpha_4 &= \alpha_1.
\end{aligned}$$

As before, the last equation gives a constant operating point $\frac{\overline{f}}{\overline{X}_1+\overline{X}_2} \equiv c = \frac{u_1}{\frac{u_4}{l_4}+\frac{u_1}{l_1}}$. However, unlike the single population case, the assumptions $\alpha_{4,1} = \alpha_{4,2}$ and $\alpha_{1,1} = \alpha_{1,2}$ leave only four independent equations to solve for the five unknown equilibrium values $(\overline{X}_1, \overline{X}_2, \overline{S}_1, \overline{S}_2, \overline{f})$. The equilibrium values are therefore not unique, and there exists an infinite number of values that satisfy the equilibrium conditions for a constant $\overline{e}$.

By inspection, the positive cone

$$\mathcal{S} = \left\{ \left(\overline{X}_1, \overline{X}_2, \overline{S}_1, \overline{S}_2, \overline{f}\right) : \overline{X}_1 > 0, \overline{X}_2 > 0, \overline{S}_1 > 0, \overline{S}_2 > 0, \overline{f} > 0 \right\}$$

is included in the set of allowable equilibrium vales, so both populations may coexist. This coexistence is consistent with other model structures with identical birth and death rates [96].

7.4 Stability

Assessing the local stability of any equilibrium by examining the eigenvalues of the linearized system leads to inconclusive results because the Jacobian has an eigenvalue at 0 (see Appendix B.3). Thus, the (input-output) stability of the nonlinear system with nonzero nutrient influx cannot be immediately determined– even if the linearized system had eigenvalues with negative real part, asymptotic stability of an equilibrium point does not imply bounded input bounded output stability.

Instead, the stability analysis will proceed in the following manner: Assume that $(X_{1,0}, X_{2,0}, S_{1,0}, S_{2,0}, f_0)$ is an equilibrium point corresponding to the input $\overline{e}$. Note that this point is not unique (see Section 7.3). Now, assume that the input is changed to $e = \overline{e} + \epsilon$, where ϵ is constant, and expand the states as power series in ϵ:

$$\begin{array}{rcccccccccc}
X_1 &=& X_{1,0} &+& X_{1,1}\epsilon &+& X_{1,2}\epsilon^2 &+& X_{1,3}\epsilon^3 &+& \cdots \\
X_2 &=& X_{2,0} &+& X_{2,1}\epsilon &+& X_{2,2}\epsilon^2 &+& X_{2,3}\epsilon^3 &+& \cdots \\
S_1 &=& S_{1,0} &+& S_{1,1}\epsilon &+& S_{1,2}\epsilon^2 &+& S_{1,3}\epsilon^3 &+& \cdots \\
S_2 &=& S_{2,0} &+& S_{2,1}\epsilon &+& S_{2,2}\epsilon^2 &+& S_{2,3}\epsilon^3 &+& \cdots \\
f &=& f_0 &+& f_1\epsilon &+& f_2\epsilon^2 &+& f_3\epsilon^3 &+& \cdots
\end{array}$$

where the coefficients of the powers of ϵ are independent of ϵ. If it can be shown that all of the coefficients of ϵ^k, $k = 1, 2, \ldots$, are bounded, then it can be concluded that the competing populations model with identical birth/death rates is bounded input bounded

output (BIBO) stable for the class of piecewise-constant inputs. Stability for this class of inputs (simply denoted as "BIBO stability" in the sequel) is sufficient for the long-term fitness maximization framework considered in this dissertation.

An examination between the relationship between the power series expansion in ϵ and a Taylor series expansion will be useful in the following analysis. Specifically, it will help in the power series expansion of $\frac{1}{X_1+X_2}$. With slight abuse of notation, consider a variable $X(\epsilon)$ expanded around some operating point at $\overline{\epsilon} = 0$, where $X_0 := X(0)$. We can write out expansions based on a power series in ϵ and in terms of deviations from the operating point $\overline{X}$.

$$\begin{aligned} X(\epsilon) &= X_0 + X_1\epsilon + X_2\epsilon^2 + X_3\epsilon^3 + \cdots \\ &= X_0 + \frac{\partial}{\partial\epsilon}(X)\bigg|_{\overline{\epsilon}} \delta\epsilon + \frac{1}{2}\,\frac{\partial^2}{\partial\epsilon^2}(X)\bigg|_{\overline{\epsilon}} (\delta\epsilon)^2 + \frac{1}{3!}\,\frac{\partial^3}{\partial\epsilon^3}(X)\bigg|_{\overline{\epsilon}} (\delta\epsilon)^3 + \cdots \end{aligned}$$

where $\delta\epsilon = \epsilon$ since $\overline{\epsilon} = 0$. Thus, we have the following relationships:

$$\begin{aligned} X_1 &= \frac{\partial}{\partial\epsilon}(X)\bigg|_{\overline{\epsilon}} \\ X_2 &= \frac{1}{2}\,\frac{\partial^2}{\partial\epsilon^2}(X)\bigg|_{\overline{\epsilon}} \\ X_3 &= \frac{1}{3!}\,\frac{\partial^3}{\partial\epsilon^3}(X)\bigg|_{\overline{\epsilon}} \\ &\vdots \end{aligned}$$

The quantity $\frac{1}{X(\epsilon)}$ can therefore be expanded as a power series in ϵ as

$$\begin{aligned} \frac{1}{X(\epsilon)} &= \sum_{n=0}^{\infty} \left(\frac{1}{X}\right)_n \epsilon^n \\ &= \sum_{n=0}^{\infty} \frac{1}{n!} \left(\frac{1}{X}\right)^{(n)}\bigg|_{\overline{\epsilon}} \epsilon^n \end{aligned}$$

where $(x)^{(n)} := \frac{\partial^n}{\partial\epsilon^n}(x)$. The coefficient of the n^{th} power of ϵ is then

$$\left(\frac{1}{X}\right)_n = \frac{1}{n!} \left(\frac{1}{X}\right)^{(n)}\bigg|_{\overline{\epsilon}}.$$

The notation for the evaluation of the derivative at $\overline{\epsilon}$ will be omitted in the sequel for simplicity.

Lemma 7.4.1. *$\left(\frac{1}{X}\right)^{(n)}$ is affine in $\frac{\partial^n}{\partial\epsilon^n}(X)$.*

Proof. This claim will be shown by induction.

For the base case $n = 1$,

$$\begin{aligned}\left(\frac{1}{X}\right)^{(1)} &= \frac{\partial}{\partial\epsilon}\left(\frac{1}{X}\right)\\ &= -\frac{1}{X_0^2}\frac{\partial}{\partial\epsilon}(X).\end{aligned}$$

Now, for the inductive step, suppose that $\left(\frac{1}{X}\right)^{(n-1)}$ is affine in $\frac{\partial^{n-1}}{\partial\epsilon^{n-1}}(X)$. Then, we can write $\left(\frac{1}{X}\right)^{(n-1)}$ as

$$\left(\frac{1}{X}\right)^{(n-1)} = C + D\frac{\partial^{n-1}}{\partial\epsilon^{n-1}}(X),$$

where C and D are not functions of $\frac{\partial^{n-1}}{\partial\epsilon^{n-1}}(X)$. Taking the derivative yields

$$\begin{aligned}\left(\frac{1}{X}\right)^{(n)} &= \frac{\partial}{\partial\epsilon}\left(\frac{1}{X}\right)^{(n-1)}\\ &= \frac{\partial C}{\partial\epsilon} + \frac{\partial D}{\partial\epsilon}\frac{\partial^{n-1}}{\partial\epsilon^{n-1}}(X) + D\frac{\partial^n}{\partial\epsilon^n}(X)\end{aligned}$$

which is affine in $\frac{\partial^n}{\partial\epsilon^n}(X)$. □

Remark 7.4.2. *This Lemma gives a very useful property. If $G = G_0 + G_1\epsilon + G_2\epsilon^2 + \cdots$, then the coefficient in front of ϵ^n for the expansion of $\frac{1}{G}$ will be linear in G_n. In other words, $\left(\frac{1}{G}\right)_n$ is linear in G_n.*

Lemma 7.4.1 can also be visualized in terms of the power series expansion of X.

Corollary 7.4.3. *If $X = X_0 + X_1\epsilon + X_2\epsilon^2 + \cdots$, then*

$$\left(\frac{1}{X}\right)_n = \frac{1}{n!}\left(\frac{1}{X}\right)^{(n)} = C_n - \frac{X_n}{X_0^2}$$

where C_n is not a function of $\frac{\partial^n}{\partial\epsilon^n}(X)$.

Proof. The claim will be shown by induction.

Recall that

$$\begin{aligned}X_1 &= \frac{\partial}{\partial\epsilon}(X)\bigg|_{\overline{\epsilon}}\\ X_2 &= \frac{1}{2}\,\frac{\partial^2}{\partial\epsilon^2}(X)\bigg|_{\overline{\epsilon}}\\ X_3 &= \frac{1}{3!}\,\frac{\partial^3}{\partial\epsilon^3}(X)\bigg|_{\overline{\epsilon}}\\ &\vdots\end{aligned}$$

For the base case ($n = 1$),

$$\begin{aligned}\left(\frac{1}{X}\right)^{(1)} &= \frac{\partial}{\partial\epsilon}\left(\frac{1}{X}\right)\\ &= -\frac{1}{X_0^2}\frac{\partial}{\partial\epsilon}(X)\\ &= -\frac{X_1}{X_0^2}\end{aligned}$$

where $C_1 = 0$ is not a function of $\frac{\partial}{\partial\epsilon}(X)$.

For the inductive step, assume that

$$\left(\frac{1}{X}\right)_{n-1} = \frac{1}{(n-1)!}\left(\frac{1}{X}\right)^{(n-1)} = C_{n-1} - \frac{X_{n-1}}{X_0^2},$$

where C_{n-1} is not a function of $\frac{\partial^{n-1}}{\partial\epsilon^{n-1}}(X)$. Then,

$$\begin{aligned}\left(\frac{1}{X}\right)^{(n)} &= \frac{\partial}{\partial\epsilon}\left(\frac{1}{X}\right)^{(n-1)}\\ &= (n-1)!\frac{\partial C_{n-1}}{\partial\epsilon} - (n-1)!\frac{\partial}{\partial\epsilon}\left(\frac{\frac{1}{(n-1)!}\frac{\partial^{n-1}}{\partial\epsilon^{n-1}}(X)}{X_0^2}\right)\\ &= (n-1)!\frac{\partial C_{n-1}}{\partial\epsilon} - \frac{X_0^2\frac{\partial^n}{\partial\epsilon^n}(X) - 2\frac{\partial^{n-1}}{\partial\epsilon^{n-1}}(X)X_0\frac{\partial}{\partial\epsilon}(X)}{X_0^4}\\ &= (n-1)!\frac{\partial C_{n-1}}{\partial\epsilon} + \frac{2\frac{\partial^{n-1}}{\partial\epsilon^{n-1}}(X)X_0\frac{\partial}{\partial\epsilon}(X)}{X_0^4} - \frac{\frac{\partial^n}{\partial\epsilon^n}(X)}{X_0^2}\\ &= \widetilde{C}_n - \frac{\frac{\partial^n}{\partial\epsilon^n}(X)}{X_0^2}\\ &= n!\left(C_n - \frac{X_n}{X_0^2}\right)\end{aligned}$$

which completes the proof. □

A more specific form of C_n can be obtained.

Corollary 7.4.4. *If* $X = X_0 + X_1\epsilon + X_2\epsilon^2 + \cdots$ *and*

$$\left(\frac{1}{X}\right)_n = C_n - \frac{X_n}{X_0^2},$$

then, for $n \geq 2$,

$$C_n = (-1)^n\frac{X_1^n}{X_0^{n+1}} + \frac{z_n y_n}{g_n}$$

where $z_n \in \mathbb{R}$, $g_n \in \{X_0, X_0^2, X_0^3, \ldots\}$ *and* y_n *is drawn from the set of monomials of* $(X_1, X_2, \ldots, X_{n-1})$ *excluding the subset of monomials of* (X_1).

Proof. The claim will be shown by induction.

For the base case ($n = 2$),

$$\begin{aligned}\left(\frac{1}{X}\right)_2 &= \frac{1}{2}\frac{\partial^2}{\partial\epsilon^2}\left(\frac{1}{X}\right)\\ &= \frac{1}{2}\left(\frac{2}{X_0^3}\left(\frac{\partial}{\partial\epsilon}(X)\right)^2 - \frac{1}{X_0^2}\frac{\partial^2}{\partial\epsilon^2}(X)\right)\\ &= \frac{X_1^2}{X_0^3} - \frac{X_2}{X_0^2}.\end{aligned}$$

Thus, $C_2 = \frac{X_1^2}{X_0^3}$ is consistent with the hypothesis with $z_2 = 0$.

For the inductive step, assume

$$\begin{aligned}\left(\frac{1}{X}\right)_{n-1} &= \frac{1}{(n-1)!}\frac{\partial^{n-1}}{\partial\epsilon^{n-1}}\left(\frac{1}{X}\right)\\ &= (-1)^{n-1}\frac{X_1^{n-1}}{X_0^n} + \frac{z_{n-1}y_{n-1}}{g_{n-1}} - \frac{X_{n-1}}{X_0^2}.\end{aligned}$$

Then,

$$\begin{aligned}\left(\frac{1}{X}\right)_n &= \frac{1}{n!}\frac{\partial^n}{\partial\epsilon^n}\left(\frac{1}{X}\right)\\ &= \frac{(n-1)!}{n!}\frac{\partial}{\partial\epsilon}\left[(-1)^{n-1}\frac{X_1^{n-1}}{X_0^n} + \frac{z_{n-1}y_{n-1}}{g_{n-1}} - \frac{X_{n-1}}{X_0^2}\right]\\ &= \frac{1}{n}\left[(-1)^{n-1}\frac{(n-1)X_0^n\left(\frac{\partial}{\partial\epsilon}(X)\right)^{n-2}\frac{\partial^2}{\partial\epsilon^2}(X) - n\left(\frac{\partial}{\partial\epsilon}(X)\right)^n X_0^{n-1}}{X_0^{2n}}\right.\\ &\qquad \left. + \frac{\partial}{\partial\epsilon}\frac{z_{n-1}y_{n-1}}{g_{n-1}} + \frac{2X_1X_{n-1}}{X_0^3} - \frac{nX_n}{X_0^2}\right]\\ &= \frac{1}{n}\left[(-1)^{n-1}\frac{2(n-1)X_1^{n-2}X_2}{X_0^n} + \frac{\partial}{\partial\epsilon}\frac{z_{n-1}y_{n-1}}{g_{n-1}} + \frac{2X_1X_{n-1}}{X_0^3}\right]\\ &\qquad + (-1)^n\frac{X_1^n}{X_0^{n+1}} - \frac{X_n}{X_0^2}\end{aligned}$$

Note that the term $\frac{\partial}{\partial\epsilon}\frac{z_{n-1}y_{n-1}}{g_{n-1}}$ is

$$\begin{aligned}\frac{\partial}{\partial\epsilon}\frac{z_{n-1}y_{n-1}}{g_{n-1}} &= z_{n-1}\frac{g_{n-1}\frac{\partial}{\partial\epsilon}(y_{n-1}) - y_{n-1}\frac{\partial}{\partial\epsilon}(g_{n-1})}{g_{n-1}^2}\\ &= z_{n-1}\frac{\frac{\partial}{\partial\epsilon}(y_{n-1})}{g_{n-1}} - z_{n-1}\frac{y_{n-1}\frac{\partial}{\partial\epsilon}(g_{n-1})}{g_{n-1}^2}\end{aligned}$$

where $\frac{\partial}{\partial \epsilon}(y_{n-1})$ and $y_{n-1}\frac{\partial}{\partial \epsilon}(g_{n-1})$ belong to the set of monomials of $(X_1, X_2, \ldots, X_{n-1})$ excluding the subset of monomials of (X_1). Indeed, the only way the subset of monomials of (X_1) could appear at this step is if y_{n-1} was drawn from this subset.

Therefore, we can express $\left(\frac{1}{X}\right)_n$ as

$$\left(\frac{1}{X}\right)_n = \frac{z_n y_n}{g_n} + (-1)^n \frac{X_1^n}{X_0^{n+1}} - \frac{X_n}{X_0^2}$$

where z_n, y_n, and g_n conform to the definitions in the corollary statement. □

Remark 7.4.5. *The description of the set from which y_n is drawn excludes polynomials such as X_1, X_1^3, X_1^{10}, etc.; the condition states that the only way X_1 shows up is when it is multiplied by another monomial of $(X_2, \ldots, X_{n-1})$.*

Remark 7.4.6. *Corollaries 7.4.3 and 7.4.4 will be useful in deriving the steady state dynamics for the coefficients of ϵ^k, $k \geq 2$ (see Theorem 7.4.12).*

Remark 7.4.7. *The set from which g_n is drawn can be shown to be limited to $\{X_0, X_0^2, \ldots, X_0^n\}$, but it is immaterial for the main purposes of this Corollary. Additionally, the set from which z_n is drawn can be shown to be $\mathbb{Z}$, but its usefulness does not merit the attention.*

We will often encounter terms such as

$$\frac{fX_1}{X_1 + X_2} = \sum_{n=0}^{\infty} \left(\frac{fX_1}{X_1 + X_2}\right)_n \epsilon^n$$

where it is of interest to find an expression for $\left(\frac{fX_1}{X_1+X_2}\right)_n$. This is a straightforward calculation:

$$\begin{aligned}\frac{fX_1}{X_1 + X_2} &= \left(\sum_{n=0}^{\infty} f_n \epsilon^n\right)\left(\sum_{n=0}^{\infty} X_{1,n}\epsilon^n\right)\left(\sum_{n=0}^{\infty}\left(\frac{1}{G}\right)_n \epsilon^n\right) \\ &= \sum_{n=0}^{\infty}\sum_{j=0}^{n}\sum_{i=0}^{j} f_i X_{1,j-i}\left(\frac{1}{G}\right)_{n-j}\epsilon^n\end{aligned}$$

where $G := X_1 + X_2$ for notational simplicity. Thus,

$$\left(\frac{fX_1}{X_1 + X_2}\right)_n = \sum_{j=0}^{n}\sum_{i=0}^{j} f_i X_{1,j-i}\left(\frac{1}{G}\right)_{n-j}.$$

Notice that this is linear in $(f_n, X_{1,n}, G_n)$ (from Lemma 7.4.1), where $G_n = X_{1,n} + X_{2,n}$. Therefore, *the coefficients in the power series expansion of the state equations will be governed by linear systems* (with possibly nonlinear forcing functions). In other words, the state equation for $X_{1,n}$ will be linear in $X_{1,n}$, $X_{2,n}$, $S_{1,n}$, $S_{2,n}$, and f_n.

Returning to the original system, assume that $c \leq \min\{\theta_1, \theta_2, \beta_1, \beta_2\}$. Since ϵ is constant, the state equations are

$$\begin{aligned}
\sum_{n=1}^{\infty} \dot{X}_{1,n}\epsilon^n &= \sum_{n=1}^{\infty} \left[\left(\frac{u_4}{l_4} + \frac{u_1}{l_1} + \frac{u_2}{\theta_1} \right) \left(\frac{fX_1}{X_1 + X_2} \right)_n - (u_1 + u_2) X_{1,n} + \frac{u_3}{\beta_1} \left(\frac{fS_1}{X_1 + X_2} \right)_n \right] \epsilon^n \\
\sum_{n=1}^{\infty} \dot{X}_{2,n}\epsilon^n &= \sum_{n=1}^{\infty} \left[\left(\frac{u_4}{l_4} + \frac{u_1}{l_1} + \frac{u_2}{\theta_2} \right) \left(\frac{fX_2}{X_1 + X_2} \right)_n - (u_1 + u_2) X_{2,n} + \frac{u_3}{\beta_2} \left(\frac{fS_2}{X_1 + X_2} \right)_n \right] \epsilon^n \\
\sum_{n=1}^{\infty} \dot{S}_{1,n}\epsilon^n &= \sum_{n=1}^{\infty} \left[u_2 X_{1,n} - \frac{u_2}{\theta_1} \left(\frac{fX_1}{X_1 + X_2} \right)_n - \frac{u_3}{\beta_1} \left(\frac{fS_1}{X_1 + X_2} \right)_n \right] \epsilon^n \\
\sum_{n=1}^{\infty} \dot{S}_{2,n}\epsilon^n &= \sum_{n=1}^{\infty} \left[u_2 X_{2,n} - \frac{u_2}{\theta_2} \left(\frac{fX_2}{X_1 + X_2} \right)_n - \frac{u_3}{\beta_2} \left(\frac{fS_2}{X_1 + X_2} \right)_n \right] \epsilon^n \\
\sum_{n=1}^{\infty} \dot{f}_n\epsilon^n &= \sum_{n=1}^{\infty} \left[-\gamma \left(X_{1,n} + X_{2,n} \right) \right] \epsilon^n + \epsilon
\end{aligned}$$

where the ϵ^0 term drops out because it is assumed that $(X_{1,0}, X_{2,0}, S_{1,0}, S_{2,0}, f_0)$ is an equilibrium corresponding to the input $\overline{e}$.

Starting with $n = 1$, the equations governing the dynamics of $X_{1,1}$, $X_{2,1}$, $S_{1,1}$, $S_{2,1}$, and f_1 can be isolated by looking at the coefficients of the ϵ^1 terms. For $X_{1,1}$,

$$\dot{X}_{1,1} = \left(\frac{u_4}{l_4} + \frac{u_1}{l_1} + \frac{u_2}{\theta_1} \right) \left(\frac{fX_1}{G} \right)_1 - (u_1 + u_2) X_{1,1} + \frac{u_3}{\beta_1} \left(\frac{fS_1}{G} \right)_1$$

where

$$\begin{aligned}
\left(\frac{fX_1}{G} \right)_1 &= \sum_{j=0}^{1} \sum_{i=0}^{j} f_i X_{1,j-i} \left(\frac{1}{G} \right)_{1-j} \\
&= -\frac{f_0 X_{1,0} G_1}{G_0^2} + \frac{f_0 X_{1,1}}{G_0} + \frac{f_1 X_{1,0}}{G_0} \\
&= -c \frac{X_{1,0}}{X_{1,0} + X_{2,0}} \left(X_{1,1} + X_{2,1} \right) + c X_{1,1} + \frac{X_{1,0}}{X_{1,0} + X_{2,0}} f_1 \\
\left(\frac{fS_1}{G} \right)_1 &= \sum_{j=0}^{1} \sum_{i=0}^{j} f_i S_{1,j-i} \left(\frac{1}{G} \right)_{1-j} \\
&= -\frac{f_0 S_{1,0} G_1}{G_0^2} + \frac{f_0 S_{1,1}}{G_0} + \frac{f_1 S_{1,0}}{G_0} \\
&= -c \frac{S_{1,0}}{X_{1,0} + X_{2,0}} \left(X_{1,1} + X_{2,1} \right) + c S_{1,1} + \frac{S_{1,0}}{X_{1,0} + X_{2,0}} f_1
\end{aligned}$$

where $c = \frac{f_0}{X_{1,0} + X_{2,0}}$. Notice that these terms are linear in $X_{1,1}$, $X_{2,1}$, $S_{1,1}$, $S_{2,1}$, and f_1. The

state equation is therefore

$$\begin{aligned}\dot{X}_{1,1} = &\left[\left(\frac{u_4}{l_4}+\frac{u_1}{l_1}+\frac{u_2}{\theta_1}\right)c\frac{X_{2,0}}{X_{1,0}+X_{2,0}} - (u_1+u_2) - \frac{u_3}{\beta_1}c\frac{S_{1,0}}{X_{1,0}+X_{2,0}}\right]X_{1,1}\\ &+\left[-\left(\frac{u_4}{l_4}+\frac{u_1}{l_1}+\frac{u_2}{\theta_1}\right)c\frac{X_{1,0}}{X_{1,0}+X_{2,0}} - \frac{u_3}{\beta_1}c\frac{S_{1,0}}{X_{1,0}+X_{2,0}}\right]X_{2,1}\\ &+\left[\frac{u_3}{\beta_1}c\right]S_{1,1} + [0]S_{2,1} + \left[\left(\frac{u_4}{l_4}+\frac{u_1}{l_1}+\frac{u_2}{\theta_1}\right)\frac{X_{1,0}}{X_{1,0}+X_{2,0}} + \frac{u_3}{\beta_1}\frac{S_{1,0}}{X_{1,0}+X_{2,0}}\right]f_1\end{aligned}$$

The other state equations can found similarly:

$$\begin{aligned}\dot{X}_{2,1} = &\left[-\left(\frac{u_4}{l_4}+\frac{u_1}{l_1}+\frac{u_2}{\theta_2}\right)c\frac{X_{2,0}}{X_{1,0}+X_{2,0}} - \frac{u_3}{\beta_2}c\frac{S_{2,0}}{X_{1,0}+X_{2,0}}\right]X_{1,1}\\ &+\left[\left(\frac{u_4}{l_4}+\frac{u_1}{l_1}+\frac{u_2}{\theta_2}\right)c\frac{X_{1,0}}{X_{1,0}+X_{2,0}} - (u_1+u_2) - \frac{u_3}{\beta_2}c\frac{S_{2,0}}{X_{1,0}+X_{2,0}}\right]X_{2,1}\\ &+[0]S_{1,1} + \left[\frac{u_3}{\beta_2}c\right]S_{2,1} + \left[\left(\frac{u_4}{l_4}+\frac{u_1}{l_1}+\frac{u_2}{\theta_2}\right)\frac{X_{2,0}}{X_{1,0}+X_{2,0}} + \frac{u_3}{\beta_2}\frac{S_{2,0}}{X_{1,0}+X_{2,0}}\right]f_1\end{aligned}$$

$$\begin{aligned}\dot{S}_{1,1} = &\left[u_2 - \frac{u_2}{\theta_1}c\frac{X_{2,0}}{X_{1,0}+X_{2,0}} + \frac{u_3}{\beta_1}c\frac{S_{1,0}}{X_{1,0}+X_{2,0}}\right]X_{1,1}\\ &+\left[\frac{u_2}{\theta_1}c\frac{X_{1,0}}{X_{1,0}+X_{2,0}} + \frac{u_3}{\beta_1}c\frac{S_{1,0}}{X_{1,0}+X_{2,0}}\right]X_{2,1}\\ &+\left[-\frac{u_3}{\beta_1}c\right]S_{1,1} + [0]S_{2,1} + \left[-\frac{u_2}{\theta_1}\frac{X_{1,0}}{X_{1,0}+X_{2,0}} - \frac{u_3}{\beta_1}\frac{S_{1,0}}{X_{1,0}+X_{2,0}}\right]f_1\end{aligned}$$

$$\begin{aligned}\dot{S}_{2,1} = &\left[\frac{u_2}{\theta_2}c\frac{X_{2,0}}{X_{1,0}+X_{2,0}} + \frac{u_3}{\beta_2}c\frac{S_{2,0}}{X_{1,0}+X_{2,0}}\right]X_{1,1}\\ &+\left[u_2 - \frac{u_2}{\theta_2}c\frac{X_{1,0}}{X_{1,0}+X_{2,0}} + \frac{u_3}{\beta_2}c\frac{S_{2,0}}{X_{1,0}+X_{2,0}}\right]X_{2,1}\\ &+[0]S_{1,1} + \left[-\frac{u_3}{\beta_2}c\right]S_{2,1} + \left[-\frac{u_2}{\theta_2}\frac{X_{2,0}}{X_{1,0}+X_{2,0}} - \frac{u_3}{\beta_2}\frac{S_{2,0}}{X_{1,0}+X_{2,0}}\right]f_1\end{aligned}$$

$$\dot{f}_1 = -\gamma\left(X_{1,1}+X_{2,1}\right)+1$$

Letting $x := [X_{1,1}\ X_{2,1}\ S_{1,1}\ S_{2,1}\ f_1]^T$, the first-order dynamics are governed by

$$\dot{x} = A_1 x + B_1 \tag{7.1}$$

where $B_1 = [0\ 0\ 0\ 0\ 1]^T$. Note that this is the same system that describes the dynamics of small deviation away from the equilibrium $(X_{1,0}, X_{2,0}, S_{1,0}, S_{2,0}, f_0)$, i.e. it is the linearized system.

Theorem 7.4.8. *If $S_{1,0}, S_{2,0}$, and f_0 are non-negative, $X_{1,0}$ and $X_{2,0}$ are positive, the birth, death, sporulation, and germination rates are finite and positive over a nonempty set of values of $\frac{f}{X_1+X_2}$, and $\gamma \ll 1$, then System (7.1) has bounded states for the class of bounded piecewise constant inputs.*

Proof. See Appendix B.3. □

Remark 7.4.9. *Like Theorem 6.4.1, the condition $\gamma \ll 1$ allows a simplified proof of the claim. Numerical simulations suggest that the condition is not necessary, but the proof then becomes extremely messy. Since γ should be chosen small to not invalidate the population-level model, the simplification is warranted.*

Remark 7.4.10. *The input to state transfer function derived in the proof reveals that all of the states will approach a constant value in response to a constant input.*

With the base case ($n = 1$) established in Theorem 7.4.8, induction may be used to show that all terms in the power series expansion are bounded. To show this, assume that all coefficients of ϵ^k, $k = 1, 2, \ldots, n-1$ are bounded. We will now argue that the coefficients of ϵ^n are also bounded, which will complete the induction and prove that the competing populations model with identical birth and death rates is BIBO stable.

Though it was established that $\left(\frac{fX_1}{X_1+X_2}\right)_n$ is linear in f_n, $X_{1,n}$, and $X_{2,n}$ (similarly for $\left(\frac{fX_2}{X_1+X_2}\right)_n$, $\left(\frac{fS_1}{X_1+X_2}\right)_n$, and $\left(\frac{fS_2}{X_1+X_2}\right)_n$), it is possible to extract more information about this term, under the conditions of Theorem 7.4.8, from the assumption that the lower order states are stable. In particular, if f_k, $X_{1,k}$, and $X_{2,k}$, $k = 1, 2, \ldots, n-1$ all approach constant values, then

$$\dot{f}_k \to 0 \text{ and } k = 1, 2, \ldots, n-1 \Rightarrow \begin{array}{l} X_{1,1} + X_{2,1} \to \dfrac{1}{\gamma}, \text{ and} \\ X_{1,j} + X_{2,j} \to 0, \ j = 2, 3, \ldots, n-1 \end{array}$$

due to the state equation for f_k, $k = 1, 2, \ldots, n-1$. In addition to the steady state values of $X_{1,k} + X_{2,k}$, stability of f_k, $X_{1,k}$, and $X_{2,k}$, also allows the computation of the steady state values of f_k, $k = 1, 2, \ldots, n-1$.

Lemma 7.4.11. *Under the conditions of Theorem 7.4.8, and if f_k, $X_{1,k}$, and $X_{2,k}$, $k = 1, 2, \ldots, n-1$ all approach constant values, then*

$$f_k \to c\left(X_{1,k} + X_{2,k}\right), \ k = 1, 2, \ldots, n-1$$

as $t \to \infty$.

Proof. The claim will be shown by induction.

For the base case ($k = 1$), if $X_{1,1}$ and $S_{1,1}$ approach constant values, then $\dot{X}_{1,1} + \dot{S}_{1,1} = 0$ as $t \to \infty$:

$$
\begin{aligned}
0 &= \dot{X}_{1,1} + \dot{S}_{1,1} \\
&= \left[\left(\frac{u_4}{l_4} + \frac{u_1}{l_1} + \frac{u_2}{\theta_1} \right) c \frac{X_{2,0}}{X_{1,0} + X_{2,0}} - (u_1 + u_2) - \frac{u_3}{\beta_1} c \frac{S_{1,0}}{X_{1,0} + X_{2,0}} \right] X_{1,1} \\
&\quad + \left[- \left(\frac{u_4}{l_4} + \frac{u_1}{l_1} + \frac{u_2}{\theta_1} \right) c \frac{X_{1,0}}{X_{1,0} + X_{2,0}} - \frac{u_3}{\beta_1} c \frac{S_{1,0}}{X_{1,0} + X_{2,0}} \right] X_{2,1} \\
&\quad + \left[\frac{u_3}{\beta_1} c \right] S_{1,1} + [0] S_{2,1} + \left[\left(\frac{u_4}{l_4} + \frac{u_1}{l_1} + \frac{u_2}{\theta_1} \right) \frac{X_{1,0}}{X_{1,0} + X_{2,0}} + \frac{u_3}{\beta_1} \frac{S_{1,0}}{X_{1,0} + X_{2,0}} \right] f_1 \\
&\quad + \left[u_2 - \frac{u_2}{\theta_1} c \frac{X_{2,0}}{X_{1,0} + X_{2,0}} + \frac{u_3}{\beta_1} c \frac{S_{1,0}}{X_{1,0} + X_{2,0}} \right] X_{1,1} \\
&\quad + \left[\frac{u_2}{\theta_1} c \frac{X_{1,0}}{X_{1,0} + X_{2,0}} + \frac{u_3}{\beta_1} c \frac{S_{1,0}}{X_{1,0} + X_{2,0}} \right] X_{2,1} \\
&\quad + \left[- \frac{u_3}{\beta_1} c \right] S_{1,1} + [0] S_{2,1} + \left[- \frac{u_2}{\theta_1} \frac{X_{1,0}}{X_{1,0} + X_{2,0}} - \frac{u_3}{\beta_1} \frac{S_{1,0}}{X_{1,0} + X_{2,0}} \right] f_1 \\
&= \left(\frac{u_4}{l_4} + \frac{u_1}{l_1} \right) c \frac{X_{1,1} X_{2,0}}{X_{1,0} + X_{2,0}} - u_1 X_{1,1} - \left(\frac{u_4}{l_4} + \frac{u_1}{l_1} \right) c \frac{X_{1,0} X_{2,1}}{X_{1,0} + X_{2,0}} \\
&\quad + \left(\frac{u_4}{l_4} + \frac{u_1}{l_1} \right) \frac{X_{1,0}}{X_{1,0} + X_{2,0}} f_1 \\
&= c \frac{X_{1,1} X_{2,0}}{X_{1,0} + X_{2,0}} - c X_{1,1} - c \frac{X_{1,0} X_{2,1}}{X_{1,0} + X_{2,0}} + \frac{X_{1,0}}{X_{1,0} + X_{2,0}} f_1 \\
&= \frac{X_{1,0}}{X_{1,0} + X_{2,0}} \left(- c X_{1,1} - c X_{2,1} + f_1 \right)
\end{aligned}
$$

which implies that $f_1 = c\left(X_{1,1} + X_{2,1}\right)$ in steady state since one of the conditions of the lemma is $X_{1,0} > 0$. Note that the same result would have been obtained if $\dot{X}_{2,1} + \dot{S}_{2,1}$ was used instead.

For the inductive step, assume that f_j, $X_{1,j}$, and $X_{2,j}$, all approach constant values and $f_j = c\left(X_{1,j} + X_{2,j}\right)$ for $j = 1, 2, \ldots, k-1$. It will be shown that if f_k, $X_{1,k}$, and $X_{2,k}$ all approach constant values, then $f_k = c\left(X_{1,k} + X_{2,k}\right)$.

Since the states are stable up to the k^{th} term in the power series expansion, then $\dot{X}_{1,j} + \dot{S}_{1,j} = 0$ in steady state for $j = 1, 2, \ldots, k$. This implies that

$$
\begin{aligned}
&\left(X_1 + X_2\right) \left[\dot{X}_{1,k+1} + \dot{X}_{2,k+1} \epsilon^{k+1} + \dot{X}_{1,k+2} + \dot{X}_{2,k+2} \epsilon^{k+2} + \cdots \right] \\
&\qquad = \left(\frac{u_4}{l_4} + \frac{u_1}{l_1} \right) f X_1 - u_1 X_1 \left(X_1 + X_2\right).
\end{aligned}
$$

Expanding f, X_1, and X_2 in their power series expansions and retaining only the coefficients

of ϵ^k yields:

$$\begin{aligned}
0 &= \left(\frac{u_4}{l_4} + \frac{u_1}{l_1}\right) \sum_{i=0}^{k} f_i X_{1,k-i} - u_1 \sum_{i=0}^{k} X_{1,i} \left(X_{1,k-i} + X_{2,k-i}\right) \\
&= \left(\frac{u_4}{l_4} + \frac{u_1}{l_1}\right) \left(f_k X_{1,0} + \sum_{i=0}^{k-1} c \left(X_{1,i} + X_{2,i}\right) X_{1,k-i}\right) - u_1 \sum_{i=0}^{k} X_{1,i} \left(X_{1,k-i} + X_{2,k-i}\right) \\
&= \left(\frac{u_4}{l_4} + \frac{u_1}{l_1}\right) \left(f_k X_{1,0} + \sum_{i=0}^{k-1} c \left(X_{1,i} + X_{2,i}\right) X_{1,k-i}\right) - u_1 \sum_{i=0}^{k} X_{1,k-i} \left(X_{1,k} + X_{2,k}\right) \\
&= \left(f_k X_{1,0} + \sum_{i=0}^{k-1} c \left(X_{1,i} + X_{2,i}\right) X_{1,k-i}\right) \\
&\qquad - c \left(X_{1,0} \left(X_{1,k} + X_{2,k}\right) + \sum_{i=0}^{k-1} X_{1,k-i} \left(X_{1,k} + X_{2,k}\right)\right) \\
&= f_k X_{1,0} - c X_{1,0} \left(X_{1,k} + X_{2,k}\right)
\end{aligned}$$

which implies that $f_k = c\left(X_{1,k} + X_{2,k}\right)$ in steady state since one of the conditions of the lemma is $X_{1,0} > 0$. □

Lemma 7.4.11 and the state equation for f therefore imply

$$f_k \to \begin{cases} \frac{c}{\gamma} & k = 1 \\ 0 & 2 \leq k \leq n-1 \end{cases}$$

if f_k, $X_{1,k}$, and $X_{2,k}$, $k = 1, 2, \ldots, n-1$ all approach constant values. With these facts and Corollary 7.4.4, it is possible to derive the steady state dynamics of the coefficients of ϵ^n.

Theorem 7.4.12. *Under the conditions of Theorem 7.4.8, and if f_k, $X_{1,k}$, and $X_{2,k}$, $k = 1, 2, \ldots, n-1$ all approach constant values, then*

$$\dot{x}_n \to A_n x_n$$

as $t \to \infty$, where $x_n := [X_{1,n}\ X_{2,n}\ S_{1,n}\ S_{2,n}\ f_n]^T$.

Proof. Corollary 7.4.4 states that $\left(\frac{1}{G}\right)_n = (-1)^n \frac{G_1^n}{G_0^{n+1}} + \frac{z_n y_n}{g_n} - \frac{G_n}{G_0^2}$, where $G := X_1 + X_2$. In steady state, it is known that $f_k = G_k = 0$ for $k = 2, 3, \ldots, n-1$ since the coefficients up to ϵ^{n-1} are bounded. This implies that $y_k \to 0$ for $k = 2, 3, \ldots, n$ since y_n is drawn from the set of monomials of $(X_1, X_2, \ldots, X_{n-1})$ excluding the subset of monomials of (X_1). Therefore,

if $0 < j < n$,

$$\begin{aligned}
\left(\frac{f}{G}\right)_j &= \sum_{i=0}^{j} f_i \left(\frac{1}{G}\right)_{j-i} \\
&= f_0 \left(\frac{1}{G}\right)_j + f_1 \left(\frac{1}{G}\right)_{j-1} \\
&= f_0 \left((-1)^j \frac{G_1^j}{G_0^{j+1}} - \frac{G_j}{G_0^2}\right) + f_1 \left((-1)^{j-1} \frac{G_1^{j-1}}{G_0^j} - \frac{G_{j-1}}{G_0^2}\right) \\
&= f_0 \left((-1)^j \frac{G_1^j}{G_0^{j+1}}\right) + f_1 \left((-1)^{j-1} \frac{G_1^{j-1}}{G_0^j}\right) \\
&= \frac{f_0}{G_0}(-1)^j \frac{G_1^j}{G_0^j} + \frac{f_1}{G_1}(-1)^{j-1} \frac{G_1 G_1^{j-1}}{G_0^j} \\
&= 0
\end{aligned}$$

where the fourth equality results from $G_j = 0$ for $1 < j < n$. Therefore, up to order n,

$$\frac{f}{G} = \frac{f_0}{G_0} + \left(\frac{f}{G}\right)_n \epsilon^n$$

in steady state. Now, extending the index to $j = n$ from the set equations above leads to

$$\begin{aligned}
\left(\frac{f}{G}\right)_n &= \sum_{i=0}^{n} f_i \left(\frac{1}{G}\right)_{n-i} \\
&= f_0 \left(\frac{1}{G}\right)_n + f_1 \left(\frac{1}{G}\right)_{n-1} + f_n \left(\frac{1}{G}\right)_0
\end{aligned}$$

since it has not been established that f_n converges to 0. Continuing,

$$\begin{aligned}
\left(\frac{f}{G}\right)_n &= f_0 \left(\frac{1}{G}\right)_n + f_1 \left(\frac{1}{G}\right)_{n-1} + f_n \left(\frac{1}{G}\right)_0 \\
&= f_0 \left((-1)^n \frac{G_1^n}{G_0^{n+1}} - \frac{G_n}{G_0^2}\right) + f_1 \left((-1)^{n-1} \frac{G_1^{n-1}}{G_0^n}\right) + \frac{f_n}{G_0} \\
&= c(-1)^n \frac{G_1^n}{G_0^n} + (-1)^{n-1} \frac{G_1^n}{G_0^n} - f_0 \frac{G_n}{G_0^2} + \frac{f_n}{G_0} \\
&= \frac{f_n}{G_0} - \frac{f_0 G_n}{G_0^2}.
\end{aligned}$$

Therefore, up to order n,

$$\frac{f}{G} = \frac{f_0}{G_0} + \left[\frac{f_n}{G_0} - \frac{f_0 G_n}{G_0^2}\right] \epsilon^n.$$

Multiplying this term by $X_1 = X_{1,0} + X_{1,1}\epsilon + X_{1,2}\epsilon^2 + \cdots$ gives

$$\frac{f}{G}X_1 = \left[\frac{f_0}{G_0} + \left[\frac{f_n}{G_0} - \frac{f_0 G_n}{G_0^2}\right]\epsilon^n\right]\left[X_{1,0} + X_{1,1}\epsilon + X_{1,2}\epsilon^2 + \cdots\right],$$

which allows the determination of $\left(\frac{fX_1}{X_1+X_2}\right)_n$:

$$\begin{aligned}\left(\frac{fX_1}{X_1+X_2}\right)_n &= \frac{f_0}{G_0}X_{1,n} + \frac{X_{1,0}}{G_0}f_n - \frac{f_0 X_{1,0}}{G_0^2}G_n \\ &= cX_{1,n} + \frac{X_{1,0}}{X_{1,0}+X_{2,0}}f_n - c\frac{X_{1,0}}{X_{1,0}+X_{2,0}}\left(X_{1,n}+X_{2,n}\right) \\ &= c\left(1 - \frac{X_{1,0}}{X_{1,0}+X_{2,0}}\right)X_{1,n} - c\frac{X_{1,0}}{X_{1,0}+X_{2,0}}X_{2,n} + \frac{X_{1,0}}{X_{1,0}+X_{2,0}}f_n.\end{aligned}$$

which is linear in the states $X_{1,n}$, $X_{2,n}$, and f_n. Similarly,

$$\begin{aligned}\left(\frac{fX_2}{X_1+X_2}\right)_n &= -c\frac{X_{2,0}}{X_{1,0}+X_{2,0}}X_{1,n} + c\left(1 - \frac{X_{2,0}}{X_{1,0}+X_{2,0}}\right)X_{2,n} + \frac{X_{2,0}}{X_{1,0}+X_{2,0}}f_n \\ \left(\frac{fS_1}{X_1+X_2}\right)_n &= c\left(1 - \frac{S_{1,0}}{X_{1,0}+X_{2,0}}\right)X_{1,n} - c\frac{S_{1,0}}{X_{1,0}+X_{2,0}}X_{2,n} + \frac{S_{1,0}}{X_{1,0}+X_{2,0}}f_n \\ \left(\frac{fS_2}{X_1+X_2}\right)_n &= -c\frac{S_{2,0}}{X_{1,0}+X_{2,0}}X_{1,n} + c\left(1 - \frac{S_{2,0}}{X_{1,0}+X_{2,0}}\right)X_{2,n} + \frac{S_{2,0}}{X_{1,0}+X_{2,0}}f_n\end{aligned}$$

are all linear in the states $X_{1,n}$, $X_{2,n}$, $S_{1,n}$, $S_{2,n}$, and f_n. Notably, *there are no constant/forcing terms.*

Therefore, the dynamics of the coefficients of the ϵ^n $(n > 1)$ are

$$\begin{aligned}\dot{X}_{1,n} &\to \left(\frac{u_4}{l_4} + \frac{u_1}{l_1} + \frac{u_2}{\theta_1}\right)\left(\frac{fX_1}{X_1+X_2}\right)_n - (u_1+u_2)X_{1,n} + \frac{u_3}{\beta_1}\left(\frac{fS_1}{X_1+X_2}\right)_n \\ \dot{X}_{2,n} &\to \left(\frac{u_4}{l_4} + \frac{u_1}{l_1} + \frac{u_2}{\theta_2}\right)\left(\frac{fX_2}{X_1+X_2}\right)_n - (u_1+u_2)X_{2,n} + \frac{u_3}{\beta_2}\left(\frac{fS_2}{X_1+X_2}\right)_n \\ \dot{S}_{1,n} &\to u_2 X_{1,n} - \frac{u_2}{\theta_1}\left(\frac{fX_1}{X_1+X_2}\right)_n - \frac{u_3}{\beta_1}\left(\frac{fS_1}{X_1+X_2}\right)_n \\ \dot{S}_{2,n} &\to u_2 X_{2,n} - \frac{u_2}{\theta_2}\left(\frac{fX_2}{X_1+X_2}\right)_n - \frac{u_3}{\beta_2}\left(\frac{fS_2}{X_1+X_2}\right)_n \\ \dot{f}_n &\to -\gamma\left(X_{1,n}+X_{2,n}\right)\end{aligned}$$

which are linear in the states as $t \to \infty$. Since there are no constant/forcing terms, the dynamics can be written as

$$\dot{x}_n = A_n x_n$$

in steady state. □

Remark 7.4.13. *Lemma 7.4.1 suggests that, for all $n \geq 1$,*

$$\dot{x}_n = A_n x_n + \mathcal{B}_n$$

where $\mathcal{B}_n$ is some (possibly nonlinear) forcing function. Theorem 7.4.12 says that the forcing goes to zero as $t \to \infty$.

From Remark 7.4.13, it is possible to conclude that the coefficients of ϵ^n are bounded as long as the eigenvalues of A_n lie in the *closed* left half plane. This will complete the inductive step for BIBO stability of the proposed model.

Lemma 7.4.14. *Under the conditions of Theorem 7.4.12, the eigenvalues of A_n lie in the closed left half plane.*

Proof. From the proof of Theorem 7.4.12, A_n can be filled out to be

$$A_n = \begin{bmatrix} a_{11} & a_{12} & a_{13} & 0 & a_{15} \\ a_{21} & a_{22} & 0 & a_{24} & a_{25} \\ a_{31} & a_{32} & a_{33} & 0 & a_{35} \\ a_{41} & a_{42} & 0 & a_{44} & a_{45} \\ a_{51} & a_{52} & 0 & 0 & 0 \end{bmatrix}$$

where

$$\begin{aligned}
a_{11} &= \left(\frac{u_4}{l_4} + \frac{u_1}{l_1} + \frac{u_2}{\theta_1}\right) c \frac{X_{2,0}}{X_{1,0} + X_{2,0}} - (u_1 + u_2) - \frac{u_3}{\beta_1} c \frac{S_{1,0}}{X_{1,0} + X_{2,0}} \\
a_{12} &= -\left(\frac{u_4}{l_4} + \frac{u_1}{l_1} + \frac{u_2}{\theta_1}\right) c \frac{X_{1,0}}{X_{1,0} + X_{2,0}} - \frac{u_3}{\beta_1} c \frac{S_{1,0}}{X_{1,0} + X_{2,0}} \\
a_{13} &= \frac{u_3}{\beta_1} c \\
a_{15} &= \left(\frac{u_4}{l_4} + \frac{u_1}{l_1} + \frac{u_2}{\theta_1}\right) \frac{X_{1,0}}{X_{1,0} + X_{2,0}} + \frac{u_3}{\beta_1} \frac{S_{1,0}}{X_{1,0} + X_{2,0}}
\end{aligned}$$

$$\begin{aligned}
a_{21} &= -\left(\frac{u_4}{l_4} + \frac{u_1}{l_1} + \frac{u_2}{\theta_2}\right) c \frac{X_{2,0}}{X_{1,0} + X_{2,0}} - \frac{u_3}{\beta_2} c \frac{S_{2,0}}{X_{1,0} + X_{2,0}} \\
a_{22} &= \left(\frac{u_4}{l_4} + \frac{u_1}{l_1} + \frac{u_2}{\theta_2}\right) c \frac{X_{1,0}}{X_{1,0} + X_{2,0}} - (u_1 + u_2) - \frac{u_3}{\beta_2} c \frac{S_{2,0}}{X_{1,0} + X_{2,0}} \\
a_{24} &= \frac{u_3}{\beta_2} c \\
a_{25} &= \left(\frac{u_4}{l_4} + \frac{u_1}{l_1} + \frac{u_2}{\theta_2}\right) \frac{X_{2,0}}{X_{1,0} + X_{2,0}} + \frac{u_3}{\beta_2} \frac{S_{2,0}}{X_{1,0} + X_{2,0}}
\end{aligned}$$

$$
\begin{aligned}
a_{31} &= u_2 - \frac{u_2}{\theta_1}\frac{X_{2,0}}{X_{1,0}+X_{2,0}} + \frac{u_3}{\beta_1}c\frac{S_{1,0}}{X_{1,0}+X_{2,0}} \\
a_{32} &= \frac{u_2}{\theta_1}c\frac{X_{1,0}}{X_{1,0}+X_{2,0}} + \frac{u_3}{\beta_1}c\frac{S_{1,0}}{X_{1,0}+X_{2,0}} \\
a_{33} &= -\frac{u_3}{\beta_1}c \\
a_{35} &= -\frac{u_2}{\theta_1}\frac{X_{1,0}}{X_{1,0}+X_{2,0}} - \frac{u_3}{\beta_1}\frac{S_{1,0}}{X_{1,0}+X_{2,0}}
\end{aligned}
$$

$$
\begin{aligned}
a_{41} &= \frac{u_2}{\theta_2}c\frac{X_{2,0}}{X_{1,0}+X_{2,0}} + \frac{u_3}{\beta_2}c\frac{S_{2,0}}{X_{1,0}+X_{2,0}} \\
a_{42} &= u_2 - \frac{u_2}{\theta_2}\frac{X_{1,0}}{X_{1,0}+X_{2,0}} + \frac{u_3}{\beta_2}c\frac{S_{2,0}}{X_{1,0}+X_{2,0}} \\
a_{44} &= -\frac{u_3}{\beta_2}c \\
a_{45} &= -\frac{u_2}{\theta_2}\frac{X_{2,0}}{X_{1,0}+X_{2,0}} - \frac{u_3}{\beta_2}\frac{S_{2,0}}{X_{1,0}+X_{2,0}}
\end{aligned}
$$

$$a_{51} = a_{52} = -\gamma$$

and $c = \frac{f_0}{X_{1,0}+X_{2,0}}$. This matrix is identical to A_1 from Theorem 7.4.8, where it was proved that the eigenvalues have non-positive real part (see Appendix B.3). Therefore, all of the eigenvalues of A_n lie in the closed left half plane. □

The induction is complete: $X_{1,n}$, $X_{2,n}$, $S_{1,n}$, $S_{2,n}$, and f_n are bounded and approach constant values for a constant input for all n. Since none of the coefficients for any power of ϵ blow up, the proposed model is BIBO stable.

7.5 Steady state approximation

Though the equilibrium values $(\overline{X}_1, \overline{X}_2, \overline{S}_1, \overline{S}_2, \overline{f})$ cannot be found in a closed-form expression, an approximate relationship between successive steady states can be found.

Suppose that $\overline{e}$ produces the steady state $(\overline{X}_1, \overline{X}_2, \overline{S}_1, \overline{S}_2, \overline{f})$, where $\overline{X}_1 + \overline{X}_2 \gg 1$ (this is required for the population-level model to remain valid). Now let the nutrient influx change to $\overline{e} + \epsilon$, where $|\epsilon| \ll \overline{e}$. Recall that the new steady state cannot be found by linearizing the system around the equilibrium $(\overline{X}_1, \overline{X}_2, \overline{S}_1, \overline{S}_2, \overline{f})$ because the Jacobian has an eigenvalue at 0 (see Appendix B.3). This makes the deviations from equilibrium in steady state undefined because the inverse of the Jacobian cannot be found.

It is possible, however, to write the new steady state solution as a power series in ϵ. For example, assume that X_1 approaches

$$\hat{X}_1 = \overline{X}_1 + X_{1,1}\epsilon + X_{1,2}\epsilon^2 + X_{1,3}\epsilon^3 + \cdots$$

where the $X_{1,n}$ are independent of ϵ. It was shown in Section 7.4 that each of the $X_{1,n}$ are bounded as long as some benign conditions are satisfied (see Theorem 7.4.8), so the proposed expansion is uniformly valid [125].

If ϵ is small enough, then the new steady state $(\hat{X}_1, \hat{X}_2, \hat{S}_1, \hat{S}_2, \hat{f})$ in response to $\overline{e} + \epsilon$ can be well-approximated by retaining only the first power of ϵ:

$$\begin{aligned}
\hat{X}_1 &= \overline{X}_1 + X_{1,1}\epsilon \\
\hat{X}_2 &= \overline{X}_2 + X_{2,1}\epsilon \\
\hat{S}_1 &= \overline{S}_1 + S_{1,1}\epsilon \\
\hat{S}_2 &= \overline{S}_2 + S_{2,1}\epsilon \\
\hat{f} &= \overline{f} + f_1\epsilon.
\end{aligned}$$

Finding closed-form expressions for $X_{i,1}, S_{i,1}$, and f_1 is not possible because of the same reason the steady states could not be found in the first place: Too many unknowns and not enough equations. Assuming that $\frac{\overline{f}}{\overline{X}_1+\overline{X}_2} \leq \min\{\theta_1, \theta_2, \beta_1, \beta_2\}$, a subset of the equations after substituting the first-order approximation are

$$\begin{aligned}
0 = &\left(\left(\frac{u_1}{l_1} + \frac{u_4}{l_4} + \frac{u_2}{\theta_1}\right)\frac{\overline{f} + f_1\epsilon}{\overline{X}_1 + \overline{X}_2 + (X_{1,1} + X_{2,1})\epsilon} - (u_1 + u_2)\right)\left(\overline{X}_1 + X_{1,1}\epsilon\right) \\
&\qquad + \frac{u_3}{\beta_1}\frac{\overline{f} + f_1\epsilon}{\overline{X}_1 + \overline{X}_2 + (X_{1,1} + X_{2,1})\epsilon}\left(\overline{S}_1 + S_{1,1}\epsilon\right) \\
0 = &\left(u_2 - \frac{u_2}{\theta_1}\frac{\overline{f} + f_1\epsilon}{\overline{X}_1 + \overline{X}_2 + (X_{1,1} + X_{2,1})\epsilon}\right)\left(\overline{X}_1 + X_{1,1}\epsilon\right) \\
&\qquad - \frac{u_3}{\beta_1}\frac{\overline{f} + f_1\epsilon}{\overline{X}_1 + \overline{X}_2 + (X_{1,1} + X_{2,1})\epsilon}\left(\overline{S}_1 + S_{1,1}\epsilon\right) \\
0 = &-\frac{1}{\gamma}\left(\overline{X}_1 + \overline{X}_2 + (X_{1,1} + X_{2,1})\epsilon\right) + \overline{e} + \epsilon
\end{aligned}$$

The equations for X_2 and S_2 are similar to the first two equalities. The expressions can be simplified for small ϵ by

$$\frac{1}{\overline{X}_1 + \overline{X}_2 + (X_{1,1} + X_{2,1})\epsilon} \sim \frac{1}{\overline{X}_1 + \overline{X}_2} - \frac{X_{1,1} + X_{2,1}}{\left(\overline{X}_1 + \overline{X}_2\right)^2}\epsilon.$$

Since the left hand sides of the equations above are identically 0, then the coefficients of the powers of ϵ must be zero. The ϵ^0 coefficients yield the original steady state equations, but the ϵ^1 coefficients yield the following:

$$\begin{aligned}
X_{1,1} + X_{2,1} &= \frac{1}{\gamma} \\
\frac{f_1}{X_{1,1} + X_{2,1}} &= c \\
\alpha_{2,1}(c)X_{1,1} &= \alpha_{3,1}(c)S_{1,1} \\
\alpha_{2,2}(c)X_{2,1} &= \alpha_{3,2}(c)S_{2,1}.
\end{aligned}$$

Except for the first equality, these equations are identical to the equilibrium conditions for the input $\overline{e}$. Notably, there are only four independent equations for five unknowns, so the new steady state $(\hat{X}_1, \hat{X}_2, \hat{S}_1, \hat{S}_2, \hat{f})$ cannot be exactly derived in the power series in ϵ.

Though exact expressions for $X_{i,1}, S_{i,1}$, and f_1 cannot be found, an approximation that is valid for small ϵ can be derived. The differential equations for $X_1 + S_1$ and $X_2 + S_2$ are

$$\begin{aligned}\dot{X}_1 + \dot{S}_1 &= (\alpha_4 - \alpha_1) X_1 \\ \dot{X}_2 + \dot{S}_2 &= (\alpha_4 - \alpha_1) X_2,\end{aligned}$$

which means that, for $X_i(0) + S_i(0) = \overline{X}_i + \overline{S}_i$ $(i = 1, 2)$ and any $t > 0$,

$$\begin{aligned}(X_1(t) + S_1(t)) - \left(\overline{X}_1 + \overline{S}_1\right) &= \int_0^t (\alpha_4(\tau) - \alpha_1(\tau)) X_1(\tau) d\tau \\ (X_2(t) + S_2(t)) - \left(\overline{X}_2 + \overline{S}_2\right) &= \int_0^t (\alpha_4(\tau) - \alpha_1(\tau)) X_2(\tau) d\tau\end{aligned}$$

As $t \to \infty$,

$$\begin{aligned}\int_0^t (\alpha_4(\tau) - \alpha_1(\tau)) X_1(\tau) d\tau &\to (X_{1,1} + S_{1,1}) \epsilon \\ \int_0^t (\alpha_4(\tau) - \alpha_1(\tau)) X_2(\tau) d\tau &\to (X_{2,1} + S_{2,1}) \epsilon.\end{aligned}$$

For small enough ϵ, it is reasonable to assume that $X_i(\tau) \approx \overline{X}_i$ for $0 < \tau \leq t$, $i = 1, 2$. This implies that, as $t \to \infty$,

$$\begin{aligned}(X_{1,1} + S_{1,1}) \epsilon &\approx \overline{X}_1 \int_0^t (\alpha_4(\tau) - \alpha_1(\tau)) d\tau \\ (X_{2,1} + S_{2,1}) \epsilon &\approx \overline{X}_2 \int_0^t (\alpha_4(\tau) - \alpha_1(\tau)) d\tau\end{aligned}$$

In other words, the change in total population level is proportional to the vegetative cell subpopulation. This is consistent with the fact that only vegetative cells grow and die, whereas spore numbers are independent of environmental factors. The approximation leaves the following relationship:

$$\begin{aligned}\frac{(X_{1,1} + S_{1,1}) \epsilon}{(X_{2,1} + S_{2,1}) \epsilon} &= \frac{\overline{X}_1 \int_0^t (\alpha_4(\tau) - \alpha_1(\tau)) d\tau}{\overline{X}_2 \int_0^t (\alpha_4(\tau) - \alpha_1(\tau)) d\tau} \\ \Rightarrow \quad \frac{X_{1,1} + S_{1,1}}{X_{2,1} + S_{2,1}} &= \frac{\overline{X}_1}{\overline{X}_2},\end{aligned}$$

or

$$\frac{X_{1,1}}{X_{2,1}} = \frac{\overline{X}_1}{\overline{X}_2} \frac{1 + \frac{\alpha_{2,2}(c)}{\alpha_{3,2}(c)}}{1 + \frac{\alpha_{2,1}(c)}{\alpha_{3,1}(c)}}$$

where $c = \frac{\overline{f}}{\overline{X}_1+\overline{X}_2}$ is the (constant) equilibrium operating point given by $\alpha_4 = \alpha_1$.

With the addition of the extra equation offered by the approximation, there are now five equations to solve for the perturbed steady state:

$$\begin{aligned} X_{1,1} + X_{2,1} &= \frac{1}{\gamma} \\ \frac{f_1}{X_{1,1} + X_{2,1}} &= c \\ \alpha_{2,1}(c)X_{1,1} &= \alpha_{3,1}(c)S_{1,1} \\ \alpha_{2,2}(c)X_{2,1} &= \alpha_{3,2}(c)S_{2,1} \\ \frac{X_{1,1}}{X_{2,1}} &= \frac{\overline{X}_1}{\overline{X}_2}\frac{1+\frac{\alpha_{2,2}(c)}{\alpha_{3,2}(c)}}{1+\frac{\alpha_{2,1}(c)}{\alpha_{3,1}(c)}}, \end{aligned}$$

which allows the perturbed steady state $(\hat{X}_1, \hat{X}_2, \hat{S}_1, \hat{S}_2, \hat{f})$ to be found in terms of the previous steady state $(\overline{X}_1, \overline{X}_2, \overline{S}_1, \overline{S}_2, \overline{f})$. For example, the total population size $A_i := \overline{X}_i + \overline{S}_i$ from one steady state to another can be written as

$$A_1(k+1) = A_1(k)\left[1 + \frac{\frac{1}{\gamma}(1+b_1(k))(1+b_2(k))^2}{A_1(k)(1+b_2(k))^2 + A_2(k)(1+b_1(k))^2}\,\epsilon(k)\right] \tag{7.2}$$

$$A_2(k+1) = A_2(k)\left[1 + \frac{\frac{1}{\gamma}(1+b_1(k))^2(1+b_2(k))}{A_1(k)(1+b_2(k))^2 + A_2(k)(1+b_1(k))^2}\,\epsilon(k)\right], \tag{7.3}$$

where k denotes the "k^{th} steady state," and

$$\begin{aligned} b_1 &:= \frac{\alpha_{2,1}(c)}{\alpha_{3,1}(c)} \\ b_2 &:= \frac{\alpha_{2,2}(c)}{\alpha_{3,2}(c)} \end{aligned}$$

map to the steady state sporulation efficiencies for each population.

Figures 7.2–7.5 provide support that the steady state approximation is valid for small ϵ. These simulations were produced with $\overline{e} = 1$, $\theta_1 = \beta_1 = 10$, and $\theta_2 = \beta_2 = 1$. As expected, the approximation becomes more accurate as $|\epsilon| \to 0$.

Figure 7.6 shows a time-domain simulation with slightly different sporulation and germination policies and $e(t) = 1 + 0.01 \cdot \mathbf{1}(t-700) - 0.03 \cdot \mathbf{1}(t-1400)$. As before, the predictive performance of the approximation degrades as ϵ gets larger.

Due to the small ϵ condition, the subsequent analysis is restricted to **slowly varying** environments. These are environments that change sufficiently slowly such that populations remain in a "quasi-steady state" operating mode. In other words, the time scale of the environment must be much longer than the time scale of the population dynamics. Though somewhat restrictive, this is necessary in order to have a closed-form steady state expression.

Equations (7.2) and (7.3) are robust to a different functional dependencies for $\alpha_{2,i}$ and $\alpha_{3,i}$ as long as $|\epsilon| \ll \overline{e}$. Specifically, suppose that α_4 and α_1 still depend on $\frac{f}{X_1+X_2}$ (so

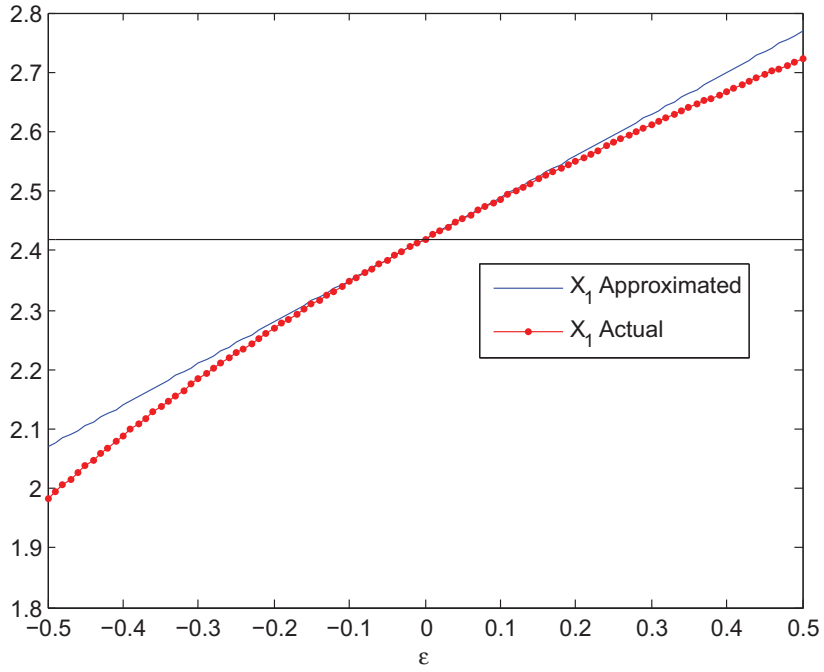

Figure 7.2: Approximated and actual X_1. The black horizontal line indicates $\overline{X}_1$.

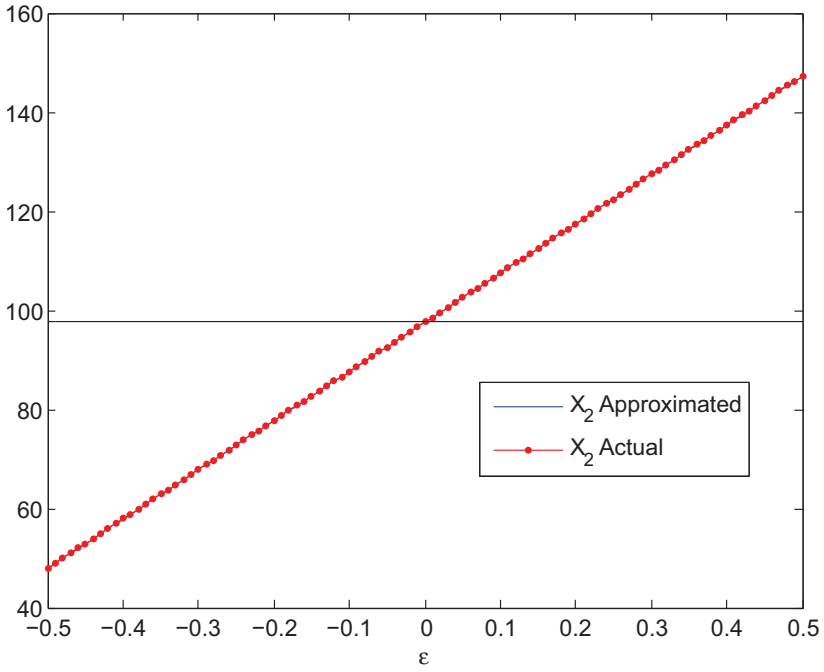

Figure 7.3: Approximated and actual X_2. The black horizontal line indicates $\overline{X}_2$.

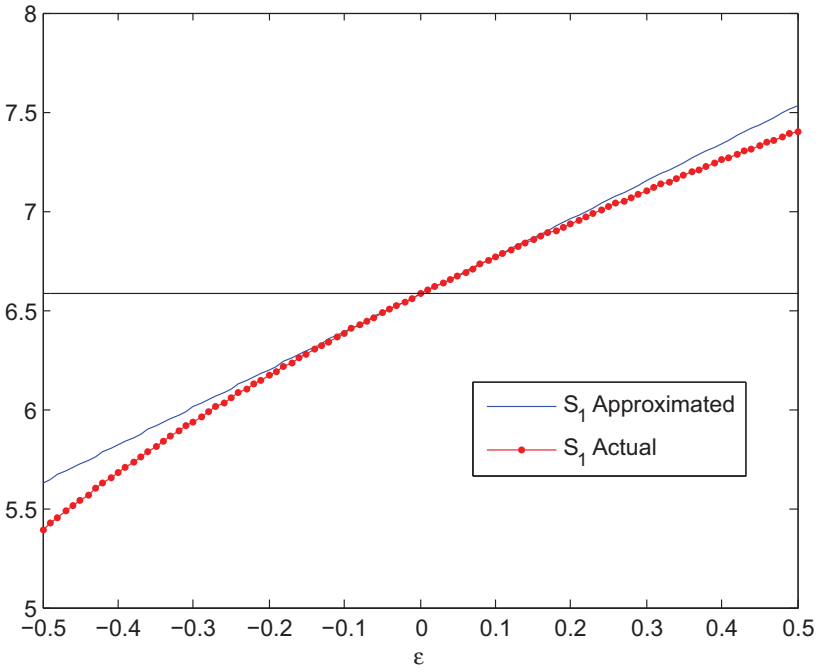

Figure 7.4: Approximated and actual S_1. The black horizontal line indicates $\overline{S}_1$.

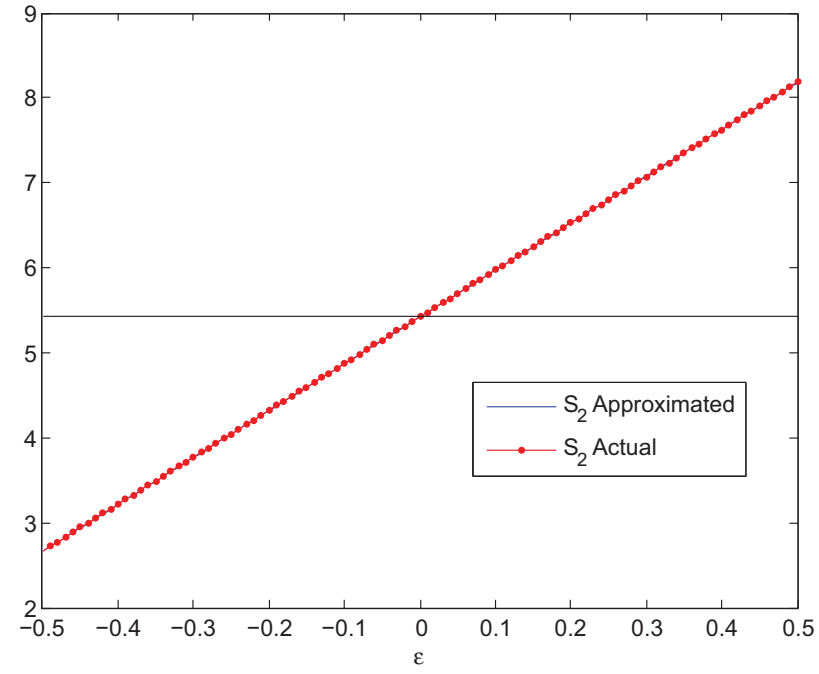

Figure 7.5: Approximated and actual S_2. The black horizontal line indicates $\overline{S}_2$.

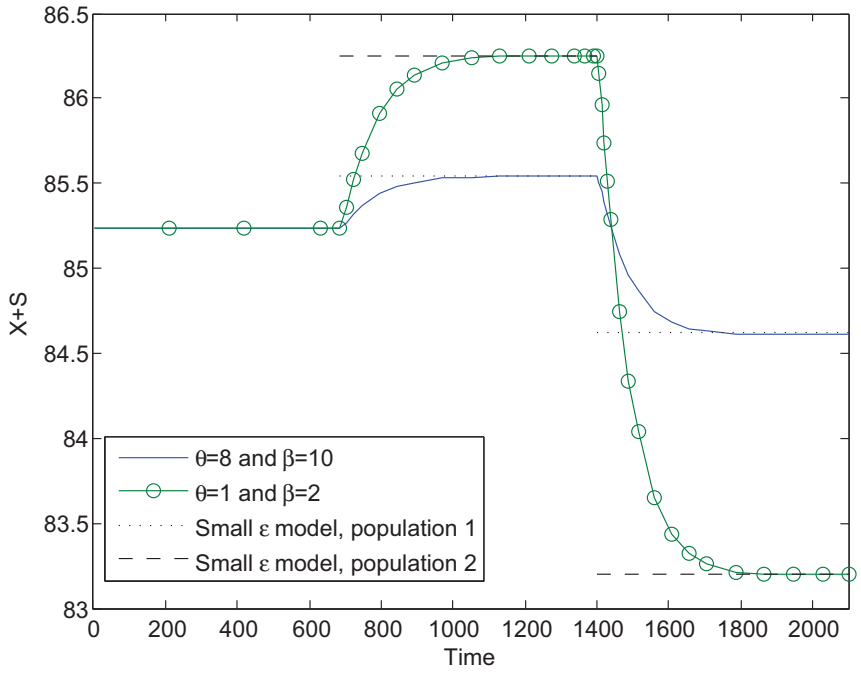

Figure 7.6: Approximated and actual total population numbers.

that logistic-like growth and death depend on the carrying capacity-like term f of the environment), but $\alpha_{2,i}$ and $\alpha_{3,i}$ are now only functions of f:

$$\alpha_{2,i} = \max\left\{0, u_2 - \frac{u_2}{\theta_i} f\right\}$$
$$\alpha_{3,i} = \min\left\{u_3, \frac{u_3}{\beta_i} f\right\}$$

for $i = 1, 2$. At equilibrium for input $\overline{e}$, there are still too many unknowns for the number of equations, though two of the equations have changed:

$$\alpha_{3,i}\left(\overline{f}\right)\overline{S}_i = \alpha_{2,i}\left(\overline{f}\right)\overline{X}_i$$
$$\Rightarrow \quad \alpha_{3,i}\left(\frac{c\overline{e}}{\gamma}\right)\overline{S}_i = \alpha_{2,i}\left(\frac{c\overline{e}}{\gamma}\right)\overline{X}_i.$$

Since the equilibrium values still depend on the initial conditions, we can apply the small ϵ

approximation to get equations for the perturbed steady state:

$$\begin{aligned}
X_{1,1} + X_{2,1} &= \frac{1}{\gamma} \\
\frac{f_1}{X_{1,1} + X_{2,1}} &= c \\
\alpha_{2,1}\left(\frac{c\overline{e}}{\gamma}\right) X_{1,1} &= \alpha_{3,1}\left(\frac{c\overline{e}}{\gamma}\right) S_{1,1} \\
\alpha_{2,2}\left(\frac{c\overline{e}}{\gamma}\right) X_{2,1} &= \alpha_{3,2}\left(\frac{c\overline{e}}{\gamma}\right) S_{2,1} \\
\frac{X_{1,1}}{X_{2,1}} &= \frac{\overline{X}_1}{\overline{X}_2} \frac{1 + \frac{\alpha_{2,2}\left(\frac{c\overline{e}}{\gamma}\right)}{\alpha_{3,2}\left(\frac{c\overline{e}}{\gamma}\right)}}{1 + \frac{\alpha_{2,1}\left(\frac{c\overline{e}}{\gamma}\right)}{\alpha_{3,1}\left(\frac{c\overline{e}}{\gamma}\right)}},
\end{aligned}$$

which lead to the following expressions for $X_{1,1} + S_{1,1}$ and $X_{2,1} + S_{2,1}$:

$$X_{1,1} + S_{1,1} = \frac{\frac{1}{\gamma}\overline{X}_1 \left(1 + \frac{\alpha_{2,2}\left(\frac{c(\overline{e}+\epsilon)}{\gamma}\right)}{\alpha_{3,2}\left(\frac{c(\overline{e}+\epsilon)}{\gamma}\right)}\right)\left(1 + \frac{\alpha_{2,1}\left(\frac{c(\overline{e}+\epsilon)}{\gamma}\right)}{\alpha_{3,1}\left(\frac{c(\overline{e}+\epsilon)}{\gamma}\right)}\right)}{\frac{\overline{X}_2+\overline{S}_2}{1+\frac{\alpha_{2,2}\left(\frac{c\overline{e}}{\gamma}\right)}{\alpha_{3,2}\left(\frac{c\overline{e}}{\gamma}\right)}}\left(1 + \frac{\alpha_{2,1}\left(\frac{c(\overline{e}+\epsilon)}{\gamma}\right)}{\alpha_{3,1}\left(\frac{c(\overline{e}+\epsilon)}{\gamma}\right)}\right) + \frac{\overline{X}_1+\overline{S}_1}{1+\frac{\alpha_{2,1}\left(\frac{c\overline{e}}{\gamma}\right)}{\alpha_{3,1}\left(\frac{c\overline{e}}{\gamma}\right)}}\left(1 + \frac{\alpha_{2,2}\left(\frac{c(\overline{e}+\epsilon)}{\gamma}\right)}{\alpha_{3,2}\left(\frac{c(\overline{e}+\epsilon)}{\gamma}\right)}\right)}$$

$$X_{2,1} + S_{2,1} = \frac{\frac{1}{\gamma}\overline{X}_2 \left(1 + \frac{\alpha_{2,2}\left(\frac{c(\overline{e}+\epsilon)}{\gamma}\right)}{\alpha_{3,2}\left(\frac{c(\overline{e}+\epsilon)}{\gamma}\right)}\right)\left(1 + \frac{\alpha_{2,1}\left(\frac{c(\overline{e}+\epsilon)}{\gamma}\right)}{\alpha_{3,1}\left(\frac{c(\overline{e}+\epsilon)}{\gamma}\right)}\right)}{\frac{\overline{X}_2+\overline{S}_2}{1+\frac{\alpha_{2,2}\left(\frac{c\overline{e}}{\gamma}\right)}{\alpha_{3,2}\left(\frac{c\overline{e}}{\gamma}\right)}}\left(1 + \frac{\alpha_{2,1}\left(\frac{c(\overline{e}+\epsilon)}{\gamma}\right)}{\alpha_{3,1}\left(\frac{c(\overline{e}+\epsilon)}{\gamma}\right)}\right) + \frac{\overline{X}_1+\overline{S}_1}{1+\frac{\alpha_{2,1}\left(\frac{c\overline{e}}{\gamma}\right)}{\alpha_{3,1}\left(\frac{c\overline{e}}{\gamma}\right)}}\left(1 + \frac{\alpha_{2,2}\left(\frac{c(\overline{e}+\epsilon)}{\gamma}\right)}{\alpha_{3,2}\left(\frac{c(\overline{e}+\epsilon)}{\gamma}\right)}\right)}.$$

If $|\epsilon| \ll \overline{e}$,

$$\frac{c(\overline{e}+\epsilon)}{\gamma} \approx \frac{c\overline{e}}{\gamma} \;\Rightarrow \frac{\alpha_{2,i}\left(\frac{c(\overline{e}+\epsilon)}{\gamma}\right)}{\alpha_{3,i}\left(\frac{c(\overline{e}+\epsilon)}{\gamma}\right)} \approx \frac{\alpha_{2,i}\left(\frac{c\overline{e}}{\gamma}\right)}{\alpha_{3,i}\left(\frac{c\overline{e}}{\gamma}\right)},$$

which implies that Equations (7.2) and (7.3) still hold. Even if $\frac{c(\overline{e}+\epsilon)}{\gamma}$ was not close to $\frac{c\overline{e}}{\gamma}$, it is still possible for $\frac{\alpha_{2,i}\left(\frac{c(\overline{e}+\epsilon)}{\gamma}\right)}{\alpha_{3,i}\left(\frac{c(\overline{e}+\epsilon)}{\gamma}\right)} \approx \frac{\alpha_{2,i}\left(\frac{c\overline{e}}{\gamma}\right)}{\alpha_{3,i}\left(\frac{c\overline{e}}{\gamma}\right)}$ if $\theta_i \approx \beta_i \gg 1$.

7.6 Sporulation efficiency as control variable

Equations (7.2) and (7.3),

$$A_1(k+1) = A_1(k)\left[1 + \frac{\frac{1}{\gamma}(1+b_1(k))(1+b_2(k))^2}{A_1(k)(1+b_2(k))^2 + A_2(k)(1+b_1(k))^2}\,\epsilon(k)\right] \tag{7.2}$$

$$A_2(k+1) = A_2(k)\left[1 + \frac{\frac{1}{\gamma}(1+b_1(k))^2(1+b_2(k))}{A_1(k)(1+b_2(k))^2 + A_2(k)(1+b_1(k))^2}\,\epsilon(k)\right], \tag{7.3}$$

are in terms of $b_1(k)$ and $b_2(k)$, which form a one-to-one map with the sporulation efficiencies $u_i(k) \in [0,1]$ of each population. Specifically, for $i = 1, 2$,

$$\begin{array}{lcl} b_i(k) = \infty & \leftrightarrow & 100\% \text{ sporulation efficiency (“conservative”)} \\ b_i(k) = 0 & \leftrightarrow & \text{no spores (“aggressive”)} \end{array}$$

For example, if $b_2(k) = \infty$ and $b_1(k) < \infty$, it is easy to verify that $A_2(k+1) = A_2(k)$ and

$$A_1(k+1) = A_1(k) + \frac{1}{\gamma}(1+b_1(k))\epsilon(k)$$

which is expected since $X_{1,1} = \frac{1}{\gamma}$ and $S_{1,1} = b_1(k)X_{1,1}$.

Since the $b_i(k)$'s dictate how well one population does relative to the other (with respect to $\max \overline{X} + \overline{S}$), these parameters (or the corresponding $u_i(k)$'s) can be labeled as the “control” for each population. The selection of the control is discussed in Section 7.8, where it is seen to be a result of natural selection. Hence, bacteria do not actively choose their $b_i(k)$ or $u_i(k)$ to maximize their own fitness, but rather the subpopulations with the “best” $b_i(k)$ or $u_i(k)$ competitively exclude the other subpopulations. Nevertheless, it is convenient to imagine the $b_i(k)$ or $u_i(k)$ as “being chosen” to try to do better than other competing populations.

Even though each $b_i(k)$ is a steady state parameter ($\frac{\alpha_{2,i}(c)}{\alpha_{3,i}(c)}$), it captures the transient trade-off associated with being too conservative. Specifically, a population with a relatively small $b_i(k)$ will devote more resources towards rapid growth when $\epsilon > 0$, but suffers more losses when $\epsilon < 0$. For example, consider two competing populations at equilibrium with $A_1(k) = A_2(k)$, or $\overline{X}_1 + \overline{S}_1 = \overline{X}_2 + \overline{S}_2$. Suppose $b_1(k) > b_2(k)$. Then, $\overline{X}_1 < \overline{X}_2$, and since only vegetative cells can grow, population 2 will increase more than population 1. This will happen even if $\theta_2 > \theta_1$ (population 2 sporulates more readily than population 1) because $b_1(k) > b_2(k)$ implies that $\beta_2 < \beta_1$, so population 2 also germinates more readily than population 1. Therefore, the vegetative subpopulation always remains relatively large in the more “aggressive” population.

Sporulation efficiencies ranging from $\approx 0\%$ (laboratory selected) to $\approx 100\%$ (naturally selected) can be found in the literature [167, 168]. However, 100% sporulation efficiency is uncommon [167]. In the model, 100% sporulation can only be obtained if there was no germination at all values of $\frac{f}{X_1+X_2}$ (or $\beta \to \infty$), which implies that there will be no vegetative cells after they all commit to sporulation (even with a re-introduction of nutrients).

Although this may seem like a poor strategy, it will be shown in Section 7.7 that this is a useful tactic under certain situations. Similarly, 0% sporulation efficiency may also be an effective survival strategy since there are many other bacteria that are not capable of forming spores (e.g. *Escherichia coli*), but they are able to flourish in a variety of different environments. Thus, the allowable values for each $b_i(k)$ will be

$$0 \leq b_i(k),$$

with no upper limit for each $b_i(k)$ to accommodate 100% sporulation. The corresponding sporulation efficiencies $u_i(k)$ are therefore limited to

$$0 \leq u_i(k) \leq 1.$$

A plot of the mapping between the $b_i(k)$ and sporulation efficiencies $u_i(k)$ is given in Figure 7.7.

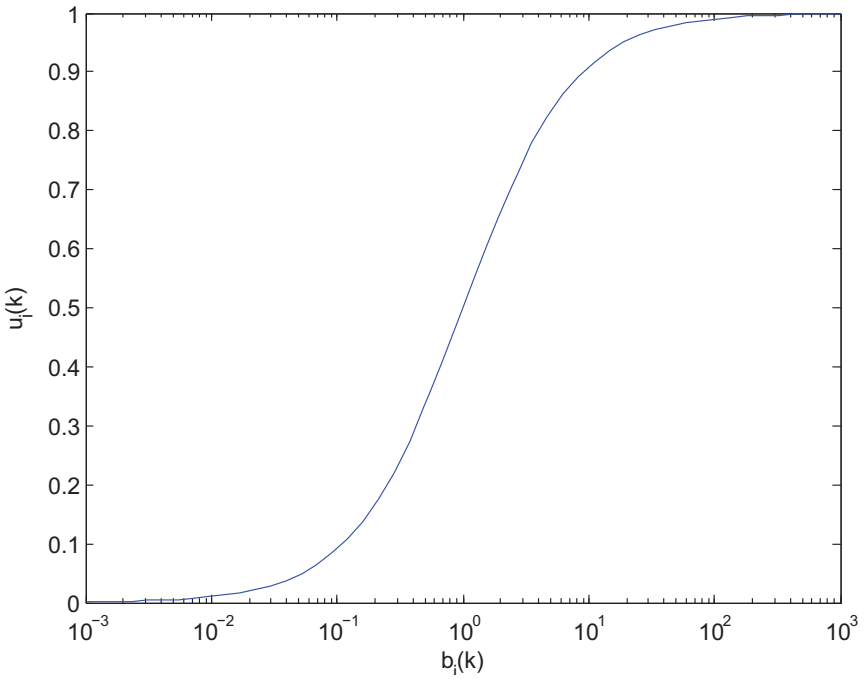

Figure 7.7: Relationship between $b_i(k)$ and the sporulation efficiency parameter $u_i(k)$.

7.7 Evolutionary stable strategies

With the "control" parameter for a sporulating *B. subtilis* colony identified, the optimal policy can now be derived. However, finding the optimal control is not as straightforward as simply maximizing the steady state total population number– in this case, the optimal policy depends on the control of the competing population. This situation calls for a game-theoretic treatment, where tools developed specifically for evolutionary biology can be utilized. Before using these tools to address the optimal sporulation problem, relevant background is provided below.

7.7.1 Game theory background

The application of game theory to evolutionary biology allowed the development of a powerful idea applicable in several different fields, from economics to psychology [99, 175]. This idea, developed by John Maynard Smith, is to model the evolution of biological traits whose advantages depend on their frequency in the population [170]. This modeling framework allowed Maynard Smith to develop theory for an evolutionary stable strategy (ESS). Intuitively, an ESS is a biological trait/strategy which, if adopted by an entire population, cannot be invaded by a small number of deviant biological traits/strategies. In other words, no further evolutionary change is possible once an ESS is established. Since its roots lie in game theory, a brief introduction to game theory will be presented before the main results of ESSs are stated.

A game involves a number of players, a set of strategies for each player, and a payoff that quantitatively describes the outcomes of every play of the game in terms of the amount that each player wins or loses [10]. This payoff function, which players typically aim to maximize, depends on the strategies of all players. For example, in a two player game where player 1 adopts strategy q_1 and player 2 adopts strategy q_2, the payoff for player 1 is $J_1(q_1, q_2) \in \mathbb{R}$ (strategy q_1 played against strategy q_2) while the payoff for player 2 is $J_2(q_1, q_2) \in \mathbb{R}$ (strategy q_2 played against strategy q_1). Though both players seek to maximize their payoffs, they do not know the strategies that the other player will use. Since each payoff depends on the strategy of the other player, this maximization must assume the other player acts in a certain way. Under the assumption that both players act *rationally*, each player will maximize his own payoff. This leads to the concept of a Nash equilibrium, which is defined to be a set of strategies (q_1^*, q_2^*) that are the best responses to each other– no player can do better by deviating from a Nash point, assuming that the other player does not deviate. Mathematically, for a two person game this corresponds to [10]

$$J_1(q_1^{NE}, q_2^{NE}) \geq J_1(q_1, q_2^{NE}) \text{ and}$$
$$J_2(q_1^{NE}, q_2^{NE}) \geq J_2(q_1^{NE}, q_2).$$

Note that a single player may have a higher payoff if both players use different strategies than (q_1^{NE}, q_2^{NE}). Also, if $J_1 = -J_2$, then a Nash equilibrium is a saddle point.

For q_1 and q_2 each played with certainty (not drawn from a probability distribution), there are conditions for the existence of at least one Nash equilibrium. If q_1 and q_2 are elements of compact and convex sets, and if the payoff functions satisfy [10]

1. J_1 and J_2 are continuous,
2. $q_1 \mapsto J_1(q_1, q_2)$ is concave for fixed q_2, and
3. $q_2 \mapsto J_2(q_1, q_2)$ is concave for fixed q_1,

then there is a Nash equilibrium for the payoff functions J_1 and J_2. These conditions are only sufficient, so Nash equilibria may exist that do not satisfy these conditions.

There are several methods for finding Nash equilibria. One such methodology involves the computation of the rational reaction sets for each player [10, 232]. For a two player game, these sets are

$$R_1 = \left\{ (q_1^*, q_2) \mid J_1(q_1^*, q_2) = \max_{q_1} J_1(q_1, q_2) \right\}$$
$$R_2 = \left\{ (q_1, q_2^*) \mid J_2(q_1, q_2^*) = \max_{q_2} J_2(q_1, q_2) \right\}$$

so each rational reaction set is the best response to the other player's (fixed) strategy. It is clear to see that the set of all Nash equilibria is given by $R_1 \cap R_2$.

It is possible for many Nash equilibria to exist for a game. Though there are several ways one may select a "correct" Nash equilibrium (which predicts the actual outcome of the game), one of the most widely used criteria is stability. An appealing definition of stability is offered by an ESS, which is stable in the following sense: No player can do better with a unilateral switch to another strategy, and there is no incentive to move to another equilibrium. In other words, once an ESS is established, no other strategy can invade [82].

It is clear that if q^* is an ESS, then (q^*, q^*) is a Nash equilibrium. Hence, it is an optimal policy under the assumption that other members also adopt their optimal policies. However, not every Nash equilibrium satisfies the stability property of an ESS. Conditions for an ESS can be derived from the following thought experiment [10]: Suppose a population is composed of many members, where pairwise conflicts between population members often occur. When these conflicts do occur, a symmetric game is played ($J_1(q_1, q_2) = J_2(q_2, q_1)$), which allows the analysis to proceed by focusing on the payoff $J = J_1$ to player 1.

For the sake of simplicity, assume the allowable strategies for the game are $q^*, q_1, q_2, \ldots, q_N$. Suppose that strategy q^* is used by most members of the population and a small proportion of the population adopts deviant strategies $q_1, q_2, \ldots, q_N$. From the point of view of player 1, let $1-p$ be the probability of playing a game with a player adopting q^*, and let p_i be the probability of playing a game with a player adopting q_i, where $\sum_{i=1}^N p_i = p$. Since q^* is used by most population members, assume $0 < p \approx 0$.

If player 1 adopts q^*, his expected fitness in a pairwise conflict with another member of the population is

$$F(q^*) = J(q^*, q^*)(1-p) + \sum_{i=1}^{N} J(q^*, q_i) p_i.$$

If player 1 adopts a deviant strategy q_k, his expected payoff is

$$F(q_k) = J(q_k, q^*)(1-p) + \sum_{i=1}^{N} J(q_k, q_i) p_i.$$

For strategy q^* to be strictly better than *any* deviant strategy q_k,

$$\begin{aligned} & F(q^*) > F(q_k) \\ \Leftrightarrow\ & J(q^*, q^*) > J(q_k, q^*) + \frac{1}{1-p} \sum_{i=1}^{N} \left[J(q_k, q_i) - J(q^*, q_i) \right] p_i \end{aligned}$$

for all $k = 1, \ldots, N$. However, since $p \approx 0$, then strategy q^* is better against any deviant strategy if

$$J(q^*, q^*) > J(q_k, q^*) \text{ for all } k = 1, \ldots, N.$$

Therefore, a population with most members adopting q^* cannot be invaded by a small population adopting deviant strategies. If $J(q^*, q^*) = J(q_k, q^*)$ for some k, it is still possible for $F(q^*) > F(q_k)$ as long as

$$J(q^*, q_i) > J(q_k, q_i) \text{ for all } i = 1, \ldots, N$$

for all of the k such that $J(q^*, q^*) = J(q_k, q^*)$.

This leads to the following definition [169, 266]: A strategy q^* is an ESS against deviant strategies $q_1, q_2, \ldots, q_N$ if either

1. $J(q^*, q^*) > J(q_k, q^*)$, for all $k = 1, \ldots, N$,
2. for any q_k such that $J(q^*, q^*) = J(q_k, q^*)$, we must have $J(q^*, q_i) > J(q_k, q_i)$ for all $i = 1, \ldots, N$.

An analogous derivation for a continuum of strategies ($N \to \infty$) will produce a similar definition of an ESS.

7.7.2 Evolutionary stable strategies for the quasi-steady state model

To make our exposition simpler, the following analysis will be performed in terms of the parameters $b_i(k)$, which form a one-to-one map with sporulation efficiencies $u_i(k)$ (see Figure 7.7).

Since evolution cannot predict the future, it is only capable of operating *in response* to each $\epsilon(k)$. For population 1, this means

$$b_1^*(k) = \arg \max_{0 \le b_1(k)} \; J_1(b_1(k), b_2(k))$$

where $J_1(b_1(k), b_2(k)) = A_1(k+1)$ represents the payoff for choosing $b_1(k)$ against the strategy $b_2(k)$. The 2^{nd} population's goal is similarly defined, where $J_2(b_1(k), b_2(k)) = A_2(k+1)$. It is easy to derive the rational reaction sets for populations 1 and 2:

$$\begin{aligned}
R_1 &= \{(b_1(k), b_2(k)) \mid b_1(k) = b_1^*(k)\} \\
&\quad \text{where } b_1^*(k) = \begin{cases} \max\left\{0, \sqrt{\frac{A_1(k)}{A_2(k)}}(1 + b_2(k)) - 1\right\} & \text{if } \epsilon(k) > 0 \\ \infty & \text{if } \epsilon(k) < 0 \end{cases} \\
R_2 &= \{(b_1(k), b_2(k)) \mid b_2(k) = b_2^*(k)\} \\
&\quad \text{where } b_2^*(k) = \begin{cases} \max\left\{0, \sqrt{\frac{A_2(k)}{A_1(k)}}(1 + b_1(k)) - 1\right\} & \text{if } \epsilon(k) > 0 \\ \infty & \text{if } \epsilon(k) < 0 \end{cases}
\end{aligned}$$

Note that R_1 and R_2 depend on the population numbers $A_1(k)$ and $A_2(k)$ when $\epsilon(k) > 0$. This is because of the density-dependent reward functions $J_1(b_1(k), b_2(k))$ and $J_2(b_1(k), b_2(k))$, which are uncommon in biological game theory applications due to the assumption of individual pairwise conflicts [170]. We may assume a similar setup with inter-population conflicts occurring between individual bacteria or small (but equally-sized) subgroups of each population, which implies that $A_1(k) = A_2(k)$ in the reward functions above. This will be called the "fair-game" assumption in the sequel.

Alternatively, we may prove that $A_1(k) = A_2(k)$ *eventually* if each population acts rationally (i.e. adopts $b_1^*(k)$ and $b_2^*(k)$) and $\epsilon(k)$ has the same sign for all k. This steady state framework is valid if we assume that both populations have been interacting for a long time in a consistently-trending environment before performing our analysis.

Assume that $A_1(k) < A_2(k)$ and $\epsilon(k) > 0\ \forall k$, and suppose $b_2^*(k)$ is given. Then $b_1^*(k) < b_2^*(k)$. Defining $\Delta A_i(k) := \frac{1}{\epsilon(k)}\left(A_i(k+1) - A_i(k)\right)$, $i = 1, 2$, it is easy to see that

$$\Delta A_1(k) = \frac{A_1(k)(1+b_1^*(k))(1+b_2^*(k))^2}{A_1(k)(1+b_2^*(k))^2 + A_2(k)(1+b_1^*(k))^2}\ \frac{1}{\gamma}$$
$$\Delta A_2(k) = \frac{A_2(k)(1+b_1^*(k))^2(1+b_2^*(k))}{A_1(k)(1+b_2^*(k))^2 + A_2(k)(1+b_1^*(k))^2}\ \frac{1}{\gamma}.$$

Since $A_i(k+1) = \left(1 + \frac{\Delta A_i(k)}{A_i(k)}\epsilon(k)\right) A_i(k)$ and $\epsilon(k) > 0$, the population with the larger $\frac{\Delta A_i(k)}{A_i(k)}$ will have the larger rate of growth. Indeed,

$$\frac{(1+b_1^*(k))(1+b_2^*(k))^2}{A_1(k)(1+b_2^*(k))^2 + A_2(k)(1+b_1^*(k))^2} > \frac{(1+b_1^*(k))^2(1+b_2^*(k))}{A_1(k)(1+b_2^*(k))^2 + A_2(k)(1+b_1^*(k))^2}$$

since $b_1^*(k) < b_2^*(k)$. Since the analysis is symmetric when $A_1(k) > A_2(k)$, we have that $A_1(k) \to A_2(k)$ as $k \to \infty$.

The set of all Nash equilibria is given by $R_1 \cap R_2$ [10, 232] under the condition that $A_1(k) = A_2(k)$. Note that, since J_1 and J_2 are not strictly concave for fixed $b_2(k)$ and $b_1(k)$, respectively, then there is no guarantee that $R_1 \cap R_2$ is not empty. However, there are Nash equilibria, which are given by

$$\left(b_1^{NE}(k), b_2^{NE}(k)\right) = \begin{cases} \left(b_2^{NE}(k), b_1^{NE}(k)\right) & \text{if } \epsilon(k) > 0 \\ (\infty, \infty) & \text{if } \epsilon(k) < 0 \end{cases}$$

which says that there are infinitely many Nash equilibria when $\epsilon(k) > 0$ and one Nash equilibria when $\epsilon(k) < 0$. Of this set of Nash equilibria, it can be shown that

$$\left(b_1^{NE}(k), b_2^{NE}(k)\right) = \begin{cases} (0, 0) & \text{if } \epsilon(k) > 0 \\ (\infty, \infty) & \text{if } \epsilon(k) < 0 \end{cases}$$

are in fact ESSs. Similar to the definition given in background section for ESSs, a strategy $b^{ESS}(k)$ from a continuum of strategies is an ESS against deviant strategies $b(k)$ if either

1. $J(b^{ESS}(k), b^{ESS}(k)) > J(b(k), b^{ESS}(k))$, for each $b(k) \neq b^{ESS}(k)$,

2. for any $b(k)$ such that $J(b^{ESS}(k), b^{ESS}(k)) = J(b(k), b^{ESS}(k))$, we must have

$$J(b^{ESS}(k), \hat{b}(k)) > J(b(k), \hat{b}(k))$$

for all $\hat{b}(k) \neq b^{ESS}(k)$,

where J can be J_1 or J_2 because it is assumed that all population members participate in symmetric games [10]. The following analysis assumes $J = J_1$, which focuses on the payoff to player 1.

It can be verified that Condition 1 of the ESS definition holds for $b^{NE}(k) = 0$ when $\epsilon(k) > 0$ and $b^{NE}(k) = \infty$ when $\epsilon(k) < 0$. Suppose that $\epsilon(k) > 0$, $A_1(k) = A_2(k)$, and consider the strategy $b^{NE}(k) = 0$. Then,

$$\begin{aligned} J(0,0) &= A_1(k)\left[1 + \frac{\frac{1}{\gamma}}{A_1(k) + A_2(k)}\epsilon(k)\right] \\ &= A_1(k) + \frac{1}{2}\frac{\epsilon(k)}{\gamma}. \end{aligned}$$

Now, playing any other strategy $b(k) > 0$, the payoff is

$$\begin{aligned} J(b(k),0) &= A_1(k)\left[1 + \frac{\frac{1}{\gamma}(1 + b(k))}{A_1(k) + A_2(k)(1 + b(k))^2}\epsilon(k)\right] \\ &= A_1(k) + \frac{1 + b(k)}{1 + (1 + b(k))^2}\frac{\epsilon(k)}{\gamma}. \end{aligned}$$

For any $b(k) > 0$, $J(0,0) > J(b(k),0)$. To see why, suppose not: $J(0,0) \leq J(b(k),0)$. Then,

$$\begin{aligned} \frac{1}{2} &\leq \frac{1 + b(k)}{1 + (1 + b(k))^2} \\ \Leftrightarrow\ 1 + (1 + b(k))^2 &\leq 2 + 2b(k) \\ \Leftrightarrow\ 1 + 2b(k) + b^2(k) &\leq 1 + 2b(k) \end{aligned}$$

which is a contradiction because $b(k) > 0$. Therefore, $b^{ESS}(k) = 0$ when $\epsilon(k) > 0$.

To show that $b^{NE}(k) = \infty$ is an ESS when $\epsilon(k) < 0$, a similar process is followed. When $A_1(k) = A_2(k)$ and $b^{NE}(k) = \infty$, there are no vegetative cells that perish as a result of the diminished nutrient supply (due to 100% sporulation efficiency). Then, by inspection,

$$J(\infty, \infty) = A_1(k+1) = A_1(k)$$

i.e. the total population is unaffected due to the assumption that spores are independent of the nutrient supply. Playing any other strategy $b(k) < \infty$, the payoff is

$$\begin{aligned} J(b(k),\infty) &= A_1(k)\left[1 + \frac{\frac{1}{\gamma}(1 + b(k))}{A_1(k)}\epsilon(k)\right] \\ &= A_1(k) + (1 + b(k))\frac{\epsilon(k)}{\gamma}. \end{aligned}$$

It is obvious that $J(\infty,\infty) > J(b(k),\infty)$ since $\epsilon(k) < 0$. Thus, $b^{NE}(k) = \infty$ is an ESS. It may seem unsettling that the stated value $J(\infty,\infty) = A_1(k)$ was not equal to

$$A_1(k) + \frac{(1+\infty)(1+\infty)^2}{(1+\infty)^2 + (1+\infty)^2}\frac{\epsilon(k)}{\gamma}.$$

However, the payoff $J(\infty,\infty) = A_1(k)$ is correct. The reason is because the asymptotic expansion for the new equilibrium,

$$\hat{X}_1 + \hat{S}_1 = \overline{X}_1 + \overline{S}_1 + (X_{1,1} + S_{1,1})\,\epsilon$$

breaks down ($(X_{1,1} + S_{1,1})\,\epsilon \sim 1$) when both sporulation efficiencies approach ∞. Therefore, Equations (7.2) and (7.3) are no longer valid, so the payoff should be calculated by referring to the original system of equations.

The ESS is therefore

$$b^{ESS}(k) = \begin{cases} 0 & \text{if } \epsilon(k) > 0 \\ \infty & \text{if } \epsilon(k) < 0 \end{cases} \tag{7.4}$$

which says that it is optimal to be "aggressive" when the nutrient supply is increasing and "conservative" when the nutrient supply is decreasing.

This ESS is robust to other reward functions. For example, suppose that $J(b_1(k), b_2(k)) = A_1(k+1) - A_2(k+1)$ (a reward function for a zero-sum game). Then, the fair-game assumption leads to the Nash equilibria

$$\left(b_1^{NE}(k), b_2^{NE}(k)\right) = \begin{cases} \left(b_2^{NE}(k), b_1^{NE}(k)\right) & \text{if } \epsilon(k) > 0 \\ (\infty,\infty) & \text{if } \epsilon(k) < 0 \end{cases}.$$

To show that Equation (7.4) is an ESS for this reward function, note that $J(b(k), b(k)) = 0$ for any $0 \le b(k)$ as long as the fair-game assumption holds. In particular,

$$\begin{aligned} J(0,0) &= 0 \\ J(\infty,\infty) &= 0. \end{aligned}$$

Now, when $\epsilon(k) > 0$ and $b(k) > 0$,

$$\begin{aligned} J(b(k),0) &= \frac{-b^2(k)(1+b(k))}{(1+b(k))^2+1}\frac{\epsilon(k)}{\gamma} \\ &< J(0,0) \end{aligned}$$

and when $\epsilon(k) < 0$ and $b(k) < \infty$,

$$\begin{aligned} J(b(k),\infty) &= (1+b(k))\frac{\epsilon(k)}{\gamma} \\ &< J(\infty,\infty) \end{aligned}$$

which implies that Equation (7.4) also gives an ESS for this zero-sum reward function.

The evolutionary optimal decision policy relies on the sign of changes in the nutrient supply. Under ideal circumstances, the *B. subtilis* population will never decrease since $u_i(k) = 1$ (100% sporulation efficiency) accompanies decreases in nutrient supply. When the nutrient supply increases, the optimal policy calls for no spores. In this sense, the decision policy resembles a bang-bang/on-off controller. Of course, from a mean population point-of-view, this does not happen to actual bacterial colonies, where the dynamics of evolutionary change limit the bandwidth of the evolutionary optimal controller.

7.8 Dynamics of evolution

7.8.1 Evolutionary dynamics background

An ESS is a policy that players will adopt because no other player can do better by adopting a deviant strategy. Since it also defines a Nash equilibrium, an ESS is optimal under the assumption that other players use their optimal strategies [10, 197]. However, since it describes the strategy which *eventually* becomes established in the population, an ESS is a steady state policy in a population with invariant payoffs. In the context of simple biological systems, an ESS corresponds to a genotype (strategy) that maximizes the fitness (payoff) of an organism in response to the maximum-fitness phenotypes adopted by other organisms. The dynamics of evolution typically preclude the possibility of a different optimal policy becoming unilaterally adopted by a population after one round of selection [172]; frequency gains of the optimal genotype (the fraction of the population adopting the optimal strategy) are usually modeled and observed to be incremental as long as genotypes produce a positive number of offspring. Over time, however, genes that give rise to maximum fitness will increase in frequency (across the population) to 1. Mathematically, the Price equation [215] and other selection equations predict this behavior. For example, the simple selection dynamics suggested by Orr [194] predict that changes in allele frequency can be modeled as

$$\Delta p = \frac{pqs}{1 - qs}$$

where p is the frequency of allele 1, $q = 1 - p$ is the frequency of allele 2, and $s \in [0, 1]$ is the selection coefficient (allele 2's fitness measured as a fraction of allele 1's fitness). For $q, p \in (0, 1)$, it is impossible for Δp to be $-p$ or $1 - p$, so a genotype offering the optimal phenotype/maximum fitness cannot overtake an entire population in one step. Indeed, these selection dynamics predict sigmoidal paths of allele frequencies. The Price equation, which models the selection dynamics differently, reproduces this behavior in the sense that "gene frequencies change so as to move towards optimality" [91]. Since the fitness of a gene is determined by its phenotype(s), the more fit traits will spread in a population through competitive interactions until the entire population is composed of the trait that offers maximum fitness, but this process takes many rounds of selection.

It can be shown that incremental increases in the optimal genotype lead to incremental changes in a population's average fitness. In other words, the average fitness across a population cannot reach its maximum fitness after one round of selection. Suppose that

$0 \leq x \leq \overline{x}$ is an allowable set of genotypes in a population, with elements ordered such that strategy $x = 0$ has the lowest fitness and $x = \overline{x}$ has the highest fitness. The fitness associated with each genotype is given by an increasing function $f(x)$. Let the distribution of phenotypes initially be $F_1(x)$ and the corresponding density be $p_1(x)$, and after one round of selection, the distribution changes incrementally to $F_2(x)$ (with corresponding density $p_2(x)$) such that $F_1(x) \geq F_2(x)\ \forall x \in [0, \overline{x}]$, with strict inequality holding for at least some x. In other words, the strategies with high fitness spread in the population while the strategies with low fitness get weeded out. Suppose that the KL divergence between $F_1(x)$ and $\mathbf{1}(\overline{x})$ is sufficiently large such that an "incremental change" results in $F_2(x) \neq \mathbf{1}(\overline{x})$, where $\mathbf{1}(\overline{x})$ is the heaviside step function. Since the genotype sets are the same for both populations, the average population fitnesses are

$$J_1 = \int_0^{\overline{x}} f(x)p_1(x)dx$$
$$J_2 = \int_0^{\overline{x}} f(x)p_2(x)dx$$

before and after the round of natural selection, respectively. Note that, since $f(x)$ is increasing in x,

$$\begin{aligned} J_2 = \int_0^{\overline{x}} f(x)p_2(x)dx &< f(\overline{x}) \int_0^{\overline{x}} p_2(x)dx \\ &= \int_0^{\overline{x}} f(x)\delta(\overline{x})dx \end{aligned}$$

where $\delta(\overline{x}) = \frac{d}{dx}\mathbf{1}(\overline{x})$, so J_2 does not achieve the maximum fitness. The average population fitness does increase, however, which can be shown by defining

$$y_1 = F_1(x)$$
$$y_2 = F_2(x)$$

so $\frac{dy_1}{dx} = p_1(x)$ and $\frac{dy_2}{dx} = p_2(x)$. This notation results in

$$J_1 = \int_0^{\overline{x}} f(x)p_1(x)dx = \int_0^1 f\left(F_1^{-1}(y_1)\right) dy_1 = \int_0^1 f\left(F_1^{-1}(y)\right) dy$$
$$J_2 = \int_0^{\overline{x}} f(x)p_2(x)dx = \int_0^1 f\left(F_2^{-1}(y_2)\right) dy_2 = \int_0^1 f\left(F_2^{-1}(y)\right) dy.$$

Since $F_1(x) \geq F_2(x)$, $F_1^{-1}(y) \leq F_2^{-1}(y)$ with strict inequality holding for at least some y. Since f is increasing, this implies that

$$\begin{aligned} \int_0^1 f\left(F_1^{-1}(y)\right) dy &< \int_0^1 f\left(F_2^{-1}(y)\right) dy \\ \Rightarrow\ J_1 &< J_2 \end{aligned}$$

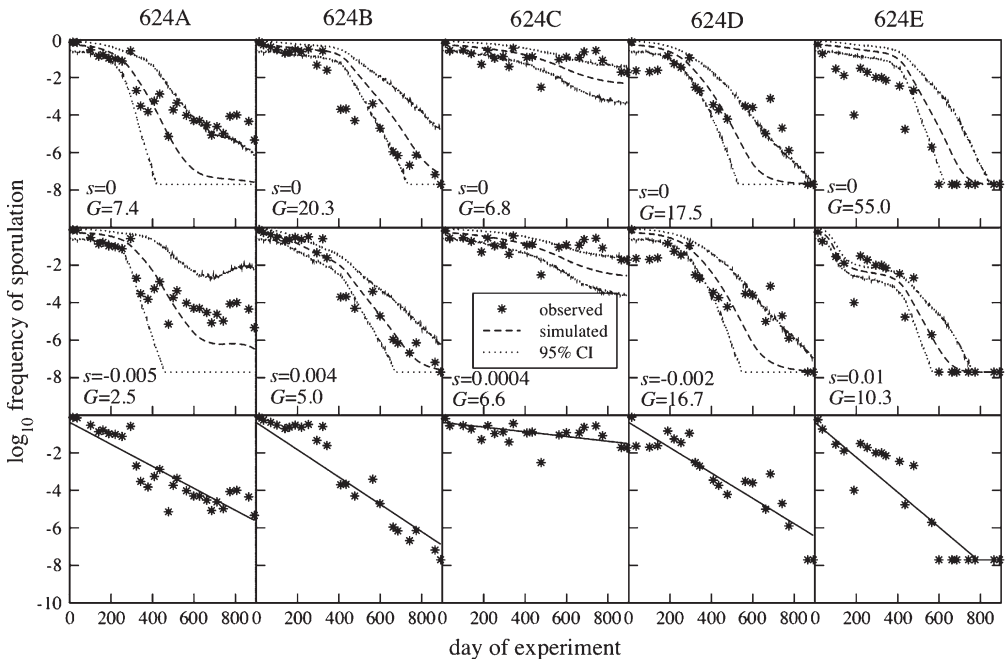

Figure 7.8: Adaptation of sporulation efficiency in *B. subtilis* populations over 6000 generations, from Maughan *et al.* [167].

so the average population fitness has increased, but because of the incremental change in the genotype distribution, it does not achieve its maximum value.

There are several records of average population fitness gains due to adaptation by natural selection in laboratory settings. In response to a new, relatively constant environment, many of these fitness gains are "initially rapid but tend to decelerate over time" [67]. Elena and Lenski [67] suggest that these dynamics indicate that the populations, after being placed in a new environment, are evolving from a region of low fitness towards an adaptive peak or plateau (adopting Wright's "fitness landscape" as a visualization model [273]). For example, in a long-term (6000 generations) experiment with several groups of *B. subtilis* populations undergoing selection against sporulation, the experimental populations showed that sporulation efficiency ($u(k)$ in the model presented) decreased exponentially to 0% (three of the five populations) or nearly 0% (two of the five populations) [167]; see Figure 7.8. Though there was no significant increase in sporulation efficiency in the five populations grown in an environment that presumably selected for sporulation [168], it was generally observed that competitive fitness (against ancestors) increased the largest during the early evolutionary stages [166]. Though the genetic details of these experiments is beyond the scope of this work, it was found that up to 27% of the genes analyzed were transcribed at significantly different levels than the ancestor [165], which indicates that these changes were in fact due to natural selection.

Other experiments demonstrate initially fast adaptation that decelerates over time. In a long-term experiment on *E. coli* that evolved for 20000 generations in a specific growing condition, it was found that the rate of improvement was $\frac{1}{10}$ as fast between generations

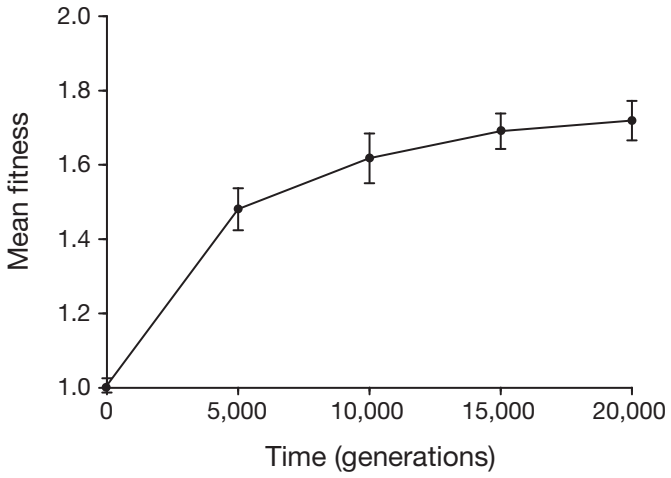

Figure 7.9: Fitness gains in *E. coli* populations over 20000 generations, from Cooper and Lenski [41].

15000-20000 compared to the first 5000 generations [41, 51]. At a higher generational resolution, it was also observed that morphology (cell size) and fitness (measured in competition with the ancestor) evolved rapidly for the first 2000 generations and was relatively static between 5000-10000 generations [153]. Data from these experiments is shown in Figure 7.9, and the authors suggested a hyperbolic model to fit the data [51, 153].

The general, qualitative dynamics of decelerating fitness gains are reproduced in other experiments with bacteria [60, 142, 268, 274] and viruses [31, 191]. One important idea that all of these data confirm is that evolution does not act instantaneously across a population at a sufficiently fine time scale. Though a single member of the population may exhibit an adaptive step change in fitness [67], the *average population fitness* changes are relatively continuous. Specifically, if a population adopts an ESS for one environment and is abruptly placed in a different environment, it will exhibit a seemingly continuous change to the new ESS [111, 112, 192]. According to the studies cited above on evolutionary dynamics, this change will decelerate over time.

7.8.2 Proposed evolutionary model

The experimental studies outlined in the previous section suggest that a simple, linear model may be an adequate way to describe changes between two evolutionary stable strategies. Additionally, the sporulation efficiency adaptation studies [165, 166, 167, 168] suggest an evolutionary model governing the dynamics of $u(k)$. Letting $u(k)$ parameterize the sporulation efficiency for the k^{th} steady state ($u(k) = 0$, no sporulation; $u(k) = 1$, 100% sporulation), the proposed model for evolutionary changes to the sporulation decision policy due

to natural selection is

$$u(k+1) = u(k) + \Delta u(k) \tag{7.5}$$
$$\Delta u(k) = \begin{cases} \eta_I \left(1 - u(k)\right) & \text{if } \epsilon(k) < 0 \\ -\eta_D u(k) & \text{if } \epsilon(k) > 0 \end{cases}$$

where η_I and η_D describe the effect of selection pressure on increases and decreases in $u(k)$, respectively. Both parameters η_I and η_D must be chosen so $0 \leq u(k) \leq 1$ $\forall k$ (i.e. no overshoot). This model agrees with the facts that evolutionary changes are non-anticipative and adaptive changes decelerate over time. Though the time scale of the model is in terms of successive steady states, $\epsilon(k)$ may be restricted to be small enough so a relatively constant number of generations is elapsed during some percentage (i.e. 95%) settling time. The linearity of the model is consistent with other evolutionary models (e.g. [271]).

The proposed evolutionary model (7.5) is similar to replicator dynamics, which are often used to illustrate the dynamics of population games in the context of ESSs. Replicator dynamics, named because of the assumption that strategies breed true in an asexual population, track the frequency of pure strategies in a population in a system of ordinary differential equations or difference equations [10, 266]. For example, if a fraction $0 \leq x_1 \leq 1$ of the population adopted strategy u_1 and the remaining fraction $x_2 = 1 - x_1$ of the population adopted u_2, then the replicator dynamics are

$$\dot{x}_1 = x_1 \left[\{\text{Expected fitness of using } u_1\} - \{\text{Expected population fitness}\}\right]$$
$$\dot{x}_2 = x_2 \left[\{\text{Expected fitness of using } u_2\} - \{\text{Expected population fitness}\}\right]$$

where the expected fitnesses are evaluated at the current strategy distribution (x_1, x_2). Then, for instance, if $x_1 = 1$ then the expected fitness of using u_1 is the same as the expected fitness of the population. The population will then remain at this vertex of the simplex of possible choices for (x_1, x_2). Discrete time difference equations for replicator dynamics take a similar form,

$$x_1(k+1) = \frac{\alpha + \{\text{Expected fitness of using } u_1\}}{\alpha + \{\text{Expected population fitness}\}} x_1(k)$$
$$x_2(k+1) = \frac{\alpha + \{\text{Expected fitness of using } u_2\}}{\alpha + \{\text{Expected population fitness}\}} x_2(k)$$

where α is chosen large enough so the numerators (and hence the denominators) are always positive [112]. The stability of replicator dynamics is often used to relate the steady state x_i to an ESS [10, 266].

It can be shown that the simpler, linear evolutionary model (7.5) is consistent with the discrete time replicator dynamics under a few assumptions and simplifications. Suppose that strategies $0 \leq u(k) \leq 1$ are gridded into n different strategies, $0 = u_1 < u_2 < \cdots < u_n = 1$. Then, if $x_i(k)$ denotes the fraction of the population adopting strategy u_i at time k,

$$u(k) = \sum_{i=1}^{n} u_i x_i(k).$$

The dynamics of each x_i are

$$x_i(k+1) = \frac{\alpha + \{\text{Expected fitness of } u_i\}}{\alpha + \{\text{Expected population fitness}\}} x_i(k),$$

which lead to the dynamics of $u(k)$:

$$\begin{aligned} u(k+1) &= \sum_{i=1}^{n} u_i x_i(k+1) \\ &= \sum_{i=1}^{n} u_i x_i(k) \frac{\alpha + \{\text{Expected fitness of } u_i\}}{\alpha + \{\text{Expected population fitness}\}} \\ &= u(k) \\ &+ \frac{\{\text{Expected population fitness}\}}{\alpha + \{\text{Expected population fitness}\}} \left[\sum_{i=1}^{n} u_i x_i(k) \frac{\{\text{Expected fitness of } u_i\}}{\{\text{Expected population fitness}\}} - u(k) \right] \end{aligned}$$

which is equivalent to (7.5) if the following conditions hold:

1. $\alpha \gg 1$ so $\frac{\{\text{Expected population fitness}\}}{\alpha + \{\text{Expected population fitness}\}} \approx$ constant.
2. If strategy m has the highest fitness, then

$$\{\text{Expected fitness of } u_i\} = \begin{cases} \approx \frac{\{\text{Expected population fitness}\}}{x_i(k)} & \text{if } i = m \\ \ll \frac{\{\text{Expected population fitness}\}}{x_i(k)} & \text{otherwise} \end{cases}.$$

Note that it is generally very difficult for a reward function to satisfy the second condition. Nonetheless, the proposed evolutionary model (7.5) is approximately consistent with the structure of the replicator dynamics model. Though differences arise if the conditions above do not hold, the simplicity of the linear model compensates for the complexities of dealing with the replicator dynamics.

Since the proposed evolutionary model is based on population-average phenotype changes (or fitness changes, since the sporulation model assigns each sporulation efficiency a fitness value), it is general enough to allow for two different scenarios at the genetic level:

1. A single genotype which gives rise to phenotypic polymorphism. In other words, the entire population adopts a single genetic strategy gives rise to the probabilistic decision policy where a cell forms a spore in steady state with probability $u(k)$.

2. Genetic polymorphism which gives rise to phenotypic polymorphism. A simple example of this scenario is a fraction $u(k)$ of the population with a genetic predisposition to form spores more readily than the remaining $1 - u(k)$ fraction of the population. Importantly, these two subpopulations are genetically distinct.

The difference between these two cases will become important when the results are compared to "bet-hedging" strategies (see Section 7.10.2).

Since evolutionary dynamics preclude the possibility of bang-bang/on-off decision policies for stabilizing η_I and η_D, it is possible for a population to arrive at a non-equilibrium decision policy as $k \to \infty$ if the sign of $\epsilon(k)$ switches frequently enough. This possibility will be explored in Sections 7.9-7.10.

7.9 Environmental model

Suppose that the environment can switch between two modes. In one mode, denoted H for "high," $\epsilon(k)$ is positive. In the other, denoted L for "low," $\epsilon(k)$ is negative. In both cases, $\epsilon(k)$ must be small in order for the steady state model to remain valid.

It is assumed that $\epsilon(k)$ has the same magnitude $\overline{\epsilon}$ while in H or L for the sake of simplicity.

The Markov model in Figure 7.9 illustrates the proposed model for transitioning between H and L.

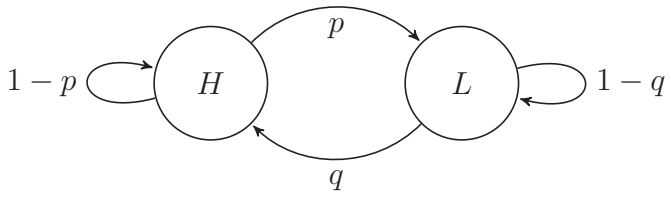

Figure 7.10: Markov model of environment. H corresponds to $\epsilon(k) = \overline{\epsilon} > 0$ and L corresponds to $\epsilon(k) = -\overline{\epsilon} < 0$.

The environment is modeled as randomly transitioning between periods of increasing nutrient supply and decreasing nutrient supply. This may be a realistic model for a periodic environment, such as nutrient variation due to changing seasons, weather, or circadian conditions. For example, it may be possible that nutrient availability from plant roots in soil (where *B. subtilis* commonly dwells) is dependent on 24-hour light cycles, temperature, and cloud cover. The environment may remain in H or L by setting p or q to zero, respectively, to model permanent trends in nutrient supply (as long as $\epsilon(k) \ll \overline{e}\ \forall k$ to preserve the validity of the model). The condition $q \approx 0$ may be applicable to desert isolates of *B. subtilis* (for example, from the Sonoran desert basalt [168]), where sustained nutrient depletion is sporadically interrupted by short periods of outgrowth.

For fixed p and q, $\epsilon(k)$ is now a random process. As k gets large, we can easily calculate $\mathbb{E}\{\epsilon(k)\}$ since the environmental Markov chain is a single class of recurrent states [22]. The stationary distribution of the Markov chain in Figure 7.9 is

$$\text{Operating mode} = \begin{cases} H & \text{with probability } \frac{q}{p+q} \\ L & \text{with probability } \frac{p}{p+q} \end{cases}$$

which implies that, as k gets large,

$$\begin{aligned} \mathbb{E}\{\epsilon(k)\} &= \overline{\epsilon}\ \Pr\{\epsilon(k) = \overline{\epsilon}\} - \overline{\epsilon}\ \Pr\{\epsilon(k) = -\overline{\epsilon}\} \\ &= \overline{\epsilon}\frac{q}{p+q} - \overline{\epsilon}\frac{p}{p+q} \\ &= \overline{\epsilon}\frac{q-p}{p+q}. \end{aligned}$$

Large k is a reasonable assumption because it is assumed that ESSs are steady state policies. One may alternatively invoke the ergodicity of the environmental Markov chain.

Due to the choice of expanding the new steady state to only the first power of ϵ, i.e. $\hat{X}_1 = \overline{X}_1 + X_{1,1}\epsilon$, and the fair-game assumption $A_1(k) = A_2(k)$, the ESS for the reward function $\mathbb{E}\{A(k+1)\}$ is

$$b^{ESS}(k) = \begin{cases} 0 & \text{if } \mathbb{E}\{\epsilon(k)\} > 0 \\ \infty & \text{if } \mathbb{E}\{\epsilon(k)\} < 0 \end{cases}$$

or

$$b^{ESS}(k) = \begin{cases} 0 & \text{if } q > p \\ \infty & \text{if } q < p \end{cases} . \tag{7.6}$$

In terms of the sporulation efficiencies, the ESSs are

$$u^{ESS}(k) = \begin{cases} 0 & \text{if } q > p \\ 1 & \text{if } q < p \end{cases} . \tag{7.7}$$

This policy is intuitive when viewed from a long-term interpretation. Denoting T_H as the (random) time spent in H and T_L as the (random) time spent in L for one complete cycle, we would expect a positive average (in time) nutrient influx if $\mathbb{E}\{T_H\} > \mathbb{E}\{T_L\}$. Thus, the optimal policy should correspond to positive nutrient influx, or $u = 0$. Note that the probability mass functions for T_H and T_L are

$$\Pr\{T_H = t_H\} = (1-p)^{t_H - 1} p$$
$$\Pr\{T_L = t_L\} = (1-q)^{t_L - 1} q$$

so

$$\mathbb{E}\{T_H\} > \mathbb{E}\{T_L\}$$
$$\Leftrightarrow \ \frac{1}{p} > \frac{1}{q}$$

which is equivalent to the condition for $u^{ESS}(k) = 0$.

Unless p or q are zero, the ESS for sporulation efficiencies will never be achieved in steady state due to the proposed evolutionary model. Notably, evolution cannot see into the future, so selection cannot take expected long-term behavior into account. For example, whenever the environment is in L, a subpopulation with $u = 1$ will out-compete a subpopulation with $u = 0$, which will shift the average total-population sporulation policy upwards. This will happen even if $\mathbb{E}\{T_H\} \gg \mathbb{E}\{T_L\}$, and it will prevent $u^{ESS} = 0$ from ever being attained.

Intuitively, it is expected that the actual value of $u(k)$ will depend on the period and "duty cycle" of the environment. For instance, if $\eta_I = \eta_D$ and $p \approx q > 0$, then $u(k)$ will be around $\frac{1}{2}$ on average. Though not optimal from an evolutionary point of view (a population with a fixed $u = 0$ or $u = 1$ would do better in the long run), the actual policy which is constrained by evolutionary dynamics will be derived in the next section.

7.10 Non-equilibrium policy

Since the dynamics of $u(k)$ depend on the sign of $\epsilon(k)$, the actual sporulation policy becomes a random process.

Theorem 7.10.1. *Suppose $q \neq 0$ and $p \neq 0$. Then, as $k \to \infty$, $\mathbb{E}\{u(k)\}$ will converge to a periodic signal with minimum value*

$$u_{min} = \frac{\left[1 - \frac{(1-\eta_I)q}{1-(1-\eta_I)(1-q)}\right] \frac{(1-\eta_D)p}{1-(1-\eta_D)(1-p)}}{1 - \frac{(1-\eta_I)q}{1-(1-\eta_I)(1-q)} \frac{(1-\eta_D)p}{1-(1-\eta_D)(1-p)}} \tag{7.8}$$

and maximum value

$$u_{max} = 1 + (u_{min} - 1)\frac{(1-\eta_I)q}{1-(1-\eta_I)(1-q)}. \tag{7.9}$$

Proof. As before, denote T_H as the (random) time spent in H and T_L as the (random) time spent in L. Without loss of generality, suppose that the environment enters L at $k = 0$. While in L, the value of $u(k)$ increases:

$$\mathbb{E}\{u(T_L)\} = \mathbb{E}\left\{u(0) + \sum_{k=0}^{T_L-1} \Delta u(k)\right\} = \mathbb{E}\{u(0)\} + \mathbb{E}\left\{\sum_{k=0}^{T_L-1} \Delta u(k)\right\}.$$

The expected summation can be broken down into two parts,

$$\begin{aligned}\mathbb{E}\left\{\sum_{k=0}^{T_L-1} \Delta u(k)\right\} &= \mathbb{E}\left\{\sum_{k=0}^{T_L-1} \eta_I\left(1 - u(k)\right)\right\} \\ &= \mathbb{E}\left\{\sum_{k=0}^{T_L-1} \eta_I\right\} - \mathbb{E}\left\{\sum_{k=0}^{T_L-1} \eta_I u(k)\right\}\end{aligned}$$

with

$$\begin{aligned}\mathbb{E}\left\{\sum_{k=0}^{T_L-1} \eta_I\right\} &= \mathbb{E}\left\{\mathbb{E}\left\{\sum_{k=0}^{T_L-1} \eta_I \middle| T_L\right\}\right\} \\ &= \mathbb{E}\{T_L\eta_I\} \\ &= \frac{1}{q}\eta_I\end{aligned}$$

and, assuming $|1-\eta_I|<1$,

$$\begin{aligned}
\mathbb{E}\left\{\sum_{k=0}^{T_L-1}\eta_I u(k)\right\} &= \mathbb{E}\left\{\mathbb{E}\left\{\sum_{k=0}^{T_L-1}\eta_I u(k)\middle| T_L\right\}\right\}\\
&= \mathbb{E}\left\{\eta_I\mathbb{E}\left\{\sum_{k=0}^{T_L-1} u(k)\middle| T_L\right\}\right\}\\
&= \mathbb{E}\left\{\eta_I\left[\sum_{k=0}^{T_L-1}\mathbb{E}\left\{u(0)\right\}(1-\eta_I)^k + \sum_{k=1}^{T_L-1}\sum_{i=0}^{k-1}(1-\eta_I)^i\eta_I\right]\right\}\\
&= \mathbb{E}\left\{\eta_I\left[\mathbb{E}\left\{u(0)\right\}\frac{1-(1-\eta_I)^{T_L}}{\eta_I} + \sum_{k=1}^{T_L-1}\left(1-(1-\eta_I)^k\right)\right]\right\}\\
&= \mathbb{E}\left\{\mathbb{E}\left\{u(0)\right\} - \mathbb{E}\left\{u(0)\right\}(1-\eta_I)^{T_L} + \eta_I(T_L-1) - \eta_I\sum_{k=1}^{T_L-1}(1-\eta_I)^k\right\}\\
&= \mathbb{E}\left\{u(0)\right\} - \mathbb{E}\left\{u(0)\right\}\mathbb{E}\left\{(1-\eta_I)^{T_L}\right\} + \eta_I\mathbb{E}\left\{T_L-1\right\}\\
&\qquad - \mathbb{E}\left\{(1-\eta_I)-(1-\eta_I)^{T_L}\right\}\\
&= \mathbb{E}\left\{u(0)\right\} - \mathbb{E}\left\{u(0)\right\}\frac{(1-\eta_I)q}{1-(1-\eta_I)(1-q)} + \eta_I\left(\frac{1}{q}-1\right)\\
&\qquad -(1-\eta_I) + \frac{(1-\eta_I)q}{1-(1-\eta_I)(1-q)}
\end{aligned}$$

or

$$\mathbb{E}\left\{\sum_{k=0}^{T_L-1}\eta_I u(k)\right\} = \left(\mathbb{E}\left\{u(0)\right\}-1\right) - \left(\mathbb{E}\left\{u(0)\right\}-1\right)\frac{(1-\eta_I)q}{1-(1-\eta_I)(1-q)} + \frac{\eta_I}{q}$$

Substituting these last two series of equalities into the original expression for $\mathbb{E}\left\{u(T_L)\right\}$ gives

$$\begin{aligned}
\mathbb{E}\left\{u(T_L)\right\} &= \mathbb{E}\left\{u(0)\right\} + \frac{\eta_I}{q} - \left(\mathbb{E}\left\{u(0)\right\}-1\right) + \left(\mathbb{E}\left\{u(0)\right\}-1\right)\frac{(1-\eta_I)q}{1-(1-\eta_I)(1-q)} - \frac{\eta_I}{q}\\
&= 1 + \left(\mathbb{E}\left\{u(0)\right\}-1\right)\frac{(1-\eta_I)q}{1-(1-\eta_I)(1-q)}. \qquad (7.10)
\end{aligned}$$

After T_L, the system spends T_H time units in H. During this time, the value of $u(k)$ decreases:

$$\begin{aligned}
\mathbb{E}\left\{u(T_L+T_H)\right\} &= \mathbb{E}\left\{u(T_L) + \sum_{k=T_L}^{T_L+T_H-1}\Delta u(k)\right\}\\
&= \mathbb{E}\left\{u(T_L)\right\} + \mathbb{E}\left\{\sum_{k=T_L}^{T_L+T_H-1} -\eta_D u(k)\right\}.
\end{aligned}$$

The second term can be computed as

$$\begin{aligned}
\mathbb{E}\left\{\sum_{k=T_L}^{T_L+T_H-1} -\eta_D u(k)\right\} &= \mathbb{E}\left\{\mathbb{E}\left\{\sum_{k=T_L}^{T_L+T_H-1} -\eta_D u(k)\middle| T_L, T_H\right\}\right\} \\
&= \mathbb{E}\left\{-\eta_D \sum_{k=T_L}^{T_L+T_H-1} \mathbb{E}\left\{u(k)\right\}\right\} \\
&= \mathbb{E}\left\{-\eta_D \mathbb{E}\left\{u(T_L)\right\} \sum_{k=T_L}^{T_L+T_H-1} (1-\eta_D)^{k-T_L}\right\} \\
&= -\mathbb{E}\left\{u(T_L)\right\} + \mathbb{E}\left\{u(T_L)\right\} \mathbb{E}\left\{(1-\eta_D)^{T_H}\right\} \\
&= -\mathbb{E}\left\{u(T_L)\right\} + \mathbb{E}\left\{u(T_L)\right\} \frac{(1-\eta_D)p}{1-(1-\eta_D)(1-p)}
\end{aligned}$$

so $\mathbb{E}\left\{u(T_L+T_H)\right\}$ can be written as

$$\begin{aligned}
\mathbb{E}\left\{u(T_L+T_H)\right\} &= \mathbb{E}\left\{u(T_L)\right\} + \left[-\mathbb{E}\left\{u(T_L)\right\} + \mathbb{E}\left\{u(T_L)\right\} \frac{(1-\eta_D)p}{1-(1-\eta_D)(1-p)}\right] \\
&= \left[1 + \left(\mathbb{E}\left\{u(0)\right\} - 1\right) \frac{(1-\eta_I)q}{1-(1-\eta_I)(1-q)}\right] \frac{(1-\eta_D)p}{1-(1-\eta_D)(1-p)}.
\end{aligned}$$

Using this equation, the dynamics of the local minima of $\mathbb{E}\left\{u(k)\right\}$ can be examined. Defining a time scale $T_n := n(T_L+T_H)$, $n = 0, 1, 2, \ldots$, the dynamics are

$$\begin{aligned}
\mathbb{E}\left\{u(T_{n+1})\right\} = \frac{(1-\eta_I)q}{1-(1-\eta_I)(1-q)} \frac{(1-\eta_D)p}{1-(1-\eta_D)(1-p)} \mathbb{E}\left\{u(T_n)\right\} \\
+ \left[1 - \frac{(1-\eta_I)q}{1-(1-\eta_I)(1-q)}\right] \frac{(1-\eta_D)p}{1-(1-\eta_D)(1-p)}. \quad (7.11)
\end{aligned}$$

Note that

$$\begin{aligned}
\frac{(1-\eta_I)q}{1-(1-\eta_I)(1-q)} &= \frac{q-q\eta_I}{1-(1-\eta_I-q+q\eta_I)} \\
&= \frac{q-q\eta_I}{\eta_I+q-q\eta_I} \\
&< 1
\end{aligned}$$

and similarly for $\frac{(1-\eta_D)p}{1-(1-\eta_D)(1-p)}$, which means that

$$\left|\frac{(1-\eta_I)q}{1-(1-\eta_I)(1-q)} \frac{(1-\eta_D)p}{1-(1-\eta_D)(1-p)}\right| < 1$$

so $\mathbb{E}\left\{u(T_n)\right\}$ approaches a constant value as $n \to \infty$. This value is determined by inspection of Equation (7.11):

$$\mathbb{E}\left\{u(T_n)\right\} \to \frac{\left[1 - \frac{(1-\eta_I)q}{1-(1-\eta_I)(1-q)}\right] \frac{(1-\eta_D)p}{1-(1-\eta_D)(1-p)}}{1 - \frac{(1-\eta_I)q}{1-(1-\eta_I)(1-q)} \frac{(1-\eta_D)p}{1-(1-\eta_D)(1-p)}}$$

which is the same as Equation (7.8), which proves that part of the theorem. For the maximum value, one simply uses Equation (7.10). □

Sporulation efficiency simulations for different environments are given in Figures 7.11 and 7.12. The upper and lower bounds for $\mathbb{E}\{u(k)\}$ (Equations (7.8) and (7.9)) are also given in the figures.

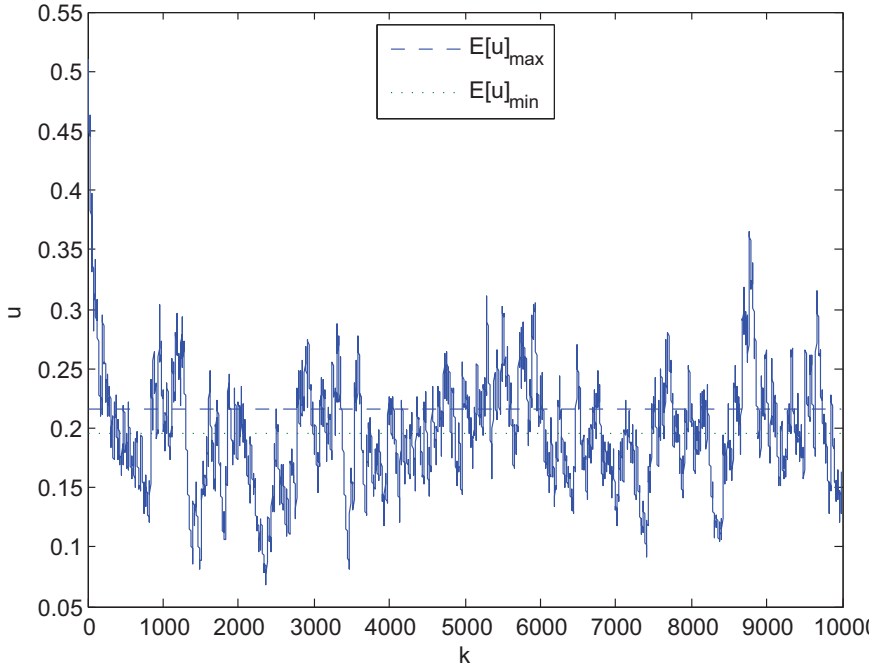

Figure 7.11: $u(k)$ for $p = 0.1$ and $q = 0.4$.

Note that the non-equilibrium policy is able to explain any sporulation efficiency between 0% and 100%, depending on the environment and model parameters. In this respect, it is consistent with the sporulation efficiencies given in Table 2.1 and the experimental data given in Section 3.4.4 (there was no observed germination, so the sporulation efficiencies were $\approx 100\%$). Though identifying the specific p and q parameters for real environments may be impossible, the qualitative behavior of the non-equilibrium policy is qualitatively consistent with observed *B. subtilis* behavior.

7.10.1 Non-equilibrium policy compared to ESS

For the environment modeled in Figure 7.9, the evolutionary optimal policy is given in Equation (7.7), repeated below:

$$u^{ESS}(k) = \begin{cases} 0 & \text{if } q > p \\ 1 & \text{if } q < p \end{cases} . \tag{7.7}$$

The actual expected policy given in the previous section is different from the evolutionary optimal policy. Notably, it allows for sporulation efficiencies between 0% and 100%.

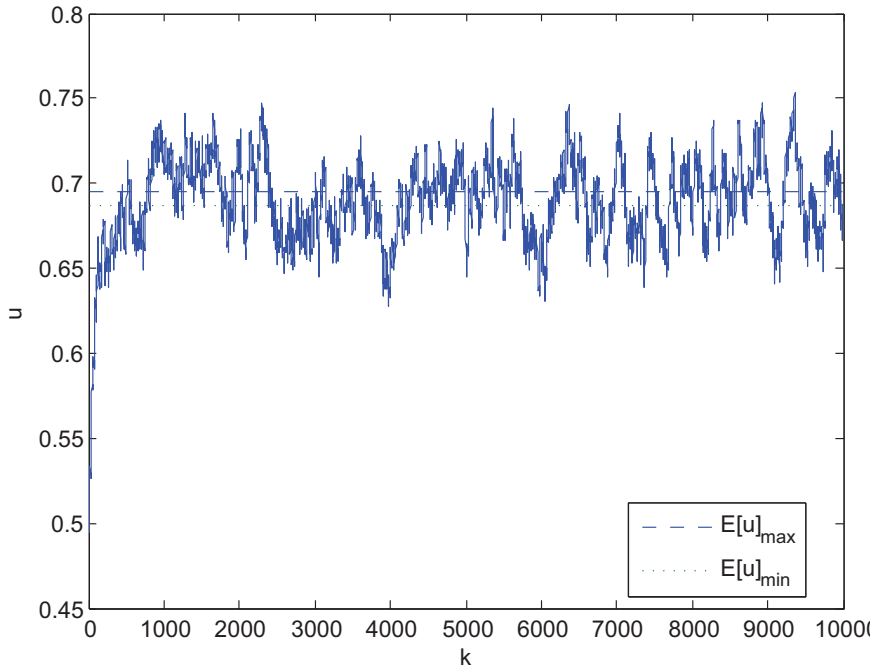

Figure 7.12: $u(k)$ for $p = 0.9$ and $q = 0.4$.

Modeling the actual expected policy as a "choice" over the optimal (ESS) policy, it can be shown that the "decision" to choose the actual expected policy exhibits risk sensitivity. Recall that the policy $u^{ESS}(k) = 0$ devotes all resources to vegetative growth while $u^{ESS}(k) = 1$ results in no vegetative cells. Since growth or death between successive steady states is proportional to the subpopulations of vegetative cells, a population with a relatively low value of $u(k)$ will exhibit more gains or losses to positive or negative $\bar{\epsilon}$ than a population with a relatively higher value of $u(k)$. Therefore, competing population 1 with $u^{ESS}(k) = 0$ against population 2 with $u(k) > 0$ will result in $A_1(k+1)$ having a higher variance than $A_2(k+1)$. Similarly, competing population 1 with $u^{ESS}(k) = 1$ against population 2 with $u(k) < 1$ will result in $A_1(k+1)$ having a lower variance than $A_2(k+1)$. Since the ESSs are optimal, populations adopting these strategies will have a higher expected payoff than populations not adopting them. Thus, there is evidence that the "choice" of $u(k) \neq u^{ESS}(k)$ is risk sensitive because:

1. If $\mathbb{E}\{\epsilon(k)\} > 0$, a policy with a lower expected value and lower variance is adopted over $u^{ESS}(k) = 0$.

2. If $\mathbb{E}\{\epsilon(k)\} < 0$, a policy with a lower expected value and higher variance is adopted over $u^{ESS}(k) = 1$.

The decision to choose the actual expected policy seems to exhibit risk aversion for positive expected gains and risk seeking for negative expected gains. This intuitive idea will be shown to be consistent with a general model of choice, and two possibly interesting ideas about bacterial expectations emerge from the analysis.

Prospect theory background

Expected utility theory arose from the observation that people make decisions that often do not maximize the expected value of their rewards. For example, it was found in 1738 that people would pay only a small monetary amount to play a game with infinite expected payoff (the Petersburg paradox) [21, 231]. Instead of maximizing the expected reward, it was postulated that people maximize the expected utility of their reward. This idea was formalized in 1944 by von Neumann and Morgenstern [262] with an axiomatic definition of rational decision-making, which allowed a logical analysis of games of chance. This expected utility theory provided a normative model of rational choice between a set of prospects. For notational convenience, define a prospect $(x_1, p_1; \ldots; x_n, p_n)$ as a contract that yields the outcome x_i with probability p_i, where $\sum_{i=1}^{n} p_i = 1$. Let $W(x_1, p_1; \ldots; x_n, p_n) \in \mathbb{R}$ be the overall utility of the prospect $(x_1, p_1; \ldots; x_n, p_n)$, which is the expected utility of the outcomes $\sum_{i=1}^{n} p_i w(x_i)$. The axioms that a rational decision maker must satisfy, according to von Neumann and Morgenstern [262], are

1. Completeness: Let $A = W(x_1, p_1; \ldots; x_n, p_n)$ and $B = W(x'_1, p'_1; \ldots; x'_n, p'_n)$. Then, either $A > B$, $A < B$, or $A = B$.

2. Transitivity: Let $C = W(\hat{x}_1, \hat{p}_1; \ldots; \hat{x}_n, \hat{p}_n)$. If $A > B$ and $B > C$, then $A > C$.

3. Independence: If $A > B$, $\lambda \in (0, 1]$, then $\lambda A + (1 - \lambda)C > \lambda B + (1 - \lambda)C$.

4. Continuity: If $x_1 > x_2 > x_3$, $\exists p \in (0, 1)$ such that $W(x_2, 1) = W(x_1, p; x_3, 1 - p)$.

Asset integration is a tenet of expected utility theory, which states that a prospect $(x_1, p_1; \ldots; x_n, p_n)$ is acceptable at asset position a iff $W(a + x_1, p_1; \ldots; a + x_n, p_n) > w(a)$ [132]. In other words, the overall utility of a prospect is calculated on the final states, not on the gains or losses.

Risk sensitivity is defined as a preference for/against a prospect $(x_1, p_1; \ldots; x_n, p_n)$ with $\sum_{i=1}^{n} x_i p_i = x$ when compared to a certain payoff x. Risk aversion is the preference of the certain payoff x over the gamble (up to a positive risk premium), and risk seeking is the preference of the gamble over the certain payoff (down to a negative risk premium). These attitudes can be represented by utility functions that are concave and convex, respectively. For example, in economic analysis w is typically concave to represent the law of diminishing returns [231], which was sufficient to explain the Petersburg paradox.

Though it is presumed that humans act rationally to maximize their expected utility, several studies have uncovered systematic inconsistencies between actual human decisions and expected utility theory [231, 250]. These inconsistencies compelled Kahneman and Tversky in 1979 to develop an alternative model of choice to explain human decision-making [132]. Their new framework, called prospect theory, postulated a descriptive model that differed from expected utility theory in three significant ways [132, 133, 250]:

1. Value function: Instead of a utility function w defined on final states, Kahneman and Tversky proposed a value function v defined on deviations from a reference point (gains/losses from a current asset position). Instead of generally being concave like

w, v is typically concave for gains and convex for losses. Additionally, v is steeper for losses than for gains (loss aversion).

2. Weighting function: Instead of weighting by actual probabilities p_i, Kahneman and Tversky proposed a weighting function $\pi(p_i)$. Unless the expectation principle holds ($\pi(p_i) = p_i$), the weighting function generally satisfies the following:

   - $\pi(p)$ is an increasing function of p, with $\pi(0) = 0$ and $\pi(1) = 1$.
   - For very small p, $\pi(p) > p$.
   - Subadditivity: $\pi(rp) > r\pi(p)$, for small p and $0 < r < 1$.
   - "Subcertainty": $\pi(p) + \pi(1-p) < 1$, $0 < p < 1$.
   - Subproportionality: If $0 < p, q, r \leq 1$, $\frac{\pi(pq)}{\pi(p)} \leq \frac{\pi(pqr)}{\pi(pr)}$.

3. Overall value of prospects: If $(x_1, p_1; x_2, p_2)$ is a regular prospect (i.e., either $p_1 + p_2 < 1$ or $x_1 \geq 0 \geq x_2$ or $x_1 \leq 0 \leq x_2$), then the overall value of the prospect is

$$V(x_1, p_1; x_2, p_2) = \pi(p_1)v(x_1) + \pi(p_2)v(x_2).$$

   For strictly positive or negative prospects, it is assumed that the prospect is edited such that there is a riskless component (the minimum gain or loss which is certain to be obtained or paid) and a risky component (the additional gain or loss which is actually at stake). For the prospect $(x_1, p_1; x_2, p_2)$, if $p_1 + p_2 = 1$ and either $x_1 > x_2 > 0$ or $x_1 < x_2 < 0$, the overall value of the prospect is

$$V(x_1, p_1; x_2, p_2) = v(x_2) + \pi(p_1)\left[v(x_1) - v(x_2)\right].$$

In addition to these modifications to expected utility theory, Kahneman and Tversky allowed the value function to be defined around a shifted reference point [11, 251]. Though it is assumed that the carriers of value are gains and losses, the *current* asset position may not always be the correct position from where to assess gains or losses. A shift in reference point may correspond to the status quo or an *asset position that one had expected to attain*; for example, an unexpected tax withdrawal from a monthly paycheck is experienced as a loss, not a reduced gain, and an entrepreneur who is weathering a slump with greater success than his competitors may interpret a small loss as a gain, relative to the larger loss he had reason to expect [132]. Other studies indicate that people often demand much more to give up an object than they would be willing to pay to acquire it (the endowment effect or status quo bias) [131, 138], which can be attributed to shifts in reference points and loss aversion encoded into the value functions. Reference points may also change due to recent changes in assets to which one had not adapted, which may explain the observation of the increased tendency to bet on long shots over the course of the betting day [132, 173].

Note that prospect theory presents a more general model of choice than expected utility theory. Setting the reference point to zero assets allows a utility function to be recovered from a value function, and setting π to the identity function allows the axioms of rational decision-making to be satisfied.

Biological applications of choice models

Beyond the applications to human behavior and psychology, expected utility theory has been used for nonhuman studies on habitat choice and territoriality, life history, and reproductive and social behaviors [14, 270]. Foraging behavior is perhaps the most widely applied example of utility theory for animals, with attention primarily focused on solitary feeding specialists with low reserves, high metabolic requirements, and periodic and relatively lengthy interruptions of foraging (e.g. long, cold nights) [270]. Payoffs are almost always food, with the underlying hypothesis that foragers make decisions to maximize the utility of food. The general findings of risk sensitive foraging behavior are [34, 54, 104, 128, 162, 174, 220]:

1. Risk insensitive behavior is rare in the animals studied (such as birds, rats, and honeybees). Research has uncovered the so-called energy budget rule, which is tested by offering a subject the choice of a variable food amount or a certain food amount equal to the expected value of the risky choice. When the certain food amount is above the required food amount to survive (positive energy budget), subjects preferred the certain reward; however, when the certain food amount is below the required food amount to survive (negative energy budget), subjects preferred the variable reward. Intuitively, survival is guaranteed by selecting the certain food amount with a positive energy budget, while the probability of survival is maximized by selecting the random food amount under a negative energy budget. If the food amount carries utility, it is postulated that the utility function is convex-concave. Below the food amount required for survival, w is convex, whereas above this value, w is concave.

2. Different cases of food variability (with positive energy budgets) exhibit different risk attitudes. Whereas the energy budget rule predicts risk aversion for food amount, experiments suggest that subjects are risk prone when choosing between a random delay until food is given and a certain delay until food is given (the amount of food for both choices in the delay experiments is fixed). The energy budget rule does not satisfactorily explain this behavior, though it is possible that aspects of prospect theory may describe it. For example, a delay in feeding time may be framed as a loss to an animal that has grown accustomed to feeding at a certain time. The temporal reference point of the previous feeding time implies that the value function is convex in the domain of the experimental feeding times.

Some studies (e.g. [162, 172]) applied prospect theory to foraging behavior, though most have been analyzed in the more specialized framework of expected utility theory.

Prospect theory applied to the decision policy choice

Suppose that population 1 adopts $b^{ESS}(k)$ and population 2 adopts $b(k) \neq b^{ESS}(k)$. Then, denoting $\Delta A_i(k) := \frac{1}{\epsilon(k)} \left(A_i(k+1) - A_i(k)\right)$,

$$A_1(k+1) = \begin{cases} A_1(k) + \Delta A_1(k)\overline{\epsilon} & \text{with Pr} \left\{\frac{q}{p+q}\right\} \\ A_1(k) - \Delta A_1(k)\overline{\epsilon} & \text{with Pr} \left\{\frac{p}{p+q}\right\} \end{cases}$$
$$A_2(k+1) = \begin{cases} A_2(k) + \Delta A_2(k)\overline{\epsilon} & \text{with Pr} \left\{\frac{q}{p+q}\right\} \\ A_2(k) - \Delta A_2(k)\overline{\epsilon} & \text{with Pr} \left\{\frac{p}{p+q}\right\} \end{cases}$$

where

$$\Delta A_1(k) = \frac{\frac{1}{\gamma}(1+b(k))^2(1+b^{ESS}(k))}{(1+b(k))^2 + (1+b^{ESS}(k))^2}$$
$$\Delta A_2(k) = \frac{\frac{1}{\gamma}(1+b(k))(1+b^{ESS}(k))^2}{(1+b(k))^2 + (1+b^{ESS}(k))^2}.$$

Without loss of generality, normalize the gains or losses for each k by $\overline{\epsilon}$ so that prospects may be represented purely in terms $\Delta A_1(k)$ and $\Delta A_2(k)$.

When $\mathbb{E}\left\{\epsilon(k)\right\} > 0$ (or $q > p$), the gains or losses are

$$\Delta A_1(k) = \frac{\frac{1}{\gamma}(1+b(k))^2}{(1+b(k))^2 + 1}$$
$$\Delta A_2(k) = \frac{\frac{1}{\gamma}(1+b(k))}{(1+b(k))^2 + 1}$$

with

$$\Pr\left\{\Delta A_i(k) > 0\right\} = \frac{q}{p+q} > \frac{1}{2}$$
$$\Pr\left\{\Delta A_i(k) < 0\right\} = \frac{p}{p+q} < \frac{1}{2}$$

for $i = 1, 2$. Note that

$$\Delta A_1(k) > \Delta A_2(k) > 0$$

since $b(k) > 0$.

When $\mathbb{E}\left\{\epsilon(k)\right\} < 0$ (or $q' < p'$), the gains or losses are

$$\Delta A_1'(k) = 0$$
$$\Delta A_2'(k) = \frac{1}{\gamma}(1+b'(k))$$

with

$$\Pr\{\Delta A_2'(k) > 0\} = \frac{q'}{p'+q'} < \frac{1}{2}$$
$$\Pr\{\Delta A_2'(k) < 0\} = \frac{p'}{p'+q'} > \frac{1}{2}.$$

No shifts of reference Straight application of prospect theory on the prospects

1. $(\Delta A_1(k), \frac{q}{p+q}; -\Delta A_1(k), \frac{p}{p+q})$
2. $(\Delta A_2(k), \frac{q}{p+q}; -\Delta A_2(k), \frac{p}{p+q})$

(when $q > p$) results in

$$\pi\left(\frac{q}{p+q}\right) v\left(\Delta A_1(k)\right) + \pi\left(\frac{p}{p+q}\right) v\left(-\Delta A_1(k)\right) < \pi\left(\frac{q}{p+q}\right) v\left(\Delta A_2(k)\right) + \pi\left(\frac{p}{p+q}\right) v\left(-\Delta A_2(k)\right) \quad (7.12)$$

since both prospects are not regular and $(\Delta A_2(k), \frac{q}{p+q}; -\Delta A_2(k), \frac{p}{p+q})$ is chosen. Similarly, the choice between the prospects

1. $(0, 1)$
2. $(\Delta A_2'(k), \frac{q'}{p'+q'}; -\Delta A_2'(k), \frac{p'}{p'+q'})$

(when $q' < p'$) results in

$$v(0) = 0 < \pi\left(\frac{q'}{p'+q'}\right) v\left(\Delta A_2'(k)\right) + \pi\left(\frac{p'}{p'+q'}\right) v\left(-\Delta A_2'(k)\right). \quad (7.13)$$

It will be shown that this simple formulation of the decision problem is not consistent with the hypotheses of prospect theory.

Equation (7.12) can be written as

$$\pi\left(\frac{q}{p+q}\right)\left[v\left(\Delta A_1(k)\right) - v\left(\Delta A_2(k)\right)\right] < \pi\left(\frac{p}{p+q}\right)\left[v\left(-\Delta A_2(k)\right) - v\left(-\Delta A_1(k)\right)\right]$$

which implies that

$$\frac{v\left(\Delta A_1(k)\right) - v\left(\Delta A_2(k)\right)}{v\left(-\Delta A_2(k)\right) - v\left(-\Delta A_1(k)\right)} < \frac{\pi\left(\frac{p}{p+q}\right)}{\pi\left(\frac{q}{p+q}\right)} < 1 \quad (7.14)$$

since $\pi(z)$ is monotonic in z and $q > p$. On the other hand, Equation (7.13) can be written as

$$-\pi\left(\frac{p'}{p'+q'}\right) v\left(-\Delta A_2'(k)\right) < \pi\left(\frac{q'}{p'+q'}\right) v\left(\Delta A_2'(k)\right)$$

which implies that

$$\frac{-v\left(-\Delta A_2'(k)\right)}{v\left(\Delta A_2'(k)\right)} < \frac{\pi\left(\frac{q'}{p'+q'}\right)}{\pi\left(\frac{p'}{p'+q'}\right)} < 1 \tag{7.15}$$

since $q' < p'$.

Equations (7.14) and (7.15) are inconsistent with each other. They respectively imply that

$$\begin{aligned} &v\left(\Delta A_1(k)\right) + v\left(-\Delta A_1(k)\right) < v\left(\Delta A_2(k)\right) + v\left(-\Delta A_2(k)\right) \\ &v\left(\Delta A_2'(k)\right) + v\left(-\Delta A_2'(k)\right) > 0. \end{aligned}$$

or

$$\begin{aligned} v\left(\Delta A_1(k)\right) &< -v\left(-\Delta A_1(k)\right) \\ v\left(\Delta A_2'(k)\right) &> -v\left(-\Delta A_2'(k)\right). \end{aligned}$$

The second inequality contradicts the first inequality and the prospect theory hypothesis that $v(x) < -v(x)$ for all $x > 0$ [132]. This discrepancy suggests that the decision problem formulation must be refined.

Including shifts of reference Introducing two shifts of reference will allow the choices to be consistent with the prospect theory model of choice. Specifically, suppose the two translations are:

- $+\Delta A_1(k)$ if $\mathbb{E}\left\{\epsilon(k)\right\} > 0$, and
- $-\Delta A_2'(k)$ if $\mathbb{E}\left\{\epsilon(k)\right\} < 0$.

The first shift results in a choice between the prospects

1. $(2\Delta A_1(k), \frac{q}{p+q}; 0, \frac{p}{p+q})$
2. $(\Delta A_1(k) + \Delta A_2(k), \frac{q}{p+q}; \Delta A_1(k) - \Delta A_2(k), \frac{p}{p+q})$

(when $q > p$), which results in

$$\begin{aligned} \pi\left(\frac{q}{p+q}\right) v\left(2\Delta A_1(k)\right) < v\left(\Delta A_1(k) - \Delta A_2(k)\right) + \\ \pi\left(\frac{q}{p+q}\right)\left[v\left(\Delta A_1(k) + \Delta A_2(k)\right) - v\left(\Delta A_1(k) - \Delta A_2(k)\right)\right] \end{aligned} \tag{7.16}$$

since $(\Delta A_1(k) + \Delta A_2(k), \frac{q}{p+q}; \Delta A_1(k) - \Delta A_2(k), \frac{p}{p+q})$ is now regular and is chosen. Similarly, the choice between the shifted prospects

1. $(-\Delta A_2'(k), 1)$

2. $(0, \frac{q'}{p'+q'}; -2\Delta A_2'(k), \frac{p'}{p'+q'})$

(when $q' < p'$) results in

$$\pi\left(\frac{p'}{p'+q'}\right) v\left(-2\Delta A_2'(k)\right) > v\left(-\Delta A_2'(k)\right). \tag{7.17}$$

It will be shown that this formulation, with shifts of reference, is consistent with the hypotheses of prospect theory.

Equation (7.16) can be written as

$$\left[1-\pi\left(\frac{q}{p+q}\right)\right] v\left(\Delta A_1(k) - \Delta A_2(k)\right) > \pi\left(\frac{q}{p+q}\right)\left[v\left(2\Delta A_1(k)\right) - v\left(\Delta A_1(k) + \Delta A_2(k)\right)\right]$$

$$\Leftrightarrow \frac{v\left(\Delta A_1(k) - \Delta A_2(k)\right)}{v\left(2\Delta A_1(k)\right) - v\left(\Delta A_1(k) + \Delta A_2(k)\right)} > \frac{\pi\left(\frac{q}{p+q}\right)}{1-\pi\left(\frac{q}{p+q}\right)}.$$

Assuming that the expectation principle holds,

$$q > p \;\Rightarrow\; \pi\left(\frac{q}{p+q}\right) > \frac{1}{2} \;\Rightarrow\; \frac{\pi\left(\frac{q}{p+q}\right)}{1-\pi\left(\frac{q}{p+q}\right)} > 1,$$

the following inequality is a result of Equation (7.16):

$$v\left(\Delta A_1(k) - \Delta A_2(k)\right) > v\left(2\Delta A_1(k)\right) - v\left(\Delta A_1(k) + \Delta A_2(k)\right). \tag{7.18}$$

Note that this is consistent with the hypothesis $v(z)$ concave for $z > 0$, since Equation (7.18) is equivalent to

$$v\left(\Delta A_1(k) - \Delta A_2(k)\right) - v\left(0\right) > v\left(2\Delta A_1(k)\right) - v\left(\Delta A_1(k) + \Delta A_2(k)\right).$$

Equation (7.17) is consistent with the conditions required to derive Equation (7.18) and the hypotheses of prospect theory. Specifically, if $v(z)$ is convex for $z < 0$,

$$v\left(0\right) - v\left(-\Delta A_2'(k)\right) > v\left(-\Delta A_2'(k)\right) - v\left(-2\Delta A_2'(k)\right)$$
$$\Leftrightarrow v\left(-2\Delta A_2'(k)\right) > 2v\left(-\Delta A_2'(k)\right).$$

Under the assumption that the expectation principle holds,

$$p' > q' \;\Rightarrow\; \pi\left(\frac{p'}{p'+q'}\right) > \frac{1}{2},$$

which, combined with the convexity condition, leads to

$$\pi\left(\frac{p'}{p'+q'}\right) v\left(-2\Delta A_2'(k)\right) > \frac{1}{2} v\left(-2\Delta A_2'(k)\right) > v\left(-\Delta A_2'(k)\right)$$

which is consistent with Equation (7.17). Equations (7.16) and (7.17) can therefore be explained by prospect theory.

Significance of prospect theory and shifts of reference

With two specific shifts of reference, it was shown that the "decision" to adopt the actual expected policy over the optimal policy is consistent with the model of choice suggested by prospect theory. This means that natural selection and evolutionary dynamics conspire in a manner to mimic an agent that exhibits risk sensitive decisions. It is interesting to note that prospect theory was originally developed to describe human economic preferences [133, 250], which may imply that evolution evaluates and "chooses" phenotypes in a way that is similar to actual human editing and decisions. These choices are optimal according to the model of choice provided by prospect theory ("postdictive" perspective [231]) . In fact, since the expectation principle was not violated in the analysis, one may argue that the choice of phenotype is rational for positive $\mathbb{E}\{\epsilon(k)\}$ (or negative $\mathbb{E}\{\epsilon(k)\}$) since the axioms of expected utility theory hold; in other words, as long as $\mathbb{E}\{\epsilon(k)\}$ remains positive (or negative), the decisions simply maximize a concave (convex) utility function with unaltered probability weights.

Perhaps more interesting are the shifts of references required to make the "choice" of the actual decision policy over the optimal policy consistent with prospect theory. Recall that the shifts were:

- $+\Delta A_1(k)$ if $\mathbb{E}\{\epsilon(k)\} > 0$, and
- $-\Delta A_2'(k)$ if $\mathbb{E}\{\epsilon(k)\} < 0$,

where $\Delta A_1(k)$ and $\Delta A_2'(k)$ are the larger gains/losses of the two choices under different environmental conditions. As mentioned in the Section 7.10.1, a shift of reference describes the status quo or the gain/loss that the deciding agent expects to see [251, 253]. Therefore, it is possible to claim that natural selection and evolutionary dynamics expect, when choosing between two prospects,

- maximum losses when $\mathbb{E}\{\epsilon(k)\} > 0$, and
- maximum gains when $\mathbb{E}\{\epsilon(k)\} < 0$.

This may imply that bacterial behavior has evolved to expect the worst when the nutrient influx is increasing on average, and expect the best when the nutrient influx is decreasing on average. Compared to the optimal ESS, the actual strategy performs better if the environment *unexpectedly* switches to the other operating mode. In other words, bacteria are **pessimistic** under good conditions and **optimistic** under bad conditions. Though similar to the prospect theory hypotheses of risk aversion for gains and risk seeking for losses, the optimistic and pessimistic labels refer to the particular beliefs that are required to provide a descriptive model of the decision policy selection. Therefore, if the mathematical modeling and assumptions for this analysis are representative of actual bacteria populations, we can claim that bacteria act both optimistically and pessimistically, depending on the environmental conditions.

The longer the environment remains in either H or L, the lower the "degree" of pessimism and optimism, respectively. For example, if two populations with the same initial

population-average strategy were placed in environment mode H, the population reintroduced to L first will more readily form spores than the population reintroduced to L later. According to the proposed evolutionary model, this is because the longer an environment remains constant, the more adapted a population will become to that particular condition (to maximize its fitness). From a bacteria colony's point of view, an interesting descriptive model that explains this behavior can be constructed. Suppose a colony has undergone t rounds of a constant environmental trend in H. It is reasonable to assume that the bacteria cannot predict the future, so they may not have knowledge of the parameter p that governs the distribution of T_H, the (random) number of steps spent in H. Even if the environment has constant p and q up to the current time, there still may be uncertainty in the estimated value of p due to unforeseen circumstances (e.g. sunlight exposure may significantly alter the availability of nutrients in soil [163]). Therefore, suppose that the bacteria colony forms an estimate $\hat{p}$ of the actual parameter p while in H. There are several heuristic ways in which this may be accomplished, simply using the fact that the realization t_H of the random variable T_H is greater than t. For example,

- $\hat{p} \leftarrow \mathbb{E}\{T_H\} > t$
- $\hat{p} \leftarrow \Pr\{T_H > t\} \geq \gamma$
- $\hat{p} \leftarrow \mathbb{E}\{T_H\} < t$ but $\mathrm{var}(T_H) > \gamma(t - \mathbb{E}\{T_H\})$

are all possible candidates for calculating $\hat{p}$ knowing only that $t_H > t$. In all of these cases, $\hat{p}$ is bounded by a decreasing function of t. Intuitively, this means that the longer one spends in H, the longer one would expect to remain in H since the distribution governing T_H is memoryless. Therefore, as the estimated probability of transitioning to L becomes smaller, the actual policy gets closer to the optimal ESS. This may lead to an "adaptive coin-flipping"-like strategy [43, 193, 233], where an individual cell will form a spore with probability $\frac{\hat{p}}{\hat{p}+\hat{q}}$ and continue to vegetatively grow with probability $\frac{\hat{q}}{\hat{p}+\hat{q}}$. This strategy gives rise to a time-varying population-average strategy that converges to $u = 0$ as $t_H \to \infty$.

The non-equilibrium strategy is sufficiently general to explain observed sporulation efficiencies in wild strains of bacteria (see Table 2.1). It captures the intuitive expectation that a bacterium should evolve higher sporulation efficiencies in nutrient-poor environments and lower sporulation efficiencies in nutrient-rich environments. Though it is impossible to claim that the proposed environmental model accurately reflects the actual conditions that wild bacteria tolerate, the qualitative agreement between experimentally-observed sporulation efficiencies and the non-equilibrium policy is encouraging.

7.10.2 Non-equilibrium policy compared to bet-hedging strategies

Bet-hedging background

Suppose that natural selection acts to maximize the long term fitness of an organism. If the fitness is of the classical Darwinian variety (number of viable progeny), assume that fitness

is governed by the dynamics

$$X(t+1) = W(t)X(t)$$

where, without loss of generality, the normalization $X(0) = 1$ is employed. If $W(t)$ depends on the organism's genotype θ, it may be postulated that evolution solves

$$\max_{\theta} \lim_{t\to\infty} X(t)$$

for the long term fitness problem. Note that the objective $J = \lim_{t\to\infty} X(t)$ is

$$J = \lim_{t\to\infty} \prod_{i=0}^{t-1} W(i),$$

and has the same arg max as

$$\begin{aligned} J_L := \log J &= \log\left(\lim_{t\to\infty} \prod_{i=0}^{t-1} W(i)\right) \\ &= \lim_{t\to\infty} \sum_{i=0}^{t-1} \log W(i). \end{aligned}$$

If each $W(i) = W$ is an i.i.d. random variable parameterized by θ, then the weak law of large numbers [228] yields

$$J_L \sim \mathcal{N}\left(\mathbb{E}\left\{\log W\right\}, \sigma^2\right)$$

so maximization of the expected long term fitness is equivalent to maximizing $\mathbb{E}\left\{\log W\right\}$. If W is a discrete random variable with distribution

$$\Pr\left\{W = w_i\right\} = p_i, \quad i = 1, 2, \ldots, n$$

the long term fitness maximization can be expressed as

$$\theta^* = \arg\max_{\theta} \mathbb{E}\left\{\log W\right\} = \arg\max_{\theta} e^{\mathbb{E}\{\log W\}}$$

since e^x is monotone increasing in x [26]. This gives

$$\begin{aligned} \theta^* &= \arg\max_{\theta} e^{\mathbb{E}\{\log W\}} \\ &= \arg\max_{\theta} e^{\sum_{i=1}^{n} \log w_i^{p_i}} \\ &= \arg\max_{\theta} \prod_{i=1}^{n} w_i^{p_i} \end{aligned}$$

which is the familiar geometric mean fitness maximization solution. Notice that maximization of the geometric mean does not necessarily maximize the mean. For example, if θ_1 corresponded to the distribution

$$\Pr\{W = 8\} = 1$$

and θ_2 corresponded to the distribution

$$\Pr\{W = 1\} = \frac{1}{2}$$
$$\Pr\{W = 19\} = \frac{1}{2},$$

then the geometric mean and mean for a random variable with θ_1's distribution are both 8, whereas the geometric mean and mean for a random variable with θ_2's distribution are 4.36 and 10, respectively. Therefore, θ_1 corresponds to a higher geometric mean but a lower mean than θ_2.

Corollary 7.10.2. *Let two non-negative random variables W_1 and W_2 have symmetric (about the mean) densities p_{W_1} and p_{W_2} with cumulative distribution functions F_{W_1} and F_{W_2}, respectively. If*

$$\mathbb{E}\{W_1\} = \mathbb{E}\{W_2\} = \mu$$
$$F_{W_1}(x) > F_{W_2}(x)$$

for $\mu < x < 2\mu$, then

$$\mathbb{E}\{\log W_1\} > \mathbb{E}\{\log W_2\}.$$

Equivalently, the geometric mean of W_1 will be greater than the geometric mean of W_2 as long as p_{W_1} and p_{W_2} are symmetric about their means and p_{W_1} is more concentrated (in a certain sense) than p_{W_2}.

Proof. Since W_1 and W_2 are non-negative and have symmetric densities, their supports are necessarily compact. Specifically, W_1 and W_2 can take on values from 0 to $2\mathbb{E}\{W_1\} = 2\mathbb{E}\{W_2\} = 2\mu$.

Preliminarily, the expected value of any function of W_1 (or W_2) can be simplified to

$$\begin{aligned}
\mathbb{E}\{g(W_1)\} &= \int_0^{2\mu} g(x)p_{W_1}(x)dx \\
&= \int_0^{\mu} g(x)p_{W_1}(x)dx + \int_{\mu}^{2\mu} g(x)p_{W_1}(x)dx \\
&= -\int_{\mu}^{0} g(\mu - y)p_{W_1}(\mu - y)dy + \int_0^{\mu} g(\mu + y)p_{W_1}(\mu + y)dy \\
&= \int_0^{\mu} \left(g(\mu - y) + g(\mu + y)\right) p_{W_1}(\mu + y)dy
\end{aligned}$$

where the last equality comes from the fact that $p_{W_1}(\mu - y) = p_{W_1}(\mu + y)$ for $0 < y < \mu$.

The condition $F_{W_1}(x) > F_{W_2}(x)$ for $\mu < x < 2\mu$ leads to

$$\begin{aligned}
& F_{W_1}(x) > F_{W_2}(x) \\
\Leftrightarrow & \int_0^x p_{W_1}(t)dt > \int_0^x p_{W_2}(t)dt \\
\Leftrightarrow & \int_0^\mu p_{W_1}(t)dt + \int_\mu^x p_{W_1}(t)dt > \int_0^\mu p_{W_2}(t)dt + \int_\mu^x p_{W_2}(t)dt \\
\Leftrightarrow & \int_\mu^x p_{W_1}(t)dt > \int_\mu^x p_{W_2}(t)dt \\
\Leftrightarrow & \int_0^{x-\mu} p_{W_1}(\mu + y)dy > \int_0^{x-\mu} p_{W_2}(\mu + y)dy
\end{aligned}$$

for $\mu < x < 2\mu$, with boundary condition

$$\int_0^\mu p_{W_1}(\mu + y)dy = \int_0^\mu p_{W_2}(\mu + y)dy = \frac{1}{2}.$$

Together, these imply that any increasing function $h(y)$ bounded between 0 and 1 on the interval $0 \leq y \leq \mu$ results in

$$\int_0^\mu h(y)p_{W_1}(\mu + y)dy < \int_0^\mu h(y)p_{W_2}(\mu + y)dy.$$

Intuitively, the function $h(y)$ weights p_{W_1} the least where the density is relatively large, while $h(y)$ weights p_{W_2} the most where the density is relatively large.

With this inequality, the following result can be derived: For $n = 1, 2, \ldots$,

$$\begin{aligned}
\mathbb{E}\left\{(W_1 - \mu)^{2n}\right\} &= \int_0^\mu \left(y^{2n} + (-y)^{2n}\right) p_{W_1}(\mu + y)dy \\
&= 2\int_0^\mu y^{2n} p_{W_1}(\mu + y)dy \\
&= 2\mu^{2n} \int_0^\mu \left(\frac{y}{\mu}\right)^{2n} p_{W_1}(\mu + y)dy \\
&< 2\mu^{2n} \int_0^\mu \left(\frac{y}{\mu}\right)^{2n} p_{W_2}(\mu + y)dy \\
&= \mathbb{E}\left\{(W_2 - \mu)^{2n}\right\}.
\end{aligned}$$

Note that this implies that the variance of W_1 is less than the variance of W_2, which is expected since it is assumed that p_{W_1} is more concentrated around μ than p_{W_2}. Additionally, for $n = 1, 2, \ldots$,

$$\begin{aligned}
\mathbb{E}\left\{(W_1 - \mu)^{2n+1}\right\} &= \int_0^\mu \left(y^{2n+1} + (-y)^{2n+1}\right) p_{W_1}(\mu + y)dy \\
&= \int_0^\mu \left(y^{2n+1} - y^{2n+1}\right) p_{W_1}(\mu + y)dy \\
&= 0.
\end{aligned}$$

i.e. the odd central moments for symmetric densities are zero.

Now, for an analytic function $f(x)$,

$$\begin{aligned}
\mathbb{E}\left\{f\left(W_1\right)\right\} &= \int_0^{2\mu} f(x) p_{W_1}(x) dx \\
&= \int_0^{2\mu} \left[f(\mu) + f'(\mu)\left(x-\mu\right) + \frac{f''(\mu)}{2}\left(x-\mu\right)^2 \right. \\
&\qquad \left. + \frac{f'''(\mu)}{6}\left(x-\mu\right)^3 + \cdots \right] p_{W_1}(x) dx \\
&= f(\mu) + f'(\mu) \int_0^{2\mu} \left[x-\mu\right] p_{W_1}(x) dx + \frac{f''(\mu)}{2} \int_0^{2\mu} \left[x-\mu\right]^2 p_{W_1}(x) dx \\
&\qquad + \frac{f'''(\mu)}{6} \int_0^{2\mu} \left[x-\mu\right]^3 p_{W_1}(x) dx + \cdots \\
&= f(\mu) + \sum_{i=1}^{\infty} \frac{1}{i!} \left. \frac{\partial^i f(x)}{\partial x^i} \right|_{\mu} \mathbb{E}\left\{ \left(W_1 - \mu\right)^i \right\} \\
&= f(\mu) + \sum_{n=1}^{\infty} \frac{1}{(2n)!} \left. \frac{\partial^{2n} f(x)}{\partial x^{2n}} \right|_{\mu} \mathbb{E}\left\{ \left(W_1 - \mu\right)^{2n} \right\}
\end{aligned}$$

For the specific case when $f(x) = \log x$,

$$\mathbb{E}\left\{\log W_1\right\} = \log \mu + \sum_{n=1}^{\infty} \frac{1}{(2n)!} \left. \frac{\partial^{2n} \log x}{\partial x^{2n}} \right|_{\mu} \mathbb{E}\left\{ \left(W_1 - \mu\right)^{2n} \right\},$$

where $\left. \frac{\partial^{2n} \log x}{\partial x^{2n}} \right|_{\mu} < 0$, $n = 1, 2, \ldots$, due to the concavity of $\log x$. W_1 and W_2 as described in the hypothesis give

$$\mathbb{E}\left\{\log W_1\right\} - \mathbb{E}\left\{\log W_2\right\} = \sum_{n=1}^{\infty} \frac{1}{2n!} \underbrace{\left. \frac{\partial^{2n} \log x}{\partial x^{2n}} \right|_{\mu}}_{(-)} \underbrace{\left[\mathbb{E}\left\{ \left(W_1 - \mu\right)^{2n} \right\} - \mathbb{E}\left\{ \left(W_1 - \mu\right)^{2n} \right\} \right]}_{(-)}$$

which implies

$$\mathbb{E}\left\{\log W_1\right\} > \mathbb{E}\left\{\log W_2\right\}$$

as desired. □

Remark 7.10.3. *Corollary 7.10.2 shows that, with everything else held constant, a reduction in fitness variance may produce a higher geometric mean fitness.*

Remark 7.10.4. *This corollary does not hold for random variables with non-symmetric densities. For example, consider*

$$X_1 = \begin{cases} 1 & \textit{with prob. } 0.2 \\ 13 & \textit{with prob. } 0.8 \end{cases}$$

$$X_2 = \begin{cases} 8 & \textit{with prob. } 0.8 \\ 21 & \textit{with prob. } 0.2 \end{cases}$$

In this case, $\mathbb{E}\{X_1\} = \mathbb{E}\{X_2\} = 10.6$*,* $\text{var}(X_1) = 23.04 < 27.04 = \text{var}(X_2)$*, but* $\mathbb{E}\{\log X_1\} = 2.052 < 2.272 = \mathbb{E}\{\log X_2\}$*.*

This idea of sacrificing mean fitness in order to increase other measures of fitness underlies the concept of bet-hedging strategies. Though several "definitions" for bet-hedging strategies exist [233], the most commonly accepted feature of bet-hedging strategies is a trade-off between an individual's mean fitness and fitness variance, or geometric mean fitness maximization [50, 193, 219, 242]. This allows an organism to persist in the face of fluctuating environmental conditions [13, 233], where variation in W is the result of environmental variation. Intuitively, a large fitness variance will negatively impact the survival of an organism because there is a greater probability of zero descendants, an event after which no progeny will exist [156]. Bet-hedging strategies that maximize an individual's geometric mean fitness are typically grouped into two broad classifications: conservative and diversified [193, 233]. A conservative bet-hedging strategy reduces the variance of an individual's fitness at the expense of expected fitness. Examples of this "one bird in the hand is worth two in the bush" or "safe" strategy are semelparous perennial plants initiating flowering early in the growth season to avoid the seasons' end [37, 243], and the investment in constant, large eggs sizes during each breeding season [193]. A diversified bet-hedging strategy, on the other hand, probabilistically diversifies the phenotype expression for a single genotype. Examples of this "don't put all of your eggs in one basket" strategy are the random germination of desert annuals [40], diverse timing of initiation of insect diapause [210], and variation in clutch sizes or egg sizes [193]. Diversified bet-hedging encompasses "adaptive coin-flipping" strategies [37, 43, 193], where the probabilistic diversification is a function of the environment stochasticity [135, 233].

In addition to geometric mean fitness maximization, other commonly accepted characteristics of bet-hedging strategies are:

1. Evolution: Bet-hedging strategies only evolve in unpredictable, temporally variable environments [13, 50, 233].

2. Genetic characterization: Bet-hedging strategies arise from a single genotype (even for diversified strategies) [13, 50, 145, 227, 233].

3. System condition: Bet-hedging strategies may give rise to an ESS if the phenotypic polymorphism in diversified strategies results from a single genotype [50, 193, 210, 233].

Note that a mixed ESS based on genetic polymorphism is not a bet-hedging strategy because some phenotypes may be worse than others, resulting in a lower geometric mean fitness for a portion of the population [210, 233]. This population is therefore not at equilibrium, as the population with lower fitness will become extinct.

Strategies that seem to hedge one's bets but are not typically considered bet-hedging are [233]:

1. Facultative development or behavioral adjustments of a phenotype in response to the current/predicted state of the environment (adaptations directly in response to the (predictable) environment);

2. Adjustments of a parameter to maximize fitness under uncertainty (over-designing for average conditions); and

3. Genetic polymorphism maintained by spatial heterogeneity of the environment, or by frequency-dependent selection (does not reduce the variance of an individual's fitness).

Examples of these strategies include *E. coli*'s pre-induction of genes needed to cope with low oxygen levels in response to temperature increases that normally precede indigestion (Pavlovian conditioning for anticipated future events) [181], bone thicknesses in excess of those needed for average daily loads [233], and genetic variation maintained by spatial environmental heterogeneity combined with low migration/gene flow rates [106], respectively.

Though it may seem that bet-hedging is equivalent to risk averse behavior [210], this is not the case. It was shown by Samuelson [228] that maximization of the expected geometric mean of a random variable does not imply maximization of the expected (concave) utility of the same random variable. Corollary 7.10.5 provides a result on the converse of this statement.

Corollary 7.10.5. *Risk averse behavior is not sufficient for a strategy to be a bet-hedging strategy.*

Proof. The claim will be shown by a counterexample to the statement "risk averse behavior is sufficient for a strategy to be a bet-hedging strategy."

Recall that a concave utility function is necessary and sufficient to give rise to risk averse behavior for all risky prospects [177], and a bet-hedging strategy is commonly accepted to maximize the geometric mean of the risky prospects (see above).

Suppose two risky prospects are (using the notation introduced in Section 7.10.2)

$$W_1 = (1 + \Delta_1, p; 1 - \Delta_1, 1 - p)$$
$$W_2 = (1 + \Delta_2, p; 1 - \Delta_2, 1 - p)$$

where $1 > \Delta_1 > \Delta_2 > 0$ and $p > \frac{1}{2}$. If the model for population growth is

$$X(t + 1) = W(t)X(t)$$

where $X(0) = 1$, the expected fitness is maximized by choosing $W(t) = W_1$ since $\mathbb{E}\{W_1\} > \mathbb{E}\{W_2\}$. Assume, however, that the expected utility is greater for prospect W_2 than for prospect W_1:

$$pu(1 + \Delta_2) + (1 - p)u(1 - \Delta_2) > pu(1 + \Delta_1) + (1 - p)u(1 - \Delta_1).$$

where $u(x)$ is the utility of outcome x. It will be shown that the geometric mean of the fitness corresponding to W_1 is not necessarily lower than the geometric mean of fitness corresponding to W_2.

The prospects

$$W_1 = (1.12, 0.553; 0.88, 0.447)$$
$$W_2 = (1.08, 0.553; 0.92, 0.447)$$

($\Delta_1 = 0.12$, $\Delta_2 = 0.08$, $p = 0.553$) with the concave utility function $u(x) = \log(x - 0.1)$ satisfy

$$\begin{aligned} pu\left(1+\Delta_1\right) + (1-p)u\left(1-\Delta_1\right) &= 0.553\log(1.02) + 0.447\log(0.78) \\ &= -1.001 \\ &< -.0999 \\ &= 0.553\log(0.98) + 0.447\log(0.82) \\ &= pu\left(w+\Delta_2\right) + (1-p)u\left(w-\Delta_2\right), \end{aligned}$$

but the geometric means of the prospects are

$$\begin{aligned} \left(1+\Delta_1\right)^p\left(1-\Delta_1\right)^{1-p} &= 1.02^{0.553}0.78^{0.447} \\ &= 1.0055 \\ &> 1.0053 \\ &= 1.08^{0.553}0.92^{0.447} \\ &= \left(1+\Delta_2\right)^p\left(1-\Delta_2\right)^{1-p}. \end{aligned}$$

Therefore, risk averse behavior does not in general imply maximization of the geometric mean. □

Remark 7.10.6. *This is a different result than Corollary 7.10.2 because the expected values of the prospects are not equal. This shows that it is possible to have a policy with higher mean fitness, higher variance, and higher geometric fitness.*

Non-equilibrium policy and bet-hedging

The idea presented in Corollary 7.10.5 can be shown to be consistent with the non-equilibrium policy derived in Section 7.10. It was shown that the "choice" of the non-equilibrium policy over the optimal policy exhibited risk-sensitive behavior, but this does not imply that the non-equilibrium policy is a bet-hedging strategy. Notably, if $\bar{\epsilon} \ll 1$, the choice of the non-equilibrium policy does not maximize the geometric mean of the organism's fitness (number of offspring).

The non-equilibrium policy can be examined for two cases:

1. $\mathbb{E}\{\epsilon(k)\} < 0$: In this case, the non-equilibrium policy calls for a lower expected fitness and a higher fitness variance than the other prospect (highest expected fitness and lowest fitness variance). This is not consistent with a typical bet-hedging strategy, which trades off a reduction in expected fitness with a reduction in fitness variance. The optimal policy (all spores) more closely resembles a conservative bet-hedging strategy due to its "one bird in the hand is worth two in the bush" characterization [233], though without the decrease in expected fitness that accompanies a true bet-hedging strategy.

2. $\mathbb{E}\{\epsilon(k)\} > 0$: In this case, the non-equilibrium policy calls for a lower expected fitness and a lower fitness variance than the other prospect (highest expected fitness and highest fitness variance). Though it may seem to be a diversified bet-hedging strategy, notice that the geometric mean of the fitness for any strategy is

$$\begin{aligned} GM = e^{\mathbb{E}\{\log A(k+1)\}} &= (A(k) + \Delta A(k)\overline{\epsilon})^{\frac{q}{p+q}} (A(k) - \Delta A(k)\overline{\epsilon})^{\frac{p}{p+q}} \\ &= A(k) \left(1 + \frac{\Delta A(k)}{A(k)}\overline{\epsilon}\right)^{\frac{q}{p+q}} \left(1 - \frac{\Delta A(k)}{A(k)}\overline{\epsilon}\right)^{\frac{p}{p+q}} \end{aligned}$$

where $\Delta A(k) := \frac{1}{\epsilon(k)}(A(k+1) - A(k))$. Normalizing by $A(k)$ and defining $\delta := \frac{\Delta A(k)}{A(k)}\overline{\epsilon}$, the geometric mean becomes

$$GM = (1+\delta)^{\frac{q}{p+q}} (1-\delta)^{1-\frac{q}{p+q}}.$$

Notice that

$$GM = \begin{cases} 1 & \text{if } \delta = 0 \\ 0 & \text{if } \delta = 1 \end{cases}$$

but GM is not monotonically decreasing in δ. In particular,

$$\begin{aligned} \frac{\partial}{\partial\delta} GM\Big|_{\delta=0} &= \frac{q}{p+q} \left(\frac{1-\delta}{1+\delta}\right)^{1-\frac{q}{p+q}}\Bigg|_{\delta=0} - \left(1 - \frac{q}{p+q}\right) \left(\frac{1+\delta}{1-\delta}\right)^{\frac{q}{p+q}}\Bigg|_{\delta=0} \\ &= \frac{q}{p+q} - \left(1 - \frac{q}{p+q}\right) \\ &= 2\frac{q}{p+q} - 1 \\ &> 0 \end{aligned}$$

where the inequality comes from $\mathbb{E}\{\epsilon(k)\} > 0 \Rightarrow q > p \Rightarrow \frac{q}{p+q} > \frac{1}{2}$. Thus, for small δ, GM increases with increasing δ. If $\overline{\epsilon} \ll 1$, then $\delta \ll 1$, so this behavior applies to the analysis of the non-equilibrium policy.

Since $\Delta A(k)$ is greater for the optimal policy than the non-equilibrium policy, the geometric mean of the fitness corresponding to the non-equilibrium policy is smaller than the geometric mean for the optimal policy. Therefore, the non-equilibrium policy does not maximize the geometric mean of the fitness, so it cannot be a bet-hedging strategy.

Despite this crucial difference, the non-equilibrium policy is similar to a bet-hedging strategy in other ways, as summarized in Table 7.1. The generality of the proposed evolutionary dynamics model allows the non-equilibrium policy to originate from a single genotype, which is consistent with bet-hedging strategy. Both strategies also arise from temporal environmental variability, though the non-equilibrium policy results from transitioning between ESSs (as opposed to a bet-hedging strategy, which is an equilibrium policy).

Table 7.1: Characteristics of bet-hedging strategies and the derived non-equilibrium strategy

	Necessary Environmental Condition	Genetic Characterization	System Condition with Strategy	Quantity Maximized
Bet-hedging strategy	*Temporal variability*	*Single genotype*	*Evolutionary stable*	*Geometric mean fitness*
Non-equilibrium strategy	*Temporal variability*	*Single or multiple genotypes*	*Non-equilibrium*	*Value of fitness*

Thus, though superficially resembling a bet-hedging strategy, the derived non-equilibrium policy is not consistent with the commonly accepted definition of a bet-hedging strategy. The most glaring difference is the non-equilibrium policy's failure to increase the geometric mean fitness over the optimal, ESS policies. Therefore, in the proposed modeling framework, the non-equilibrium policy does not mitigate the probability of extinction, as expected. This fact was due to the small $\bar{\epsilon}$ assumption, which provides a foundation for the major drawbacks of this analysis.

7.11 Concluding remarks

This chapter examined the special case of two competing populations with identical birth and death rates. This condition was necessary because it allowed the coexistence of the two competing populations, which permitted the behavior of an "aggressive" policy ($< 100\%$ sporulation) to be examined. BIBO stability of this model was analytically proved based on the coefficients of power series expansion in the nutrient supply, where it was inductively shown that they were all bounded. Though the identical birth and death rates assumption resulted in non-unique steady states, an approximation was used to track population changes from one steady state to another. These population changes were dependent on both populations' steady state sporulation efficiencies, and the optimal efficiencies were found using game theory tools. Since these optimal policies depended on the sign of the nutrient change, an environmental model that alternates between positive and negative nutrient changes was introduced. With a natural selection-based evolutionary model describing the dynamics of the population-average sporulation efficiency, a non-equilibrium policy was derived that depended on the expected value of the nutrient change. Generally, an environment with a increasing (on average) nutrient infusion will select for a low sporulation efficiency, while an environment with a decreasing (on average) nutrient infusion will select for a high sporulation efficiency. The "choice" of the non-equilibrium policy over the optimal policies was examined in the framework of prospect theory, where it was found to be optimistic and risk seeking when nutrient infusion decreases (on average), and pessimistic and risk averse when nutrient infusion increases (on average). Finally, the derived non-equilibrium policy was compared to the general class of bet-hedging strategies, where it was concluded that

the non-equilibrium policy is not a bet-hedging strategy. In particular, the non-equilibrium policy does not diminish the probability of extinction.

There are several drawbacks with the analysis performed in this chapter. Perhaps most glaring are the effects of the small $\bar{\epsilon}$ assumption. Three inconsistencies with expected behavior arise because only small changes are allowed in the nutrient supply:

1. The purpose of sporulation: It was shown in Chapter 4 that sporulation may have evolved to deal with catastrophic environmental conditions. However, when $|\epsilon(k)| \ll \bar{e}$, catastrophic changes cannot be modeled. In this setting, the supposed main benefit of sporulation is not revealed, and the biological application of results based on this restriction may be questioned. This drawback is emphasized in Section 7.10.2, where it was shown that a population with spores has a lower geometric mean fitness than a population without spores, i.e. spores do not decrease the probability of extinction. Clearly, this result is not consistent with the main purpose of sporulation, and it was directly a result of $|\epsilon(k)|$ being small (a large $|\epsilon(k)|$ will give the desired result). Many researchers have labeled sporulation as a bet-hedging strategy [57, 145, 257], which seems to be more consistent with the physiological characterization of a bacterial spore.

2. Sporulation efficiency as a function of $\overline{f}$: Though mentioned in Section 5.4, there is a valid argument for parameterizing the sporulation and germination rates as functions of f, not $\frac{f}{X_1+X_2}$. This will allow the sporulation efficiency to be dependent on nutrient level, which agrees with the expectation that more spores should be formed as nutrient levels drop [76, 184, 224, 245]. However, due to the small $|\epsilon(k)|$ assumption, these changes to the sporulation and germination rates do not affect the results (see the end of Section 7.5). The optimal policies may be significantly different and more similar to experimental results with these different rate dependencies.

3. Adiabatic conditions: Though it is still possible to model large changes in nutrient influx as a series of several small changes, this approximation will not capture the interesting transient response of large changes in nutrient supply. This is important because the transient response is where the benefit of a vegetative population is revealed, which is how we arrived at a competing populations model in the first place. Adiabatic conditions may also lead to a reduced biological relevance of the derived ESSs (see below).

These inconsistencies cannot be ignored, and much time was spent trying to drop the small $|\epsilon(k)|$ assumption. However, without this assumption, a closed-form solution describing changes between two successive steady states could not be found. Therefore, the assumption was retained out of necessity and the desire to derive clean, analytical (non-numerical) results.

Another drawback of the analysis is that the derived ESSs may not be consistent with experimental findings. In the situation where $\epsilon(k) < 0$, it might be expected that the reduction in the carrying capacity of the environment is converted to spores, so there is no decrease in total population number. However, unlike the derived ESS (100% sporulation),

this policy allows the population to be more sensitive to increases in nutrient influx. Thus, this policy seems to be able to invade a population of organisms adopting the derived ESS. This discrepancy is the result of the sporulation and germination rate dependencies and the assumed one-step optimization horizon. Changing the rate dependencies to f would allow non-constant sporulation efficiencies (see above), and increasing the horizon over which the payoffs are calculated will account for decreases in nutrient influx followed by increases. Though increasing the optimization horizon may result in more intuitive ESSs, the one-step horizon was chosen because it is analytically tractable. With a longer horizon, the payoffs become density dependent, which may lead to complex stable strategies that may depend on initial population conditions [62, 107, 112]. This would be unavoidable with a longer horizon because the fair-game assumption cannot be enforced at each time step, since it would negate the whole purpose of using a longer horizon in the first place. In addition to density dependent payoff functions, longer horizons for the random environment would not have clean, closed-form ESSs due to the fact that the approximated populations at $k+1$ are nonlinear in the populations at k. Therefore, the one-step horizon was retained due to the convenient application of the fair-game assumption and the clean expected payoff function. This simplification comes at the expense of ESSs that may not agree with intuition.

Finally, the competing populations model with identical birth and death rates is not able to capture a particular, possibly important behavior. With a constant nutrient influx ($\epsilon(k) \equiv 0$), it is expected that mutation and selection in both populations will lead to changes in the steady state numbers for both population sizes. Though the restriction of equal birth and death rates precludes the possibility of competitive exclusion, competitive interactions that change steady state numbers would be an interesting feature to model. There is evidence that this occurs in natural ecosystems with nearly constant environmental conditions, as mentioned in Section 7.8.1. However, the proposed model does not allow any changes when $\epsilon(k) \equiv 0$, once a steady state is established.

There is a clear need to modify the proposed model so the results have more biological relevance. In order to start addressing the obvious drawbacks mentioned above, a methodology must be developed to find the solution to the nonlinear differential equations for large changes in nutrient supply. Though it may not be possible to allow large $\epsilon(k)$ for this particular model structure, it must be a prerequisite for any subsequent sporulation model focusing on the sporulation decision policy. Large changes in nutrient influx will allow the incorporation of changing sporulation efficiencies in response to absolute nutrient level, which may give rise to more intuitive and meaningful ESSs. If the steady state relationships are simple enough, the effect of payoff horizon length can also be examined. Though there are likely many additional ways to improve the biological relevance of the results, these areas seem to be the most critical.

Chapter 8

Conclusion

The material presented in this dissertation addressed the general research aims presented in Chapter 1. Using a *B. subtilis* research platform, reasons for the existence of sporulation, the optimal sporulation policies under different environmental conditions, and some characteristics and comparisons between the optimal and observed policies were conjectured using a framework of evolutionary optimality. Elucidating these research goals necessitated the development of various population-level sporulation models and a few mathematical results. Although many of the mathematical results were only proved for the specific models in this dissertation, many of the general results should be valid for many similar sporulation models. This would increase the biological significance of the presented work, which is admittedly limited due to tractability constraints and the desire for analytical cleanliness. However, if an actual colony of *B. subtilis* was well approximated by the proposed models, then the results of this research would be very intriguing from a biological point of view. In particular, the optimistic and risk seeking versus pessimistic and risk averse characterizations of bacterial behavior would provide a fascinating account of the effects of evolution on a simple organism.

Nonetheless, there are significant criticisms of the presented research. Aside from the specific remarks in the last sections of Chapters 3–7, there are some potential pitfalls that must be considered in the assumed modeling and analysis framework. Most conspicuous is the validity of the evolutionary optimality framework and the associated question "does evolution maximize fitness?" It is beyond the scope of this dissertation to provide an exhaustive list of examples to support or refute the fitness maximization assumption, but even if it was true, evolutionary optimality may be difficult to observe. Unless the experimental conditions are very similar to the environment in which an organism evolved, optimality would not be exhibited in the resulting behavioral mechanisms. For example, a population of microbes adapted to high density growth will have a low fitness in low density growth environments since they are specialists in resources exploitation instead of high replication rate [25]. It is possible to ensure that the experimental setting is reflective of the evolutionary environment by evolving the bacteria in the experimental environment for many generations, which would require a burn in time on the order of years for *B. subtilis* [166, 168]. However, even if we could observe an evolutionary optimal behavior in the correct environmental setting, corroborating theoretical findings with experimental results would still be difficult. There is

a large gap between experimental and modeling conditions, especially when dealing with nutrient availability. Since there is no easy way to measure nutrient conditions *in vivo*, model validation and parameter estimation are not reliable. The appropriateness of any proposed sporulation model is therefore questionable, which may contribute to biologically-useless results. Finally, even if all of the aforementioned issues were resolved, new mathematical tools would need to be developed to deal with the analytical challenges of finding solutions to nonlinear differential equations. The research in Chapter 7 was able to work around this by imposing small changes in the input, but as mentioned in Section 7.11, this is probably not appropriate for a real sporulation situation.

The work presented in this dissertation provided only a small sampling of the possible ways to study *B. subtilis* decision policies– there are many directions for future work. Besides addressing the general criticisms in the preceding paragraph and the remarks at the ends of Chapters 3–7, it would be interesting to examine sporulation in the context of other *B. subtilis* survival strategies such as natural competence, degradative enzyme synthesis, chemotaxis, and motility. These are all interrelated subsystems that are expressed in response to nutrient limitation [184], and examination of more survival strategies will lead to a more holistic point of view in the resulting analysis. It will also provide a better reason for the evolution of sporulation since the environmental niche that is addressed by sporulation will be highlighted and isolated. Studying *B. subtilis* survival by only considering sporulation is similar to examining the safety of an aircraft based only on aileron design; though some interesting results may emerge, a true appreciation and appraisal of aircraft safety can only be made by considering all of the safety mechanisms. The effects of the other survival subsystems on sporulation (and vice versa) are always considered by a researcher with sufficient domain knowledge, but explicitly including them in the modeling and analysis will provide a better understanding of the role of this survival strategy. The work in this dissertation only scratched the surface of a complete quantitative characterization of sporulation, and it is obvious that there are a considerable number of criticisms that need to be addressed and work to be done.

Perhaps more than most other organisms, bacteria like *B. subtilis* are often the focus of quantitative studies due to their relatively well-understood behavior, ease of genetic manipulation, and short experimental turnaround time. However, bacteria only represent a fraction (albeit very large) of the lifeforms on earth [267], and they are definitely not the only ones which are interesting to study from a control theory perspective (see Sections 1.1 and 1.2 for some examples). In fact, control systems in the Animal kingdom may be more interesting because we are more familiar with the organisms and can more easily relate to them. Though potentially more difficult to analyze quantitatively, biological systems from other domains still harbor feedback systems based on environmental sensing and suitable responses to ensure survival. In this respect, the control-based ideas and analysis methods utilized in this dissertation should be applicable to the study of many other biological organisms and systems. Integral control, for example, is likely ubiquitous in biological systems, underlying processes such as homeostatic control, sensor adaptation, and evolutionary adaptation [46, 276].

Control theory is but one of many engineering disciplines from which to study biological

organisms. Though interesting due to their pervasiveness in biological systems, feedback control principles are often not the appropriate lens to look through. For example, the analysis of biocompatibility, mechanical properties, degradation, or responsiveness for tissue engineering, stent design, or dental implant manufacturing requires a materials science point of view [148]; analysis of blood flow through arteries in search of fluid conditions that are associated with and contribute to atherosclerotic disease requires a fluid mechanics point of view [144]; and understanding the design of hearing and acoustic-producing apparatuses (such as ears or throats) requires an acoustic engineering and vibration theory point of view [77]. Just as the design of a passenger airplane requires the interdisciplinary collaboration of several engineers, a thorough analysis of a biological system requires ideas from many engineering fields. This comprehensive perspective is needed to appreciate the intricacy and sophistication of biological systems and organisms, which are truly marvels of engineering design.

References

[1] M. Acar, J. Mettental, and A. van Oudenaarden, *Stochastic switching as a survival strategy in fluctuating environments*, Nature Genetics, 40 (2008), pp. 471–475.

[2] B. Alberts, D. Bray, J. Lewis, M. Raff, K. Roberts, and J. Watson, *Molecular Biology of the Cell*, Garland Publishing, Inc., New York, NY, third ed., 1994.

[3] M. Andersson, A. Axelsson, and G. Zacchi, *Diffusion of glucose and insulin in a swelling n-isopropylacrylamide gel*, Int. J. Pharm., 157 (1997), pp. 199–208.

[4] C. Antoniewski, B. Savelli, and P. Stragier, *The spoIIJ gene, which regulates early developmental steps in Bacillus subtilis, belongs to a class of environmentally responsive genes*, J. Bacteriol., 172 (1990), pp. 86–93.

[5] R. Armstrong and R. McGehee, *Coexistence of species competing for shared resources*, Theor. Popul. Biol., 9 (1976), pp. 317–328.

[6] ——, *Competitive exclusion*, Am. Naturalist, 115 (1980), pp. 151–170.

[7] N. Balaban, J. Merrin, R. Chalt, L. Kowalik, and S. Leibler, *Bacterial persistence as a phenotypic switch*, Science, 305 (2004), pp. 1622–1625.

[8] T. Barbosa, C. Serra, R. La Ragione, M. Woodward, and A. Henriques, *Screening for Bacillus isolates in the broiler gastrointestinal tract*, Appl. Env. Microbiol., 71 (2005), pp. 968–978.

[9] J. Barker, *Defining fitness in natural and domesticated populations*, in Adaptation and Fitness in Animal Populations: Evolutionary and Breeding Perspectives on Genetic Resource Management, J. van der Werf, H.-U. Graser, R. Frankham, and C. Gondro, eds., Springer Netherlands, 2009, pp. 3–14.

[10] E. Barron, *Game Theory: An Introduction*, John Wiley and Sons, Inc., Hoboken, NJ, 2008.

[11] I. Bateman, A. Munro, B. Rhodes, C. Starmer, and R. Sugden, *A test of the theory of reference-dependent preferences*, Quart. J. Econ., 112 (1997), pp. 479–506.

[12] B. Batt and D. Kompala, *Verification of immune response optimality through cybernetic modeling*, J. Theor. Biol., 142 (1990), pp. 317–340.

[13] H. Beaumont, J. Gallie, C. Kost, G. Ferguson, and P. Rainey, *Experimental evolution of bet hedging*, Nature, 462 (2009), pp. 90–93.

[14] P. Bednekoff, *Risk-sensitive foraging, fitness, and life histories: Where does reproduction fit into the big picture?*, Amer. Zool., 36 (1996), pp. 471–483.

[15] C. Bell, *Growth of Agrobacterium tumefaciens under octopine limitation in chemostats*, Appl. Env. Microbiol., 56 (1990), pp. 1775–1781.

[16] R. Bellazzi, G. Nucci, and C. Cobelli, *The subcutaneous route to insulin-dependent diabetes therapy: closed-loop and partially closed-loop control strategies for insulin delivery and measuring glucose concentration*, IEEE Eng. Med. Biol., 20 (2001), pp. 54–64.

[17] J. Benardini, J. Sawyer, K. Venkateswaran, and W. Nicholson, *Spore UV and acceleration resistance of endolithic Bacillus pumilus and Bacillus subtilis isolates obtained from Sonoran Desert basalt: implications for lithopanspermia*, Astrobiol., 3 (2003), pp. 709–717.

[18] M. Bennett and J. Hasty, *Microfluidic devices for measuring gene network dynamics in single cells*, Nat. Rev. Genetics, 10 (2009), pp. 628–638.

[19] J. Benyus, *Biomimicry: Innovation Inspired by Nature*, William Morrow & Company, Inc., New York, NY, 1997.

[20] W. Bequette, *A critical assessment of algorithms and challenges in the development of a closed-loop artificial pancreas*, Diabetes Technol. The., 7 (2005), pp. 28–47.

[21] D. Bernoulli, *Exposition of a new theory on the measurement of risk*, Econometrica, 22 (1954), pp. 23–36.

[22] D. Bertsekas and J. Tsitsiklis, *Introduction to Probability*, Athena Scientific, Belmont, MA, 2002.

[23] C. Birky, *Uniparental inheritance of mitochondrial and chloroplast genes: Mechanisms and evolution*, Proc. Natl. Acad. Sci., 92 (1995), pp. 11331–11338.

[24] I. Bischofs, J. Hug, A. Liu, D. Wolf, and A. Arkin, *Complexity in bacterial cell-cell communication: quorum signal integration and subpopulation signaling in the Bacillus subtilis phosphorelay*, Proc. Natl. Acad. Sci., 106 (2009), pp. 6459–6464.

[25] A. Borderia and S. Elena, *r- and k-selection in experimental populations of vesicular stomatitis virus*, Infect. Genet. Evol., 2 (2002), pp. 137–143.

[26] S. Boyd and L. Vandenberghe, *Convex Optimization*, Cambridge University Press, Cambridge, UK, 2004.

[27] E. Boye and K. Nordstrom, *Coupling the cell cycle to cell growth: a look at the parameters that regulate cell-cycle events*, EMBO Rep., 4 (2003), pp. 757–760.

[28] S. S. Branda, J. E. Gonzlez-Pastor, S. Ben-Yehuda, R. Losick, and R. Kolter, *Fruiting body formation by Bacillus subtilis*, Proc. Natl. Acad. Sci., 98 (2001), p. 1162111626.

[29] R. Brandon, *Adaptation and Environment*, Princeton University Press, Princeton, NJ, 1990.

[30] D. Brune, *Isolation and characterization of sulfur globule proteins from Chromatium vinosum and Thiocapsa roseopersicina*, Arch. Microbiol., 163 (1995), pp. 391–399.

[31] J. Bull, M. Badgett, H. Wichman, J. Huelsenbeck, D. Hillis, A. Gulati, C. Ho, and I. Molineux, *Exceptional convergent evolution in a virus*, Genetics, 147 (1997), pp. 1497–1507.

[32] D. Burbulys, K. Trach, and J. Hoch, *Initiation of sporulation in b. subtilis is controlled by a multicomponent phosphorelay*, Cell, 64 (1991), pp. 545–552.

[33] J. Cairns, J. Overbaugh, and S. Miller, *The origin of mutants*, Nature, 335 (1988), pp. 142–145.

[34] T. Caraco, *On foraging time allocation in a stochastic environment*, Ecology, 61 (1980), pp. 119–128.

[35] A. Carpenter, T. Jones, M. Lamprecht, C. Clarke, I. H. Kang, O. Friman, D. Guertin, J. H. Chang, R. Lindquist, J. Moffat, P. Golland, and D. Sabatini, *CellProfiler: image analysis software for identifying and quantifying cell phenotypes*, Genome Biol., 7 (2006), p. R100.

[36] F. Chandra, G. Buzi, and J. Doyle, *Glycolytic oscillations and limits on robust efficiency*, Science, 333 (2011), pp. 187–192.

[37] D. Childs, C. Metcalf, and M. Rees, *Evolutionary bet-hedging in the real world: empirical evidence and challenges revealed by plants*, Proc. R. Soc. B, 277 (2010), pp. 3055–3064.

[38] J. Chung, G. Stephanopoulos, K. Ireton, and A. Grossman, *Gene expression in single cells of Bacillus subtilis: evidence that a threshold mechanism controls the initiation of sporulation*, J. Bacteriol., 176 (1994), pp. 1977–1984.

[39] D. Claus and D. Fritze, *Taxonomy of Bacillus*, in *Bacillus*, C. Harwood, ed., Plenum Press, New York, NY, 1989, pp. 5–26.

[40] D. Cohen, *Optimizing reproduction in a randomly varying environment*, J. Theor. Biol., 12 (1966), pp. 119–129.

[41] V. Cooper and R. Lenski, *The population genetics of ecological specialization in evolving Escherichia coli populations*, Nature, 407 (2000), pp. 736–739.

[42] W. Cooper, *Expected time to extinction and the concept of fundamental fitness*, J. Theor. Biol., 107 (1984), pp. 603–629.

[43] W. Cooper and R. Kaplan, *Adaptive "coin-flipping": a decision-theoretic examination of natural selection for random individual variation*, J. Theor. Biol., 94 (1982), pp. 135–151.

[44] W. S. Cooper, *Decision theory as a branch of evolutionary theory: a biological derivation of the savage axioms*, Psychol. Rev., 94 (1987), pp. 395–411.

[45] J. Costerton, P. Stewart, and E. Greenberg, *Bacterial biofilms: a common cause of persistent infections*, Science, 284 (1999), pp. 1318–1322.

[46] M. Csete and J. Doyle, *Reverse engineering of biological complexity*, Science, 295 (2002), pp. 1664–1669.

[47] C. Darwin, *On The Origin of Species*, Cambridge University Press, New York, NY, 2009.

[48] I. Dawes, D. Kay, and J. Mandelstam, *Determining effect of growth medium on the shape and position of daughter chromosomes and on sporulation in Bacillus subtilis*, Nature, 230 (1971), pp. 567–569.

[49] M. de Heij, P. van den Hout, and J. Tinbergen, *Fitness cost of incubation in great tits (Parus major is related to clutch size*, Proc. R. Soc. B, 273 (2006), pp. 2353–2361.

[50] I. de Jong, P. Haccou, and O. Kuipers, *Bet hedging or not? a guide to proper classification of microbial survival strategies*, Bioessays, 33 (2011), pp. 215–223.

[51] A. de Visser and R. Lenski, *Long-term experimental evolution in Escherichia coli. XI. rejection of non-transitive interactions as cause of declining rate of adaptation*, BMC Evol. Biol., 2 (2002), p. 19.

[52] M. Dickinson, C. Farley, R. Full, M. Koehl, R. Kram, and S. Lehman, *How animals move: an integrative view*, Science, 288 (2000), pp. 100–106.

[53] D. Dragon and R. Rennie, *The ecology of anthrax spores: tough but not invincible*, Can. Vet. J., 36 (1995), pp. 295–301.

[54] T. Drezner-Levy and S. Shafir, *Parameters of variable reward distributions that affect risk sensitivity of honey bees*, J. Exper. Biol., 210 (2007), pp. 269–277.

[55] A. Driks, *Overview: Development in bacteria: spore formation in Bacillus subtilis*, Cell. Mol. Life Sci., 59 (2002), pp. 389–391.

[56] D. Dubnau, *Genetic competence in Bacillus subtilis*, Microbiol. Rev., 55 (1991), pp. 395–424.

[57] D. Dubnau and R. Losick, *Bistability in bacteria*, Mol. Microbiol., 61 (2006), pp. 564–572.

[58] R. Dudley and C. Gans, *A critique of symmorphosis and optimality models in physiology*, Physiol. Zool., 64 (1991), pp. 627–637.

[59] J. Dworkin and I. Shah, *Exit from dormancy in microbial organisms*, Nat. Rev. Microbiol., 8 (2010), pp. 890–896.

[60] D. Dykhuizen, *Experimental studies of natural selection in bacteria*, Annu. Rev. Ecol. Syst., 21 (1990), pp. 373–398.

[61] O. Dzyubachy, J. Essers, W. van Cappellen, C. Baldeyron, A. Inagaki, W. Niessen, and E. Meijering, *Automated analysis of time-lapse fluorescence microscopy images: from live cell images to intracellular foci*, Bioinformatics, 26 (2010), pp. 2424–2430.

[62] J. Eadie and J. Fryxell, *Density dependence, frequency dependence, and alternative nesting strategies in goldeneyes*, Am. Nat., 140 (1992), pp. 621–641.

[63] A. Earl, R. Losick, and R. Kolter, *Ecology and genomics of Bacillus subtilis*, Trends Microbiol., 16 (2008), pp. 269–275.

[64] A. Edwards, *The Fundamental Theorem of Natural Selection*, Biol. Rev., 69 (1994), pp. 443–474.

[65] H. El Samad and M. Khammash, *Modelling and analysis of gene regulatory network using feedback control theory*, Int. J. Syst. Sci., 41 (2010), pp. 17–33.

[66] H. El Samad, M. Khammash, C. Homescu, and L. Petzold, *Optimal performance of the heat-shock regulatory network*, Proc. 16th IFAC World Cong., Prague, (2005).

[67] S. Elena and R. Lenski, *Evolution experiments with microorganisms: The dynamics and genetic bases of adaptation*, Nat. Rev. Genet., 4 (2003), pp. 457–469.

[68] R. Elner and A. Campbell, *Force, function and mechanical advantage in the chelae of the American lobster Homarus americanus (Decapoda: Crustacea)*, J. Zool., 193 (1981), pp. 269–286.

[69] J. Errington, *Bacillus subtilis sporulation: regulation of gene expression and control of morphogenesis*, Microbiol. Rev., 57 (1993), pp. 1–33.

[70] ——, *Determination of cell fate in Bacillus subtilis*, Trends Genet., 12 (1996), pp. 31–34.

[71] ——, *Regulation of endospore formation in Bacillus subtilis*, Nat. Rev. Microbiol., 1 (2003), pp. 117–126.

[72] P. Eswaramoorthy, J. Dinh, D. Duan, O. A. Igoshin, and M. Fujita, *Single cell measurement of the levels and distributions of the phosphorelay components in a population of sporulating Bacillus subtilis cells*, Microbiology, (2010).

[73] W. Ewens, *An interpretation and proof of the Fundamental Theorem of Natural Selection*, Theor. Popul. Biol., 36 (1989), pp. 167–180.

[74] R. Fisher, *The Genetical Theory of Natural Selection*, Clarendon Press, Oxford, 1930.

[75] R. Fisher, *The evolution of dominance*, Biol. Rev., 6 (1931), pp. 345–368.

[76] S. Fisher and A. Sonenshein, *Control of carbon and nitrogen metabolism in Bacillus subtilis*, Annu. Rev. Microbiol., 45 (1991), pp. 107–135.

[77] N. Fletcher and S. Thwaites, *Physical models for the analysis of acoustical systems in biology*, Quart. Rev. Biophys., 12 (1979), pp. 25–65.

[78] M. Fujita and R. Losick, *Evidence that entry into sporulation in Bacillus subtilis is governed by a gradual increase in the level and activity of the master regulator spo0a*, Genes & Develop., 19 (2005), pp. 2236–2244.

[79] D. Futuyma, *Evolutionary Biology*, Sinauer Associates, Inc., Sunderland, MA, 1979.

[80] A. Gardner, S. West, and A. Griffin, *Is bacterial persistence a social trait?*, PLOS One, 8 (2007), p. e752.

[81] O. Gefen and N. Balaban, *The importance of being persistent: heterogeneity of bacterial populations under antibiotic stress*, FEMS Microbiol. Rev., 33 (2009), pp. 704–717.

[82] S. Geritz, J. Metz, E. Kisdi, and G. Meszena, *Dynamics of adaptation and evolutionary branching*, Phys. Rev. Lett., 78 (1997), pp. 2024–2027.

[83] J. Gerke, C. Chen, and B. Cohen, *Natural isolates of Saccharomyces cerevisiae display complex genetic variation in sporulation efficiency*, Genetics, 174 (2006), pp. 985–997.

[84] S. Ghosh and P. Setlow, *Isolation and characterization of superdormant spores of Bacillus species*, J. Bacteriol., 191 (2009), pp. 1787–1797.

[85] J. Gibb, *The breeding biology of the great and blue titmice*, Ibis, 92 (1950), pp. 507–539.

[86] R. Gilbert, P. Turnbull, J. Parry, and J. Kramer, *Bacillus cereus and other Bacillus species: Their part in food poisoning and other clinical infections*, in The Aerobic Endospore-forming Bacteria: Classification and Identification, R. Berkeley and M. Goodfellows, eds., Academic Press, London, 1981, pp. 297–314.

[87] J. Gonzalez-Pastor, *Cannibalism: a social behavior in sporulation Bacillus subtilis*, FEMS Microbiol. Rev., 35 (2010), pp. 415–424.

[88] J. Gonzalez-Pastor, E. Hobbs, and R. Losick, *Cannibalism by sporulating bacteria*, Science, 301 (2003), pp. 510–513.

[89] B. Goodwin, *Oscillatory behavior in enzymatic control processes*, Adv. Enzyme Regul., 3 (1965), pp. 425–428.

[90] S. Gould and R. Lewontin, *The Spandrels of San Marco and the Panglossian paradrigm: a critique of the adaptationist programme*, Proc. R. Soc. Lond. B., 205 (1979), pp. 581–598.

[91] A. Grafen, *The simplest formal argument for fitness optimization*, J. Genet., 87 (2008), pp. 421–433.

[92] J. Griffith, *Mathematics of cellular control processes: I. negative feedback to one gene*, J. Theoret. Biol., 20 (1968), pp. 202–208.

[93] A. Grossman, *Integration of developmental signals and the initiation of sporulation B. subtilis*, Cell, 65 (1991), pp. 5–8.

[94] ——, *Genetic networks controlling the initiation of sporulation and the development of genetic competence in Bacillus subtilis*, Annu. Rev. Genetics, 29 (1995), pp. 477–508.

[95] A. Grossman and R. Losick, *Extracellular control of spore formation in Bacillus subtilis*, Proc. Natl. Acad. Sci., 85 (1988), pp. 4369–4373.

[96] J. Grover, *Resource Competition*, Chapman & Hall, London, 1997.

[97] R. Gupta, Q. Beg, and P. Lorenz, *Bacterial alkaline proteases: molecular approaches and industrial applications*, Appl. Microbiol. Biotechnol., 59 (2002), pp. 15–32.

[98] J. Hale and A. Somolinos, *Competition for a fluctuating nutrient*, J. Math. Biol., 18 (1983), pp. 255–280.

[99] P. Hammerstein and E. Hagen, *The second wave of evolutionary economics in biology*, TRENDS Ecol. Evol., 20 (2005), pp. 604–609.

[100] A. Handel and D. Rozen, *The impact of population size on the evolution of asexual microbes on smooth versus rugged fitness landscapes*, BMC Evol. Biol., 9 (2009), p. 236.

[101] S. Hansen and S. Hubbell, *Single nutrient microbial competition: qualitative agreement between experimental and theoretically-forecast outcomes*, Science, 207 (1980), pp. 1491–1493.

[102] C. Harwood, *Introduction to the biotechnology of Bacillus*, in *Bacillus*, C. Harwood, ed., Plenum Press, New York, NY, 1989, pp. 1–4.

[103] C. Harwood and S. Cutting, *Molecular Biological Methods for Bacillus*, John Wiley and Sons, Ltd., New York, NY, 1990.

[104] T. Hastjarjo, A. Silberberg, and S. Hursh, *Risky choice as a gunction of amount and variance in food supply*, J. Exper. Anal. Behav., 53 (1990), pp. 155–161.

[105] S. Hedges, *The origin and evolution of model organisms*, Nat. Rev. Genetics, 3 (2002), pp. 838–849.

[106] P. Hedrick, M. Ginevan, and E. Ewing, *Genetic polymorphism in heterogeneous environments*, Annu. Rev. Ecol. Syst., 7 (1976), pp. 1–32.

[107] W. Hines, *Evolutionary stable strategies: a review of basic theory*, Theor. Pop. Biol., 31 (1987), pp. 195–272.

[108] A. D. Hitchins and R. A. Slepecky, *Bacterial spore formation as a modified procaryotic cell division*, Nature, 223 (1969), pp. 804–807.

[109] J. A. Hoch, *Regulation of the phosphorelay and the initiation of sporulation in Bacillus subtilis*, Anu. Rev. Microbiol., 47 (1993), pp. 441–465.

[110] A. Hodgkin and A. Huxley, *A quantitative description of membrane current and its application to conduction and excitation in nerve*, J. Physiol., 117 (1952), pp. 500–544.

[111] J. Hofbauer and K. Sigmund, *Adaptive dynamics and evolutionary stability*, Appl. Math. Lett., 3 (1990), pp. 75–79.

[112] ——, *Evolutionary game dynamics*, Bull. Am. Math. Soc., 40 (2003), pp. 479–519.

[113] T. Hoffman, N. Frankenberg, M. Marino, and D. Jahn, *Ammonification in Bacillus subtilis utilizing dissimilatory nitrite reductase is dependent on resDE*, J. Bacteriol., 180 (1998), pp. 186–189.

[114] D. Hogan and R. Kolter, *Why are bacteria refractory to antimicrobials?*, Curr. Opin. Microbiol., 5 (2002), pp. 472–477.

[115] H. Hong, L. H. Duc, and S. Cutting, *The use of bacterial spore formers as probiotics*, FEMS Microbiol. Rev., 29 (2005), pp. 813–835.

[116] H. Hong, R. Khaneja, N. Tam, A. Cazzato, S. Tan, M. Urdaci, A. Brisson, A. Gasbarrini, I. Barnes, and S. Cutting, *Bacillus subtilis isolated from the human gastrointestinal tract*, Res. Microbiol., 160 (2009), pp. 134–143.

[117] A. Houston, C. Clark, J. McNamara, and M. Mangel, *Dynamic models in behavioral and evolutionary ecology*, Nature, 332 (1988), pp. 29–34.

[118] R. Hovorka, *Continuous glucose monitoring and closed-loop systems*, Diabetes Med., 23 (2005), pp. 1–12.

[119] A. Hsu, T. Hagobian, K. Jacobs, H. Attallah, and A. Friedlander, *Effects of heat removal through the hand on metabolism and performance during cycling exercise in the heat*, Can. J. Appl. Physiol., 30 (2005), pp. 87–104.

[120] Y. Inatsu, N. Nakamura, Y. Yuriko, T. Fushimi, L. Watanasiritum, and S. Kawamoto, *Characterization of Bacillus subtilis strains in Thua nao, a traditional fermented soybean food in northern Thailand*, Letters Appl. Microbiol., 43 (2006), pp. 237–242.

[121] K. Indest, W. Buchholz, J. Faeder, and P. Setlow, *Germination and elucidating reasons for germination heterogeneity*, J. Food Sci., 74 (2009), pp. R73–R78.

[122] F. Jacob and J. Monod, *Genetic regulatory mechanisms in the synthesis of proteins*, J. Mol. Biol., 3 (1961), pp. 318–356.

[123] H. Jannasch, *Enrichments of aquatic bacteria in continuous culture*, Microbiol., 59 (1967), pp. 165–173.

[124] G. Jeronimidis, *The fracture behavior of wood and the relations between toughness and morphology*, Proc. R. Soc. Lond. B., 208 (1980), pp. 447–460.

[125] R. Johnson, *Singular Perturbation Theory: Mathematical and Analytical Techniques with Applications to Engineering*, Springer Science+Business Media, Inc., New York, NY, 2005.

[126] C. Jones, N. Padula, and P. Setlow, *Effect of mechanical abrasion on the viability, disruption and germination of spores of Bacillus subtilis*, J. Appl. Microbiol., 99 (2005), pp. 1484–1494.

[127] S. Jones and J. Lennon, *Dormancy contributes to the maintenance of microbial diversity*, Proc. Natl. Acad. Sci., 107 (2010), pp. 5881–5886.

[128] A. Kacelnik and F. Brito e Abreu, *Risky choice and Weber's Law*, J. Theor. Biol., 194 (1998), pp. 289–298.

[129] S. Kadam and G. Velicer, *Variable patterns of density-dependent survival in social bacteria*, Behav. Ecol., 17 (2006), pp. 833–838.

[130] D. Kadouri, E. Jurkevitch, Y. Okon, and S. Castro-Sowinski, *Ecological and agricultural significance of bacterial polyhydroxyalkanoates*, Crit. Rev. Microbiol., 31 (2005), pp. 55–67.

[131] D. Kahneman, J. Knetsch, and R. Thaler, *Anomalies: The endownment effect, loss aversion, and status quo bias*, J. Econ. Perspect., 5 (1991), pp. 193–206.

[132] D. Kahneman and A. Tversky, *Prospect theory: an analysis of decision under risk*, Econometrica, 47 (1979), pp. 263–291.

[133] ——, *Choices, values, and frames*, Amer. Psychol., 39 (1984), pp. 341–50.

[134] M. Kanehisa and S. Goto, *KEGG: Kyoto Encyclopedia of Genes and Genomes*, Nucl. Acids Res., 28 (2000), pp. 27–30.

[135] R. Kaplan and W. Cooper, *The evolution of developmental plasticity in reproductive characteristics: an application of the "adaptive coin-flipping" principle*, Am. Nat., 123 (1984), pp. 393–410.

[136] A. Karniel and G. Inbar, *Human motor control: learning to control a time-varying, nonlinear, many-to-one system*, IEEE Trans. Syst. Man Cy. C., 30 (2000), pp. 1–11.

[137] S. Kaur and A. Singh, *Natural occurence of Bacillus thuringiensis in leguminous phylloplanes in the New Delhi region of India*, World J. Microbiol. Biotech., 16 (2000), pp. 679–682.

[138] J. Knetsch, *The endownment effect and evidence of nonreversible indifference curves*, Amer. Econ. Rev., 79 (1989), pp. 1277–1284.

[139] K. Kobayashi, S. Ehrlich, A. Albertini, G. Amati, K. Andersen, M. Arnaud, K. Asai, S. Ashikaga, S. Aymerich, P. Bessieres, F. Boland, S. Brignell, S. Bron, K. Bunai, J. Chapuis, L. Christiansen, A. Danchin, M. Debarbouille, E. Dervyn, E. Deuerling, K. Devine, S. Devine, O. Dreesen, J. Errington, S. Fillinger, S. Foster, Y. Fujita, A. Galizzi, R. Gardan, C. Eschevins, T. Fukushima, K. Haga, C. Harwood, M. Hecker, D. Hosoya, M. Huulo, H. Kakeshita, D. Karamata, Y. Kasahara, F. Kawamura, K. Koga, P. Koski, R. Kuwana, D. Imamura, M. Ishimaru, S. Ishikawa, I. Ishio, D. Le Coq, A. Masson, C. Mauel, R. Meima, R. Mellado, A. Moir, S. Moriya, E. Nagakawa, H. Nanamiya, S. Nakai, P. Nygaard, M. Ogura, T. Ohanan, M. O'Reilly, M. O'Rourke, Z. Pragai, H. Pooley, G. Rapoport, J. Rawlins, L. Rivas, C. Rivolta, A. Sadaie, Y. Sadaie, M. Sarvas, T. Sato, H. Saxild, E. Scanlan, W. Schumann, M. Simon, P. Stragier, R. Studer, H. Takamatsu, T. Tanaka, M. Takeuchi, H. Thomaides, V. Vagner, J. can Dijl, K. Watabe, A. Wipat, H. Yamamoto, M. Yamamoto, Y. Yamamoto, K. Yamane, K. Yata, K. Yoshida, H. Yoshikawa, U. Zuber, and N. Ogasawara, *Essential Bacillus subtilis genes*, Proc. Natl. Acad. Sci., 100 (2003), pp. 4678–4683.

[140] L. Kominek and H. Halvorson, *Metabolism of poly-β-hydroxybutyrate and acetoin in Bacillus cereus*, J. Bacteriol., 90 (1965), pp. 1251–1259.

[141] E. Koonin and Y. Wolf, *Is evolution Darwinian or/and Lamarckian*, Biol. Direct, 4 (2009), p. 42.

[142] A. Kraigsley and S. Finkel, *Adaptive evolution in single species bacterial biofilms*, FEMS Microbiol. Lett., 293 (2009), pp. 135–140.

[143] K. Kreutz-Delgado, M. Long, and H. Seraji, *Kinematic analysis of 7-DOF manipulators*, Int. J. Robot. Res., 11 (1992), pp. 469–481.

[144] D. Ku, *Blood flow in arteries*, Annu. Rev. Fluid Mech., 29 (1997), pp. 399–434.

[145] E. Kussell, R. Kishony, N. Balaban, and S. Leibler, *Bacterial persistence: a model of survival in changing environments*, Genetics, 169 (2005), pp. 1807–1814.

[146] E. Kussell and S. Leibler, *Phenotypic diversity, population growth, and information in fluctuating environments*, Science, 309 (2005), pp. 2075–2078.

[147] H. Laanbroek, A. Smit, G. Klein, and H. Veldkamp, *Competition for L-glutamate between specialized and versatile Clostridium species*, Arch. Microbiol., 120 (1979), pp. 61–66.

[148] R. Langer and D. Tirrell, *Designing materials for biology and medicine*, Nature, 428 (2004), pp. 487–492.

[149] A. Lazaris, S. Arcidiacono, Y. Huang, J.-F. Zhou, F. Duguay, N. Chretien, E. Welsh, J. Soares, and C. Karatzas, *Spider silk fibers spun from soluble recombinant silk produced in mammalian cells*, Science, 295 (2002), pp. 472–476.

[150] E. L. Lehmann, S. Fienberg, and G. Casella, *Theory of Point Estimation*, Springer-Verlag, New York, NY, 1998.

[151] A. Lehninger, D. Nelson, and M. Cox, *Principles of Biochemistry, with an extended discussion of oxygen-binding proteins*, Worth Publishers, New York, NY, second ed., 1993.

[152] R. E. Lenski, J. A. Mongold, P. D. Sniegowski, M. Travisano, F. Vasi, P. J. Gerrish, and T. M. Schmidt, *Evolution of competitive fitness in experimental populations of e. coli: What makes one genotype a better competitor than another?*, Antonie van Leeuwenhoek, 73 (1998), pp. 35–47.

[153] R. E. Lenski and M. Travisano, *Dynamics of adaptation and diversification: A 10,000-generation experiment with bacterial populations*, Proc. Natl. Acad. Sci., 91 (1994), pp. 6808–6814.

[154] T. Leser, A. Knarreborg, and J. Worm, *Germination and outgrowth of Bacillus subtilis and Bacillus licheniformis spores in the gastrointestinal tract of pigs*, J. Appl. Microbiol., 104 (2007), pp. 1025–1033.

[155] R. Levins, *Coexistence in a variable environment*, Am. Naturalist, 114 (1979), pp. 765–783.

[156] R. Lewontin and D. Cohen, *On population growth in a randomly varying environment*, Proc. Natl. Acad. Sci., 62 (1969), pp. 1056–1060.

[157] N. Lopez, M. Floccari, A. Steinbuchel, A. Garcia, and B. Mendez, *Effect of poly(3-hydroxybutyrate) (phb) content on the starvation-survival of bacteria in natural waters*, FEMS Microbiol. Ecol., 16 (1995), pp. 95–102.

[158] M. Lorenz and W. Wackernagel, *Bacterial gene transfer by natural genetic transformation in the environment*, Microbiol. Mol. Biol. Rev., 58 (1994), pp. 563–602.

[159] C. Macken, P. Hagan, and A. Perelson, *Evolutionary walks on rugged landscapes*, SIAM J. Appl. Math., 51 (1991), pp. 799–827.

[160] T. Malik and H. Smith, *Does dormancy increase fitness of bacterial populations in time-varying environments?*, Bull. Math. Biol., 70 (2008), pp. 1140–1162.

[161] J. Mandelstam and S. Higgs, *Induction of sporulation during synchronized chromosome replication in Bacillus subtilis*, J. Bacteriol., 120 (1974), pp. 38–42.

[162] B. Marsh and A. Kacelnik, *Framing effects and risky decisions in starlings*, Proc. Natl. Acad. Sci., 99 (2002), pp. 3352–3355.

[163] D. Massimino, M. Andre, C. Richaud, A. Daguenet, J. Massimino, and J. Vivoli, *The effect of a day at low irradiance of a maize crop i: Root respiration and update of N, P, and K*, Physiol. Plant., 51 (1981), pp. 150–155.

[164] A. Matin and H. Veldkamp, *Physiological basis of the selective advantage of a Spirillum sp. in a carbon-limited environment*, J. Gen. Microbiol., 105 (1978), pp. 187–197.

[165] H. Maughan, C. Birky, and W. Nicholson, *Transriptome divergence and the loss of plasticity in B. subtilis after 6,000 generations of evolution under relaxed selection for sporulation*, J. Bacteriol., 191 (2009), pp. 428–433.

[166] H. Maughan, V. Callicotte, A. Hancock, C. Birky, W. Nicholson, and J. Masel, *The population genetics of phenotypic deterioration in experimental population of B. subtilis*, Evolution, 60 (2006), pp. 686–695.

[167] H. Maughan, J. Masel, C. Birky, and W. Nicholson, *The roles of mutation accumulation and selection in loss of sporulation in experimental populations of B. subtilis*, Genetics, 177 (2007), pp. 937–948.

[168] H. Maughan and W. Nicholson, *Stochastic processes influence stationary-phase decisions in B. subtilis*, J. Bacteriol., 186 (2004), pp. 2212–2214.

[169] J. Maynard Smith, *Models in Ecology*, Cambridge University Press, Cambridge, 1974.

[170] ——, *Evolution and the Theory of Games*, Cambridge University Press, Cambridge, 1982.

[171] ——, *The Theory of Evolution*, Cambridge University Press, Cambridge, Canto ed., 1993.

[172] R. McDermott, J. Fowler, and O. Smirnov, *On the evolutionary origin of prospect theory preferences*, J. Politics, 70 (2008), pp. 335–350.

[173] W. McGlothlin, *Stability of choices among uncertain alternatives*, Amer. J. Psych., 69 (1956), pp. 604–615.

[174] J. McNamara and A. Houston, *Risk-sensitive foraging: a review of the theory*, Bull. Math. Biol., 54 (1992), pp. 355–378.

[175] L. Mealey, *The sociobiology of sociopathy: An integrated evolutionary model*, Behav. Brain Sci., 18 (1995), pp. 523–541.

[176] R. Megee, J. Drake, A. Frederickson, and H. Tsuchiya, *Studies in microbial symbiosis: Saccharomyces cerevisiae and Lactobacillus casei*, Can. J. Microbiol., 52 (1971), pp. 1733–1742.

[177] C. Menezes and D. Hanson, *On the theory of risk aversion*, Int. Econ. Rev., 11 (1970), pp. 481–487.

[178] D. Merugu, B. Prabhakar, and N. Rama, *An incentive mechanism for decongesting the roads: a pilot program in Bangalore*, in ACM Workshop on the Economics of Networked Systems, NetEcon, 2009.

[179] J. Metz, R. Nisbet, and S. Geritz, *How should we define 'fitness' for general ecological scenarios?*, Trends Ecol. Evol., 7 (1992), pp. 198–202.

[180] I. Miko, *Epistasis: gene interaction and phenotype effects*, Nat. Edu., 1 (2008).

[181] A. Mitchell, G. Romano, B. Groisman, A. Yona, E. Dekel, M. Kupiec, O. Dahan, and Y. Pilpel, *Adaptive prediction of environmental changes by microorganisms*, Nature, 460 (2009), pp. 220–224.

[182] S. Monteiro, J. Clemente, A. Henriques, R. Gomes, M. Carrondo, and A. Cunha, *A procedure for high-yield spore production by Bacillus subtilis*, Biotechnol. Prog., 21 (2005), pp. 1026–1031.

[183] H. Moyed and K. Bertrand, *hipA, a newly recognized gene of Escherichia coli k-12 that affects frequency of persistence after inhibition of murein synthesis*, J. Bacteriol., 155 (1983), pp. 768–775.

[184] T. Msadek, *When the going gets tough: survival strategies and environmental signaling networks in Bacillus subtilis*, TRENDS Microbiol., 7 (1999), pp. 201–207.

[185] J. Mueller, G. Bukusoglu, and A. Sonenshein, *Transcriptional regulation of Bacillus subtilis glucose starvation-inducible genes: control of gsiA by the ComP-ComA signal transduction system*, J. Bacteriol., 174 (1992), pp. 4361–4373.

[186] H. Nakata, *Role of acetate in sporogenesis of Bacillus cereus*, J. Bacteriol., 91 (1966), pp. 784–788.

[187] H. Ngugi, S. Dedej, K. Delaplane, A. Savelle, and H. Scherm, *Effect of flower-applied Serenade biofungicide (Bacillus subtilis) on pollination-related variables in rabbiteye blueberry*, Biol. Control, 33 (2005), pp. 32–38.

[188] W. Nicholson, N. Munakata, G. Horneck, H. Melosh, and P. Setlow, *Resistance of Bacillus endospores to extreme terrestrial and extraterrestrial environments*, Microbiol. Mole. Biol. Rev., 64 (2000), pp. 548–572.

[189] D. Noble, *From the Hodgkin-Huxley axon to the virtual heart*, J. Physiol., 580 (2007), pp. 15–22.

[190] J. Norris and J. Wolf, *A study of antigens of the aerobic sporeforming bacteria*, J. Appl. Microbiol., 24 (1961), pp. 42–56.

[191] I. Novella, E. Duarte, S. Elena, A. Moya, E. Domingo, and J. Holland, *Exponential increases of RNA virus fitness during large population transmissions*, Proc. Natl. Acad. Sci., 92 (1995), pp. 5841–5844.

[192] M. Nowak and K. Sigmund, *Evolutionary dynamics of biological games*, Science, 303 (2004), pp. 793–799.

[193] H. Olofsson, J. Ripa, and N. Jonzen, *Bet-hedging as an evolutionary game: the trade-off between egg size and number*, Proc. R. Soc. B., 276 (2009), pp. 2963–2969.

[194] H. Orr, *Fitness and its role in evolutionary genetics*, Nat. Rev. Genet., 10 (2009), pp. 531–539.

[195] Z. Palkova, *Multicellular microorganisms: laboratory versus nature*, EMBO Reports, 5 (2004), pp. 470–476.

[196] H. Park and H. Choi, *Aerodynamic characteristics of flying fish in gliding flight*, J. Exp. Biol., 213 (2010), pp. 3269–3279.

[197] G. A. Parker and J. M. Smith, *Optimality theory in evolutionary biology*, Nature, 348 (1990), pp. 27–33.

[198] G. F. Parker, R. A. Daniel, and J. Errington, *Timing and genetic regulation of commitment to sporulation in Bacillus subtilis*, Microbiology, 142 (1996), pp. 3445–3452.

[199] R. Parker, F. Doyle, and N. Peppas, *The intravenous route to blood glucose control: a review of control algorithms for noninvasive monitoring and regulation in type i diabetic patients*, IEEE Eng. Med. Biol., 20 (2001), pp. 65–73.

[200] J. Patrick and D. Kearns, *Laboratory strains of Bacillus subtilis do not exhibit swarming motility*, J. Bacteriol., 191 (2009), pp. 7129–7133.

[201] D. Paul, *The selection of the "survival of the fittest"*, J. Hist. Biol., 21 (1988), pp. 411–424.

[202] S. Payot, E. Guedon, M. Desvaux, E. Gelhaye, and E. Petitdemange, *Effect of dilution rate, cellobiose and ammonium availabilities on Clostridium cellulolyticum sporulation*, Appl. Microbiol. Biotechnol., 52 (1999), pp. 670–674.

[203] M. Perego, *Multiple protein-aspartate phosphatases provide a mechanism for the integration of diverse signals in the control of development in B. subtilis*, Cell, 79 (1994), pp. 1047–1055.

[204] ——, *A peptide export-import control circuit modulating bacterial development regulates protein phosphotases of the phosphorelay*, Proc. Natl. Acad. Sci., 94 (1997), pp. 8612–8617.

[205] M. Perego, S. Cole, D. Burbulys, K. Trach, and J. Hoch, *Characterization of the gene for a protein kinase which phosphorylated the sporulation-regulatory proteins spo0a and spo0f of Bacillus subtilis*, J. Bacteriol., 171 (1989), pp. 6187–6196.

[206] M. Perego and J. Hoch, *Cell-cell communication regulates the effects of protein aspartate phosphatases on the phosphorelay controlling development in B. subtilis*, Proc. Natl. Acad. Sci., 93 (1996), pp. 1549–1553.

[207] A. Perez-Escudero, M. Rivera-Alba, and G. de Polavieja, *Structure of deviations from optimality in biological systems*, Proc. Natl. Acad. Sci., 106 (2009), pp. 20544–20549.

[208] T. Perkins and P. Swain, *Strategies for cellular decision-making*, Mol. Syst. Biol., 5 (2009), p. 326.

[209] E. Petitdemange, F. Caillet, J. Giallo, and C. Gaudin, *Clostridium cellulolyticum sp. nov., a cellulolytic, mesophilic species from decayed grass*, Int. J. Syst. Bacteriol., 34 (1984), pp. 155–159.

[210] T. Philippi and J. Seger, *Hedging one's evolutionary bets, revisited*, Trends Ecol. & Evol., 4 (1989), pp. 41–44.

[211] P. Piggot and D. Hilbert, *Sporulation of Bacillus subtilis*, Curr. Opin. Microbiol., 7 (2004), pp. 579–586.

[212] A. Plutynski, *What was Fisher's fundamental theorem of natural selection and what was it for?*, Stud. Hist. Phil. Biol. & Biomed. Sci., 37 (2006), pp. 59–82.

[213] C. F. Pope, T. D. McHugh, and S. H. Gillespie, *Methods to determine fitness in bacteria*, Methods Mol. Biol., 642 (2010), pp. 113–121.

[214] M. Pottathil and B. Lazazzera, *The extracellular phr peptide-rap phosphatase signaling circuit of B. subtilis*, Front Biosci., 8 (2003), pp. D32–D45.

[215] G. Price, *Selection and covariance*, Nature, 227 (1970), pp. 520–521.

[216] G. Price, *Fisher's 'fundamental theorem' made clear*, Ann. Hum. Genet., 36 (1972), pp. 129–140.

[217] F. Priest, *Isolation and identification of aerobic endospore-forming bacteria*, in *Bacillus*, C. Harwood, ed., Plenum Press, New York, NY, 1989, pp. 27–56.

[218] G. Pyke, *Optimal foraging theory: a critical review*, Ann. Rev. Ecol. Syst., 15 (1984), pp. 523–575.

[219] W. Ratcliff and F. Denison, *Individual-level bet hedging in the bacterium Sinorhizobium meliloti*, Curr. Biol., 20 (2010), pp. 1740–1744.

[220] L. Real and T. Caraco, *Risk and foraging in stochastic environments*, Annu. Rev. Ecol. Syst., 17 (1986), pp. 371–390.

[221] D. Reinkensmeyer, P. Lum, and S. Lehman, *Human control of a simple two-hand grasp*, Biol. Cybern., 67 (1992), pp. 553–564.

[222] W. Reznikoff, *The lactose operon-controlling elements: a complex paradigm*, Mole. Microbiol., 6 (1992), pp. 2419–2422.

[223] D. Rosen and D. Renouf, *Seasonal changes in blubber distribution in Atlantic harbor seals: indications of thermodynamic considerations*, Mar. Mammal Sci., 13 (1997), pp. 229–240.

[224] D. Roszak and R. Colwell, *Survival strategies of bacteria in the natural environment*, Microbiol. Rev., 51 (1987), pp. 365–379.

[225] S. Rowland, W. Burkholder, K. Cunningham, M. Maciejewski, A. Grossman, and G. King, *Structure and mechanism of action of Sda, an inhibitor of the histidine kinases that regulate initiation of sporulation in Bacillus subtilis*, Mol. Cell, 13 (2004), pp. 689–701.

[226] S. Sahoo, R. Verma, A. Suresh, K. Rao, J. Bellare, and G. Suraishkumar, *Macro-level and genetic-level repsonses of Bacillus subtilis to shear stress*, Biotechnol., 19 (2003), pp. 1689–1696.

[227] M. Salathe, J. Van Cleve, and M. Feldman, *Evolution of stochastic switching rates in asymmetric fitness landscapes*, Genetics, 182 (2009), pp. 1159–1164.

[228] P. Samuelson, *The "fallacy" of maximizing the geometric mean in long sequences of investing or gambling*, Proc. Natl. Acad. Sci., 68 (1971), pp. 2493–2496.

[229] L. Scardovi, M. Arcak, and E. Sontag, *Synchronization of interconnected systems with applications to biochemical networks: an input-output approach*, IEEE T. Automat. Contr., 55 (2010), pp. 1367–1379.

[230] P. Schaeffer, J. Millet, and J.-P. Aubert, *Catabolic repression of bacterial sporulation*, Microbiology, 54 (1965), pp. 704–711.

[231] P. Schormaker, *The expected utility model: Its variants, purposes, evidence and limitations*, J. Econ. Lit., 20 (1982), pp. 529–563.

[232] M. Sefrioui and J. Perlaux, *Nash genetic algorithms: examples and applications*, in Proc. 2000 Cong. Evol. Comp., 2000, pp. 509–516.

[233] J. Seger and J. Brockmann, *What is bet-hedging?*, in Oxford Surveys in Evolutionary Biology, Volume 4, P. Harvey and L. Partridge, eds., Oxford University Press, Cary, NC, 1987, pp. 192–211.

[234] J. Selinummi, J. Seppala, O. Yli-Harja, and J. Puhakka, *Software for quantification of labeled bacteria from digital microscope images by automated image analysis*, BioTechniques, 39 (2005), pp. 859–863.

[235] P. Setlow, *Spore germination*, Curr. Opinion Microbiol., 6 (2003), pp. 550–556.

[236] ——, *Spores of Bacillus subtilis: their resistance to and killing by radiation, heat and chemicals*, J. Appl. Microbiol., 101 (2006), pp. 514–525.

[237] ——, *Dormant spores receive an unexpected wake-up call*, Cell, 135 (2008), pp. 410–412.

[238] I. Shah, M.-H. Laaberki, D. Popham, and J. Dworkin, *A eukaryotic-like Ser/Thr kinase signals bacteria to exit dormancy in response to peptidoglycan fragments*, Cell, 135 (2008), pp. 486–496.

[239] T. Shiba, K. Tsutsumi, K. Ishige, and T. Noguchi, *Inorganic polyphosphate and polyphosphate kinase: their novel biological functions and applications*, Biochem., 65 (2000), pp. 375–384.

[240] A. Siala, I. Hill, and T. Gray, *Populations of spore-forming bacteria in an acid forest soil, with special reference to Bacillus subtilis*, J. Gen. Microbiol., 81 (1974), pp. 183–190.

[241] H. Simon, *Altruism and economics*, Am. Econ. Rev., 83 (1993), pp. 156–161.

[242] A. Simons, *Fluctuating natural selection accounts for the evolution of diversification bet hedging*, Proc. R. Soc. B., 276 (2009), pp. 1987–1992.

[243] A. Simons and M. Johnston, *Suboptimal timing of reproduction in Lobelia inflata may be a conservative bet-hedging strategy*, J. Evol. Biol., 16 (2003), pp. 233–243.

[244] E. Sober, *The two faces of fitness*, in Thinking about Evolution: Historical, Philosophical, and Political Perspectives, R. Singh, D. Paul, C. Krimbas, and J. Beatty, eds., Cambridge University Press, 2001, pp. 309–321.

[245] A. Sonenshein, *Control of sporulation initiation in Bacillus subtilis*, Curr. Opin. Microbiol., 3 (2000), pp. 561–566.

[246] N. Stanley and B. Lazazzera, *Environmental signals and regulatory pathways that influence biofilm formation*, Mole. Microbiol., 52 (2004), pp. 917–924.

[247] J. M. Sterlini and J. Mandelstam, *Commitment to sporulation in Bacillus subtilis and its relationship to development of actinomycin resistance*, Biochem. J., 113 (1969), pp. 29–37.

[248] N. Tam, N. Uyen, H. Hong, L. Duc, T. Hoa, C. Serra, A. Henriques, and S. Cutting.

[249] J. Thoday, *Natural selection and biological progress*, in A Century of Darwin, S. Barnett, ed., Heinemann, 1958, pp. 313–333.

[250] A. Tverksy and D. Kahneman, *Rational choice and the framing of decisions*, J. Business, 59 (1986), pp. 5251–78.

[251] ——, *Loss aversion in riskless choice: A reference-dependent model*, Quarterly J. Econ., 106 (1991), pp. 1039–61.

[252] J. Tyson, *Biochemical oscillations*, in Computational Cell Biology, C. Fall, E. Marland, J. Wagner, and J. Tyson, eds., Springer-Verlag, New York, NY, 2002, pp. 230–260.

[253] B. Van Praag, *The individual welfare function of income in Belgium: an empirical investigation*, Euro. Econ. Rev., 20 (1971), pp. 337–369.

[254] J. Veening, L. Hamoen, and O. Kuipers, *Phosphotases modulate the bistable sporulation gene expression pattern in Bacillus subtilis*, Molec. Microbiol., 56 (2005), pp. 1481–1494.

[255] J. Veening, W. Smits, L. Hamoen, and O. Kuipers, *Single cell analysis of gene expression patterns of competence development and initiation of sporulation in Bacillus subtilis grown on chemically defined media*, J. Appl. Microbiol., 101 (2006), pp. 531–541.

[256] J.-W. Veening, H. Murray, and J. Errington, *A mechanism for cell cycle regulation of sporulation initiation in Bacillus subtilis*, Genes & Develop., 23 (2009), pp. 1959–1970.

[257] J.-W. Veening, E. Stewart, T. Berngruber, F. Taddei, O. Kuipers, and L. Hamoen, *Bet-hedging and epigenetic inheritance in bacterial cell development*, Proc. Natl. Acad. Sci., 105 (2008), pp. 4393–4398.

[258] K. Venkateswaran, M. Satomi, S. Chung, R. Kern, R. Koukol, C. Basic, and D. White, *Molecular microbial diversity of a spacecraft assembly facility*, System. Appl. Microbiol., 24 (2001), pp. 311–320.

[259] G. Vermeij, *The evolutionary interaction among species: selection, escalation, and coevolution*, Annu. Rev. Ecol. Syst., 25 (1994), pp. 219–236.

[260] C. Viney, *Silk fibres: Origins, nature and consequences of structure*, in Structural Biological Materials: Design and Structure: Property Relationships, M. Elices, ed., Elsevier Science & Technology, New York, NY, 2000, pp. 295–333.

[261] V. Volterra, *Variations and fluctuations of the number of individuals in animal species living together*, J. Cons. Int. Explor. Mer., 3 (1928), pp. 3–51.

[262] J. von Neumann and O. Morgenstern, *Theory of Games and Economic Behavior*, Princeton University Press, Princeton, NJ, 1944.

[263] J. Wang and L. Bakken, *Screening of soil bacteria for poly-β-hydroxybutyric acid production and its role in the survival of starvation*, Microb. Ecol., 35 (1998), pp. 94–101.

[264] J. D. Wang and P. A. Levin, *Metabolism, cell growth and the bacterial cell cycle*, Nat. Rev. Microbiol., 7 (2009), pp. 822–827.

[265] P. Ward, J. Botha, R. Buick, M. De Kock, D. Erwin, G. Garrison, J. Kirschvink, and R. Smith, *Abrupt and gradual extinction among late Permian land vertibrates in the Karoo Basin, South Africa*, Sci., 307 (2005), pp. 709–714.

[266] J. Weibull, *Evolutionary Game Theory*, MIT Press, Cambridge, MA, 1995.

[267] W. Whitman, D. Coleman, and W. Wiebe, *Prokaryotes: the unseen majority*, Proc. Natl. Acad. Sci., 95 (1998), pp. 6578–6583.

[268] L. Wick, H. Weilenmann, and T. Egli, *The apparent clock-like evolution of Escherichia coli in glucose-limited chemostats is reproducible at large but not at small population sized and can be explained with Monod kinetics*, Microbiol., 148 (2002), pp. 2889–2902.

[269] E. Widmaier, H. Raff, and K. Strang, *Vander's Human Physiology: The Mechanisms of Body Function*, McGraw-Hill, New York, NY, tenth ed., 2006.

[270] B. Winterhalder, F. Lu, and B. Tucker, *Risk-sensitive adaptive tactics: Models and evidence from subsistence studies in biology and anthropology*, J. Archaeol. Research, 7 (1999), pp. 301–348.

[271] D. Wolf, V. Vazirani, and A. P. Arkin, *Diversity in times of adversity: probabilistic strategies in microbial survival games*, J. Theor. Biol., 234 (2005), pp. 227–253.

[272] D. Woods and D. Jones, *Physiological responses of Bacteroides and Clostridium strains to environmental stress factors*, in Advances in Microbial Physiology, Volume 28, A. Rose and D. Tempest, eds., Academic Press Inc. (London) Ltd., London, 1987, pp. 1–64.

[273] S. Wright, *The roles of mutation, inbreeding, crossbreeding and selection in evolution*, Proc. Sixth Internat. Cong. Genet., 1 (1932), pp. 356–366.

[274] L. Yang, L. Jelsbak, R. Lykke Marvig, S. Damkiaer, C. Workman, M. Holm Rau, S. Kirkelund Hansen, A. Folkesson, H. Krogh Johansen, O. Ciofu, N. Hoiby, M. Sommer, and S. Molin, *Evolutionary dynamics of bacteria in a human host environment*, Proc. Natl. Acad. Sci., 108 (2011), pp. 7481–7486.

[275] M. Yeo and K. Chater, *The interplay of glycogen metabolism and differentiation provides an insight into the developmental biology of Streptomyces coelicolor*, Microbiol., 151 (2005), pp. 855–861.

[276] T.-M. Yi, Y. Huang, M. Simon, and J. Doyle, *Robust perfect adaptation in bacterial chemotaxis through integral feedback control*, Proc. Natl. Acad. Sci., 97 (2000), pp. 4649–4653.

[277] X. Yi and P. Setlow, *Studies of the commitment step in the germination of spores of Bacillus species*, J. Bacteriol., 192 (2010), pp. 3424–3433.

[278] H. Yoshikawa, A. O'Sullivan, and N. Sueoka, *Sequential replication of the Bacillus subtilis chromosome. III. Regulation of initiation*, Proc. Natl. Acad. Sci., 52 (1964), pp. 973–980.

[279] J. W. Zyskind and D. W. Smith, *DNA replication, the bacterial cell cycle, and cell growth*, Cell, 69 (1992), pp. 5–8.

Appendix A

Numerical values for $\alpha_i(t)$ parameterizations

The data used in the following calculations comes from the following experiments, which were *B. subtilis* strain 168 resuspension experiments in SM.

1. 090731_49_82_86, Point 04 (JT082). This is denoted Experiment 1 in the sequel.
2. 090810_49_82_86, Point 02 (JT082). This is denoted Experiment 2 in the sequel.

A.1 Estimating α_4

Under conditions of "high" food, the death rate $\alpha_1 \approx 0$ and the sporulation rate $\alpha_2 \approx 0$. Assuming that no spores are in the colony, the number of vegetative cells can then be written as

$$X(t) = e^{\alpha_4 t} X(0),$$

and the doubling time of the vegetative cells can be used to find the maximum growth rate. In Experiments 1 and 2, the colonies exhibit exponential growth for a short time before sporulation, with a doubling time of ≈ 1 hour. This gives the value of $\alpha_4 = \ln 2$. I arbitrarily assigned $\frac{f}{X} = 10$ at this value of α_4.

The doubling times in Experiments 1 and 2 do not reflect the minimum doubling times for *B. subtilis*. Others have reported doubling times as small as 20 minutes [200]. I will saturate the growth rate for this smaller doubling time to complete the α_4 parameterization.

A.2 Estimating α_1

As $\frac{f}{X} \to 0$, we expect that $\alpha_4 \to 0$ and $\alpha_3 \to 0$. The death rate can be estimated by assuming no sporulation (so the cells actually die) and looking at the number of vegetative cells at "low" food:

$$X(t) = e^{-\alpha_1 t} X(0).$$

After about $\frac{3}{\alpha_1}$ hours, the colony will be extinct. Since colony extinction data is impossible to find for *B. subtilis*, I assume that a cell can survive one cell cycle under conditions of extreme nutrient deprivation before perishing. Note that cell cycle time is variable and depends on nutrient level [264, 27, 279, 278]; the more nutrients, the shorter the cell cycle, and vice versa. Experiments 1 and 2 suggest that the cell cycle length is ≈ 10 hours when nutrients are scarce. The maximum death rate is therefore $\frac{3}{10}$.

The value of $\frac{f}{X}$ at which no death occurs can be estimated from Experiments 1 and 2. In both of these experiments, the minimum cell cycle time (which I assume corresponds to the maximum $\frac{f}{X}$ in the experiment) corresponds to a value of $\frac{f}{X}$ that is $\approx 10\times$ larger than the value of $\frac{f}{X}$ at which vegetative cell death begins to be observed. Therefore, I will assume $\alpha_1 = 0$ for $\frac{f}{X} \geq 1$.

A.3 Estimating α_2

When nutrients are limited, the dynamics for spore formation are

$$\dot{S} = \alpha_2 X.$$

The spore number data from Experiments 1 and 2 were collected assuming a spore is formed when the prespore appears, which may potentially occur several hours after the actual commitment to sporulation (when, for example, SpoIIA$\sim$P crosses some threshold). However, when the cell cycle times are relatively short, this delay does not introduce much error in the data. The earliest sporulation times must therefore be used from the data in Experiments 1 and 2, since the cell cycle times are shortest (relatively) during this first wave of sporulation.

For Experiment 1, for $10.5 \leq t \leq 12.5$,

$$\begin{aligned} \dot{S}_{\text{avg}} &\approx 40 \\ X_{\text{avg}} &\approx 160 \\ \Rightarrow \alpha_2 &= 0.25. \end{aligned}$$

For Experiment 2, for $7.5 \leq t \leq 9.5$,

$$\begin{aligned} \dot{S}_{\text{avg}} &\approx 25 \\ X_{\text{avg}} &\approx 100 \\ \Rightarrow \alpha_2 &= 0.25. \end{aligned}$$

Both of these time periods correspond to ≈ 0.5 of the population committing to sporulation at some point during their cell cycles, which means that this estimate for α_2 corresponds to one-half of the maximum sporulation rate.

A.4 Estimating α_3

I do not know much about spore germination dynamics except that the process occurs relatively quickly (Adam Arkin says it occurs on the order of minutes). I will set the maximum

spore germination rate equal to the maximum birth rate by making the assumption that the germination process takes one cell cycle to complete.

Appendix B

Competing populations stability

B.1 Proof of Theorem 6.4.1

Without loss of generality, assume $c_1 < c_2$.

Theorem. *If X_1, X_2, S_1, S_2, and f are non-negative, the birth, death, sporulation, and germination rates are positive over a nonempty set of values of $\frac{f}{X_1+X_2}$ and finite, and $\gamma \ll 1$, then Equilibrium 1 is locally stable and Equilibrium 2 is locally unstable.*

Proof. The proof will examine the stability of the linearized systems governing the dynamics of small deviations from Equilibria 1 and 2.

The positive rate assumption implies that $u_{1,i} > 0$, $u_{4,i} > 0$, $u_j > 0$, $i = 1, 2$ and $j = 2, 3$.

Assume $c_i \leq \min\{\theta_1, \theta_2, \beta_1, \beta_2\}$, $i = 1, 2$. The linearized dynamics around an equilibrium point $\left(\overline{X}_1, \overline{X}_2, \overline{S}_2, \overline{S}_2, \overline{f}\right)$ are

$$\frac{d}{dt}\begin{bmatrix} \delta X_1 \\ \delta X_2 \\ \delta S_1 \\ \delta S_2 \\ \delta f \end{bmatrix} = \begin{bmatrix} a_{11} & a_{12} & a_{13} & 0 & a_{15} \\ a_{21} & a_{22} & 0 & a_{24} & a_{25} \\ a_{31} & a_{32} & a_{33} & 0 & a_{35} \\ a_{41} & a_{42} & 0 & a_{44} & a_{45} \\ a_{51} & a_{52} & 0 & 0 & 0 \end{bmatrix} \begin{bmatrix} \delta X_1 \\ \delta X_2 \\ \delta S_1 \\ \delta S_2 \\ \delta f \end{bmatrix} + \begin{bmatrix} 0 \\ 0 \\ 0 \\ 0 \\ 1 \end{bmatrix} \delta e$$

where

$$a_{11} = \left(\frac{u_{4,1}}{l_{4,1}} + \frac{u_{1,1}}{l_{1,1}} + \frac{u_2}{\theta_1}\right) c\frac{\overline{X}_2}{\overline{X}_1 + \overline{X}_2} - (u_{1,1} + u_2) - \frac{u_3}{\beta_1} c\frac{\overline{S}_1}{\overline{X}_1 + \overline{X}_2}$$

$$a_{12} = -\left(\frac{u_{4,1}}{l_{4,1}} + \frac{u_{1,1}}{l_{1,1}} + \frac{u_2}{\theta_1}\right) c\frac{\overline{X}_1}{\overline{X}_1 + \overline{X}_2} - \frac{u_3}{\beta_1} c\frac{\overline{S}_1}{\overline{X}_1 + \overline{X}_2}$$

$$a_{13} = \frac{u_3}{\beta_1} c$$

$$a_{15} = \left(\frac{u_{4,1}}{l_{4,1}} + \frac{u_{1,1}}{l_{1,1}} + \frac{u_2}{\theta_1}\right) \frac{\overline{X}_1}{\overline{X}_1 + \overline{X}_2} + \frac{u_3}{\beta_1} c\frac{\overline{S}_1}{\overline{X}_1 + \overline{X}_2}$$

$$a_{21} = -\left(\frac{u_{4,2}}{l_{4,2}} + \frac{u_{1,2}}{l_{1,2}} + \frac{u_2}{\theta_2}\right) c\frac{\overline{X}_2}{\overline{X}_1 + \overline{X}_2} - \frac{u_3}{\beta_2} c\frac{\overline{S}_2}{\overline{X}_1 + \overline{X}_2}$$
$$a_{22} = \left(\frac{u_{4,2}}{l_{4,2}} + \frac{u_{1,2}}{l_{1,2}} + \frac{u_2}{\theta_2}\right) c\frac{\overline{X}_1}{\overline{X}_1 + \overline{X}_2} - (u_{1,2} + u_2) - \frac{u_3}{\beta_2} c\frac{\overline{S}_2}{\overline{X}_1 + \overline{X}_2}$$
$$a_{24} = \frac{u_3}{\beta_2} c$$
$$a_{25} = \left(\frac{u_{4,2}}{l_{4,2}} + \frac{u_{1,2}}{l_{1,2}} + \frac{u_2}{\theta_2}\right) \frac{\overline{X}_2}{\overline{X}_1 + \overline{X}_2} + \frac{u_3}{\beta_2} c\frac{\overline{S}_2}{\overline{X}_1 + \overline{X}_2}$$

$$a_{31} = u_2 - \frac{u_2}{\theta_1} c\frac{\overline{X}_2}{\overline{X}_1 + \overline{X}_2} + \frac{u_3}{\beta_1} c\frac{\overline{S}_1}{\overline{X}_1 + \overline{S}_2}$$
$$a_{32} = \frac{u_2}{\theta_1} c\frac{\overline{X}_1}{\overline{X}_1 + \overline{X}_2} + \frac{u_3}{\beta_1} c\frac{\overline{S}_1}{\overline{X}_1 + \overline{X}_2}$$
$$a_{33} = -\frac{u_3}{\beta_1} c$$
$$a_{35} = -\frac{u_2}{\theta_1}\frac{\overline{X}_1}{\overline{X}_1 + \overline{X}_2} - \frac{u_3}{\beta_1}\frac{\overline{S}_1}{\overline{X}_1 + \overline{X}_2}$$

$$a_{41} = \frac{u_2}{\theta_2} c\frac{\overline{X}_2}{\overline{X}_1 + \overline{X}_2} + \frac{u_3}{\beta_2} c\frac{\overline{S}_1}{\overline{X}_1 + \overline{X}_2}$$
$$a_{42} = u_2 - \frac{u_2}{\theta_2} c\frac{\overline{X}_1}{\overline{X}_1 + \overline{X}_2} + \frac{u_3}{\beta_2} c\frac{\overline{S}_2}{\overline{X}_1 + \overline{S}_2}$$
$$a_{44} = -\frac{u_3}{\beta_2} c$$
$$a_{45} = -\frac{u_2}{\theta_2}\frac{\overline{X}_2}{\overline{X}_1 + \overline{X}_2} - \frac{u_3}{\beta_2}\frac{\overline{S}_2}{\overline{X}_1 + \overline{X}_2}$$

$$a_{51} = a_{52} = -\gamma$$

and $c = \frac{\overline{f}}{\overline{X}_1 + \overline{X}_2}$.

If the characteristic equation for the linearized A matrix is

$$-\lambda^5 + l_4\lambda^4 + l_3\lambda^3 + l_2\lambda^2 + l_1\lambda + l_0 = 0,$$

then necessary and sufficient conditions for all of A's eigenvalues to have negative real part are:

1. $b_1 = l_3 + \frac{l_2}{l_4} < 0$; and
2. $c_1 = l_2 - l_4\frac{b_2}{b_1} < 0$, where $b_2 = l_1 + \frac{l_0}{l_4}$; and

3. $d_1 = b_2 - b_1 \frac{l_0}{c_1} < 0$; and

4. $l_0 < 0$; and

5. $l_4 < 0$,

which were obtained from the standard Routh array. Since $a_{13} = -a_{33}$, $a_{24} = -a_{44}$, and $a_{51} = a_{52} =: a_5$, the expressions for the coefficients of the characteristic polynomial are

$$\begin{aligned}
l_0 &= a_{33}a_{44}a_5 \{a_{35}[a_{41} - a_{42} + a_{21} - a_{22}] + a_{45}[a_{32} - a_{31} + a_{12} - a_{11}] \\
&\quad + a_{25}[a_{32} - a_{31} + a_{12} - a_{11}] + a_{15}[a_{41} - a_{42} + a_{21} - a_{22}]\} \\
l_1 &= a_{33}a_{44}[a_{32}a_{41} - a_{31}a_{42} + a_{21}a_{32} - a_{31}a_{22} + a_{41}a_{12} - a_{11}a_{42} + a_{12}a_{21} - a_{11}a_{22}] \\
&\quad - a_{33}a_5a_{25}[a_{32} - a_{31} + a_{11} - a_{12}] - a_{33}a_5a_{35}[a_{21} - a_{22}] \\
&\quad - a_{44}a_5a_{15}[a_{41} - a_{42} + a_{21} - a_{22}] + a_{44}a_5a_{25}[a_{11} - a_{12}] \\
&\quad - a_{44}a_5a_{45}[a_{12} - a_{11}] + a_{33}a_{15}a_5[a_{22} - a_{21}] \\
&\quad + a_{33}a_{44}a_5[a_{25} + a_{45} + a_{15} + a_{35}] \\
l_2 &= a_{33}[-a_{21}a_{32} - a_5a_{35} + a_{31}a_{22} + a_{11}a_{22} - a_5a_{15} - a_{21}a_{12} - a_5a_{25}] \\
&\quad + a_{44}[a_{42}a_{11} - a_5a_{45} - a_{12}a_{41} + a_{11}a_{22} - a_5a_{15} - a_{21}a_{12} - a_5a_{25}] \\
&\quad + a_{33}a_{44}[a_{31} + a_{42} + a_{11} + a_{22}] + a_5[a_{12}a_{25} + a_{21}a_{15} - a_{22}a_{15} - a_{25}a_{11}] \\
l_3 &= -a_{33}[a_{31} + a_{22} + a_{11}] - a_{44}[a_{42} + a_{11} + a_{22}] - a_{11}a_{22} - a_{33}a_{44} \\
&\quad + a_5[a_{15} + a_{25}] + a_{21}a_{12} \\
l_4 &= a_{11} + a_{22} + a_{33} + a_{44}
\end{aligned}$$

Note that, by inspection, $l_4 < 0$.

For Equilibrium 1, it will be shown that all of the stability conditions are true. For Equilibrium 2, it will be shown that at least one condition is violated.

1. **Equilibrium 1:** The equilibrium point is

$$\left(\overline{X}_1, \overline{X}_2, \overline{S}_1, \overline{S}_2, \overline{f}\right) = \left(\frac{\overline{e}}{\gamma}, 0, \frac{\alpha_{2,1}(c_1)}{\alpha_{3,1}(c_1)}\overline{X}_1, 0, c_1\overline{X}_1\right)$$

where

$$c_1 = \frac{\overline{f}}{\overline{X}_1} = \frac{u_{1,1}}{\frac{u_{4,1}}{l_{4,1}} + \frac{u_{1,1}}{l_{1,1}}}.$$

Since $c_1 < c_2$,

$$\begin{aligned}
&\alpha_{4,2}(c_1) - \alpha_{1,2}(c_1) < 0 \\
\Leftrightarrow\ &\left(\frac{u_{4,2}}{l_{4,2}} + \frac{u_{1,2}}{l_{1,2}}\right) c_1 < u_{1,2}. \qquad \text{(B.1)}
\end{aligned}$$

The entries of the A matrix are

$$
\begin{aligned}
a_{11} &= -(u_{1,1} + u_2) - \frac{u_3}{\beta_1} c_1 \frac{\overline{S}_1}{\overline{X}_1} \\
a_{12} &= -\left(\frac{u_{4,1}}{l_{4,1}} + \frac{u_{1,1}}{l_{1,1}} + \frac{u_2}{\theta_1} \right) c_1 - \frac{u_3}{\beta_1} c_1 \frac{\overline{S}_1}{\overline{X}_1} \\
a_{13} &= \frac{u_3}{\beta_1} c_1 \\
a_{15} &= \left(\frac{u_{4,1}}{l_{4,1}} + \frac{u_{1,1}}{l_{1,1}} + \frac{u_2}{\theta_1} \right) + \frac{u_3}{\beta_1} \frac{\overline{S}_1}{\overline{X}_1} \\
a_{21} &= 0 \\
a_{22} &= \left(\frac{u_{4,2}}{l_{4,2}} + \frac{u_{1,2}}{l_{1,2}} + \frac{u_2}{\theta_2} \right) c_1 - (u_{1,2} + u_2) \\
a_{24} &= \frac{u_3}{\beta_2} c_1 \\
a_{25} &= 0 \\
a_{31} &= u_2 + \frac{u_3}{\beta_1} c_1 \frac{\overline{S}_1}{\overline{X}_1} \\
a_{32} &= \frac{u_2}{\theta_1} c_1 + \frac{u_3}{\beta_1} c_1 \frac{\overline{S}_1}{\overline{X}_1} \\
a_{33} &= -\frac{u_3}{\beta_1} c_1 \\
a_{35} &= -\frac{u_2}{\theta_1} - \frac{u_3}{\beta_1} \frac{\overline{S}_1}{\overline{X}_1} \\
a_{41} &= 0 \\
a_{42} &= u_2 - \frac{u_2}{\theta_2} c_1 \\
a_{44} &= -\frac{u_3}{\beta_2} c_1 \\
a_{45} &= 0
\end{aligned}
$$

where $u_2 - \frac{u_2}{\theta_i} c_1 \geq 0$, $i = 1, 2$, by the assumption that $c_1 \leq \min\{\theta_1, \theta_2\}$. With these expressions, the conditions for stability can now be checked.

(a) $l_0 < 0$:
Plugging in the A matrix zero elements into the expression for l_0 yields:

$$
\begin{aligned}
l_0 &= a_{33} a_{44} a_5 \left\{ a_{35}[-a_{42} - a_{22}] + a_{15}[-a_{42} - a_{22}] \right\} \\
&= -\underbrace{a_{33}}_{(-)} \underbrace{a_{44}}_{(-)} \underbrace{a_5}_{(-)} \underbrace{(a_{35} + a_{15})}_{(+)} \underbrace{(a_{42} + a_{22})}_{(-)} \\
&< 0
\end{aligned}
$$

since

$$a_{35} + a_{15} = \frac{u_{4,1}}{l_{4,1}} + \frac{u_{1,1}}{l_{1,1}}$$
$$a_{22} + a_{42} = \left(\frac{u_{4,2}}{l_{4,2}} + \frac{u_{1,2}}{l_{1,2}}\right) c_1 - u_{1,2}$$

which are positive and negative, respectively, because of the non-negative rate assumption and Equation B.1.

(b) $b_1 = l_3 + \frac{l_2}{l_4} < 0$:
First, note that $l_4 < 0$ by inspection (since $a_{11} < 0$, $a_{22} < 0$, $a_{33} < 0$, and $a_{44} < 0$). The condition $b_1 < 0$ is therefore equivalent to showing that

$$l_3 l_4 > -l_2.$$

To show this, suppose it is not true, $l_3 l_4 \leq -l_2$. Then, after plugging in the values of the elements of the A matrix and canceling several terms, the following inequality is obtained:

$$\begin{aligned}
&a_{11}a_{33}u_{1,1} - a_{11}^2(a_{22} + a_{44}) - a_{11}a_{33}(a_{22} + a_{44}) + a_{11}a_{15}a_5 - a_{11}a_{22}(a_{22} + a_{44}) \\
&- a_{22}a_{33}(a_{22} + a_{44}) - a_{22}a_{44}(a_{22} + a_{42}) + a_{33}^2 u_{1,1} - a_{11}a_{33}(a_{22} + a_{44}) \\
&- a_{33}^2(a_{22} + a_{44}) + a_5 a_{33}\left(\frac{u_2}{\theta_1} + \frac{u_3}{\beta_1}\frac{\overline{S}_1}{\overline{X}_1}\right) - a_{11}a_{44}(a_{22} + a_{44}) \\
&- a_{33}a_{44}(a_{22} + a_{44}) - a_{44}^2(a_{22} + a_{42}) \leq 0
\end{aligned}$$

but since

$$\begin{aligned}
a_{22} + a_{44} &= \left(\frac{u_{4,2}}{l_{4,2}} + \frac{u_{1,2}}{l_{1,2}} + \frac{u_2}{\theta_2}\right) c_1 - (u_{1,2} + u_2) - \frac{u_3}{\beta_2} c_1 \\
&= \left[\left(\frac{u_{4,2}}{l_{4,2}} + \frac{u_{1,2}}{l_{1,2}}\right) c_1 - u_{1,1}\right] - \left[u_2 - \frac{u_2}{\theta_2} c_1\right] - \frac{u_3}{\beta_2} c_1 \\
&< 0
\end{aligned}$$

due to the non-negative rate assumption and Equation B.1, and since it was previously shown that $a_{22} + a_{42} < 0$, then all of the terms on the left hand side of the inequality are positive. This leads to a contradiction in the inequality, which implies that

$$b_1 < 0.$$

(c) $c_1 = l_2 - l_4 \frac{b_2}{b_1} < 0$:
Plugging in the expressions for b_1 and b_2 leads to the condition that needs to be proved, in terms of the coefficients of the characteristic polynomial:

$$l_2 - l_4 \frac{l_1 + \frac{l_0}{l_4}}{l_3 + \frac{l_2}{l_4}} < 0.$$

Since $b_1 < 0 \Rightarrow l_3 l_4 + l_2 > 0$, this condition is equivalent to

$$\begin{aligned} & l_2(l_3 l_4 + l_2) - l_4(l_1 l_4 + l_0) < 0 \\ \Leftrightarrow\ & l_2^2 - l_1 l_4^2 < -l_2 l_3 l_4 + l_0 l_4. \end{aligned}$$

Invoking the assumption that $\gamma \ll 1$ will simplify the algebra while checking this condition. As $-\gamma = a_5 \to 0^-$ (from the negative direction), the coefficients of the characteristic polynomial are

$$\begin{aligned} & l_0 \to 0^- \\ & l_1 \to u_{1,1} a_{33} a_{44} (a_{22} + a_{42}) \\ & l_2 \to -u_{1,1} a_{33} (a_{22} + a_{44}) + a_{11} a_{44} (a_{22} + a_{42}) + a_{33} a_{44} (a_{22} + a_{42}) \\ & l_3 \to u_{1,1} a_{33} - a_{11} (a_{22} + a_{44}) - a_{33} (a_{22} + a_{44}) - a_{44} (a_{22} + a_{42}) \\ & l_4 = a_{11} + a_{22} + a_{33} + a_{44}. \end{aligned}$$

With this simplification, we can verify that the inequality $l_2^2 - l_1 l_4^2 < -l_2 l_3 l_4 + l_0 l_4$ holds. To do so, suppose it does not hold, $l_2^2 - l_1 l_4^2 \geq -l_2 l_3 l_4 + l_0 l_4$. Then, after several cancellations, the hypothesis yields

$$\begin{aligned} - u_{1,1} a_{33} a_{44} (a_{22} + a_{42}) l_4^2 \geq & -u_{1,1} a_{33} (a_{11} + a_{33}) l_2 + (a_{11} + a_{33})(a_{22} + a_{44}) l_2 l_4 \\ & + a_{44} (a_{22} + a_{44})(a_{22} + a_{42}) l_2 \\ \Leftrightarrow\ - 2 u_{1,1} a_{33} a_{44} (a_{22} + a_{42}) \geq & \ u_{1,1}^2 a_{33}^2 + a_{44}^2 (a_{22} + a_{42})^2 \\ & - u_{1,1} a_{33} (a_{11} + a_{33})(a_{22} + a_{44}) \\ & - u_{1,1} a_{33} (a_{22} + a_{42})(a_{22} + a_{44}) \\ & + (a_{11} + a_{33})^2 (a_{22} + a_{42}) a_{44} \\ & + (a_{11} + a_{33})(a_{22} + a_{44})(a_{22} + a_{42}) a_{44}, \end{aligned}$$

but further cancellations yields the equivalent inequality

$$\begin{aligned} 0 \geq & \ u_{1,1}^2 a_{33}^2 + a_{44}^2 (a_{22} + a_{42})^2 - u_{1,1} a_{33} (a_{11} + a_{33})(a_{22} + a_{44}) \\ & - u_{1,1} a_{33} (a_{22} + a_{42})(a_{22} + a_{44}) + (a_{11}^2 + a_{33}^2)(a_{22} + a_{42}) a_{44} \\ & - \left(u_2 + \frac{u_3}{\beta_1} c_1 \frac{\overline{S}_1}{\overline{X}_1} \right) 2 a_{33} a_{44} (a_{22} + a_{42}) \\ & + (a_{11} + a_{33})(a_{22} + a_{44})(a_{22} + a_{42}) a_{44}. \end{aligned}$$

All of the terms on the right hand side of the inequality are positive, which is a contradiction. Therefore, with the additional assumption that $\gamma \ll 1$, we have shown that

$$c_1 < 0.$$

(d) $d_1 = b_2 - b_1 \frac{l_0}{c_1} < 0$:
Plugging in the expressions for b_1, b_2, and c_1 gives an equation for d_1 in terms of the coefficients of the characteristic polynomial.

$$\begin{aligned} d_1 &= \left(l_1 + \frac{l_0}{l_4}\right) - \left(l_3 + \frac{l_2}{l_4}\right) \frac{l_0}{l_2 - l_4 \frac{l_1 + \frac{l_0}{l_4}}{l_3 + \frac{l_2}{l_4}}} \\ &= \frac{(l_1 l_4 + l_0)[l_2 l_3 l_4 + l_2^2 - l_1 l_4^2 - l_0 l_4] - (l_3 l_4 + l_2)[l_0 l_3 l_4 + l_0 l_2]}{l_4[l_2 l_3 l_4 + l_2^2 - l_1 l_4^2 - l_0 l_4]} \end{aligned}$$

which is extremely difficult to deal with analytically. However, under the assumption that $\gamma \ll 1$, this expression simplifies considerably to

$$d_1 \to l_1$$

as $\gamma \to 0$. Therefore, it suffices to check if $l_1 < 0$ for the remaining stability condition.
Plugging in the elements of the A matrix for Equilibrium 1 into the expression for l_1 gives

$$\begin{aligned} l_1 &= -a_{33}a_{44}a_{31}(a_{22} + a_{42}) - a_{33}a_{44}a_{11}(a_{22} + a_{42}) + a_{33}a_5a_{22}(a_{35} + a_{15}) \\ &\quad + a_{44}a_5a_{15}(a_{22} + a_{42}) + a_{33}a_{44}a_5(a_{15} + a_{35}) \\ &= (a_{22} + a_{42})[-a_{33}a_{44}(a_{31} + a_{11}) + a_{44}a_5a_{15}] + (a_{15} + a_{35})a_{33}a_5(a_{22} + a_{44}) \\ &= \underbrace{(a_{22} + a_{42})}_{(-)}\underbrace{[-a_{33}a_{44}(-u_{1,1})}_{(+)}\underbrace{+a_{44}a_5a_{15}]}_{(+)} + \underbrace{\left(\frac{u_{4,1}}{l_{4,1}} + \frac{u_{1,1}}{l_{1,1}}\right)}_{(+)}\underbrace{a_{33}a_5}_{(+)}\underbrace{(a_{22} + a_{44})}_{(-)} \\ &< 0, \end{aligned}$$

Thus, if $\gamma \ll 1$, then this condition is equivalent to

$$d_1 < 0.$$

Since all of the Routh conditions are satisfied, the linearized system's A matrix has eigenvalues in the left half plane. Therefore, Equilibrium 1 is locally stable.

2. **Equilibrium 2:** The equilibrium point is

$$\left(\overline{X}_1, \overline{X}_2, \overline{S}_1, \overline{S}_2, \overline{f}\right) = \left(0, \frac{\overline{e}}{\gamma}, 0, \frac{\alpha_{2,2}(c_2)}{\alpha_{3,2}(c_2)}\overline{X}_2, c_2\overline{X}_2\right)$$

where

$$c_2 = \frac{\overline{f}}{\overline{X}_2} = \frac{u_{1,2}}{\frac{u_{4,2}}{l_{4,2}} + \frac{u_{1,2}}{l_{1,2}}}.$$

Since $c_1 < c_2$,

$$\begin{aligned} & \alpha_{4,1}(c_2) - \alpha_{1,1}(c_2) > 0 \\ \Leftrightarrow & \left(\frac{u_{4,1}}{l_{4,1}} + \frac{u_{1,1}}{l_{1,1}}\right) c_2 > u_{1,1}. \end{aligned} \tag{B.2}$$

The entries of the A matrix are

$$\begin{aligned} a_{11} &= \left(\frac{u_{4,1}}{l_{4,1}} + \frac{u_{1,1}}{l_{1,1}} + \frac{u_2}{\theta_1}\right) c_2 - (u_{1,1} + u_2) \\ a_{12} &= 0 \\ a_{13} &= \frac{u_3}{\beta_1} c_2 \\ a_{15} &= 0 \end{aligned}$$

$$\begin{aligned} a_{21} &= -\left(\frac{u_{4,2}}{l_{4,2}} + \frac{u_{1,2}}{l_{1,2}} + \frac{u_2}{\theta_2}\right) c_2 - \frac{u_3}{\beta_2} c_2 \frac{\overline{S}_2}{\overline{X}_2} \\ a_{22} &= -(u_{1,2} + u_2) - \frac{u_3}{\beta_2} c_2 \frac{\overline{S}_2}{\overline{X}_2} \\ a_{24} &= \frac{u_3}{\beta_2} c_2 \\ a_{25} &= \left(\frac{u_{4,2}}{l_{4,2}} + \frac{u_{1,2}}{l_{1,2}} + \frac{u_2}{\theta_2}\right) + \frac{u_3}{\beta_2} \frac{\overline{S}_2}{\overline{X}_2} \end{aligned}$$

$$\begin{aligned} a_{31} &= u_2 - \frac{u_2}{\theta_1} c_2 \\ a_{32} &= 0 \\ a_{33} &= -\frac{u_3}{\beta_1} c_2 \\ a_{35} &= 0 \end{aligned}$$

$$\begin{aligned} a_{41} &= \frac{u_2}{\theta_2} c_2 + \frac{u_3}{\beta_2} c_2 \frac{\overline{S}_2}{\overline{X}_2} \\ a_{42} &= u_2 + \frac{u_3}{\beta_2} c_2 \frac{\overline{S}_2}{\overline{X}_2} \\ a_{44} &= -\frac{u_3}{\beta_2} c_2 \\ a_{45} &= -\frac{u_2}{\theta_2} - \frac{u_3}{\beta_2} \frac{\overline{S}_2}{\overline{X}_2} \end{aligned}$$

where $u_2 - \frac{u_2}{\theta_i} c_2 \geq 0$, $i = 1, 2$, by the assumption that $c_2 \leq \min\{\theta_1, \theta_2\}$. With these expressions, it will be shown that at least one condition for stability is violated; specifically, it will be shown that $l_0 > 0$.

Plugging in the elements of the A matrix into the expression for l_0 yields

$$\begin{aligned} l_0 &= a_{33}a_{44}a_5 \left\{-a_{45}a_{31} - a_{25}a_{31} - a_{45}a_{11} - a_{25}a_{11}\right\} \\ &= -a_{33}a_{44}a_5(a_{25} + a_{45})(a_{11} + a_{31}), \end{aligned}$$

where

$$\begin{aligned} a_{25} + a_{45} &= \left(\frac{u_{4,2}}{l_{4,2}} + \frac{u_{1,2}}{l_{1,2}} + \frac{u_2}{\theta_2}\right) + \frac{u_3}{\beta_2}\frac{\overline{S}_2}{\overline{X}_2} - \frac{u_2}{\theta_2} - \frac{u_3}{\beta_2}\frac{\overline{S}_2}{\overline{X}_2} \\ &= \left(\frac{u_{4,2}}{l_{4,2}} + \frac{u_{1,2}}{l_{1,2}}\right) \\ &> 0 \\ a_{11} + a_{31} &= \left(\frac{u_{4,1}}{l_{4,1}} + \frac{u_{1,1}}{l_{1,1}} + \frac{u_2}{\theta_1}\right) c_2 - (u_{1,1} + u_2) + u_2 - \frac{u_2}{\theta_1} c_2 \\ &= \left(\frac{u_{4,1}}{l_{4,1}} + \frac{u_{1,1}}{l_{1,1}}\right) c_2 - u_{1,1} \\ &> 0 \end{aligned}$$

where the last inequality comes from Equation B.2. Therefore,

$$\begin{aligned} l_0 &= \underbrace{-a_{33}a_{44}a_5}_{(+)}\underbrace{(a_{25} + a_{45})}_{(+)}\underbrace{(a_{11} + a_{31})}_{(+)} \\ &> 0, \end{aligned}$$

which implies that the linearized A matrix has at least one eigenvalue in the right half plane (at least one sign change in the first column of the Routh array). Thus, Equilibrium 2 is locally unstable.

It can be showed that the stability claims are valid even if the sporulation and/or germination rates are saturated ($c_i > \min\{\theta_1, \theta_2, \beta_1, \beta_2\}$). Note that the signs of the elements of A are invariant under different values of sporulation and germination parameters by inspection, so I will omit showing these claims in the sequel.

1. **Equilibrium 1:**

   (a) $l_0 < 0$:

This condition relied on the fact that $a_{15} + a_{35} > 0$ and $a_{22} + a_{42} < 0$. Note that

$$\begin{aligned}
a_{15} &= \left(\frac{u_{4,1}}{l_{4,1}} + \frac{u_{1,1}}{l_{1,1}}\right) + \mathbb{I}\{c_1 < \theta_1\}\frac{u_2}{\theta_1} + \mathbb{I}\{c_1 < \beta_1\}\frac{u_3}{\beta_1}\frac{\overline{S}_1}{\overline{X}_1} \\
a_{35} &= -\mathbb{I}\{c_1 < \theta_1\}\frac{u_2}{\theta_1} - \mathbb{I}\{c_1 < \beta_1\}\frac{u_3}{\beta_1}\frac{\overline{S}_1}{\overline{X}_1} \\
a_{22} &= \left(\frac{u_{4,2}}{l_{4,2}} + \frac{u_{1,2}}{l_{1,2}}\right)c_1 - u_{1,2} - \mathbb{I}\{c_1 < \theta_2\}\left(u_2 - \frac{u_2}{\theta_2}c_1\right) \\
a_{42} &= \mathbb{I}\{c_1 < \theta_2\}\left(u_2 - \frac{u_2}{\theta_2}c_1\right)
\end{aligned}$$

where $\mathbb{I}\{\cdot\}$ is the indicator function. Thus, it is still true that

$$a_{15} + a_{35} = \left(\frac{u_{4,1}}{l_{4,1}} + \frac{u_{1,1}}{l_{1,1}}\right) > 0 a_{22} + a_{42} \quad = \left(\frac{u_{4,2}}{l_{4,2}} + \frac{u_{1,2}}{l_{1,2}}\right)c_1 - u_{1,2} < 0,$$

where the second inequality comes from Equation B.1.

(b) $b_1 = l_3 + \frac{l_2}{l_4} < 0$:
This condition was verified from $a_{11} + a_{31} = -u_{1,1}$, $a_{22} + a_{44} < 0$, and $a_{15} - \left(\frac{u_{4,1}}{l_{4,1}} + \frac{u_{1,1}}{l_{1,1}}\right) \geq 0$. Note that

$$\begin{aligned}
a_{11} &= -u_{1,1} - \mathbb{I}\{c_1 < \theta_1\}u_2 - \mathbb{I}\{c_1 < \beta_1\}\frac{u_3}{\beta_1}c_1\frac{\overline{S}_1}{\overline{X}_1} \\
a_{31} &= \mathbb{I}\{c_1 < \theta_1\}u_2 + \mathbb{I}\{c_1 < \beta_1\}\frac{u_3}{\beta_1}c_1\frac{\overline{S}_1}{\overline{X}_1} \\
a_{44} &= -\mathbb{I}\{c_1 < \beta_2\}\left[\frac{u_3}{\beta_2}c_1 - u_3\right] - u_3
\end{aligned}$$

The desired equalities and inequalities still hold:

$$\begin{aligned}
a_{11} + a_{31} &= -u_{1,1} - \mathbb{I}\{c_1 < \theta_1\}u_2 - \mathbb{I}\{c_1 < \beta_1\}\frac{u_3}{\beta_1}c_1\frac{\overline{S}_1}{\overline{X}_1} + \mathbb{I}\{c_1 < \theta_1\}u_2 \\
&\quad + \mathbb{I}\{c_1 < \beta_1\}\frac{u_3}{\beta_1}c_1\frac{\overline{S}_1}{\overline{X}_1} \\
&= -u_{1,1} \\
a_{22} + a_{44} &= \left(\frac{u_{4,2}}{l_{4,2}} + \frac{u_{1,2}}{l_{1,2}}\right)c_1 - u_{1,2} - \mathbb{I}\{c_1 < \theta_2\}\left(u_2 - \frac{u_2}{\theta_2}c_1\right) \\
&\quad - \mathbb{I}\{c_1 < \beta_2\}\left[\frac{u_3}{\beta_2}c_1 - u_3\right] - u_3 \\
&< 0
\end{aligned}$$

and

$$a_{15} - \left(\frac{u_{4,1}}{l_{4,1}} + \frac{u_{1,1}}{l_{1,1}}\right) = \mathbb{I}\{c_1 < \theta_1\}\frac{u_2}{\theta_1} + \mathbb{I}\{c_1 < \beta_1\}\frac{u_3}{\beta_1}\frac{\overline{S}_1}{\overline{X}_1}$$
$$\geq 0.$$

(c) $c_1 = l_2 - l_4\frac{b_2}{b_1} < 0$:
In addition to the previous inequalities, the only additional condition needed is

$$a_{11} \leq -u_{1,1}$$

which is readily obtained by inspection.

(d) $d_1 = b_2 - b_1\frac{l_0}{c_1} < 0$:
The previous inequalities are enough to verify that this condition still holds.

Thus, Equilibrium 1 is still locally stable even when the sporulation and/or germination rates have saturated.

2. **Equilibrium 2:** In order to show that $l_0 > 0$ even when the sporulation and/or germination rates have saturated, we simply need to prove that $a_{25} + a_{45} > 0$ and $a_{11} + a_{31} > 0$. Note that

$$a_{25} = \left(\frac{u_{4,2}}{l_{4,2}} + \frac{u_{1,2}}{l_{1,2}}\right) + \mathbb{I}\{c_2 < \theta_2\}\frac{u_2}{\theta_2} + \mathbb{I}\{c_2 < \beta_2\}\frac{u_3}{\beta_2}\frac{\overline{S}_2}{\overline{X}_2}$$
$$a_{45} = -\mathbb{I}\{c_2 < \theta_2\}\frac{u_2}{\theta_2} - \mathbb{I}\{c_2 < \beta_2\}\frac{u_3}{\beta_2}\frac{\overline{S}_2}{\overline{X}_2}$$
$$a_{11} = \left(\frac{u_{4,1}}{l_{4,1}} + \frac{u_{1,1}}{l_{1,1}}\right)c_2 - u_{1,1} - \mathbb{I}\{c_2 < \theta_1\}\left[u_2 - \frac{u_2}{\theta_1}c_2\right]$$
$$a_{31} = \mathbb{I}\{c_2 < \theta_1\}\left[u_2 - \frac{u_2}{\theta_1}c_2\right]$$

It is still true that

$$\begin{aligned}
a_{25} + a_{45} &= \left(\frac{u_{4,2}}{l_{4,2}} + \frac{u_{1,2}}{l_{1,2}}\right) + \mathbb{I}\{c_2 < \theta_2\}\frac{u_2}{\theta_2} + \mathbb{I}\{c_2 < \beta_2\}\frac{u_3}{\beta_2}\frac{\overline{S}_2}{\overline{X}_2} \\
&\quad - \mathbb{I}\{c_2 < \theta_2\}\frac{u_2}{\theta_2} - \mathbb{I}\{c_2 < \beta_2\}\frac{u_3}{\beta_2}\frac{\overline{S}_2}{\overline{X}_2} \\
&= \left(\frac{u_{4,2}}{l_{4,2}} + \frac{u_{1,2}}{l_{1,2}}\right) \\
&> 0 \\
a_{11} + a_{31} &= \left(\frac{u_{4,1}}{l_{4,1}} + \frac{u_{1,1}}{l_{1,1}}\right)c_2 - u_{1,1} - \mathbb{I}\{c_2 < \theta_1\}\left[u_2 - \frac{u_2}{\theta_1}c_2\right] \\
&\quad + \mathbb{I}\{c_2 < \theta_1\}\left[u_2 - \frac{u_2}{\theta_1}c_2\right] \\
&= \left(\frac{u_{4,1}}{l_{4,1}} + \frac{u_{1,1}}{l_{1,1}}\right)c_2 - u_{1,1} \\
&> 0
\end{aligned}$$

from Equation B.2. Therefore, Equilibrium 2 remains locally unstable.

□

B.2 Stability of $(0, 0, 0, 0, f(t))$ for different birth/death rates

Theorem B.2.1. *If the birth, death, sporulation, and germination rates are positive over a nonempty set of values of* $\frac{f}{X_1+X_2}$ *and finite, then the point* $(0, 0, 0, 0, f(t))$ *is locally unstable.*

Proof. Suppose that the point $(0, 0, 0, 0, f(t))$ is perturbed to $(\delta X_1, \delta X_2, \delta S_1, \delta S_2, f(t))$, where $f(t) > 0$ and the perturbed states are very small (so $\frac{f}{X_1+X_2} \gg 1$). The dynamics after this perturbation are (note that $X_1 = \delta X_1$, etc.)

$$\frac{d}{dt}\begin{bmatrix} X_1 \\ X_2 \\ S_1 \\ S_2 \\ f \end{bmatrix} = \begin{bmatrix} u_{4,1} & 0 & u_3 & 0 & 0 \\ 0 & u_{4,2} & 0 & u_3 & 0 \\ 0 & 0 & -u_3 & 0 & 0 \\ 0 & 0 & 0 & -u_3 & 0 \\ -\gamma & -\gamma & 0 & 0 & 0 \end{bmatrix}\begin{bmatrix} X_1 \\ X_2 \\ S_1 \\ S_2 \\ f \end{bmatrix} + \begin{bmatrix} 0 \\ 0 \\ 0 \\ 0 \\ 1 \end{bmatrix}\overline{e}$$

from which it is easy to obtain the characteristic equation for the linearized A matrix:

$$\lambda(\lambda - u_{4,1})(\lambda - u_{4,2})(\lambda + u_3)^2.$$

Since $u_{4,i} > 0$, $i = 1, 2$, the point $(0, 0, 0, 0, f(t))$ is locally unstable. □

B.3 Proof of Theorem 7.4.8

Theorem. *If $S_{1,0}, S_{2,0}$, and f_0 are non-negative, $X_{1,0}$ and $X_{2,0}$ are positive, the birth, death, sporulation, and germination rates are positive over a nonempty set of values of $\frac{f}{X_1+X_2}$ and finite, and $\gamma \ll 1$, then System (7.1) is BIBO stable.*

Proof. System (7.1) is

$$\dot{x} = A_1 x + B_1 \tag{7.1}$$

where

$$A_1 = \begin{bmatrix} a_{11} & a_{12} & a_{13} & 0 & a_{15} \\ a_{21} & a_{22} & 0 & a_{24} & a_{25} \\ a_{31} & a_{32} & a_{33} & 0 & a_{35} \\ a_{41} & a_{42} & 0 & a_{44} & a_{45} \\ a_{51} & a_{52} & 0 & 0 & 0 \end{bmatrix}$$

$$B_1 = \begin{bmatrix} 0 \\ 0 \\ 0 \\ 0 \\ 1 \end{bmatrix}$$

and the elements of A_1 are

$$a_{11} = \left(\frac{u_4}{l_4} + \frac{u_1}{l_1} + \frac{u_2}{\theta_1}\right) c\frac{X_{2,0}}{X_{1,0}+X_{2,0}} - (u_1+u_2) - \frac{u_3}{\beta_1} c\frac{S_{1,0}}{X_{1,0}+X_{2,0}}$$

$$a_{12} = -\left(\frac{u_4}{l_4} + \frac{u_1}{l_1} + \frac{u_2}{\theta_1}\right) c\frac{X_{1,0}}{X_{1,0}+X_{2,0}} - \frac{u_3}{\beta_1} c\frac{S_{1,0}}{X_{1,0}+X_{2,0}}$$

$$a_{13} = \frac{u_3}{\beta_1} c$$

$$a_{15} = \left(\frac{u_4}{l_4} + \frac{u_1}{l_1} + \frac{u_2}{\theta_1}\right) \frac{X_{1,0}}{X_{1,0}+X_{2,0}} + \frac{u_3}{\beta_1}\frac{S_{1,0}}{X_{1,0}+X_{2,0}}$$

$$a_{21} = -\left(\frac{u_4}{l_4} + \frac{u_1}{l_1} + \frac{u_2}{\theta_2}\right) c\frac{X_{2,0}}{X_{1,0}+X_{2,0}} - \frac{u_3}{\beta_2} c\frac{S_{2,0}}{X_{1,0}+X_{2,0}}$$

$$a_{22} = \left(\frac{u_4}{l_4} + \frac{u_1}{l_1} + \frac{u_2}{\theta_2}\right) c\frac{X_{1,0}}{X_{1,0}+X_{2,0}} - (u_1+u_2) - \frac{u_3}{\beta_2} c\frac{S_{2,0}}{X_{1,0}+X_{2,0}}$$

$$a_{24} = \frac{u_3}{\beta_2} c$$

$$a_{25} = \left(\frac{u_4}{l_4} + \frac{u_1}{l_1} + \frac{u_2}{\theta_2}\right) \frac{X_{2,0}}{X_{1,0}+X_{2,0}} + \frac{u_3}{\beta_2}\frac{S_{2,0}}{X_{1,0}+X_{2,0}}$$

$$a_{31} = u_2 - \frac{u_2}{\theta_1}\frac{X_{2,0}}{X_{1,0}+X_{2,0}} + \frac{u_3}{\beta_1}c\frac{S_{1,0}}{X_{1,0}+X_{2,0}}$$
$$a_{32} = \frac{u_2}{\theta_1}c\frac{X_{1,0}}{X_{1,0}+X_{2,0}} + \frac{u_3}{\beta_1}c\frac{S_{1,0}}{X_{1,0}+X_{2,0}}$$
$$a_{33} = -\frac{u_3}{\beta_1}c$$
$$a_{35} = -\frac{u_2}{\theta_1}\frac{X_{1,0}}{X_{1,0}+X_{2,0}} - \frac{u_3}{\beta_1}\frac{S_{1,0}}{X_{1,0}+X_{2,0}}$$

$$a_{41} = \frac{u_2}{\theta_2}c\frac{X_{2,0}}{X_{1,0}+X_{2,0}} + \frac{u_3}{\beta_2}c\frac{S_{2,0}}{X_{1,0}+X_{2,0}}$$
$$a_{42} = u_2 - \frac{u_2}{\theta_2}\frac{X_{1,0}}{X_{1,0}+X_{2,0}} + \frac{u_3}{\beta_2}c\frac{S_{2,0}}{X_{1,0}+X_{2,0}}$$
$$a_{44} = -\frac{u_3}{\beta_2}c$$
$$a_{45} = -\frac{u_2}{\theta_2}\frac{X_{2,0}}{X_{1,0}+X_{2,0}} - \frac{u_3}{\beta_2}\frac{S_{2,0}}{X_{1,0}+X_{2,0}}$$

$$a_{51} = a_{52} = -\gamma$$

and $c = \frac{f_0}{X_{1,0}+X_{2,0}}$. Note the following identities, which will be used throughout the remainder

of this proof.

$$a_{11} = a_{12} - \left(u_2 - \frac{u_2}{\theta_1}c\right) \tag{B.3}$$

$$a_{22} = a_{21} - \left(u_2 - \frac{u_2}{\theta_2}c\right) \tag{B.4}$$

$$a_{31} = a_{32} + \left(u_2 - \frac{u_2}{\theta_1}c\right) \tag{B.5}$$

$$a_{42} = a_{41} + \left(u_2 - \frac{u_2}{\theta_2}c\right) \tag{B.6}$$

$$a_{15} + a_{35} = \left(\frac{u_4}{l_4} + \frac{u_1}{l_1}\right)\frac{X_{1,0}}{X_{1,0} + X_{2,0}} \tag{B.7}$$

$$a_{25} + a_{45} = \left(\frac{u_4}{l_4} + \frac{u_1}{l_1}\right)\frac{X_{2,0}}{X_{1,0} + X_{2,0}} \tag{B.8}$$

$$a_{21} + a_{41} = -\left(\frac{u_4}{l_4} + \frac{u_1}{l_1}\right)c\frac{X_{2,0}}{X_{1,0} + X_{2,0}} \tag{B.9}$$

$$a_{12} + a_{32} = -\left(\frac{u_4}{l_4} + \frac{u_1}{l_1}\right)c\frac{X_{1,0}}{X_{1,0} + X_{2,0}} \tag{B.10}$$

$$a_{42} + a_{22} = -\left(\frac{u_4}{l_4} + \frac{u_1}{l_1}\right)c\frac{X_{2,0}}{X_{1,0} + X_{2,0}} \tag{B.11}$$

$$a_{11} + a_{31} = -\left(\frac{u_4}{l_4} + \frac{u_1}{l_1}\right)c\frac{X_{1,0}}{X_{1,0} + X_{2,0}} \tag{B.12}$$

$$a_{11}a_{32} - a_{12}a_{31} = (a_{12} - a_{32})\left(u_2 - \frac{u_2}{\theta_1}c\right) \tag{B.13}$$

Additionally, note that $a_{24} = -a_{44}$ and $a_{13} = a_{33}$.

The characteristic equation for A_1 is

$$-\lambda^5 + l_4\lambda^4 + l_3\lambda^3 + l_2\lambda^2 + l_1\lambda + l_0 = 0,$$

where the coefficients are identical to the general case in the proof for Theorem 6.4.1. The term l_0 is

$$\begin{aligned} l_0 = a_{33}a_{44}a_5\{&a_{35}[a_{41} - a_{42} + a_{21} - a_{22}] + a_{45}[a_{32} - a_{31} + a_{12} - a_{11}] \\ &+a_{25}[a_{32} - a_{31} + a_{12} - a_{11}] + a_{15}[a_{41} - a_{42} + a_{21} - a_{22}]\} \end{aligned}$$

where the aforementioned identities (Equations (B.3)-(B.6)) can be used to simplify the

terms in the curly brackets. Specifically,

$$a_{25}[a_{32} - a_{31} + a_{12} - a_{11}] = a_{25}\left[-\left(u_2 - \frac{u_2}{\theta_1}c\right) + \left(u_2 - \frac{u_2}{\theta_1}c\right)\right] = 0$$
$$a_{15}[a_{41} - a_{42} + a_{21} - a_{22}] = a_{15}\left[-\left(u_2 - \frac{u_2}{\theta_2}c\right) + \left(u_2 - \frac{u_2}{\theta_2}c\right)\right] = 0$$
$$a_{35}[a_{41} - a_{42} + a_{21} - a_{22}] = a_{35}\left[-\left(u_2 - \frac{u_2}{\theta_2}c\right) + \left(u_2 - \frac{u_2}{\theta_2}c\right)\right] = 0$$
$$a_{45}[a_{32} - a_{31} + a_{12} - a_{11}] = a_{45}\left[-\left(u_2 - \frac{u_2}{\theta_1}c\right) + \left(u_2 - \frac{u_2}{\theta_1}c\right)\right] = 0$$

so $l_0 = 0$. The characteristic equation can therefore be written as

$$\lambda\left(-\lambda^4 + l_4\lambda^3 + l_3\lambda^2 + l_2\lambda + l_1\right) = 0,$$

which means that A_1 has an eigenvalue at 0.

The remaining eigenvalues of A_1 can be analyzed by the equation

$$-\lambda^4 + l_4\lambda^3 + l_3\lambda^2 + l_2\lambda + l_1 = 0,$$

for which the Routh array gives necessary and sufficient conditions for all roots to have negative real part:

1. $l_4 < 0$; and
2. $l_1 < 0$; and
3. $b_1 = l_3 + \frac{l_2}{l_4} < 0$; and
4. $c_1 = l_2 - l_4\frac{l_1}{b_1} < 0$.

Note that the condition $l_4 < 0$ is satisfied by inspection. It will be shown that the coefficients of the characteristic equation satisfy the remaining conditions, so all of the eigenvalues of A_1 are in the closed left half plane.

1. $l_1 < 0$:
   The expression for l_1 is

$$\begin{aligned} l_1 = {} & a_{33}a_{44}[a_{32}a_{41} - a_{31}a_{42} + a_{21}a_{32} - a_{31}a_{22} + a_{41}a_{12} - a_{11}a_{42} + a_{12}a_{21} - a_{11}a_{22}] \\ & - a_{33}a_5a_{25}[a_{32} - a_{31} + a_{11} - a_{12}] - a_{33}a_5a_{35}[a_{21} - a_{22}] \\ & - a_{44}a_5a_{15}[a_{41} - a_{42} + a_{21} - a_{22}] + a_{44}a_5a_{25}[a_{11} - a_{12}] \\ & - a_{44}a_5a_{45}[a_{12} - a_{11}] + a_{33}a_{15}a_5[a_{22} - a_{21}] \\ & + a_{33}a_{44}a_5[a_{25} + a_{45} + a_{15} + a_{35}] \end{aligned}$$

which can be simplified considerably using Equations (B.3) – (B.6) to

$$\begin{aligned} l_1 &= -a_{33}a_5\left(u_2 - \frac{u_2}{\theta_2}c\right)(a_{35}+a_{15}) - a_{44}a_5\left(u_2 - \frac{u_2}{\theta_1}c\right)(a_{45}+a_{25}) \\ &\quad + a_{33}a_{44}a_5(a_{45}+a_{25}+a_{35}+a_{15}) \\ &= -a_5\left(\frac{u_4}{l_4}+\frac{u_1}{l_1}\right)\left[a_{33}\left(u_2 - \frac{u_2}{\theta_2}c\right)\frac{X_{1,0}}{X_{1,0}+X_{2,0}}\right. \\ &\quad \left. + a_{44}\left(u_2 - \frac{u_2}{\theta_1}c\right)\frac{X_{2,0}}{X_{1,0}+X_{2,0}} - a_{33}a_{44}\right] \end{aligned}$$

where the second equality was obtained by application of Equations (B.7) and (B.8). Plugging in the values of a_{33}, a_{44}, and a_5 gives the result

$$\begin{aligned} l_1 = -\gamma &\left(\frac{u_4}{l_4}+\frac{u_1}{l_1}\right)\left(u_2 - \frac{u_2}{\theta_1}c\right)\left(u_2 - \frac{u_2}{\theta_2}c\right) \\ &\cdot\left[\frac{X_{1,0}X_{2,0}}{S_{1,0}S_{2,0}} + \frac{X_{1,0}^2}{S_{1,0}\left(X_{1,0}+X_{2,0}\right)} + \frac{X_{2,0}^2}{S_{2,0}\left(X_{1,0}+X_{2,0}\right)}\right] \end{aligned}$$

which is less than zero under the conditions of the theorem. Note that the algebra and identities will be altered if $X_{i,0}$ or $S_{i,0}$, $i = 1, 2$, are zero, or if $c > \min\{\theta_1, \theta_2, \beta_1, \beta_2\}$, but the inequality is still valid.

2. $b_1 = l_3 + \frac{l_2}{l_4} < 0$:
First, l_2 is

$$\begin{aligned} l_2 &= a_{33}[-a_{21}a_{32} - a_5a_{35} + a_{31}a_{22} + a_{11}a_{22} - a_5a_{15} - a_{21}a_{12} - a_5a_{25}] \\ &\quad + a_{44}[a_{42}a_{11} - a_5a_{45} - a_{12}a_{41} + a_{11}a_{22} - a_5a_{15} - a_{21}a_{12} - a_5a_{25}] \\ &\quad + a_{33}a_{44}[a_{31}+a_{42}+a_{11}+a_{22}] + a_5[a_{12}a_{25} + a_{21}a_{15} - a_{22}a_{15} - a_{25}a_{11}] \\ &= a_5\left[a_{33}a_{45} - a_{33}\left(\frac{u_4}{l_4}+\frac{u_1}{l_1}\right) + a_{44}a_{35} - a_{44}\left(\frac{u_4}{l_4}+\frac{u_1}{l_1}\right)\right. \\ &\quad - a_{35}\left(u_2 - \frac{u_2}{\theta_2}c\right) - a_{45}\left(u_2 - \frac{u_2}{\theta_1}c\right) \\ &\quad \left. + \left(\frac{u_4}{l_4}+\frac{u_1}{l_1}\right)\left[\left(u_2 - \frac{u_2}{\theta_2}c\right)\frac{X_{1,0}}{X_{1,0}+X_{2,0}} + \left(u_2 - \frac{u_2}{\theta_2}c\right)\frac{X_{2,0}}{X_{1,0}+X_{2,0}}\right]\right] \\ &\quad - \frac{l_1c}{a_5} \\ &= a_5\left[a_{33}\left(a_{45} - \left(\frac{u_4}{l_4}+\frac{u_1}{l_1}\right)\right) + a_{44}\left(a_{35} - \left(\frac{u_4}{l_4}+\frac{u_1}{l_1}\right)\right)\right. \\ &\quad \left. + a_{15}\left(u_2 - \frac{u_2}{\theta_2}c\right) + a_{25}\left(u_2 - \frac{u_2}{\theta_1}c\right)\right] - \frac{l_1c}{a_5} \\ &= D_2 - \frac{l_1c}{a_5} \end{aligned}$$

where the "simplified" form was obtained with the help of Equations (B.3) – (B.10), and $D_2 < 0$ since $a_{45} < 0$, $a_{35} < 0$, $a_{15} > 0$, and $a_{25} > 0$.

Next, l_3 is

$$\begin{aligned} l_3 &= -a_{33}[a_{31} + a_{22} + a_{11}] - a_{44}[a_{42} + a_{11} + a_{22}] - a_{11}a_{22} - a_{33}a_{44} \\ &\quad + a_5[a_{15} + a_{25}] + a_{21}a_{12} \\ &= D_3 - \frac{l_1}{a_5\left(\frac{u_4}{l_4} + \frac{u_1}{l_1}\right)} \end{aligned}$$

where

$$\begin{aligned} D_3 &= -a_{33}\left[a_{31} + a_{22} + a_{11} + \left(u_2 - \frac{u_2}{\theta_2}c\right)\frac{X_{1,0}}{X_{1,0} + X_{2,0}}\right] \\ &\quad - a_{44}\left[a_{42} + a_{11} + a_{22} + \left(u_2 - \frac{u_2}{\theta_2}c\right)\frac{X_{1,0}}{X_{1,0} + X_{2,0}}\right] \\ &\quad - a_{11}a_{22} - a_{33}a_{44} + a_5[a_{15} + a_{25}] + a_{21}a_{12} \\ &= -a_{33}\left[-u_1 - u_2\frac{X_{2,0}}{X_{1,0} + X_{2,0}} - \frac{u_3}{\beta_2}c\frac{S_{2,0}}{X_{1,0} + X_{2,0}}\right] \\ &\quad - a_{44}\left[-u_1 - u_2\frac{X_{1,0}}{X_{1,0} + X_{2,0}} - \frac{u_3}{\beta_1}c\frac{S_{1,0}}{X_{1,0} + X_{2,0}}\right] \\ &\quad - a_{11}a_{22} - a_{33}a_{44} + a_5[a_{15} + a_{25}] + a_{21}a_{12} \\ &< 0 \end{aligned}$$

since all of the terms are negative except for $a_{12}a_{21}$, but

$$\begin{aligned} -a_{11}a_{22} + a_{12}a_{21} &= -\left(u_2 - \frac{u_2}{\theta_1}c\right)\left(u_2 - \frac{u_2}{\theta_2}c\right) \\ &\quad - \left(u_2 - \frac{u_2}{\theta_2}c\right)\left[\left(\frac{u_4}{l_4} + \frac{u_1}{l_1} + \frac{u_2}{\theta_1}\right)c\frac{X_{1,0}}{X_{1,0} + X_{2,0}}\right. \\ &\quad \left. + \frac{u_3}{\beta_1}c\frac{S_{1,0}}{X_{1,0} + X_{2,0}}\right] \\ &\quad - \left(u_2 - \frac{u_2}{\theta_1}c\right)\left[\left(\frac{u_4}{l_4} + \frac{u_1}{l_1} + \frac{u_2}{\theta_2}\right)c\frac{X_{2,0}}{X_{1,0} + X_{2,0}}\right. \\ &\quad \left. + \frac{u_3}{\beta_2}c\frac{S_{2,0}}{X_{1,0} + X_{2,0}}\right] \\ &< 0 \end{aligned}$$

The sign of the quantity $D_2 + l_4 D_3$ will be of interest shortly. The claim is that

$D_2 + l_4 D_3 > 0$. To show this, suppose not. Then,

$$
\begin{aligned}
& D_2 + l_4 D_3 \leq 0 \\
\Leftrightarrow\ & 0 \leq a_5 \left(u_2 - \frac{u_2}{\theta_1} c\right) \left[\left(\frac{u_4}{l_4} + \frac{u_1}{l_1} + \frac{u_2}{\theta_1}\right) \frac{X_{1,0}}{X_{1,0} + X_{2,0}} + \frac{u_3}{\beta_1} \frac{S_{1,0}}{X_{1,0} + X_{2,0}}\right] \\
& \quad + a_5 \left(u_2 - \frac{u_2}{\theta_2} c\right) \left[\left(\frac{u_4}{l_4} + \frac{u_1}{l_1} + \frac{u_2}{\theta_2}\right) \frac{X_{2,0}}{X_{1,0} + X_{2,0}} + \frac{u_3}{\beta_2} \frac{S_{2,0}}{X_{1,0} + X_{2,0}}\right] \\
& \quad (u_1 + u_2) a_5 \left[\left(\frac{u_4}{l_4} + \frac{u_1}{l_1}\right) + \frac{u_2}{\theta_1} \frac{X_{1,0}}{X_{1,0} + X_{2,0}} + \frac{u_3}{\beta_1} \frac{S_{1,0}}{X_{1,0} + X_{2,0}}\right. \\
& \qquad \left. + \frac{u_2}{\theta_2} \frac{X_{2,0}}{X_{1,0} + X_{2,0}} + \frac{u_3}{\beta_2} \frac{S_{2,0}}{X_{1,0} + X_{2,0}}\right] \\
& \quad + a_5 \frac{u_3}{\beta_1} c \left[+ \frac{u_2}{\theta_1} \frac{X_{1,0}}{X_{1,0} + X_{2,0}} + \frac{u_3}{\beta_1} \frac{S_{1,0}}{X_{1,0} + X_{2,0}}\right] \\
& \quad + a_5 \frac{u_3}{\beta_2} c \left[+ \frac{u_2}{\theta_2} \frac{X_{2,0}}{X_{1,0} + X_{2,0}} + \frac{u_3}{\beta_2} \frac{S_{2,0}}{X_{1,0} + X_{2,0}}\right] \\
& \quad - l_4 \frac{u_3}{\beta_1} c \left[-u_1 - u_2 \frac{X_{2,0}}{X_{1,0} + X_{2,0}} - \frac{u_3}{\beta_2} c \frac{S_{2,0}}{X_{1,0} + X_{2,0}}\right] \\
& \quad - l_4 \frac{u_3}{\beta_2} c \left[-u_1 - u_2 \frac{X_{1,0}}{X_{1,0} + X_{2,0}} - \frac{u_3}{\beta_1} c \frac{S_{1,0}}{X_{1,0} + X_{2,0}}\right] \\
& \quad - l_4 [a_{12} a_{21} - a_{11} a_{22}]
\end{aligned}
$$

which is a contradiction since all of the terms on the right hand side of the inequality are non-negative (recall that $-a_{11}a_{22} + a_{12}a_{21} < 0$), with at least one term strictly positive. Therefore, $D_2 + l_4 D_3 > 0$

Now, to show that $l_3 + \frac{l_2}{l_4} < 0$, suppose not; that is, suppose that $l_3 + \frac{l_2}{l_4} \geq 0$. Then,

$$
\begin{aligned}
& - l_3 l_4 \geq l_2 \\
\Leftrightarrow\ & - l_4 D_3 + \frac{l_1 l_4}{a_5 \left(\frac{u_4}{l_4} + \frac{u_1}{l_1}\right)} \geq D_2 - \frac{l_1 c}{a_5} \\
\Leftrightarrow\ & l_1 \left[\frac{l_4 + u_1}{a_5 \left(\frac{u_4}{l_4} + \frac{u_1}{l_1}\right)}\right] \geq D_2 + l_4 D_3
\end{aligned}
$$

where $l_4 + u_1 < 0$ (by inspection), $a_5 < 0$, and $l_1 < 0$. This leads to a contradiction because the inequality states that a negative number is greater than or equal to a strictly positive number. Therefore, $b_1 = l_3 + \frac{l_2}{l_4} < 0$.

3. $c_1 = l_2 - l_4 \frac{l_1}{b_1} < 0$:

This condition can be expressed as

$$\begin{aligned} & l_2 - l_4^2 \frac{l_1}{l_2 + l_3 l_4} < 0 \\ \Leftrightarrow\ & l_2(l_2 + l_3 l_4) < l_4^2 l_1 \\ \Leftrightarrow\ & \frac{l_2(l_2 + l_3 l_4)}{l_1} > l_4^2 \end{aligned}$$

since $b_1 < 0 \Rightarrow l_2 + l_3 l_4 > 0$ and $l_1 < 0$. Substituting in expressions from the previous condition gives

$$\begin{aligned} & \frac{1}{l_1}\left(D_2 - \frac{l_1 c}{a_5}\right)\left(D_2 - \frac{l_1 c}{a_5} + \left(D_3 - \frac{l_1}{a_5\left(\frac{u_4}{l_4} + \frac{u_1}{l_1}\right)}\right) l_4\right) > l_4^2 \\ \Leftrightarrow\ & \frac{1}{l_1}\left(D_2 - \frac{l_1 c}{a_5}\right)\left(D_2 + l_4 D_3 - \frac{l_1}{a_5}\left(\frac{u_1 + l_4}{\frac{u_4}{l_4} + \frac{u_1}{l_1}}\right)\right) > l_4^2 \end{aligned}$$

Now, to show that $l_2 - l_4 \frac{l_1}{b_1} < 0$, suppose not. Then,

$$\begin{aligned} & \left(D_2 - \frac{l_1 c}{a_5}\right)\left(D_2 + l_4 D_3 - \frac{l_1}{a_5}\left(\frac{u_1 + l_4}{\frac{u_4}{l_4} + \frac{u_1}{l_1}}\right)\right) \leq l_4^2 \\ \Leftrightarrow\ & \frac{D_2}{l_1}\left(D_2 + l_4 D_3\right) - \frac{c}{a_5}\left(D_2 + l_4 D_3\right) - \frac{D_2}{a_5}\left(\frac{u_1 + l_4}{\frac{u_4}{l_4} + \frac{u_1}{l_1}}\right) + \frac{l_1 c}{a_5^2}\left(\frac{u_1 + l_4}{\frac{u_4}{l_4} + \frac{u_1}{l_1}}\right) \leq l_4^2 \end{aligned}$$

where every term on the left hand side of the inequality is positive. Invoking the assumption that $\gamma \ll 1$, notice that

$$\frac{l_1 c}{a_5^2}\left(\frac{u_1 + l_4}{\frac{u_4}{l_4} + \frac{u_1}{l_1}}\right) \sim -\frac{1}{a_5}$$

since l_4 is independent of γ. Therefore, for some γ small enough, the inequality is violated. This contradiction leads to the conclusion that $c_1 = l_2 - l_4 \frac{l_1}{b_1} < 0$.

In summary, we have shown that the equation

$$-\lambda^5 + l_4\lambda^4 + l_3\lambda^3 + l_2\lambda^2 + l_1\lambda + l_0 = 0$$

has one root at the origin and the remaining roots have negative real part.

This is not sufficient for BIBO stability. For example, the system

$$\dot{x} = \begin{bmatrix} 1 & 0 \\ 0 & 0 \end{bmatrix} x + \begin{bmatrix} 0 \\ 1 \end{bmatrix} u$$

has an A matrix with eigenvalues in the closed left half plane, but it is not BIBO stable (the state integrates the input).

In order to establish BIBO stability for System (7.1), it will be shown that there is pole-zero cancellation at the origin.

The transfer function from the input to the states for System (7.1) is

$$\begin{aligned} H(s) &= (sI - A_1)^{-1} B_1 \\ &= \begin{bmatrix} H_1(s) \\ H_2(s) \\ H_3(s) \\ H_4(s) \\ H_5(s) \end{bmatrix} \frac{1}{\det(sI - A_1)} \\ &= \begin{bmatrix} H_1(s) \\ H_2(s) \\ H_3(s) \\ H_4(s) \\ H_5(s) \end{bmatrix} \frac{1}{s(-s^4 + l_4 s^3 + l_3 s^2 + l_2 s + l_1)} \end{aligned}$$

which is the last column of $(sI - A_1)^{-1}$ due to the structure of B_1. For $H_i(s)$, $i = 1, 2, \ldots, 5$, it will be shown that there is a zero at the origin.

1. $H_1(s)$:

$$\begin{aligned} H_1(s) = a_{24} &\left[a_{12}a_{45}(s - a_{33}) - a_{13}a_{35}a_{42} - a_{15}a_{42}(s - a_{33}) + a_{45}a_{13}a_{32}\right] \\ &- (s - a_{44}) \left[-a_{13}a_{25}a_{32} - a_{15}(s - a_{22})(s - a_{33})\right] \\ &- (s - a_{44}) \left[-a_{12}a_{25}(s - a_{33}) - a_{13}a_{35}(s - a_{22})\right] \\ = h_{13}s^3 &+ h_{12}s^2 + h_{11}s + h_{10} \end{aligned}$$

The coefficient in front of the s^0 term, h_{10}, is

$$\begin{aligned} h_{10} = a_{24} &\left[-a_{12}a_{45}a_{33} - a_{13}a_{35}a_{42} + a_{33}a_{15}a_{42} + a_{45}a_{13}a_{32}\right] \\ &a_{44} \left[-a_{13}a_{25}a_{32} - a_{15}a_{22}a_{33} + a_{12}a_{25}a_{33} + a_{22}a_{13}a_{35}\right] \\ = a_{33}a_{44} &\left[-(a_{22} + a_{42})(a_{15} + a_{35}) + (a_{45} + a_{25})(a_{12} + a_{32})\right] \\ = a_{33}a_{44} &\left[-(a_{21} + a_{41}) \left(\frac{u_4}{l_4} + \frac{u_1}{l_1}\right) \frac{X_{1,0}}{X_{1,0} + X_{2,0}} \right. \\ &\left. + \left(\frac{u_4}{l_4} + \frac{u_1}{l_1}\right) \frac{X_{2,0}}{X_{1,0} + X_{2,0}} (a_{12} + a_{32})\right] \\ = a_{33}a_{44} &\left(\frac{u_4}{l_4} + \frac{u_1}{l_1}\right)^2 \left[\frac{X_{1,0}X_{2,0}}{(X_{1,0} + X_{2,0})^2} - \frac{X_{1,0}X_{2,0}}{(X_{1,0} + X_{2,0})^2}\right] \\ = 0 \end{aligned}$$

where the third equality was obtained from Equations (B.3)–(B.8) and the fourth equality was obtained from Equations (B.9)–(B.10). Therefore,

$$H_1(s) = s\left(h_{13}s^2 + h_{12}s + h_{11}\right)$$

has a zero at the origin.

2. $H_2(s)$:

$$\begin{aligned}
H_2(s) &= -a_{24}\left[-a_{45}(s-a_{11})(s-a_{33}) - a_{13}a_{35}a_{41} - a_{15}a_{41}(s-a_{33}) + a_{13}a_{31}a_{45}\right] \\
&\quad - (s-a_{44})\left[-a_{31}a_{13}a_{25} + a_{15}a_{21}(s-a_{33})\right] \\
&\quad - (s-a_{44})\left[+a_{25}(s-a_{33})(s-a_{11}) + a_{13}a_{21}a_{35}\right] \\
&= h_{23}s^3 + h_{22}s^2 + h_{21}s + h_{20}
\end{aligned}$$

The coefficient in front of the s^0 term, h_{20}, is

$$\begin{aligned}
h_{20} &= -a_{24}\left[-a_{11}a_{45}a_{33} - a_{13}a_{35}a_{41} + a_{33}a_{15}a_{41} + a_{45}a_{13}a_{31}\right] \\
&\quad - a_{44}\left[-a_{13}a_{25}a_{31} - a_{15}a_{21}a_{33} + a_{11}a_{25}a_{33} + a_{21}a_{13}a_{35}\right] \\
&= a_{33}a_{44}\left[-(a_{25}+a_{45})(a_{11}+a_{31}) + (a_{41}+a_{21})(a_{15}+a_{35})\right] \\
&= a_{33}a_{44}\left(\frac{u_4}{l_4} + \frac{u_1}{l_1}\right)^2\left[\frac{X_{1,0}X_{2,0}}{(X_{1,0}+X_{2,0})^2} - \frac{X_{1,0}X_{2,0}}{(X_{1,0}+X_{2,0})^2}\right] \\
&= 0
\end{aligned}$$

where the third equality was obtained from Equations (B.7)–(B.9) and (B.12). Therefore,

$$H_2(s) = s\left(h_{23}s^2 + h_{22}s + h_{21}\right)$$

has a zero at the origin.

3. $H_3(s)$:

$$\begin{aligned}
H_3(s) &= a_{24}\left[a_{32}a_{45}(s-a_{11}) - a_{12}a_{35}a_{41} - a_{15}a_{31}a_{42} + a_{15}a_{32}a_{41}\right] \\
&\quad + a_{24}\left[-a_{35}a_{42}(s-a_{11}) + a_{45}a_{12}a_{31}\right] \\
&\quad - (s-a_{44})\left[-a_{35}(s-a_{11})(s-a_{22}) - a_{12}a_{25}a_{31} - a_{15}a_{21}a_{32}\right] \\
&\quad - (s-a_{44})\left[-a_{15}a_{31}(s-a_{22}) - a_{25}a_{32}(s-a_{11}) + a_{35}a_{12}a_{21}\right] \\
&= h_{33}s^3 + h_{32}s^2 + h_{31}s + h_{30}
\end{aligned}$$

The coefficient in front of the s^0 term, h_{30}, is

$$\begin{aligned}
h_{30} &= a_{44}\left[a_{11}a_{32}a_{45} + a_{12}a_{35}a_{41} + a_{15}a_{31}a_{42} - a_{15}a_{32}a_{41} - a_{11}a_{35}a_{42} - a_{45}a_{12}a_{31}\right. \\
&\quad \left. -a_{11}a_{22}a_{35} - a_{12}a_{25}a_{31} - a_{15}a_{21}a_{32} + a_{15}a_{31}a_{22} + a_{25}a_{32}a_{11} + a_{35}a_{12}a_{21}\right] \\
&= a_{44}\left[(a_{11}a_{32} - a_{12}a_{31})(a_{45}+a_{25}) + (a_{12}a_{35} - a_{15}a_{32})(a_{41}+a_{21})\right] \\
&\quad + a_{44}\left[(a_{15}a_{31} - a_{11}a_{35})(a_{22}+s_{42})\right] \\
&= a_{44}\left(\frac{u_4}{l_4} + \frac{u_1}{l_1}\right)c^2\frac{X_{2,0}}{X_{1,0}+X_{2,0}}\left(u_2 - \frac{u_2}{\theta_1}c\right)\left[-\left(\frac{u_4}{l_4} + \frac{u_1}{l_1}\right)\frac{X_{1,0}}{X_{1,0}+X_{2,0}}\right. \\
&\quad -2\frac{u_2}{\theta_1}\frac{X_{1,0}}{X_{1,0}+X_{2,0}} - 2\frac{u_3}{\beta_1}\frac{S_{1,0}}{X_{1,0}+X_{2,0}} + \left(\frac{u_4}{l_4} + \frac{u_1}{l_1} + \frac{u_2}{\theta_1}\right)\frac{X_{1,0}}{X_{1,0}+X_{2,0}} \\
&\quad \left. +\frac{u_3}{\beta_1}\frac{S_{1,0}}{X_{1,0}+X_{2,0}} + \frac{u_2}{\theta_1}\frac{X_{1,0}}{X_{1,0}+X_{2,0}} + \frac{u_3}{\beta_1}\frac{S_{1,0}}{X_{1,0}+X_{2,0}}\right] \\
&= 0
\end{aligned}$$

where the third equality was obtained from Equations (B.3), (B.5), (B.8), (B.9), (B.11), and (B.13). Therefore,

$$H_3(s) = s\left(h_{33}s^2 + h_{32}s + h_{31}\right)$$

has a zero at the origin.

4. $H_4(s)$:

$$\begin{aligned}
H_4(s) &= a_{13}\left[-a_{21}a_{32}a_{45} + a_{41}a_{35}(s-a_{22}) - a_{25}a_{31}a_{42} + a_{25}a_{32}a_{41}\right] \\
&\quad + a_{13}\left[a_{35}a_{42}a_{21} - a_{31}a_{45}(s-a_{22})\right] \\
&\quad - (s-a_{33})\left[-a_{45}(s-a_{11})(s-a_{22}) - a_{12}a_{25}a_{41} - a_{15}a_{21}a_{42}\right] \\
&\quad - (s-a_{33})\left[-a_{41}a_{14}(s-a_{22}) + a_{12}a_{21}a_{45} - a_{25}a_{42}(s-a_{11})\right] \\
&= h_{43}s^3 + h_{42}s^2 + h_{41}s + h_{40}
\end{aligned}$$

The coefficient in front of the s^0 term, h_{40}, is

$$\begin{aligned}
h_{40} &= a_{33}\left[a_{21}a_{32}a_{45} + a_{41}a_{35}a_{22} + a_{25}a_{31}a_{42} - a_{25}a_{32}a_{41} - a_{21}a_{35}a_{42} - a_{45}a_{22}a_{31}\right. \\
&\quad \left. -a_{11}a_{22}a_{45} - a_{12}a_{25}a_{41} - a_{15}a_{21}a_{42} + a_{15}a_{41}a_{22} + a_{12}a_{21}a_{45} + a_{25}a_{42}a_{11}\right] \\
&= a_{33}\left(\frac{u_4}{l_4} + \frac{u_1}{l_1}\right)\frac{X_{1,0}}{X_{1,0}+X_{2,0}}\left[a_{45}c(a_{22}-a_{21}) + a_{25}c(a_{41}-a_{42})\right. \\
&\quad \left. + a_{41}\left(a_{21} - \left(u_2 - \frac{u_2}{\theta_2}c\right)\right) - a_{21}a_{42}\right] \\
&= a_{33}\left(\frac{u_4}{l_4} + \frac{u_1}{l_1}\right)\frac{X_{1,0}}{X_{1,0}+X_{2,0}}\left(u_2 - \frac{u_2}{\theta_2}c\right)\left[-c(a_{25}+a_{45}) - (a_{21}+a_{41})\right] \\
&= a_{33}\left(\frac{u_4}{l_4} + \frac{u_1}{l_1}\right)^2\frac{X_{1,0}}{X_{1,0}+X_{2,0}}\left(u_2 - \frac{u_2}{\theta_2}c\right)\left[-c\frac{X_{2,0}}{X_{1,0}+X_{2,0}} + c\frac{X_{2,0}}{X_{1,0}+X_{2,0}}\right] \\
&= 0
\end{aligned}$$

where the second equality was obtained from Equations (B.4), (B.7), (B.10), and (B.12), the third equality was obtained from Equations (B.4) and (B.6), and the fourth equality was obtained from Equations (B.8)–(B.9) . Therefore,

$$H_4(s) = s\left(h_{43}s^2 + h_{42}s + h_{41}\right)$$

has a zero at the origin.

5. $H_5(s)$:

$$\begin{aligned}
H_5(s) &= a_{33}\left[a_{21}a_{32}(s-a_{44}) - a_{24}a_{31}a_{42} + a_{31}(s-a_{22})(s-a_{44}) + a_{24}a_{32}a_{41}\right] \\
&\quad - (s-a_{44})\left[(s-a_{11})(s-a_{22})(s-a_{44}) - a_{12}a_{24}a_{41}\right] \\
&\quad - (s-a_{44})\left[-a_{24}a_{42}(s-a_{11}) - a_{12}a_{21}(s-a_{44})\right] \\
&= h_{54}s^4 + h_{53}s^3 + h_{52}s^2 + h_{51}s + h_{50}
\end{aligned}$$

The coefficient in front of the s^0 term, h_{50}, is

$$\begin{aligned}
h_{50} &= a_{33}a_{44}\left[-a_{21}a_{32} + a_{31}a_{42} - a_{32}a_{41} + a_{31}a_{22}\right] \\
&\quad + a_{33}a_{44}\left[a_{11}a_{22} - a_{12}a_{41} + a_{42}a_{11} - a_{12}a_{21}\right] \\
&= a_{33}a_{44}\left[(a_{22}+a_{42})(a_{11}+a_{31}) - (a_{41}+a_{21})(a_{32}+a_{12})\right] \\
&= a_{33}a_{44}c^2\left(\frac{u_4}{l_4} + \frac{u_1}{l_1}\right)^2\left[\frac{X_{1,0}X_{2,0}}{(X_{1,0}+X_{2,0})^2} - \frac{X_{1,0}X_{2,0}}{(X_{1,0}+X_{2,0})^2}\right] \\
&= 0
\end{aligned}$$

where the third equality was obtained from Equations (B.9)–(B.12). Therefore,

$$H_5(s) = s\left(h_{54}s^4 + h_{53}s^3 + h_{52}s^2 + h_{51}\right)$$

has a zero at the origin.

Thus, the transfer function from the input to the states for System (7.1) is

$$\begin{aligned}
H(s) &= (sI - A_1)^{-1}B_1 \\
&= \begin{bmatrix} H_1(s) \\ H_2(s) \\ H_3(s) \\ H_4(s) \\ H_5(s) \end{bmatrix} \frac{1}{s(-s^4 + l_4s^3 + l_3s^2 + l_2s + l_1)} \\
&= \begin{bmatrix} s\left(h_{13}s^2 + h_{12}s + h_{11}\right) \\ s\left(h_{23}s^2 + h_{22}s + h_{21}\right) \\ s\left(h_{33}s^2 + h_{32}s + h_{31}\right) \\ s\left(h_{43}s^2 + h_{42}s + h_{41}\right) \\ s\left(h_{54}s^4 + h_{53}s^3 + h_{52}s^2 + h_{51}\right) \end{bmatrix} \frac{1}{s(-s^4 + l_4s^3 + l_3s^2 + l_2s + l_1)} \\
&= \begin{bmatrix} h_{13}s^2 + h_{12}s + h_{11} \\ h_{23}s^2 + h_{22}s + h_{21} \\ h_{33}s^2 + h_{32}s + h_{31} \\ h_{43}s^2 + h_{42}s + h_{41} \\ h_{54}s^4 + h_{53}s^3 + h_{52}s^2 + h_{51} \end{bmatrix} \frac{1}{-s^4 + l_4s^3 + l_3s^2 + l_2s + l_1}.
\end{aligned}$$

Since it was shown that the roots of the polynomial

$$-s^4 + l_4s^3 + l_3s^2 + l_2s + l_1 = 0$$

have negative real part, System (7.1) is therefore BIBO stable.

The conclusion still holds for $c \geq \min\{\theta_1, \theta_2, \beta_1, \beta_2\}$. Though several of the useful identities are altered (e.g. Equation (B.3) will be $a_{11} = a_{12}$ if $c > \theta_1$ and Equation (B.6) will be $a_{42} = a_{41}$ if $c > \theta_2$), the important inequalities derived throughout this proof are easily checked to remain valid. □